STANDING STOCKS AND FAUNAL ZONATION OF DEEP-SEA BENTHOS: PATTERNS AND PREDICTIONS ACROSS SCALES

A Dissertation

by

CHIH-LIN WEI

Submitted to the Office of Graduate Studies of
Texas A&M University
in partial fulfillment of the requirements for the degree of

DOCTOR OF PHILOSOPHY

May 2011

Major Subject: Oceanography

Standing Stocks and Faunal Zonation of Deep-Sea Benthos: Patterns and Predictions across Scales

STANDING STOCKS AND FAUNAL ZONATION OF DEEP-SEA BENTHOS: PATTERNS AND PREDICTIONS ACROSS SCALES

A Dissertation

by

CHIH-LIN WEI

Submitted to the Office of Graduate Studies of
Texas A&M University
in partial fulfillment of the requirements for the degree of

DOCTOR OF PHILOSOPHY

Approved by:

Chair of Committee,	Gilbert T. Rowe
Committee Members,	Jay R. Rooker
	Antonietta Quigg
	Daniel C. O. Thornton
Head of Department,	Piers Chapman

May 2011

Major Subject: Oceanography

ABSTRACT

Standing Stocks and Faunal Zonation of Deep-Sea Benthos: Patterns and Predictions across Scales. (May 2011)

Chih-Lin Wei, B.S., National Chung-Hsing University (Taiwan);

M.S., Texas A&M University

Chair of Advisory Committee: Dr. Gilbert T. Rowe

The deep ocean (> 200-m depth) covers more than 65% of earth's surface and is known as the largest active carbon sink of the planet. Photosynthesis fixes inorganic carbon into organic rich-compounds to fuel the biological production in the upper ocean. A small portion of the photosynthetic carbon eventually sinks to the seafloor to support diverse deep-sea life. In this dissertation, the phytoplankton production and export flux of particulate organic carbon (POC) to the seafloor were linked to standing stocks and compositional changes of the deep-sea soft bottom assemblages. The pattern and processes of energy transfer from the surface ocean to the deep sea was examined by modeling the global benthic bacteria, meiofauna, macrofauna, and megafauna biomass from remotely sensed ocean color images and the seafloor relief. The analysis was then scaled down to the macrofauna of the Gulf of Mexico (GoM) to examine the global pattern on regional oceanic features with contrasting productivity regimes. These results suggested a universal decline of benthic standing stocks down the continental margins that is caused by an exponential decrease of export POC flux with depth. A revisit of

historical epibenthic invertebrate sampling in the North Atlantic showed that both individual species and multi-species assemblages occurred in narrow depth bands that hugged the topography from the upper continental slope out to the Hatteras Abyssal Plain. The continuum compositional change suggested that the continuous decline of benthic food supply with depth was the potential driving force for the pattern of bathymetric faunal zonation. A broad, systematic survey across multiple depth transects in the northern GoM suggested that macrofauna zonation is not only taking place across isobaths, but also form the northeast to the northwest GoM due to a horizontal productivity gradient created by the nutrient-laden Mississippi River. Analyses of long-term demersal fish data from 1964 to 2002 in the northern GoM showed no evidence of large-scale faunal change across different sampling times. Base on the pooled data, a shift in rate of fish species replacement may be caused by complex biological interactions or changes in environmental heterogeneity along depth or productivity gradients.

ACKNOWLEDGEMENTS

I would like to thank my committee chair, Dr. Gilbert T. Rowe, and committee members, Dr. Jay R. Rooker, Dr. Antonietta Quigg, and Dr. Dan C. O. Thornton, for their guidance, encouragement, and support throughout the course of my dissertation research. Their office doors were always open for me while searching for advice and invaluable discussions. I am grateful to Dr. Fain Hubbard, our formal lab manager and graduate student mentor, who oversaw our day-to-day macrofauna sorting activity. He passed away shortly after completion of the DGoMB project, but his influence has imprinted on the many student researchers of the deep GoM benthos.

Thanks go to Archie Ammons, Clif Nunnally, Lindsey Loughry, Min Chen, Matt Ziegler, Xiaojia Chen, and Yuning Wang for the wonderful time working together at sea and sample sorting in the lab. To Amélie Scheltema, Fain Hubbard, George Wilson, Iorgu Petrescu, John Foster, Mary Wicksten, Min Chen, Roe Davenport, Yuning Wang, and Yousria Soliman for macrofauna identification, and to John McEachran for the deepwater fish identification.

I would like to thank my co-authors of publications and manuscripts generated from this dissertation including Gilbert Rowe, Elva Escobar-Briones, Antje Boetius, Thomas Soltwedel, Julian Caley, Yousria Soliman, Falk Huettmann, Fangyuan Qu, Zishan Yu, Roland Pitcher, Richard Haedrich, Mary Wicksten, Michael Rex, Jeffrey Baguley, Jyotsna Sharma, Roberto Danovaro, Ian MacDonald, Clifton Nunnally, Jody Deming,

Paul Montagna, Mélanie Lévesque, Jan Marcin Weslawski, Maria Wlodarska-Kowalczuk, Baban Ingole, Brian Bett, David Billet, Andrew Yool, Bodil Bluhm, Katrin Iken, Bhavani Narayanaswamy, Amélie Scheltema, George Wilson, Iorgu Petrescu, John Foster, Min Chen, Roe Davenport, Yuning Wang, and Greg Boland. Thanks also go to Bob Carney, Michael Rex, Ron Etter, Paul Snelgrove, and anonymous reviewers for the comments and suggestions on my manuscripts and to Roland Pitcher, Peter Lawton, Nick Ellis, Stephen Smith, Lewis Incze, Michelle Greenlaw, Nicholas Wolff, Tom Shirley, and Paul Snelgrove for valuable discussions on data analysis.

Thanks go to the men and women on board the R/V Eastwood, R/V Alaminos and R/V Gyre for their enthusiasm and devotion to explore deep ocean life. The North Atlantic epibenthic invertebrate data was derived from a dissertation at Duke University by Gilbert T. Rowe under the direction of Robert J. Menzies. This dissertation was supported by Minerals Management Service (MMS), now the Bureau of Ocean Energy Management, Regulation and Enforcement (BOEMRE). Thanks go to Erma Lee and Luke Mooney, the Oceanography Department (TAMU) and Marine Biology Department (TAMUG) for conference travel support. Additional funding thanks to Cross-Project Synthesis and Continental Margin Ecosystems (COMARGE) of Census Marine Life (CoML) that was supported by Alfred P. Sloan Foundation.

Thanks to my friends, colleagues, department faculty and staff for making my time at the College Station and Galveston campuses an enjoyable memory. Finally, I would like to

thank my parents, family, friends in Taiwan, and my wife, Shih-Ying for their encouragement, patience and love.

TABLE OF CONTENTS

CHAPTER Page

LIST OF FIGURES

FIGURE Page

FIGURE Page

LIST OF TABLES

CHAPTER I

INTRODUCTION

The deep ocean (> 200 m depth) covers more than 65% of earth's surface and is known as the largest active carbon sink of the planet. Inorganic carbon is fixed into organic rich-compounds by photosynthesis and then is transported through food webs where it has a verity of fates, usually a return to CO_2. A small portion of the particulate organic carbon (POC) eventually will reach the seafloor to support diverse deep-sea life or buried within anoxic marine sediments. The cycling of surface phytoplankton production though various compartments of deep-sea food webs has implications on ocean carbon sequestration to compensate the increasing anthropogenic carbon dioxide. It is also a key to the understanding of deep-sea biodiversity, because the rain of POC is the ultimate limiting factor for benthic population growth, reproduction and recruitment (Rowe 1983, Rex et al. 2006, Wei et al. 2010a) and also the main driving force for biological interactions such as competition and predation (Rex 1976, 1977, Rex & Etter 2010). In this dissertation, variation of phytoplankton production and export POC flux were linked to the standing stocks and compositional changes of the deep-sea soft bottom assemblages to examine how energy transfer from the surface ocean to the deep sea may affect the standing stocks and species composition across benthic size groups and taxa at spatial and temporal scales.

This dissertation follows the style of Marine Ecology Progress Series.

The second chapter, "*Global Patterns and Predictions of Seafloor Biomass Using Random Forests*", starts with a global synthesis of the benthic standing stocks on 4 major size classes including bacteria, meiofauna, macrofauna, and megafauna (Wei et al. 2010b). The machine-learning algorithm, Random Forests, was employed to model and predict seafloor standing stocks from surface primary production, water-column integrated and export particulate organic matter (POM), seafloor relief, and bottom water properties. The goal is to generate a global map of living organic carbon on the seafloor and examine the large-scale (ocean-basin-wise and latitudinal) variation with limited numbers of data. The third chapter, "*Standing Stocks and Body Size of Deep-Sea Macrofauna: A Baseline Prior to the 2010 BP Oil Spill in the Northern Gulf of Mexico*", scaled down to examine the distribution of benthic stocks within a semi-enclosed basin. A special focus is to evaluate the stock conditions prior to the *Deepwater Horizon* oil spill incident on April 20, 2010. Since no previous sampling had been conducted at the spill site, predicted models based on high resolution bathymetry and ocean color images were employed to map the biomass in the vicinity of spill site and the entire Gulf of Mexico (GoM). The standing stocks were examined for the oceanic features and regions with contrasting productivity regimes including continental slope, submarine canyons, small basins, steep escarpments, deep abyssal plain, northern GoM with pronounce influence from the Mississippi River, and southern GoM with limited riverine inputs. Moreover, temporal variation was also examined between the historical and most current data in the northern GoM. This chapter aims to provide a pristine, baseline condition for the potential post-spill effect assessment in the future.

It has been well established that the distribution of soft-bottom assemblages are zoned with depth in the deep ocean, usually as distinct narrow depth bands parallel to the isobaths (Rowe & Menzies 1969). A general explanation has been a depth-dependent loss of food supply to the benthos (Rowe 1983, Rex et al. 2006). Multiple biological and physical factors contribute to the zonation pattern but also correlate with water depth (Carney et al. 1983, Carney 2005, Rex & Etter 2010). In the forth chapter, "*Faunal zonation of large epibenthic invertebrates off North Carolina revisited*", I re-analyzed the classic work conducted by Rowe and Menzies (1969) using contemporary computing methods and geographic information system (GIS) to examine the pattern of bathymetric zonation along a large depth gradient from the upper continental slope out to the Hatteras Abyssal Plain in the North Atlantic (Wei & Rowe 2009). Besides a prominent depth zonation, the changes of faunal constituents or zonal boundaries have been suggested to occur along the isobaths (Markle & Musick 1974, Hecker 1990). Nevertheless, these previous studies only covered a narrow depth extends along the isobaths and the thus was uncertain whether the observed horizontal patterns can be extended at all depths. In the fifth chapter, "*Bathymetric Zonation of Deep-Sea Macrofauna in Relation to Export of Surface Phytoplankton Production*", a broad, systematic survey was conducted to examine the zonation of macrofauna communities in the northern Gulf of Mexico (GoM). I proposed that faunal zonation is not only taking place across isobaths, but also horizontally form the northeast to the northwest GoM due to the influence of the Mississippi River. The horizonatal productivity gradient in the northern GoM (Biggs et al. 2008) also provides a unique opportunity to tease out the

potential effect of food supply on zonation independent of the depth variation. Temporal changes in taxon or species composition has been observed and linked to long-term, climate driven variations in surface production (Ruhl 2008, Ruhl et al. 2008, Smith et al. 2009, Billett et al. 2010, Kalogeropoulou et al. 2010). Based on these observations, it might be possible to infer that the temporal faunal changes may extend to areas with similar oceanographic conditions; hence, in the sixth chapter, "*Long-Term Observations of Epibenthic Fish Zonation in the Deep Northern Gulf of Mexico*", I examined three large-scale deep-sea surveys between years 1964 and 2002 and proposed that the pattern of faunal zonation might alter at the contemporary time scale. Benthic macrofauna biomass from Chapter III was used as a surrogate for export POC flux on the seafloor (Smith et al. 1997, Johnson et al. 2007) to examine a potential productivity-zonation relationship.

CHAPTER II

GLOBAL PATTERNS AND PREDICTIONS OF SEAFLOOR BIOMASS USING RANDOM FORESTS

2.1. Overview

A comprehensive seafloor biomass and abundance database has been constructed from 24 oceanographic institutions worldwide within the Census of Marine Life (CoML) field projects. The machine-learning algorithm, Random Forests, was employed to model and predict seafloor standing stocks from surface primary production, water-column integrated and export particulate organic matter (POM), seafloor relief, and bottom water properties. The predictive models explain 63% to 88% of stock variance among the major size groups. Individual and composite maps of predicted global seafloor biomass and abundance are generated for bacteria, meiofauna, macrofauna, and megafauna (invertebrates and fishes). Patterns of benthic standing stocks were positive functions of surface primary production and delivery of the particulate organic carbon (POC) flux to the seafloor. At a regional scale, the census maps illustrate that integrated biomass is highest at the poles, on continental margins associated with coastal upwelling and with broad zones associated with equatorial divergence. Lowest values are consistently encountered on the central abyssal plains of major ocean basins The shift of biomass dominance groups with depth is shown to be affected by the decrease in average body size rather than abundance, presumably due to decrease in quantity and quality of food supply. This biomass census and associated maps are vital components of mechanistic

deep-sea food web models and global carbon cycling, and as such provide fundamental information that can be incorporated into evidence-based management.

2.2. Introduction

2.2.1. Rationale

A ‘census’, according to our dictionaries, was originally a counting of individuals for the purpose of taxation. The Census of Marine Life (CoML) is on the other hand an attempt to make a comprehensive assessment of what lives in the world’s oceans. CoML is attempting to document, describe, list, archive and map as many species of organisms as possible in all marine ecosystems, independent of an individual species’ population size. A natural by-product of CoML however has been new tabulations of animal abundances and biomass by CoML field projects. The purpose of this CoML biomass synthesis has been to capture all the new information on biomass that has been uncovered during CoML into a single data base, independent of species composition. This project has thus archived and mapped a broad spectrum of biomass data from CoML projects from around the world, added data from a number of previous comprehensive reviews, and, as a result, produced maps of biomass of a limited number of size groups living on the sea floor on a world wide basis.

While the causes of biodiversity remain obscure to a large degree, there is general agreement that biomass is a function of food supply to or within any particular habitat. As a result, standing stock biomass has been used as a surrogate for biomass production

and carbon flow to and through an ecosystem, without necessarily defining the taxa contributing to the biomass. On the other hand, by analyzing the statistical relationships of diversity to biomass, it might be possible to make some practical inferences about the effects that productivity might have on diversity (Rowe & Wei In preparation), as this is an open question that has generated considerable conjecture (Rex & Etter 2010). While the biomass census is not related to 'taxation' in the classic sense, it directly links marine populations to carbon as an ecosystem model currency. Inorganic carbon is fixed into organic-rich compounds by photosynthesis and then transferred through food webs where it has a variety of fates, usually a return to CO2. However, it is also harvested by fishers and it thus ends up in markets around the world. A biomass census therefore has relevance to societies because human populations are putting a 'tax' on the ocean biota in the form of valuable protein in fisheries products.

2.2.2. Historical background

The earliest quantitative sampling of the sea floor began at the beginning of the 20th century as an attempt to determine food resources available to bottom-dwelling fish in European waters (Petersen 1913, Petersen 1918). A good review of the mechanical instruments developed for the early shallow-water surveys (Holme & McIntyre 1971) pictures a wide variety of grab-like samplers, many still in use today. By the middle of the 20th century, the macrofauna of many continental shelves and estuaries had been sampled quantitatively by a relatively standard set of instruments. For demersal fishes and vagile megafaunal invertebrates, the most common sampling methods are trawling

and photography. Both methods have weaknesses: for example, trawling tends to capture only surface-dwelling and slow species. It may be impossible to positively identify animals to species from photographs. However, to this day neither is fool proof. With smaller forms (meiofauna, microfauna, bacteria and viruses), sampling problems are solved seemingly easily by utilizing small-diameter cores, but care has to be taken not to lose organisms by either washing or bow-wake of sampling devices. For these groups, the problem is that they have not yet been sampled comprehensively on global or ocean-basin scales.

Generalizations about the controls of sea floor biomass began to emerge by the middle of the 20th century. Expeditions sponsored by Union of Soviet Socialist Republics (USSR: dissolved in 1991) reached every corner of the globe. This large body of work concluded that biomass declines sharply with depth and with distance from land. They observed that high latitudes tended to have higher biomass than low latitudes. The major food supply to both pelagic and sea floor communities was the rain of particulate detritus, enhanced by a ladder of vertical migration (Vinogradov & Tseitlin 1983). Sea floor biomass likewise declines precipitously with depth, but is also tightly coupled to primary production in surface layers. Regression equations of the variation in benthic biomass as a function of depth and primary production established in the 1970's initially (reviewed in (Rowe 1983)) are still reasonable estimates of deep benthic biomass today (Rex et al. 2006). The slopes of the biomass regressions have been equated to the rate at which the delivery of POC to the sea floor declines, but the height or zero intercept of the regression line is a function of the mean primary production in the photic zone.

Previous reviews of seafloor standing stocks focused on bathymetric standing stock patterns in which the distribution of biomass and abundance was fitted to a linear function of water depth or direct measurement of sinking particle flux (Rowe 1983, Deming & Yager 1992, Soltwedel 2000, Rex et al. 2006). Applying such equations is conceptually intuitive but the relationships tend sometimes to fall apart in large scale predictive mapping. In this paper, we explore a novel machine-learning algorithm, Random Forests (Breiman 2001), to model the complex and potentially non-linear relationships between oceanic properties and seafloor standing stocks. Random Forests (RF) is a data mining method widely used in the fields of bioinformatics (Cutler & Stevens 2006), speech recognition (Xu & Jelinek 2004), and drug design and development (Svetnik et al. 2003). Recently RF is gaining popularity in terrestrial ecology (Prasad et al. 2006, Cutler et al. 2007, De'ath 2007); however, so far, only a handful of studies have applied RF in marine ecosystems (Oppel & Huettmann 2010, Pitcher et al. In preparation). In short, RF, as the name suggested, is an ensemble of many decision trees with binary divisions. Each tree is grown from a bootstrap sample of response variable and each node is guided by a predictor value to maximize differences in offspring branches. The fit of the tree is examined using the data not in the bootstrap selection; hence, cross-validation with external data is not necessary. Predictive accuracy requires low bias and low correlation between decision trees (Breiman 2001). RF achieves these by growing a large number of trees and then averaging the predictions. At the same time, the node decision is chosen from a random subset of predictors to make the trees look as different as possible. RF does not assume any data distribution and does

not require formal selection of predictors. RF is robust to outlier and unbalanced data, making it a better choice than traditional statistical methods (Cutler & Stevens 2006).

2.3. Materials and Methods

2.3.1. Response variables

Biomass and abundance of bacteria, meiofauna, macrofauna, megafauna (invertebrates+fishes), invertebrates, and fishes were assembled from literature and the Census of Marine Life (CoML) field projects (Fig. 2.1 and Appendix B Table S1). The "CoML Fresh Biomass Database" includes 4872 biomass records, 5511 abundance records, and 4196 records with both biomass and abundance from 175 studies. Additional datasets include nematodes (230 records from 10 studies) and pelagic decapods (17 records from 1 study); however, they were not included in this analysis. The complete list of references and detailed data information are available in Appendix B Table S1 and Appendix E File S1.

Categories of benthic fauna are usually defined by size classes. In this paper, we refer to the term "bacteria" to include both bacterial and archaeal domains. We have not included viruses. The metazoan meiofauna and macrofauna are small infauna invertebrates sampled by core or grab devices and retained on 20 to 74-µm and 250 to 520-µm sieves, respectively. Megafauna refers to large epibenthic invertebrates and demersal fishes (usually larger than 1 cm) caught or recorded by bottom trawling and photographic survey. Many studies deal with trawl invertebrates and fishes separately;

hence, 3 categories were created for the megafauna, including the invertebrates plus fishes, invertebrates, and fishes. Here the "megafauna" dataset includes both invertebrates and fishes. Estimates of meiofaunal and macrofaunal standing stocks are affected by the gear design, sampling area, and sieve sizes (Rowe 1983, Bett et al. 1994, Gage et al. 2002, Gage & Bett 2005). These factors however have been suggested to be minor compared to water depth at a global scale and do not significantly affect the overall level and pattern of stock-depth relationships (Rex et al. 2006, Rex & Etter 2010). Only studies reporting standing stocks for the whole assemblage of a size category were used in these analyses. Benthic foraminiferans were not included due to difficulty differentiating between living biomass from empty tests or shells (Soltwedel 2000, Rex et al. 2006). Throughout this analysis, the abundance was standardized to cells (for bacteria) or individuals (for meiofauna, macrofauna, and megafauna) per square meter. The biomass was standardized to milligrams carbon per square meter using appropriate conversion factors from wet or dry weight to organic carbon weight (Rowe 1983, Soltwedel 2000).

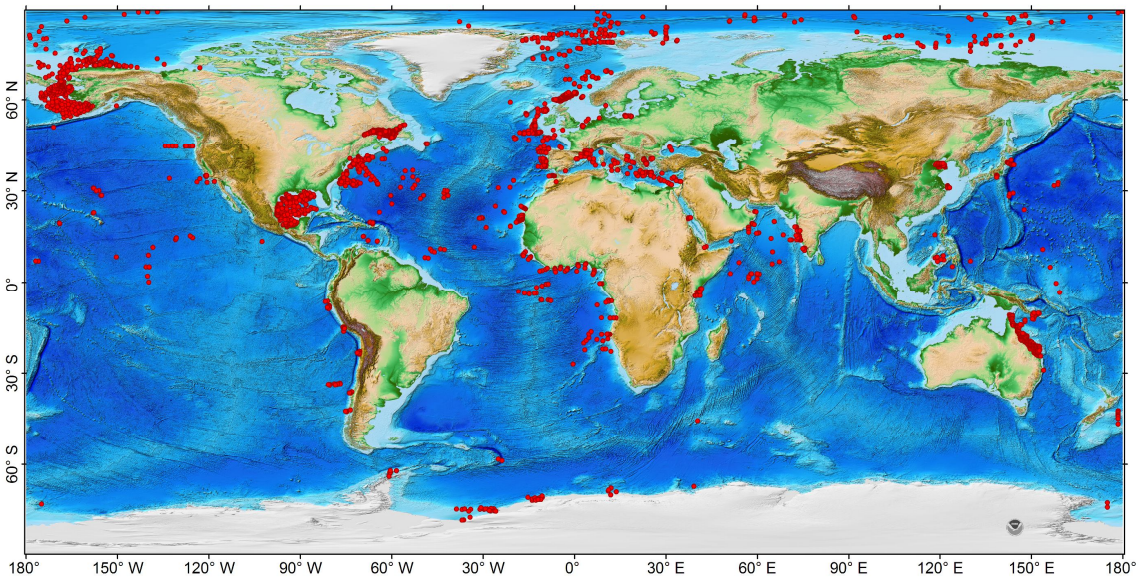

Fig. 2.1. Distribution of abundance and biomass records in the "CoML Fresh Biomass Database". References and locations for each size class are given in Appendix B Table S1 and Appendix E File S1. Bathymetric layer uses NOAA ETOPO 1 Global Relief Model (Amante & Eakins 2009).

Table 2.1. Global datasets of environmental predictors. The mean value was extracted for abundance and biomass records with catchment area of 3 x 3 or 1 x 1 cells. The datasets are divided into 4 categories, including 1) primary productivity variables, 2) water column variables, 3) bottom water properties, and 4) water depth. The table abbreviations follow: Res. = data resolution, Cell = cell size for extraction, Abbrev. = variable abbreviation.

Res.	Cell	Abbrev.	Variable	Unit
Primary Production: Decadal mean & standard deviation of monthly data from January 1998 to December 2007 (Ocean Productivity, OSU)				
5''	3x3	chl	Chlorophyll a concentration (SeaWiFS)	mg m-3
5.3''	3x3	sst	Sea Surface Temperature (AVHRR)	°C
5''	3x3	par	Photosynthetically available radiation (SeaWiFS)	Einstein m-2 day-1
5''	3x3	bbp	Particulate backscatter (SeaWiFS)	m-1
10''	1x1	mld	Mixed layed depth	m
5''	3x3	growth	Phytoplankton growth rate	divisions day-1
5''	3x3	carbon	Carbon concentration	mg m-3
5''	3x3	vgpm	Chlorophyll based net primary production	mg C m-2 day-1
5''	3x3	cbpm	Carbon based net primary production	mg C m-2 day-1
Water column: Decadal mean of monthly model simulation from January 1995 to December 2004 (Yool et al. 2009)				
1°	1x1	int.c	Integrate C to 500 m above seafloor	mg C m-2
1°	1x1	int.n	Integrate N to 500 m above seafloor	mg N m-2
1°	1x1	det.c	Integrate detrital C to 500 m above seafloor	mg C m-2
1°	1x1	det.n	Integrate detrital N to 500 m above seafloor	mg N m-2
1°	1x1	phyt	Integrate phytoplankton to 500 m above seafloor	mg N m-2
1°	1x1	zoop	Integrate zooplankton to 500 m above seafloor	mg N m-2
1°	1x1	det.c.flx	Detrital C flux at 500 m above seafloor	mg C m-2 day-1
1°	1x1	det.n.flx	Detrital N flux at 500 m above seafloor	mg N m-2 day-1

Table 2.1. Continued.

Res.	Cell	Abbrev.	Variable	Unit
Bottom Water: Annual mean & seasonal standard deviation (World Ocean Atlas 2009)				
1°	1x1	temp	Temperature	°C
1°	1x1	salin	Salinity	ppm
1°	1x1	oxyg	Oxygen concentration	milliters liter-1
1°	1x1	nitra	Nitrate concentration	micromoles liter-1
1°	1x1	phos	Phosphate concentration	micromoles liter-1
1°	1x1	si	Silicate concentration	micromoles liter-1
Water Depth: ETOPO1 Global Relief (NOAA Geophysical Data Center)				
1°	NA	depth	Water depth	m

2.3.2. Environmental predictors

Environmental variables with global coverage were utilized to characterize 1) the surface ocean climate relating to phytoplankton production, 2) water column processes associated with export POC flux, 3) bottom water properties characterizing the seafloor habitats, and 4) seafloor relief (water depth) as a proxy of declining export POC flux arriving at the ocean floor (Table 2.1 and Appendix A Fig. S1). Contemporaneous environmental and standing stocks data were not always available; therefore, mean and standard deviation (S.D.) of the predictors were calculated for the longest time periods possible. The variables are listed as:

1) Primary productivity variables: Decadal mean and standard deviation (S.D.) of monthly net primary production (NPP) models (cbpm, vgpm), and the data inputs for the NPP models (Behrenfeld & Falkowski 1997, Westberry et al. 2008) including chlorophyll concentration (chl), sea surface temperature (sst), photosynthetic available irradiance (par), mixed layer depth (mld), particle backscatter (bbp), phytoplankton growth rate (growth), and carbon concentration (carbon), all calculated between years of 1998 and 2007. The monthly data were obtained from the Ocean Productivity Group, Oregon State University, as products of the Sea Viewing Wide Field-of-view Sensor (SeaWiFS r2009.1) and Advanced Very High Resolution Radiometer (AVHRR).

2) Water column processes: Decadal mean of water-column integrated total carbon (int.c) and nitrogen (int.n), detrital carbon (det.c) and nitrogen (det.n), phytoplankton (phyt) and zooplankton (zoop), as well as export flux of detrital carbon (det.flx.c) and

nitrogen (det.flx.n), obtained from a 10-year simulation of monthly model outputs from 1995 to 2004 using Ocean Circulation and Climate Advanced Model (OCCAM) driven by a nitrogen based Nutrient Phytoplankton Zooplankton Detritus (NPZD) Model (Yool et al. 2009).

3) Bottom water properties: Annual mean and seasonal standard deviation (S.D.) of bottom water temperature, salinity, oxygen, nitrate, phosphate, and silicate concentration were obtained from World Ocean Atlas 2009, NOAA National Oceanographic Data Center.

4) Global ocean depths were obtained from the ETOPO1 Global Relief Model ,NOAA National Geophysical Data Center (Amante & Eakins 2009).

2.3.3. Data analyses and modeling

We used partial regression analysis to examine the relationships between standing stocks and depth when the latitude and longitude are held constant. The multiple regression residuals of stocks against latitude and longitude were used as dependent variables to regress against depth. To bring the dependent variable back to an appropriate scale, the y-intercept from the multiple regression was added to the residuals. The partial regression was also used in the pre-treatment of the depth-integrated bacteria data to standardize sediment penetration depths (from 0.5 to 29.5 cm; >83% are between 5 and 15 cm). Similar approaches has been developed and tested in Rex et al. (Rex et al. 2006).

A stochastic model between standing stocks and 39 environmental predictors (Table 2.1 and Appendix A Fig. S1) was constructed using Random Forests (RF) (Breiman 2001).

RF is a member of Regression Tree Analyses (RTA) (Breiman et al. 1984). In RTA, the response variable (standing stocks) is recursively partitioned into small successive binary splits. Each split is based on a single value of predictor from an exhaustive search of all available predictors to maximize the differences between the offspring branches. In RF, the response variable was bootstrap resampled before conducting RTA to generate large numbers of un-pruned decision trees (1000 trees in this study). Unlike traditional RTA, the RF algorithm searches the best split from a random subset of predictors (1/3 of all variables) and the prediction can be made from new data (environmental) by averaging the model outputs of all trees. At each bootstrap resampling step, 2/3 of the data (in-bag) were selected to build the decision tree. The other 1/3 of the data (out-of-bag, or OOB) were used to carry out an internal examination of model (decision tree) prediction error and estimate variable importance. The OOB data can generate predictions using the tree grown from the in-bag data. These OOB predictions were aggregated (by averaging the outputs of all trees) to compare with the observations and estimated the prediction error. The performance of the RF model was examined as percent variance explained: $R^2 = 1 - MSE_{OOB}$ / observed variance, where MSE_{OOB} is the mean square error between observations and OOB predictions. Predictor Importance was determined by how much worse the OOB predictions can be if the data for that predictor are randomly permuted. This essentially mimicked what would happen with or without the help of that predictor. The increase of prediction error (MSE_{OOB}) after the permutation was used to measure its contribution to the prediction accuracy. This

accuracy importance measure (increase of MSE_{OOB}) was computed for each tree and averaged over the forest (1000 trees).

2.3.4. Construction of random forest models

Standing stocks (biomass and abundance) were logarithm (base 10) transformed before conducting RF analysis. Environmental data were extracted based on the latitude and longitude of the stock records by averaging a box of size 3 x 3 or 1 x 1 cells (Table 2.1). Mean value of the box was matched to the corresponding stocks record. RF algorithm was then run independently on each of the 12 datasets. Most primary productivity predictors have declining temporal coverage at the high latitudes between years of 1998 and 2007 due to prolonged winter darkness or cloud cover preventing SeaWiFS ocean color measurements (Appendix A Fig. S2). This can be a source of error during the RF modeling, because decadal mean and standard deviation of the predictors was only calculated from the available monthly data. In order to evaluate the model stability, we conducted 4 RF simulations for each dataset. The simulations were based on different data selection scenarios, including: 1) all standing stocks and environmental data were included; 2) only data calculated from > 30 months of SeaWiFS measurements were included; 3) only data calculated from > 60 months of SeaWiFS measurements were included; 4) only data calculated from > 90 months of SeaWiFS measurements were included. In other words, Scenario 1 retained all the data and Scenario 4 excluded much of the high latitude data (>50° N or S, see Appendix A Fig. S2). The mean and standard deviation (S.D.) of the model performance (R2) and variable importance were calculated

to evaluate the model sensitivity. In the following text, the "simulations" refer to the RF runs under the 4 data selection scenarios.

2.3.5. Global prediction of seafloor standing stocks

Environmental data were averaged to the same grid resolution (1 arc degree grids) before using them as model inputs for global standing stocks predictions (Appendix A Fig. S1). For each dataset, 4 global predictions were generated from RF simulations. The mean and coefficient of variation (S.D. / mean * 100%) were calculated for each grid to optimize the predictions and examine the output stability. In order to produce a smooth predicted surface, the predictions were interpolated to 0.1 degree cell resolution using Inverse Distance Weighting (IDW). The predicted map of standing stocks is displayed in color classes using Jenks Natural Breaks Optimization method to maximize the differences between the classes. The global integral of benthic biomass was integrated from each cell value multipling the cell area on predicted map based on equidistant cylindrical projection. The calculations were based on the formula: Global integral = Σ map cell value (in per unit area) * cell area at equator (~12343 km2) * cosine (latitude). Statistical analyses and RF modeling used R 2.11.0 (R Development Core Team 2010) and R package randomForest (Liaw & Wiener 2002). Geostatistical analyses and mapping used ESRI® ArcMapTM 9.2 and R package sp (Bivand et al. 2008) .

2.4. Results

2.4.1. Partial linear regressions

Our results confirmed the conclusions of Rex et al. (Rex et al. 2006) and suggested significantly negative log-linear relationships of biomass, abundance, and body size for 3 large size classes with depth; however, none of these parameters showed statistically significant depth dependency for bacteria (Table 2.2). We adapted figure legends from Rex et al. (Rex et al. 2006) and raised the y-intercepts of their regression equations 3 orders of magnitude (converting the unit from g C m^{-2} to mg C m^{-2}) for comparison with our current results. Our regression y-intercepts were slightly lower than the previous synthesis (2.4 vs. 2.5 for bacteria.; 2.2 vs. 2.3 for meiofauna.; 3.1 vs. 3.2 for macrofauna.; 1.8 vs. 2.3 for megafauna.), while the rate of decline biomass with depth was steeper for meiofauna ($-2.4x10^{-4}$ vs. $-1.7x10^{-4}$) and macrofauna ($-5.2x10^{-4}$ vs. $-4.5x10^{-4}$), but more gradual for megafauna ($-3.1x10^{-4}$ vs. $-3.9x10^{-4}$, Table 2.2). The biomass hierarchy among size groups was similar between the 2 studies: macrofauna dominated the shelves and bacteria and meiofauna dominated the abyssal plains (Fig. 2.2). The only apparent difference was a cross of the regression lines between macrofauna and megafauna at ~6000 m depth, or a reversal of their biomass hierarchies. The lower y-intercepts and steeper slopes for the meiofauna and macrofauna suggested that the biomass levels were lower in this study than in the previous synthesis. The rate of declining biomass with depth was highest for macrofauna, followed by megafauna and meiofauna. Except for meiofauna, the y-intercept of the abundance-depth regressions were slightly lower in this study (13.3 vs. 14.1 for bacteria.; 3.5 vs. 3.6 for macrofauna.; -0.7 vs. -0.3 for

megafauna.) while the slopes were more gradual (-2x10-4 vs. -2.8x10-4 for macrofauna.; -2.8x10-4 vs. -3.7x10-4 for megafauna., Table 2.2). The rate of declining abundance with depth was sharpest for megafauna, followed by macrofauna and meiofauna (Fig. 2.3, Table 2.2). Average body size for each size class was calculated as biomass divided by abundance. The average sizes of all 3 large groups showed significant depth dependency with the rates of declining mean size with depth being the most rapid for macrofauna, followed by megafauna and meiofauna (Table 2.2 and Fig. 2.4). The rapid decline in average macrofaunal size was likely overestimated at abyssal depths, because the regression line was apparently higher at shelf depths due to extremely large values (>10 mg C individual^{-1}) at high latitude areas.

2.4.2. Random forests

On average, RF models explained 78% to 81% of total variance (R^2) for bacteria, meiofauna, and macrofauna biomass (Fig. 2.5a). Compared to the small size classes, the RF performance was subordinate for megafauna, invertebrates, and fishes, in which the models only explained 63% to 68% of the observed biomass variance. The RF algorithm appears to perform better for abundance with the models explaining 77% to 88% of total variance for each size class. The RF performance among different simulation scenarios was generally stable (S.D $\leq$ 1%). The variability was only slightly higher for macrofauna and invertebrates with S.D. between 2% to 3%. A scatter plot between observed and predicted biomass (Fig. 2.5b) suggests that the OOB predictions were in proper scale (regression slopes = ~1) with modest deviations from the observations.

Table 2.2. Regression analyses of biomass, abundance, and body size against depth for bacteria, meiofauna, macrofauna, and megafauna. Response variables are log10 transformed biomass (mg C m-2), abundance (individual m-1), and body size (µg C individual-1). Predictor is depth (m). Scatter plots of the response variables against predictor and regression lines are given in Figure 2-4. Abbreviations: N = number of samples; *** denotes P<0.001; n.s. = not significant.

Regression	Equations	N	F
Log_{10} Biomass (mg C m^{-2})			
Bacteria	Y= 2.4 - (1.22e-06) X	525	<0.01 n.s.
Meiofauna	Y = 2.18 - (2.39e-04) X	689	244.1***
Macrofauna	Y =3.05 - (5.15e-04) X	2552	1885***
Megafauna	Y = 1.81 - (3.07e-04) X	282	136.2***
Log_{10} Abundance (individual m^{-1})			
Bacteria	Y = 13.27 - (3.58e-05) X	515	2.82 n.s.
Meiofauna	Y = 5.73 - (1.25e-04) X	1148	184.7***
Macrofauna	Y = 3.5 - (1.95e-04) X	2734	618.2***
Megafauna	Y = -0.68 - (2.82e-04) X	253	32.92***
Log_{10} Body Size(µg C $individual^{-1}$)			
Bacteria	Y = -7.79 +(1.35e-05) X	451	2.28 n.s.
Meiofauna	Y = -0.61 - (6.81e-05) X	616	27.6***
Macrofauna	Y = 2.62 - (3.63e-04) X	2393	637.3***
Megafauna	Y = 6.17 - (1.57e-04) X	136	43.58***

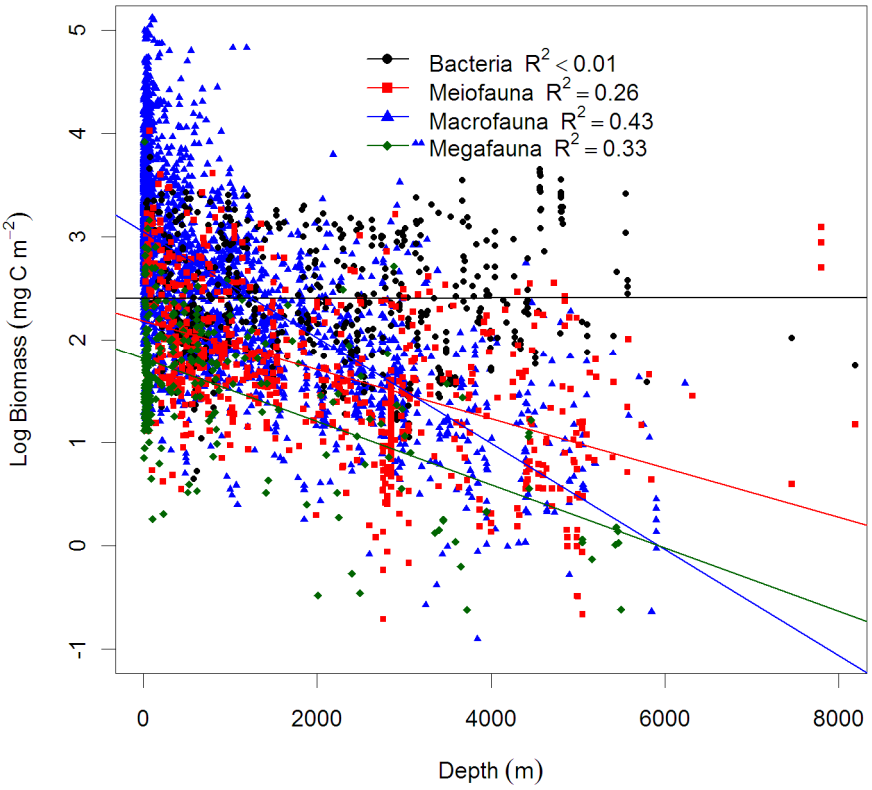

Fig. 2.2. Biomass as a function of depth for bacteria, meiofauna, macrofauna, and megafauna. Biomass was log10 transformed and the effects of latitude and longitude were removed by partial regression. Figure legend follows Rex et al. (Rex et al. 2006) for comparison. References of data source are available in Appendix B Table S1 and Appendix E File S1. Regression equations and test statistics for each size categories are available in Table 2.2.

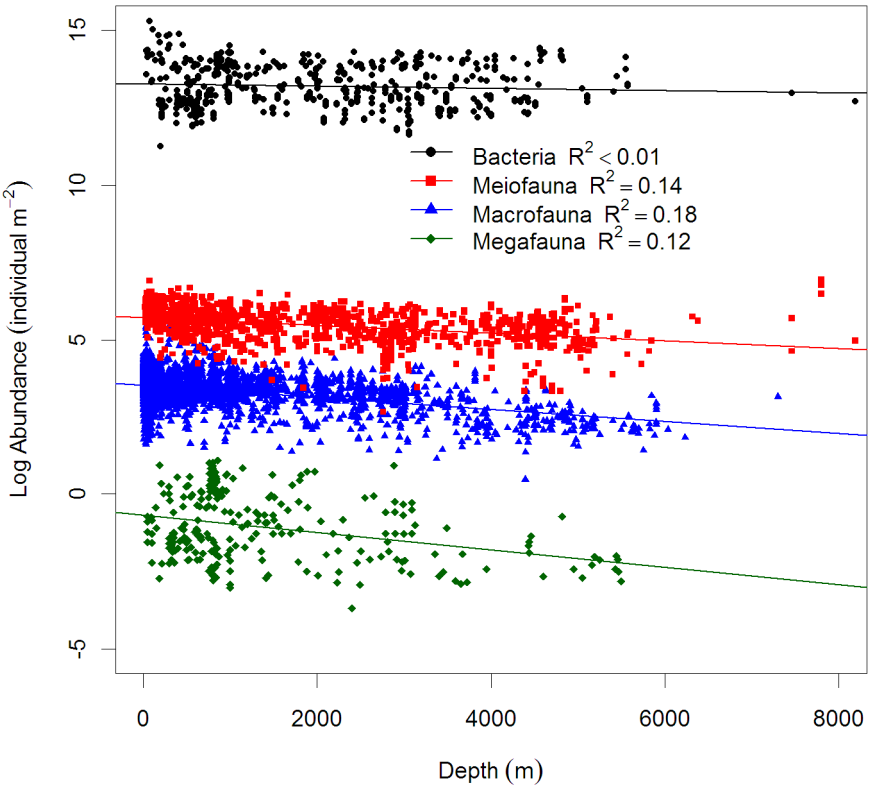

Fig. 2.3. Abundance as a function of depth for bacteria, meiofauna, macrofauna, and megafauna. Abundance was log10 transformed and the effects of latitude and longitude were removed by partial regression. Figure legend follows Rex et al. (Rex et al. 2006) for comparison. References of data source are available in Appendix B Table S1 and Appendix E File S1. Regression equations and test statistics for each size category are available in Table 2.2.

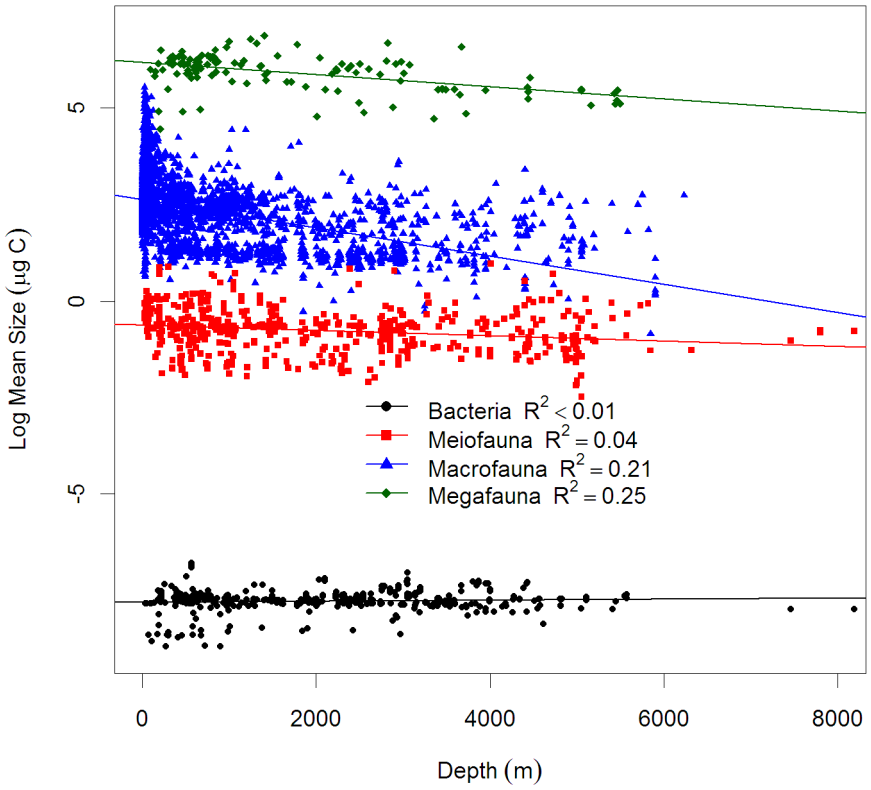

Fig. 2.4. Average body size as a function of depth for bacteria, meiofauna, macrofauna, and megafauna. The average size was calculated by dividing biomass with abundance. The body size was log10 transformed and the effects of latitude and longitude were removed by partial regression. Figure legend follows Rex et al. (Rex et al. 2006) for comparison. References of data source are available in Appendix B Table S1 and Appendix E File S1. Regression equations and test statistics for each size categories are available in Table 2.2.

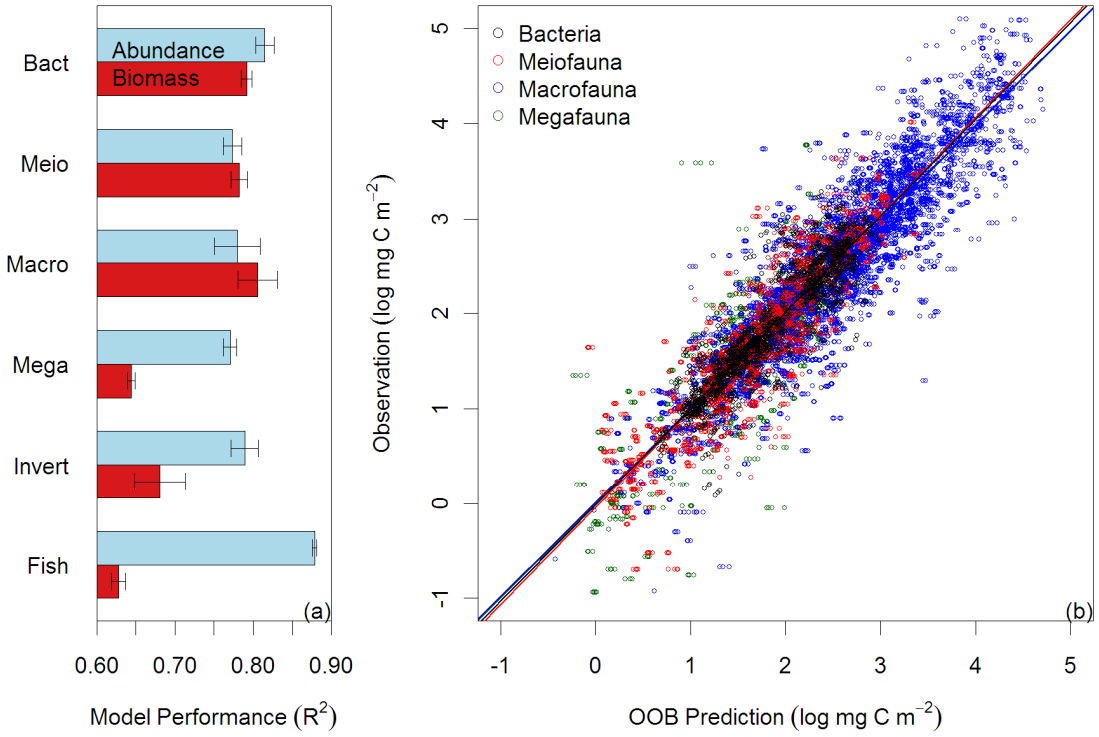

Fig. 2.5. Random Forests (RF) performance on biomass and abundance of each size class. (a) Mean percent variance explained by the RF model ± S.D. (error bar) from 4 RF simulations. Abbreviations: Bact = bacteria, Meio = meiofauna, Macro = macrofauna, Mega = megafauna, and invert = invertebrates. (b) Observed against OOB predicted biomass from the 4 RF simulations. Color legends indicate 4 major size classes.

We combined predictor importance from bacteria, meiofauna, macrofauna, and megafauna (Appendix A Fig. S3) to examine the predictor importance on total benthic biomass. This was only done for the biomass datasets because they were converted to a unified currency in mg C per square meter. With the exception of bacteria, depth was ranked highly important for the 3 larger size classes (Fig. 2.6). To our surprise, neither net primary production (vgpm, cbpm) nor flux of detrital organic matter to seafloor (det.c.flx, det.n.flx) was considered the most important for the total benthic biomass. Instead, water depth and the data inputs for the NPP models (carbon, bbp, sst, par, mld, chl) were among the top 10 most important variables. Nonetheless, when the predictor importance was examined for the size classes, NPP models (vgpm, cbpm) had considerable importance for bacterial, meiofaunal, and macrofaunal biomass but appeared less important for megafaunal biomass. Decadal mean and S.D. of the predictors generally ranked in similar orders suggesting high correlation between them; however, it may also suggest that overall levels and seasonal fluctuations of the predictors were both important in predicting the biomass. The predictors associated with water column processes (Table 2.1) appeared not significant to the total biomass; however, the decadal mean of water column-integrated zooplankton (zoop.mean), total organic matter (int.c.mean, int.n.mean), and detrital organic matter (det.c.mean, det.n.mean), were among the most important predictors for megafaunal standing stocks, especially for abundance (see Appendix A Fig. S3d and Fig. S4d). Annual mean salinity (salin.mean) was the only bottom water property ranked within the top 10 most important predictors for the total biomass (Fig. 2.6).

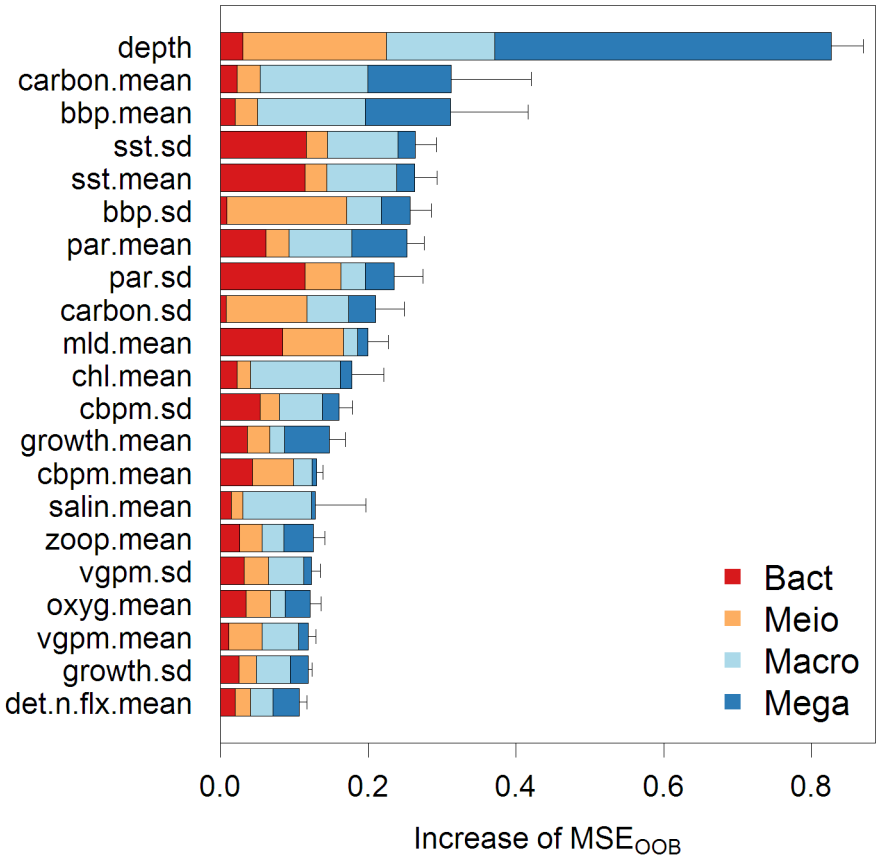

Fig. 2.6. Mean predictor importance on total seafloor biomass. The predictor importance of major size classes were combined (Appendix A Fig. S3) and mean ± S.D. (error bar) was calculated from 4 RF simulations. The top 20 most important variables are shown in descending order. Increase of mean square error (MSEOOB) indicates the contribution to RF prediction accuracy for that variable.

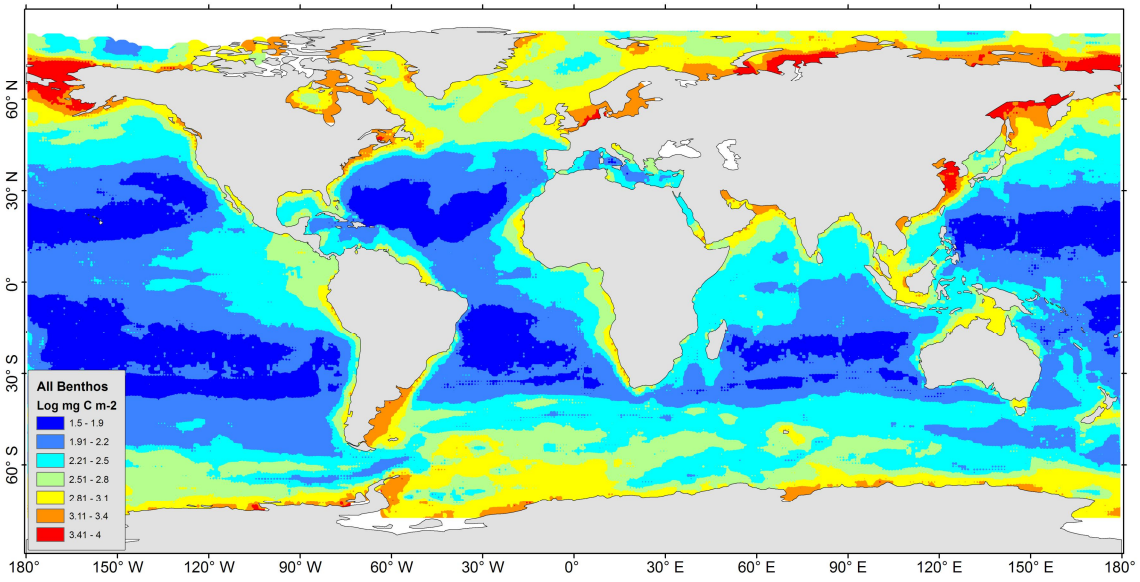

Fig. 2.7. Distribution of seafloor biomass predictions. The total biomass was combined from predictions of bacteria, meiofauna, macrofauna, and megafauna biomass (Appendix A Fig. 5a, b, c, d). Map was smoothed using Inverse Distance Weighting interpolation to 0.1 degree resolution and displayed in logarithm scale (base of 10).

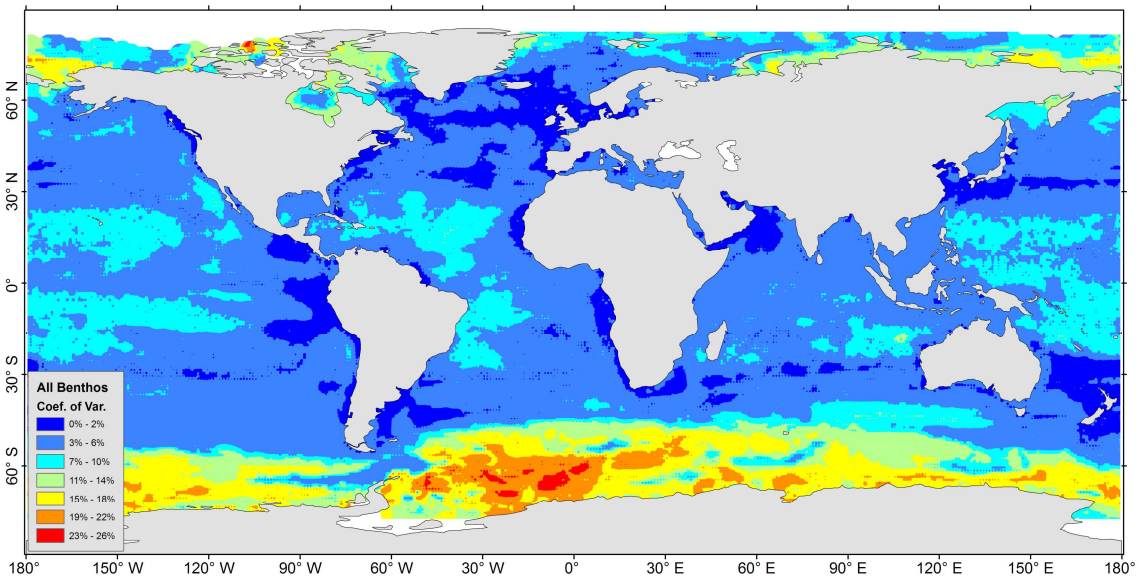

Fig. 2.8. Coefficient of variation (C.V.) for mean seafloor biomass prediction. The C.V. was computed as S.D. /mean * 100% from 4 RF simulations. Map was smoothed using Inverse Distance Weighting interpolation to 0.1 degree resolution.

2.4.3. Patterns of predicted biomass

No biomass predictions were given near the northern tip of the Arctic Ocean and part of the Antarctic shores due to a lack of SeaWiFS satellite data as a result of permanent sea ice cover (Appendix A Fig. S2). The predictions of major size classes (Appendix A Fig. S5a, b, c, d) were combined to estimate the total benthic biomass. The maximum biomass of 2.6 to 10 g C per square meter occurred on the shelves of the north frigid zones (e.g. Kara Sea, Siberian Sea, and Chukchi/Bering Sea) and temperate areas (e.g. Yellow sea and North Sea, see Fig. 2.7, red color). These predictions however were lower than the empirical maximum found in the Chukchi/Bering Sea, where the infauna biomass as high as 40 to 100 g C m^{-2} were reported (Grebmeier et al. 2006). The discrepancy is probably associated with high prediction uncertainty in the areas (C.V. = 15% to 22%, Fig. 2.8) or unexplained variability in the models (Fig. 2.5a). The weaker maximum (orange color) between 1.3 to 2.5 g C per square meter occurred on the polar to temperate shelves and subtropical coastal areas (e.g. East/South China Sea, Arabian Sea, and Persian Gulf). The lowest biomass prediction between 30 and 80 mg C per square meter occurred on the abyssal plains of the Pacific, Atlantic, and Indian Ocean; however, relatively higher biomass was predicted on the seafloor of the east side of Pacific and Atlantic basins under the productive equatorial divergence and coastal upwelling areas (Williams & Follows 2003). For these largest ocean areas, the model outputs were stable among 4 RF simulations with S.D. less than 10% of the mean predictions (Fig. 2.8, light blue to dark blue colors). Any high uncertainties were usually associated with high predicted biomass. The Southern Ocean for example had the

highest uncertainty with S.D. between 15% and 26% of the mean (yellow to red class), where most of the uncertainty was derived from the unstable predictions for macrofauna biomass (Appendix A Fig. S6). The S.D. of some Arctic shelves were slightly lower than the Southern Ocean, mostly between 11% and 18% of the mean (green to yellow class, Fig. 2.8). The log10 predictied biomass (mg C m^{-2}) and abundance (individual m^{-2}) for each size class are available in Appendix E File S2 and File S3, respectively. Global maps showing the mean of abundance prediction and coefficient of variation for each size class are given in Appendix A Fig. S7 and Fig. S8, respectively.

A total of 110.3 ± 48.2 (Mean ± S.D. from 4 RF simulations) megatons of living carbon biomass were estimated based on the global integral of the predicted map cells (Fig. 2.7), in which bacteria, meiofauna, macrofauna, and megafauna contributed 31.4%, 12.9%, 50.7%, and 5% of the global integral, respectively. Previous workers estimated that global POC flux to the seafloor was 3.76 to 3.91 megaton C day-1 (Dunne et al. 2007, Yool et al. 2009) and carbon burial was about 0.82 megaton C day-1 (Dunne et al. 2007). By dividing the total mass by the flux (Rowe et al. 1991, Rowe et al. 2008b), we estimated that the mean residence time for the seafloor living carbon was 36.6±16 days (mean ± S.D.). Generally, the predictions were highest on the continental shelves, which account for 21.1% of the global integral biomass but cover merely 5.9% of the total seafloor area (≤ 200 m water depth, Fig. 2.9a). Water depths deeper than 3000 m harbor more then 50% of the global benthic biomass due to their vast area (covering > 75% of seafloor). The predictions were also high at high latitudes (> 60˚N or S) and the tropical ocean (< 23.5˚N or S) of the northern and southern hemisphere, in which the biomass

contributed 25.4% and 28.8% of the global integral on 13.4% and 40.7% of the ocean area, respectively (Fig. 2.9b). As a rule of thumb, the total biomass of all size classes (except for bacteria) dissipates along the continental margins to the abyssal plains (Fig. 2.2) but this is accompanied by a major shift in size classes in the predictions, with the biomass composition changing from metazoan dominated (meiofauna + macrofauna) for the first couple hundred-meter zonal integrals to bacteria dominated on the abyssal plain (Fig. 2.9a). Along the latitudinal zonal integrals, the biomass composition also shifted from the majority of large-size macrofauna at high latitudes to the small-size meiofauna and bacteria dominated at the tropics (Fig. 2.9b).

Regional variability among the major ocean basin is apparent when predicted biomass was plotted against depth (Fig. 2.10). Generally, the declining trends of biomass with depth were similar but the overall levels differed by basin, with the predictions bounded between the higher end of the Southern Ocean and the lower end of the Mediterranean Sea (Fig. 2.10h). In the Atlantic and Arctic Ocean, high density at bathyal depths near the upper end of the biomass–depth distribution (Fig. 2.10a, e) appeared responsible for elevated biomass levels above the Pacific, Indian Ocean, and Gulf of Mexico (Fig. 2.10). These high values corresponded to the high biomass predictions in the North Atlantic to Arctic Ocean (Fig. 2.7) under the productive subpolar gyre north of the Gulf Stream (Williams & Follows 2003). The high density at the bottom of the biomass-depth distribution for the Atlantic and Pacific Oceans (Fig. 2.10a, b) illustrates the low predicted biomass on the vast abyssal plains. In the Indian Ocean, the extraordinary high predicted values between ~1200 to 3000-m water depths (Fig. 2.10c) single out the

Oman and Pakistan Margin, where the benthic biomass between 1.3 and 2.5 g C per square meter is as high as continental shelf values (Fig. 2.7, orange color). We believe that the high predictions derive mainly from the monsoon dynamics and seasonal fluctuation of export POC flux (Pfannkuche & Lochte 2000) rather than the mid-water Oxygen Minimum Zones (OMZ), because resolution of our bottom oxygen data (Table 2.1) is probably not sufficient to detect OMZ influences. At hadal depths (>6000 m), the biomass predictions were meager in general (< 0.2 g C m^{-2}, Fig. 2.10a, b); however, relatively high values (0.5~0.7 g C m^{-2}) were predicted near the Kurile-Kamchatka Trench of the Northwest Pacific Basin (Fig. 2.10b) and the South Sandwich Trench near the southern tip of the South America and Antarctic Peninsula (Fig. 2.10d).

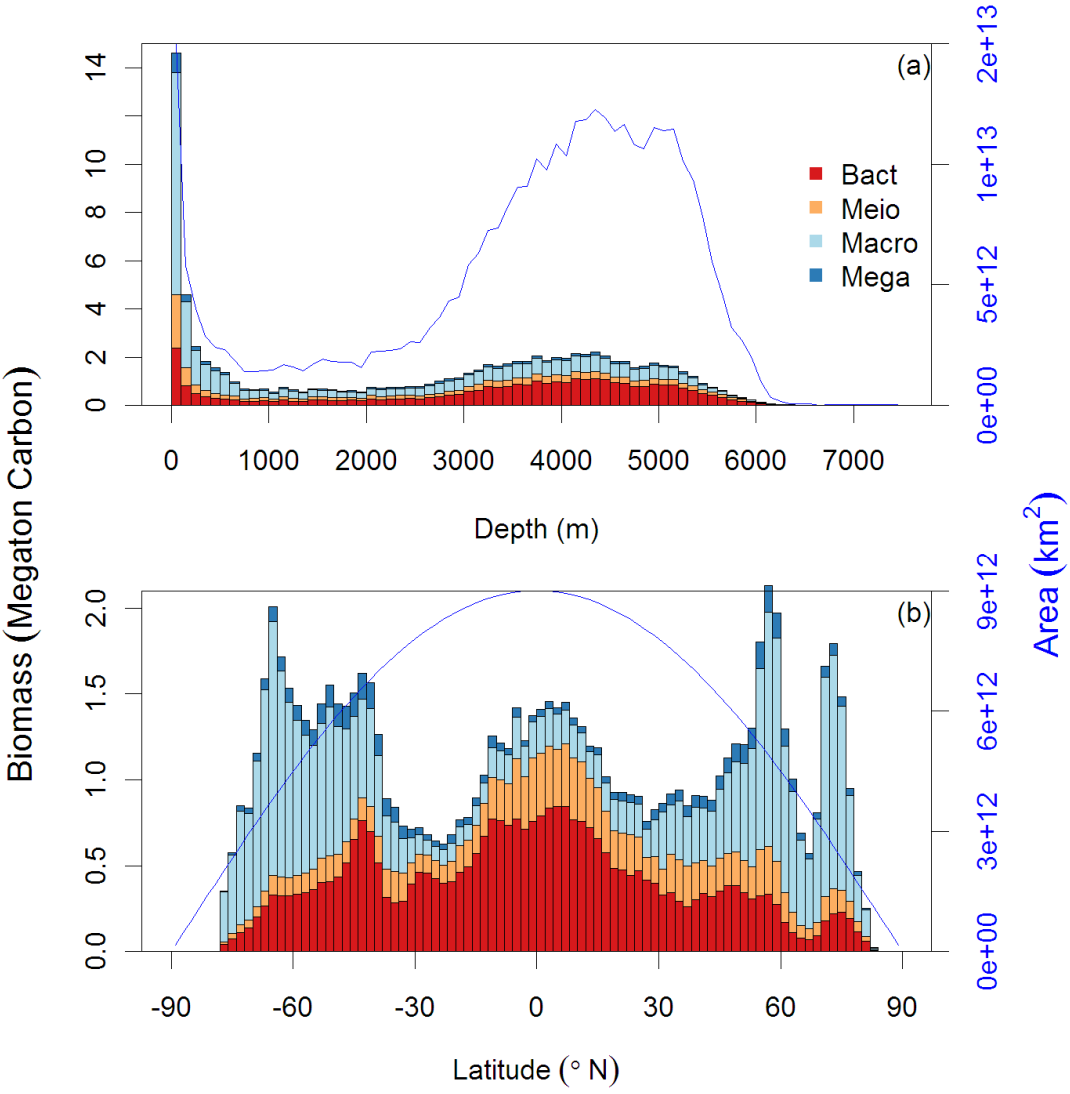

Fig. 2.9. Global zonal integrals of benthic biomass (bars) in unit of megaton carbon based on 100-m bins (a) and 2-latitude-degree bins (b). The blue line shows integrals of seafloor area in unit of square kilometer. Color legends indicate 4 major size classes.

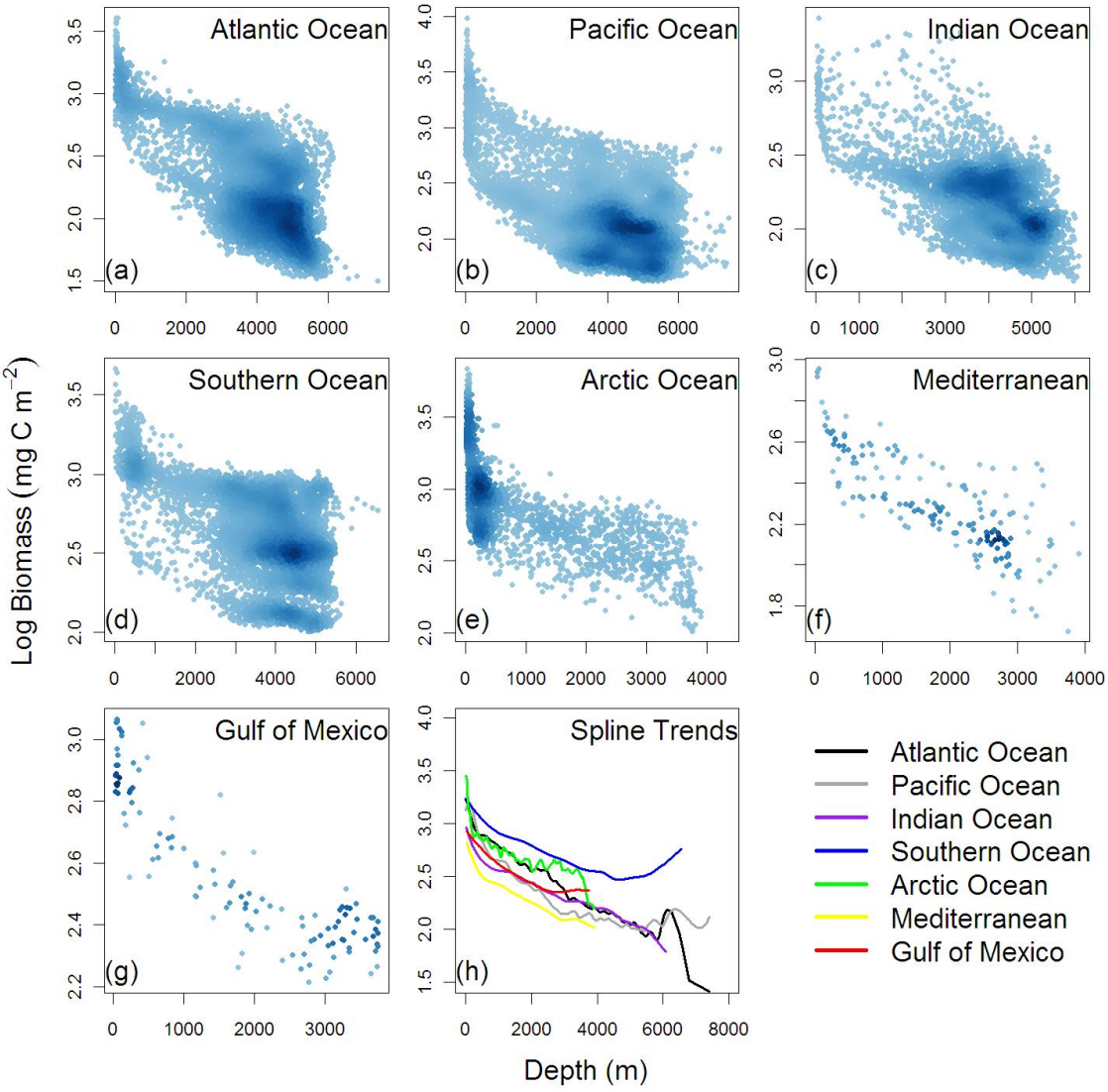

Fig. 2.10. Seafloor biomass predictions against depths for major ocean basins. (a) Atlantic Ocean; (b) Pacific Ocean; (c) Indian Ocean; (d) Southern Ocean; (e) Arctic Ocean; (f) Mediterranean Sea; and (g) Gulf of Mexico. Blue color gradient indicates kernel density estimates. Panel (h) shows the regional predicted trends based on smoothing spline function. Color legend indicates the spline trends for each basin.

2.5. Discussion

2.5.1. Observed and predicted patterns

In this study, classic log-linear declines of seafloor biomass and abundance with depth were demonstrated for meiofauna, macrofauna, and megafauna (Rowe 1983, Soltwedel 2000, Rex et al. 2006). These widely recognized patterns have been attributed to the decreasing quantity and quality of sinking phytodetritus with increasing depth and distance from the productive coastal waters and river runoff (Rowe 1983, Gage & Tyler 1991). Although the selection pressure (food limitation) may be the same, responses differed among the size groups along the depth gradients, showing disparate rates of declining biomass and shifts of biomass hierarchy from macrofauna domination on the shelves and upper slope to meiofauna and bacteria domination on the abyssal plains (Rowe et al. 1991, Heip et al. 2001, Rex et al. 2006, Rowe et al. 2008b). Fig. 2.4 suggests that these observed biomass patterns among size groups are governed by the rate of declining average body size rather than by the rate of declining abundance with depth. The decrease of animal size in the deep-sea has been explained by energy constraints and the need to maintain viable density for successful reproduction (Thiel 1975, Rex et al. 2006). Recent evidence from terrestrial environments also suggests a potential link between the animal body size and food quality (Ho et al. 2010). It has been suggested that the macrofauna may compete for fresh settled phytodetritus with bacteria (Witte et al. 2003, Sweetman & Witte 2008, van Nugteren et al. 2009, Rowe & Deming In Press), while the meiofauna may prefer bacterial carbon over phytodetitus (Ingels et al. 2010). Hence, the rapid decline of macrofaual average size with depth could be related

to the exponential decrease of sinking detrital carbon or the refractory organic matter in the deep-sea sediments. The meiofauna, on the contrary, may be less affected by the deterioration of the food influx and experienced a relatively gradual decline of average size with depth; however, the actual causes of this discrepancy in size-structure remain unclear.

Interestingly, our predicted biomass not only has captured the shifts of dominant size groups with depth but also with latitude (Fig. 2.9), supporting the dominance of macrofaunal biomass (Clough et al. 2005, Grebmeier et al. 2006) and meager importance of bacteria at the high latitudes (Rowe et al. 1997) due, potentially, to strong benthic-pelagic coupling, short food chain, and weaker microbial loop in the overlying water (Grebmeier & Barry 2007, Kirchman et al. 2009). Other intriguing features from our predictions include the apparent increase of bacterial, meiofaunal, and decrease of macrofaunal biomass integrals from high latitudes toward the tropical oceans (Fig. 2.9b). In fact, the increasing bacterial and meiofaunal integrals were a function of the increasing cell areas toward the equator due to the map projection, which in turn makes the decrease of macrofaunal integrals seemingly even more convincing. This cross-latitude comparison however could be biased by a potential interaction with water depth, because the tropical oceans comprise many deep basins and the high latitudes, such as Chukchi/Bering Sea, have extended shelf areas. We tested this by using partial regression to statistically remove the effect of water depth and longitude. When depth was held constant, macrofaunal biomass could be fitted to a positive parabolic function

of latitude (R^2 =0.17, P <0.001), supporting the elevated macrofaunal biomass at high latitudes (Rowe 1983).

From a global perspective, the results of regressions (Fig. 2.2-2.4) reinforced the weak to no depth-dependency of bacterial standing stocks (Deming & Baross 1993, Dixon & Turley 2000, Rex et al. 2006). Despite immense variation in declining POC flux at depth, the surface sediments supported a remarkably constant bacterial stock spanning only ~2 orders of magnitude difference worldwide (30 to 2220 mg C m-2 and 1.3x1012 to 1.9x1014 cells m^{-2}, 5th to 95th percentile, n = 525); nonetheless, regional and local studies in our database do indicate dependency of bacterial standing stocks with depth or POC flux (Deming & Yager 1992, Lochte 1992, Deming & Carpenter 2008). The high bacterial stocks at the supposedly depauperate abyssal depths have been attributed to their barophilic adaption (Deming & Colwell 1985, Patching & Eardly 1997). As bacteria are transported with phytoditrital aggregates to the deep sea (Lochte & Turley 1988), a large number of the bacteria could be dormant or inactive because of the extreme pressure and frigid temperature (Deming & Baross 2000, Quéric et al. 2004), while the active microbes are supported by carbon deposition flux (Witte et al. 2003), viral lysis of the infected prokaryotes (Danovaro et al. 2008), extracellular enzymatic activities (Boetius & Lochte 1994, Vetter et al. 1998), and benthic metazoan sloppy feeding (Rowe & Deming In Press). It is worth noting that many studies have applied a uniformed conversion factor to estimate the biomass from bacterial numbers, which may be the main reason that no statistical relationship was detected between the bacterial cell size and water depth (Fig. 2.4). Based on direct measurements of the cell volume over a

wide range of water depths in the northern Gulf of Mexico, Deming and Carpenter (Deming & Carpenter 2008) concluded that the greater ocean depths generally harbored smaller bacterial cells despite the abundance remaining constant. That is, the constancy of bacterial biomass with depth that we observed here could be an artifact because the cell volumes were not measured directly at all depths. To our surprise, even though no depth-dependency was evident for the bacterial standing stocks, the RF algorithm performed well in predicting the bacterial biomass (R^2 = 79 ± 0.6%) and abundance (R^2 = 81 ± 1.2%, mean ± S.D, n=4). High predictor importance of sea surface temperature (sst), irradiance (par), mixed layer depth (mld), and carbon-based primary production model (cbpm) support the idea that the sedimentary bacterial biomass may be imported in the form of sinking particles (Deming & Colwell 1985, Lochte & Turley 1988). The high bacterial biomass predictions on the abyssal plains of semi-enclosed basins, such as the Gulf of Mexico, Arabian Sea, and East Mediterranean (Appendix A Fig. S5a), supported potential lateral advection of detritus from the margins due to relatively large area of shelves and margins compared to basin volume (Deming & Carpenter 2008).

2.5.2. Anomalies not explained by random forests

Although multiple predictors were obtained to cover as many aspects and processes that could affect the distribution of benthic standing stocks, around 19% to 36% of observed variances are still unexplainable in the current RF models. Some important predictors, such as sediment grain size (Flach et al. 2002), organic composition (Danovaro et al. 1995), bioturbation (Smith 1992, Clough & Ambrose 1997), and community oxygen demand (Smith & Hinga 1983, Rowe et al. 2008a), were not included due to sparse data

availability; others such as oxygen minimums (Levin et al. 2000, Quiroga et al. 2005) or abrupt changes in thermal dynamic regimes (Narayanaswamy et al. 2010), could also be left undetected due to the coarse resolution in available hydrographic data. Nevertheless, the largest unexplained variability was probably derived from our non-contemporaneous predictors that do not account for the seasonal or inter-annual changes of benthic standing stocks as a result of climate-induced variations on productivity and export POC flux (Smith et al. 2009, Billett et al. 2010). The seafloor organisms depend on diverse sources of energy (Rowe & Staresinic 1979), including large food falls (Smith et al. 1998), hydrocarbons from cold seeps and hydrothermal vents (Brooks & Kennicutt 1987, Van Dover 2000), lateral resource advection from continental margins (Rowe et al. 1994), accumulation of organic matter in submarine canyons (Rowe et al. 1982) and trenches (Danovaro et al. 2002), and rapid energy transfers on seamounts (Boehlert & Genin 1987). In addition, benthic foraminifera, sometimes accounting for more than 50% of eukaryote biomass (Gooday et al. 1992), are not included in our datasets. These anomalies are not in the scope of this analysis and should be estimated separately elsewhere in a global context. For example, at the head of the New Zealand's Kaikoura Canyon (data not in the database), the extremely high macrofauna and megafauna biomass (89 g C m^{-2}) was about 100-fold more than our total biomass prediction (0.94 g C m^{-2}) (De Leo et al. 2010). Within the datasets, extraordinary high "total biomass" was also reported at the head of the Mississippi Submarine Canyon (Rowe et al. 2008b) due to dominance of a "carpet of worms" (Soliman & Wicksten 2007). The observed biomass was still more than 4-fold higher than our prediction. This is partially because

the Gulf of Mexico basin had very high background bacterial biomass (Deming & Carpenter 2008). When the bacteria component is removed, the prediction still under estimates the observed biomass by about 50%. Hence, the total living carbon prediction in this study (Fig. 2.7) should be considered as a conservative estimate for the soft bottom communities solely reling on sinking phytodetritus, with the anomalies causing the observed biomass to deviate from this baseline (Fig. 2.5b).

2.5.3. Predictor importance

We tested the RF algorithm using only the primary productivity predictors (decadal mean and S.D. of chl, sst, par, bbp, mld, growth, carbon, vgpm, and cbpm) and depth (Table 2.1). We found that the reduced models only experienced modest deterioration in performance (R2reduced = 75% - 80.3% for biomass of 3 small size classes and R2reduced = 63% for megafauna biomass; R2reduced = 76.3% - 80.6% for abundance of 4 major size classes), suggesting that these productivity/depth predictors alone can explain much of the observed stock variances. It is also evident that these satellite-based ocean color parameters and depth are among the most important predictors when the full RF models were constructed (Fig. 2.6). Their importance was even greater than the model estimates of export phytodetritus flux (det.c.flx & det.n.flx, Table 2.1) that have been considered important for benthic communities (Lochte & Turley 1988, Smith et al. 1997, Witte et al. 2003, Wei et al. 2010). One possibility is that not all export flux is utilized by the benthos (Rowe et al. 2008b) and the combination of productivity/depth predictors simply explain the stock variances better; however, the spurious correlations between these predictors could also make them all rank highly important. Strobl et al.

(Strobl et al. 2008) recommended "Conditional Permutation" while calculating the variable importance to reduce the effect of spurious correlations. We did not attempt this analysis because our focus was on prediction rather than pinpointing the exact contribution of each predictor.

2.5.4. Conclusions

The fate of sinking phytodetritus flux to the ocean floor and the energy transfer to the benthos is a complex biogeochemical process. The combination of mechanistic primary productivity models (Behrenfeld & Falkowski 1997, Westberry et al. 2008) and empirical relationship of export POC flux at depth (Pace et al. 1987) may not properly reflect the actual benthic food influx and consumption. In this study, we demonstrated that the combination of multivariate predictors and machine-learning algorithm was superior to conventional regression models using only water depth or export POC flux to predict benthic standing stocks (Rex et al. 2006, Johnson et al. 2007). Conceptually, the RF predicted biomass presented here (Fig. 2.7) can be seen as non-linear transformation of the surface primary production through a sophisticated decision network and is thus potentially a more realistic reflection of benthic food supply or utilization. Benthic biomass is essential to understand the dynamic processes of global carbon cycling (Rowe & Pariente 1992) and productivity-diversity relationship in the deep sea (Rex & Etter 2010, Rowe & Wei In preparation). Predictive mapping of this kind can fill the gaps where critical biomass information is lacking, since a true 'census' of global living carbon is expensive and practically impossible. Accurate prediction of benthic biomass can facilitate Ecosystem Based Management (EBM) on socioeconomically important

species (Pikitch et al. 2004). It is also extremely useful for generating and testing large scale hypotheses (e.g. latitudinal and cross-basin comparison) and planning shipboard surveys. Moreover, the reduced RF models mentioned above can be used to perform fine-scale predictions with high resolution ocean color images (5 arc minute grids) and the global relief model (1 arc minute grids, Table 2.1), and potentially reveal more heterogeneous biomass patterns at local scale than the current coarse analysis framework. The ocean color/depth predictors also make it possible to do contemporaneous modeling with recent sampling (SeaWiFS data are only available since 1997) or data collected in the future. This study presents an initial framework for archiving the seafloor standing stock data. More training datasets from diverse environments matched in space and time are urgently needed to improve the model performance and prediction accuracy, and perhaps, in due course, the seafloor standing stocks can be now-casted using the current ocean climate or even forecasted under the future climate scenarios (IPCC 2007 Climate Change 2007).

CHPTER III

STANDING STOCKS AND BODY SIZE OF DEEP-SEA MACROFAUNA: A BASELINE PRIOR TO THE 2010 BP OIL SPILL IN THE NORTHERN GULF OF MEXICO

3.1. Overview

A comprehensive database based on 9 benthic surveys from years 1971 to 2002 was constructed to evaluate the distribution of macrofaunal standing stocks in the deep Gulf of Mexico (GoM) prior to the *Deepwater Horizon* oil spill incident. Predictive models based on high resolution bathymetry and ocean color images were employed to map the stock distribution in the vicinity of spill site and the entire GoM basin because no previous sampling had been conducted at the exact location. The composite dataset for the GoM suggested strong benthic-pelagic coupling, with the stock distribution and animal body size being positive functions of surface productivity and delivery of particulate organic carbon to the seafloor. The variation of animal size with depth, however, was a function of a shift of dominant abundance from large *sensu-stricto* macrofauna to small macrofauna-size meiofauna. At a local scale, high benthic biomass in the N GoM was associated with the enhanced productivity by the nutrient-laden Mississippi River outflows, eddy transport of the river plumes, and upwelling along the Loop Current edges. The apparent biomass enhancement at the Mississippi and De Soto Canyon and deep sediment fan was presumably related to lateral advections of organic carbon from the surrounding continental shelf and slope. Except for the Campeche Bank,

the meager biomass of the Mexican margin may reflect the characteristic low productivity Caribbean water that enters the GoM with the Loop Currents. Benthic biomass in the N GoM was not statistically different between comprehensive surveys in the 1983 to 1985 and 2000 to 2002. The historical stock assessment based 685 core or grab sampling from 188 locations provide an important baseline of the sediment-dwelling fauna that may be under immediate or long-term impacts of the oil spill.

3.2. Introduction

3.2.1. BP *Deepwater Horizon* oil spill

On April 20, 2010, a giant bubble of methane gas erupted ~1,500 m below the sea surface from the Macondo well (Mississippi Canyon Block 252 or MC252), triggered massive explosions at the British Petroleum (BP) *Deepwater Horizon* Platform. A series of efforts to shut off the leaking well failed, and crude oil gushed from the seafloor for 85 consecutive days, releasing 4.4 ± 20% million barrels of oil, causing the largest oil spill in US history (Crone & Tolstoy 2010). Owing to the extreme depths of leakage, only ~25% of oil was recovered from the wellhead or burned/skimmed at the surface. The remaining ~75% of oil evaporated, was degraded naturally through microbial oxidation with the aid of chemical dispersants, formed aggregates with suspended sediments and sank to the seabed or entered bays and estuaries (Lehr et al. 2010). Studies showed that the spill oil entered the marine food web (Graham et al. 2010, Hazen et al. 2010, Valentine et al. 2010) and eventually may affect the benthic community when the assimilated oil carbon sank to the seafloor (Joye & MacDonald

2010). The sessile benthic community could be at further risks due to bottom hypoxia induced by the excessive microbial methane oxidation (Adcroft et al. 2010, Kessler et al. 2011), as well as the application >2 million gallons of chemical dispersants around the wellhead and at the surface with unknown toxicity consequences to the aquatic life (Judson et al. 2010, Kujawinski et al. 2011).

3.2.2. Implication of BP spill to deep-sea macrobenthos

Benthic infauna such as spionid and capitellid polychaetes and ampeliscid amphipods have been studied extensively as bio-indicator due to their resilience or sensitivity to oil contamination (Gesteira & Dauvin 2000, Dean 2008). For example, a dense mat of tube-dwelling amphipod species (>12,000 individuals m-2), *Ampelisca Mississppiana*, was discovered at ~500-m depth of the Mississippi Canyon head prior to the BP spill (Soliman & Wicksten 2007). Their tissues showed preferential bioaccumulation of polycyclic aromatic hydrocarbons (PAHs), presumably related to drilling activities in the N GoM and the advection of contaminated organic matters to the submarine canyon (Soliman & Wade 2008). High macrofaunal density can also be found within the NW Arabian Sea and SE Pacific oxygen minimum zone (OMZ), where shifts of species composition and biomass-size spectra were documented (Levin et al. 2000, Quiroga et al. 2005). Although some macrobenthos have substantial tolerance to hydrocarbons and low oxygen, environmental disasters of this magnitude are almost unprecedented. Based on previous studies in shallow water and estuaries, the standing stocks of benthic macrobenthos may decline immediately after initial oil spill impact (Grassle et al. 1981,

Gesteira & Dauvin 2000). The recovery of the sub-tidal community is expected to be slower than the exposed shores, because the habitat has been contaminated by sedimentation of oil-polluted particles with no practical clean up strategies (Kingston 2002). At ~1,500 m near the wreckage of *Deepwater Horizon*, frigid temperature (4˚C) and lack of sunlight do little to help degrading oil in the sediments; hence, the recovery could be long. The worst case scenario could be the subsurface mixture of oil and dispersant plumes being trapped in deepwater for prolonged periods of time, thus harming the seafloor community (Adcroft et al. 2010, Camilli et al. 2010, Kujawinski et al. 2011).

3.2.3. Standing stock pattern in general and in the N Gulf of Mexico

Generally, standing stocks of macrofauna decline exponentially with depth due to deteriorating quantity and quality of photosynthetic carbon that sinks to the seafloor (Rowe 1983, Rex et al. 2006, Wei et al. 2010b). The overall level of stocks varies among continental margins, depending on surface production, width of the continental shelf, latitude, and terrestrial runoff (Rowe 1983, Gage & Tyler 1991). Moreover, the macrofaunal standing stocks have been considered as a surrogate for benthic food supplies arriving on the seafloor (Smith et al. 1997, Johnson et al. 2007). *In-situ* experiments suggest that the macrobenthos can rapidly respond to the pulse of phytodetritus to the seabed (Witte et al. 2003, Sweetman & Witte 2008). It has been suggested that the ability of direct movement and structuring sediments may benefit metazoans for seizing the limited resources over the bacteria (Rowe & Deming In Press).

In the N GoM, the surface production and the flux of carbon to the benthic environment were estimated to be higher in the northeast than in the northwest basin due to higher surface primary production (Biggs et al. 2008). Furthermore, the Mississippi Submarine Canyon is an active conduit of organic matter between the productive continental shelf receiving major riverine inputs (e.g. the Mississippi River) and the sediment fan adjacent to the nutrient-poor abyssal plain at the middle of the GoM basin (Bianchi et al. 2006, Santschi & Rowe 2008). The slope of NW GoM is also known for its complex physiography (Bryant et al. 1991), where numerous salt diapirs and small basins may work as funnels to trap organic materials. These intriguing productivity regimes may affect or limit the distribution and standing stocks of deep-sea macrobenthos. The earliest quantitative macrofaunal sampling in the GoM began in the 70's (Rowe & Menzel 1971, Rowe et al. 1974). These studies suggested that the standing stocks of macrobenthos were depauperate compared to the NW Atlantic due to low surface productivity associated with the Caribbean offshore water. The paucity has also been explained by a faster turnover of living organic carbon in the warmer deepwater in the GoM (4°C vs. 2˚C in the Atlantic). In the 80s', Pequegnat et al. (1990) sampled three transects on the continental slope of the N GoM and discovered a seasonal pattern in the macrofaunal abundance. They also found that the abundance along the central transect was higher than the west and east transects. The unexpected high abundance in the deepwater of the central transect was attributed to the influence of natural hydrocarbon seeps in the vicinity.

3.2.4. Census of marine life efforts and study objectives

Given the mounting challenges of climate change and anthropogenic impacts on marine ecosystems, the Census of Marine Life (CoML) was launched in 2000 to document the global baseline on marine biodiversity (McIntyre 2010, Snelgrove 2010). A Census affiliated field project, the Deep Gulf of Mexico Benthos (DGoMB) program, sponsored by the Mineral Management Service (MMS), now the Bureau of Ocean Energy Management, Regulation and Enforcement (BOEMRE) of US Department of Interior, began a 3-year deep-sea survey to understand the structure and function of benthic communities prior to ultra-deepwater drilling in N GoM (Rowe & Kennicutt 2008). In this analysis, we will focus on the DGoMB data to examine macrofaunal standing stocks among major oceanic features in the N GoM with contrasting productivity regimes. The standing stocks were also compared with the historical data in the N GoM and information from the S GoM. The goal is to provide a comprehensive ecological baseline for future assessment of the BP oil spill impacts. Since no previous sediment samples had been taken at the spill site (MC252), the macrofaunal standing stocks were re-constructed using predictive models based on bathymetry and remote-sensed ocean color images. Similar modeling has been utilized by the CoML Fresh Biomass Synthesis to predict global seafloor biomass with encouraging accuracy (Wei et al. 2010b).

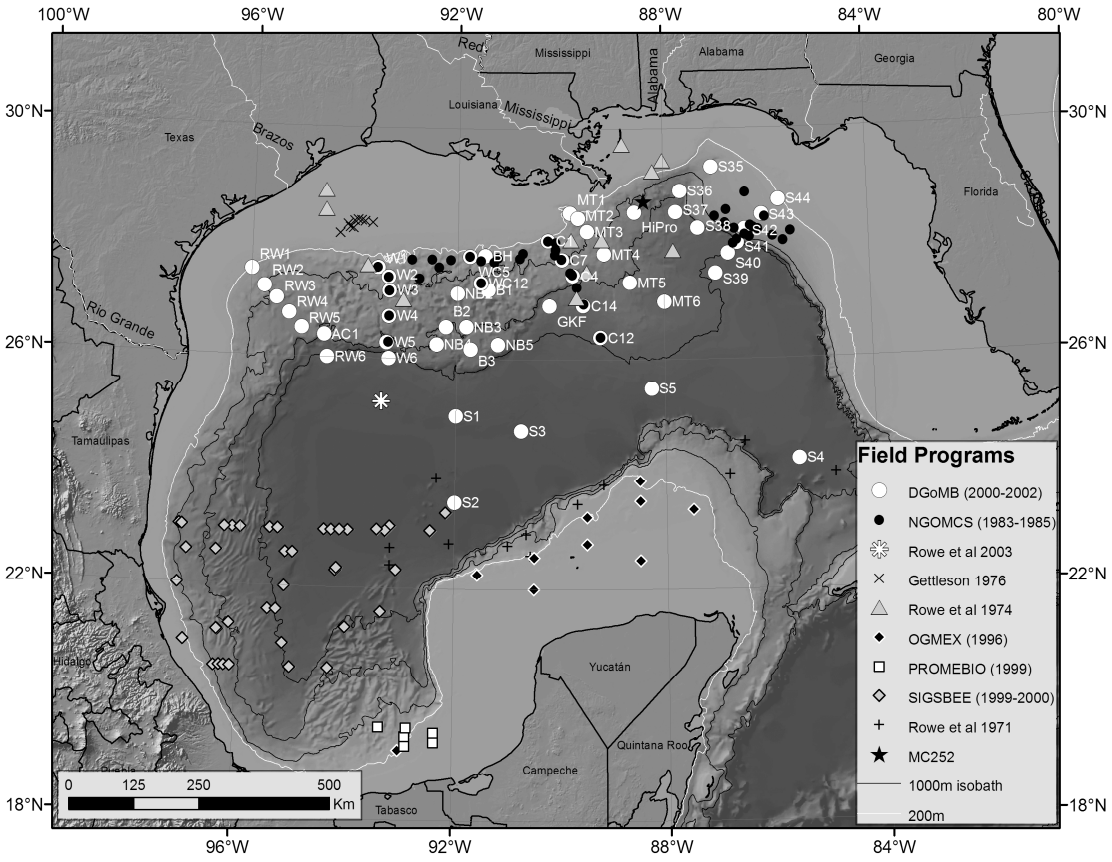

Fig. 3.1. Locations of quantitative deep-sea macrofauna sampling in the Gulf of Mexico. The white line indicates depth of 200m. The black lines indicate 1,000m isobaths. The station names show the DGoMB sampling. The star symbol indicates the location of the *Deepwater Horizon* oil platform.

3.3. Materials and Methods

3.3.1. Northern Gulf of Mexico (GoM) sampling

During the Deep Gulf of Mexico Benthos (DGoMB) field work (years 2000 to 2002, Rowe & Kennicutt 2008, Rowe & Kennicutt 2009), benthic macrofauna were sampled using a 0.2-m^2 version of the GoMEX box corer (Boland & Rowe 1991). A total of 51 locations (Fig. 3.1, Table S3.1) was sampled from which the distribution of macrofauna standing stocks and mean size along the continental slope and abyssal plain were determined (from 213 m to 3,732 m). At least 5 box cores were deployed at each location and overall 271 box cores were collected for a total sampled area of 54 m^2. Standard sample processing procedures for deep-sea benthos were used on board and in the laboratory (detailed descriptions can be found in Wei et al. 2010a). Density was estimated from specimens retained in the 300-μm sieve. Macrofauna *sensu-stricto* density (excluding large size meiofauna such as nematodes, copepods, and ostracodes) was also estimated (Gage et al. 2002). At selected slope sites (C7, MT1, MT3, MT6, S36, and S42), bio-volume of each specimen was measured using an ocular micrometer from 3 sub-cores (12.4 cm diameter) with appropriate geometric formulae. The volume was converted to wet weight using seawater density of 1.1 (mg/mm^3). Organic carbon weights were calculated from preserved wet weights based on conversion factors for each taxonomic group (Rowe 1983). Total biomass at each location was estimated by summation of density multiplying by the mean weight for each taxon (Table S3.2).

Northern Gulf of Mexico Continental Slope (NGoMCS) Study (years 1983 to 1985, Gallaway 1988, Pequegnat et al. 1990) used a 0.06-m² version of the GoMEX box corer. Animal density was estimated using the same sampling procedure (e.g. 300-μm sieve) for 45 sites based on 324 core replications from 298 to 2,951-m depth (Fig. 3.1, Table S3.3). Macrofaunal body size was not measured directly during NGoMCS; therefore, the biomass was estimated by multiplying the abundance with mean weight of major taxonomic groups from the DGoMB sampling (Table S3.2). Additional historical data on the Texas and Louisiana continental shelf and slope (Rowe et al. 1974, Gettleson 1976) and Sigsbee Abyssal Plain (Rowe et al. 2003) were listed in the supporting information (Fig. 3.1, Table S3.4). Except for a slightly smaller sieve size (250μm), Rowe et al. (2003) used the same GOMEX box corer and sampling procedures as the DGoMB study. The data from Rowe et al. (1974) and Gettleson (1976) were not included in the analyses due to gear (0.2-m^2 version of the van Veen grab) and sieve size (420 to 500 μm) difference. The preserved wet weights of the whole macrofauna community in Rowe et al. (1974) and Gettleson (1976) were multiplied by a conversion factor of 0.043 to estimate organic carbon weights (Rowe 1983).

3.3.2. Southern Gulf of Mexico (GoM) Sampling

Macrofaunal data of the S GoM were provided by Universidad Nacional Autónoma de México (UNM) for comparison. A total of 56 stations from 38 m to 3,795-m depth were sampled in the 1996 to 2000 during the Oceanografía del Golfo de México (OGMEX, Escobar-Briones & Soto 1997), Procesos Oceánicos y Mecanismos de Producción

Biológica en el sur del Golfo de México (PROMEBIO, Escobar-Briones et al. 2008a), and SIGSBEE Cruises (Escobar-Briones et al. 2008b). The infauna specimens were collected using a 0.2-m^2 Smith McIntyre Grab (OGMEX), 0.16-m^2 USNEL box corer (PROMEBIO), and 0.25-m^2 USNEL box corer (SIGSBEE) with a 250-µm sieve based on standard sampling procedures for deep-sea benthos (Fig. 3.1, Table S3.4). Preserved wet weights were measured directly on a microbalance after sorting to major taxa. Historical data of the S GoM (Rowe & Menzel 1971) were collected with an anchor dredge, counted, weighed wet, dried in the laboratory, and analyzed for organic carbon contents using an elemental analyzer. These data were provided in the supporting information but not included in the analyses (Fig. 3.1, Table S3.4).

3.3.3. Hypothesis testing and statistical analyses

During the DGoMB study, a total of 7 depth transects was sampled across the continental margin of the N GoM (Fig. 3.1, Table S3.1) including: Far West Slope (RW Transect): Stations RW1 to RW6 and Station AC1; West Slope (W Transect): Stations W1 to W6; West Central Slope (WC Transect): Stations WC5, WC12, NB2 to NB5, and BH; Central Slope (C Transect): Stations C1, C7, C4, C14, and C12; Mississippi Canyon (MT Transect): Stations MT1 to MT6; De Soto Canyon (DS Transect): Stations S35 to S38; and Florida Slope (FL Transect): Stations S44 to S39. In year 2002, part of the slope sites were revisited and additional 5 sites were sampled on the Sigsbee (Stations S1, S2 S3 and S5) and Florida Abyssal Plains (Station S4).

Macrofaunal standing stocks were contrasted between the active Mississippi Canyon (MT Transect) and adjacent continental slope (C, WC, W, and RW Transects; Null Hypothesis 1), between the inactive De Soto Canyon (DS Transect) and adjacent FL Slope Transect (Null Hypothesis 2), and between the FL Transect cutting through the steep Florida Escarpment and the RW & W Transect across the relatively gradual Sigsbee Escarpment (Null Hypothesis 3). In addition, macrofauna sampled within the continental slope basins (B stations) were compared with the adjacent non-basin slope (NB stations; Null Hypothesis 4).

Macrofaunal standing stocks were standardized to individual and milligram organic carbon per square meter and then log transformed (Log_{10}) to approximate normality and equal variance assumption before analyses. We used analysis of covariance (ANCOVA) to compare the slope and elevation of regression lines (depth as functions of standing stocks) among transects and to remove unexplained variability associated with sampling depths (covariate). When the regression slopes were homogeneous, the elevations of regression lines were compared using Tukey's Honest Significance Difference (HSD) test (Zar 1984). When the slopes were heterogeneous (significant interaction between treatment and covariate), Tukey's HSD test was applied to identify which pairs of transects having significantly different regression slopes (Zar 1984). These transect pairs were compared using Johnson-Neyman (J-N) test (Huitema 1980) to pinpoint the specific depth ranges where the regression elevations were not significantly different. The depths outside of the non-significant ranges (based on the J-N test) and overlapped between the transect pairs (with heterogeneous regression slopes) were reported.

In addition, ANCOVA was also conducted to test that macrofaunal standing stocks were not different between the current DGoMB and historical NGoMCS (Gallaway 1988, Pequegnat et al. 1990) sampling (Null Hypothesis 5). In selected transects (C stations, Stations W1 to W5, Stations WC5 and WC12), the DGoMB study repeated the historical NGoMCS sampling (Fig. 3.1). Three sites on the FL Transect, Stations S41 to S43, were also sampled in the proximity of historical NGoMCS sites (~7.1 to 10.5 km apart). Hence, the Null Hypothesis 5 was also tested using randomized complete block (RCB) analysis of variance (ANOVA), with the blocking factor being the sampling sites along the selected transect. Finally, the macrofaunal standing stocks in the N GoM (DGoMB + NGoMCS) were compared with the data from the S GoM basin (Null Hypothesis 6).

Table 3.1. Environmental data for Random Forest modeling. The mean value was extracted for standing stock records with catchment area of 3 x 3 or 1 x 1 cells. The table abbreviations follow: Res = data resolution (arcminute), Cell = cell size for data extraction, Abb = variable abbreviation.

Data Type	Res	Cell	Abb	Variable	Unit
Ocean Color Image: (decadal mean & SD of monthly data from Jan 1998 to Dec 2007)	5	3x3	chl	Chlorophyll a concentration	mg m^{-3}
	5.3	3x3	sst	Sea Surface Temperature	°C
	5	3x3	par	Photosynthetic radiation	einstein m^{-2} d^{-1}
	5	3x3	bbp	Particulate backscatter	m^{-1}
	10	1x1	mld	Mixed layer depth	m
	5	3x3	growth	Phytoplankton growth rate	divisions d^{-1}
	5	3x3	carbon	Carbon concentration	mg m^{-3}
	5	3x3	vgpm	Chlorophyll based net primary production	mg C m^{-2} d^{-1}
	5	3x3	cbpm	Carbon based net primary production	mg C m^{-2} d^{-1}
Water Depth	1	NA	depth	Water depth	m

3.3.4. Modeling and prediction of macrofaunal standing stocks

Random Forest (RF) models (Breiman 2001) were constructed between macrofaunal standing stocks and environmental predictors. In the RF, the stock records (from core replications) were bootstrap re-sampled and subjected to successive binary divisions. At each split, an optimal value from a random subset of environmental predictors (2/3 of total) was chosen to maximize the stock difference between the divisions. Each tree-like structure from a bootstrap re-sampling (repeat 1,000 trees in this study) was grown fully until no division could be made and then collected as "Random Forests". Similar to a regression model with a mathematical equation, the RF can make predictions if new data are available for each predictor. The outputs from each tree were then averaged as the final prediction. The model fit (R^2) was examined by comparing the predictions with the observations not in the bootstrap selection. The importance of a predictor was evaluated by permuting the predictor values to mimic the absence of that variable during modeling. The increase of prediction error (deterioration of the model) after permutation was used to evaluate the variable importance on making the accurate RF model. Detailed description of the RF algorithm can be found in Wei et al (2010b).

In this study, the predictors used decadal mean and standard deviations of monthly ocean color images measured between years of 1998 and 2007 from the Sea Viewing Wide Field-of-view Sensor (SeaWiFS r2009.1) and Advanced Very High Resolution Radiometer (AVHRR). Net primary production models including Vertical General Production Model (vgpm) and Carbon Based Production Model (cbpm) as well as the

model inputs including chlorophyll concentration, sea surface temperature (sst), photosynthetic available irradiance (par), mixed layer depth (mld), particle backscatter (bbp), phytoplankton growth rate (growth), and carbon concentration (carbon) were obtained from the Ocean Productivity web page, Oregon State University (Table 3.1). Bathymetry (water depth) was derived from the ETOPO1 global relief model, NOAA Geophysical Data Center. The mean values of ocean color images were extracted based on a box of 3-by-3 or 1-by-1 grid cells to match to the coordinates of box core samples. During the RF modeling, water depth used the original measurements during the core sampling. Part of the environmental predictors (sst, mld, and depth) were re-gridded to 5 arc-minutes before combining with other variables as new data for standing stock prediction. The predictions were made based on the established RF models using the new data matrix with high resolution coverage of the entire Gulf of Mexico. The stock predictions were then classified using Jenks Natural Breaks Optimization to maximize the differences between classes.

Statistical analyses and RF modeling used R 2.11.0 (R Development Core Team 2010) and R package randomForest (Liaw & Wiener 2002). Geostatistical analyses and mapping used ESRI® ArcMapTM 9.2.

3.4. Results

3.4.1. Standing stocks and average size estimates in DGoMB sampling

A total of 147,270 specimens was collected and sorted into 39 macrofaunal taxa during the DGoMB study. Nematodes had the highest total abundance (30.3%) followed by polychaetes (26.2%), amphipods (13.8%), and harpacticoids (6.3%), etc. (Fig 3.2a, Table S3.5). The total density showed a significantly negative log-linear relationship with depth (Fig 3.3a, $\log_{10}$ density = 3.97 - 0.23 *depth, $R^2 = 0.56$, $F_{1, 49} = 63.38$, $P < 0.001$). The head of Mississppi Canyon (Station MT1, Fig. 3.1) had the highest density (Table 3.2, 21,801 ± 7,659 individuals m^{-2}, mean ± s.d., n = 10). The second highest density (~11,000 individuals m^{-2}) occurred in the upper Desoto Canyon (Stations S35 and S36). The next level of animal density (~7,000 to 9,000 individuals m^{-2}) was found in the upper Mississippi Canyon (Stations MT2 and MT3) and upper slope (Stations RW1, W1, and S43). Surprisingly, the deepest site on the Mississippi Sediment Fan (Station S5 at 3,314-m depth) had one of the highest animal densities (7,075 ± 217 individuals m^{-2}, n = 2). All other abyssal sites at similar depths (Stations S1 to S4 at 3,409 to 3,732-m depth) only had ~800 to 1,600 individuals m^{-2}, suggesting a 4 to 8-fold enrichment of animal density at Station S5.

When the macrofauna-size meiofauna taxa (copepods, nematodes, and ostracodes) were removed from the macrofauna *sensu-stricto*, the animal density declined more rapidly with depth and the linear model fits were improved (Figure 3.3b, $\log_{10}$ density =3.83 - 0.32 *depth, $R^2 = 0.74$, $F_{1, 49} = 140.4$, $P < 0.001$). The hierarchy of animal density

among sites showed an apparent shift. The head of the Mississippi Canyon (Station MT1, Fig. 3.1) still had the greatest density (Table 3.2, 21,633 ± 7,903 individuals m^{-2}, mean ± s.d., n = 10). The second highest densities were only ~6,000 individuals m^{-2} at the upper Mississippi Canyon (Station MT2) and the shelf break of the far-west slope (Station RW1). The next level of 5,000 or so individuals m^{-2} occurred at the head of Desoto Canyon (Station S35) or the shelf break of the Texas (Station W1) and Florida Slope (Station S44). Despite its mid-slope depth (1,572 m), the Station HiPro had a surprisingly high density (5,076 ± 1,279 individuals m-2, n = 5) southeast of the mouth of the Mississippi River. After removing the large sized meiofauna, the animal density on the deep Mississippi Sediment Fan (S5) dropped dramatically to only 1,545 ± 438 individuals m^{-2} (n = 2); nonetheless, it was still 3 to 5-fold more abundant than the *sensu-stricto* density at Station S1 to S4 (294 to 516 individuals m^{-2}) on the abyssal plain.

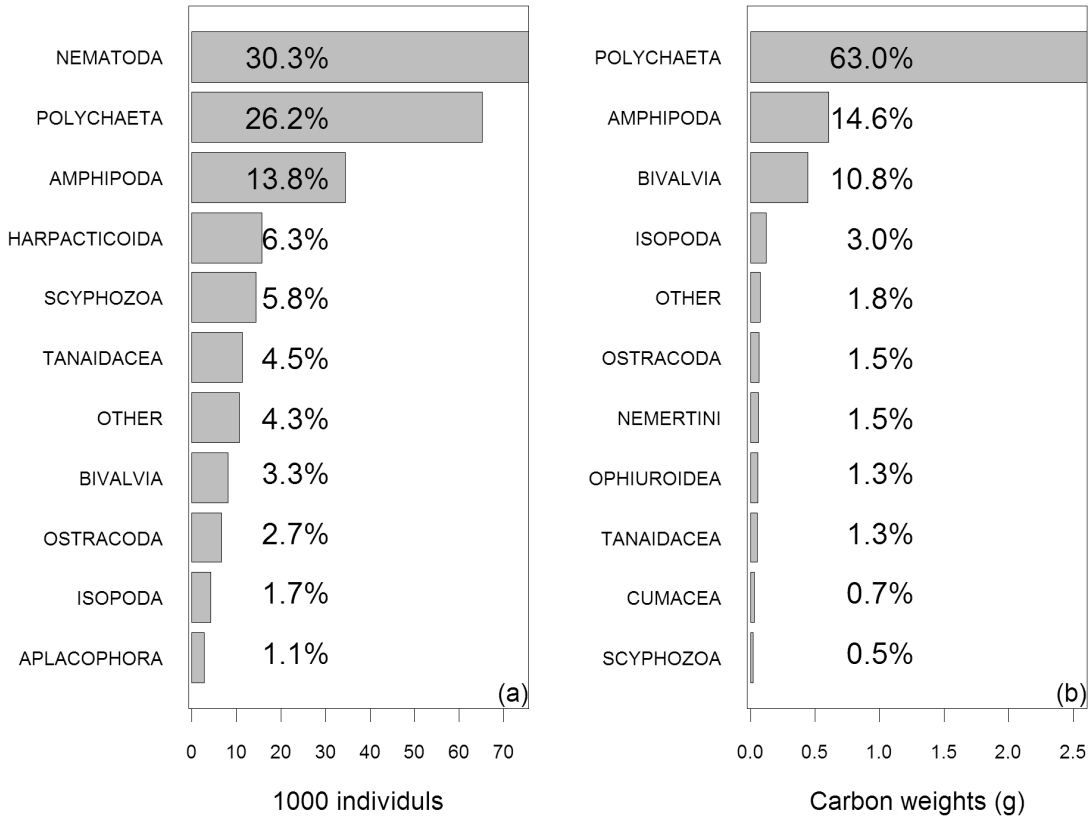

Fig. 3.2. Total macrofauna abundance and organic carbon biomass collected during the DGoMB study. Bar charts show the top-ten macrofaunal taxa with highest (a) abundance and (b) organic carbon weights. The 11th to 39th most abundant taxa were combined as category “OTHER”. Following the bar charts is relative abundance (a) or biomass (b) for each taxon (%).

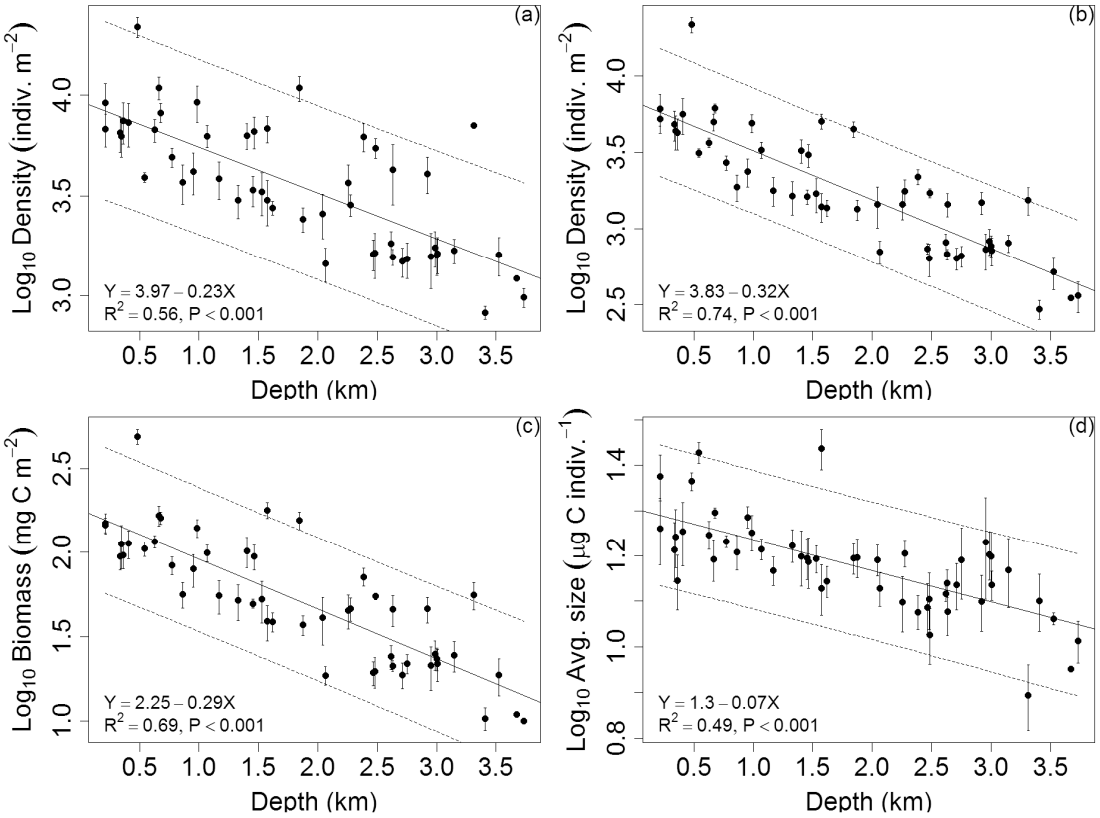

Fig. 3.3. Log10-transformed (a) total density, (b) macrofauna *sensu-stricto* density, (c) organic carbon weight, and (d) average body size as functions of water depth for DGoMB sampling. Linear regressions (solid line) with 95% confidence interval (between dash lines) were conducted on the station averages from 271 core replications. The standard error is shown as error bar.

Table 3.2. Macrofaunal standing stocks and average size for DGoMB sampling. n = number of sample, D = density (individual m^{-2}), Dx = macrofauna *sensu-stricto* density (exclude nematodes, harpacticoids, ostracodes), B = preserved wet weight. (mg m^{-2}), BC = organic carbon weight. (mg C m^{-2}), W = average size (mg $individual^{-1}$), WC = average size (mg C $individual^{-1}$).

Station	n	D	s.d.	Dx	s.d.	B	s.d.	BC	s.d	W	WC
RW1	5	9202	4893	6137	3211	3257.1	728.79	145.7	32.73	0.41	0.018
RW2	5	4183	2196	2370	1087	1807.9	773.01	79.6	39.56	0.45	0.019
RW3	5	3011	1270	1641	906	1116.6	625.22	51.7	27.98	0.36	0.017
RW4	5	3009	1708	1399	660	935.2	526.50	39.1	20.60	0.32	0.013
RW5	5	2754	488	1372	378	900.8	276.63	38.6	11.13	0.32	0.014
RW6	5	1624	752	715	335	513.9	242.83	21.9	10.58	0.32	0.014
W1	5	7332	4030	5626	3334	2504.7	1022.14	112.9	47.43	0.40	0.018
W2	4	6729	1739	3662	542	2600.4	424.87	116.1	19.08	0.40	0.018
W3	5	3690	1810	1883	841	1345.3	525.30	56.3	21.59	0.38	0.016
W4	5	3377	1296	1621	400	1123.3	193.34	49.6	6.63	0.35	0.016
W5	5	1533	688	659	233	496.2	169.37	21.9	6.47	0.35	0.016
W6	5	1682	518	804	233	580.7	225.20	24.5	11.14	0.35	0.015
WC5	5	6248	2946	4382	2435	2419.3	1456.01	112.2	71.83	0.38	0.017
WC12	5	3843	1802	1787	856	1281.6	608.96	55.4	27.89	0.34	0.015
B1	5	3681	1866	1446	664	1040.4	519.53	45.3	23.16	0.29	0.013
B2	5	1566	321	676	125	504.4	70.76	21.2	3.44	0.33	0.014
B3	5	1827	599	814	246	608.1	224.56	24.1	8.71	0.33	0.013
NB2	5	3323	1779	1700	946	1202.7	702.13	52.7	33.04	0.36	0.016
NB3	5	2420	755	1342	454	846.8	254.00	37.1	11.12	0.36	0.016
NB4	5	2582	1452	1443	966	963.2	625.75	41.1	28.78	0.37	0.016
NB5	5	1454	625	706	275	441.5	150.02	18.7	5.35	0.31	0.013
C1	5	6504	2925	4829	2419	2079.9	766.10	94.7	35.63	0.36	0.016
C7	10	6272	2485	3293	1230	2245.7	772.69	99.6	35.64	0.37	0.016
C4	5	6599	2669	3045	1167	2161.5	755.53	94.4	36.00	0.35	0.015
C14	5	5467	1358	1709	255	1275.8	82.92	54.8	5.47	0.25	0.011

Table 3.2. Continued.

Station	n	D	s.d.	Dx	s.d.	B	s.d.	BC	s.d	W	WC
C12	5	4079	1865	1485	550	1091.2	415.28	46.1	17.72	0.30	0.013
MT2	4	8194	1777	6172	828	3643.2	618.64	160.4	26.98	0.45	0.020
MT3	10	9219	6047	4924	2087	3212.2	1239.16	139.5	53.23	0.41	0.018
MT4	5	6317	2070	3262	1252	2228.7	956.84	101.8	46.34	0.35	0.016
MT5	5	2859	783	1763	736	1055.5	358.20	46.2	15.98	0.37	0.016
MT6	9	1485	731	638	315	430.3	208.44	18.8	9.72	0.32	0.014
S35	5	10887	3103	5019	1404	3739.1	1033.66	166.2	51.25	0.35	0.016
S36	12	10859	5302	4481	1808	3488.5	1317.49	155.3	64.73	0.36	0.016
S37	5	6231	2232	2192	532	1611.3	400.43	71.5	19.33	0.27	0.012
S38	5	4268	3184	1445	566	1014.4	473.56	45.8	21.22	0.26	0.012
S44	5	6776	2815	5262	2337	3141.2	901.75	150.0	46.26	0.50	0.024
S43	5	7456	3834	4265	2198	2412.0	904.70	96.6	37.41	0.35	0.014
S42	9	4917	1628	2709	858	1893.8	625.08	83.7	29.80	0.39	0.017
S40	4	1572	968	729	392	504.5	268.70	21.4	12.40	0.43	0.017
S41	8	1744	986	828	461	563.9	309.43	24.9	13.89	0.36	0.016
S39	5	1595	744	769	284	533.9	186.09	23.5	7.95	0.36	0.016
S5	2	7075	217	1545	438	1384.8	343.26	55.7	14.61	0.20	0.008
S4	4	825	124	294	84	248.0	82.15	10.4	3.18	0.30	0.013
S1	2	1612	500	516	173	414.2	140.03	18.7	6.52	0.26	0.012
S3	1	1223	N.A.	348	N.A.	260.2	N.A.	10.9	N.A.	0.21	0.009
S2	2	983	152	362	119	235.0	20.16	10.0	0.05	0.24	0.010
BH	5	3899	477	3143	465	2349.1	430.17	105.3	23.09	0.60	0.027
HiPro	5	6826	2257	5076	1279	3949.4	919.31	178.8	43.02	0.60	0.027
GKF	5	1622	634	737	132	485.5	186.87	19.3	7.01	0.30	0.012
AC1	5	1638	924	637	344	451.0	217.16	19.7	8.98	0.29	0.013

Preserved wet weights and organic carbon weights were estimated by multiplying density (Appendix C Table S4) by the mean weight of each taxon (Appendix C Table S2). Polychaetes contributed more than half (63.0%) of the organic carbon biomass, followed by amphipods (14.6%), bivalves (10.8%), and isopods (3.0%), etc. (Fig. 3.2b, Appendix C Table S6). The carbon biomass-depth trend (Fig. 3.3c) was similar to the trend for the *sensu-stricto* density against depth (Fig. 3.3b). The Mississippi Canyon head (Table 3.2, Station MT1, 492.1 ± 159.88 mg C m^{-2}, mean ± s.d., n = 10) still had the highest biomass; however, the vicinity of Mississippi River mouth (Station HiPro, 178.8 ± 43.02 mg C m^{-2}, n = 5) and the upper De Soto Canyon (Station S35, 166.2 ± 51.25 mg C m^{-2}, n = 5; Station S36, 155.3 ± 64.73 mg C m^{-2}, n = 12) joined the upper Mississippi Canyon (Station MT2, 160.4 ± 26.98 mg C m^{-2}, n = 4) to have the second highest biomass (Fig. 3.3c). The biomass of the deep Mississippi Sediment Fan (Table 3.2, Station S5, 55.7 ± 14.61 mg C m^{-2}, n = 2) was still 3 to 6-fold higher than the other abyssal plain areas (Stations S1 to S4, 10 to 18.7 mg C m^{-2}).

The organic carbon weights (Fig. 3.3c, slope = - 0.29) declined more rapidly with depth than the animal density (Fig. 3.3a, slope = -0.23), indicating that the average animal size (organic carbon weight divided by density) also decline with depth (Figure 3.3d, $\log_{10}$ average size = 1.3 - 0.07 *depth, $R^2 = 0.49$, $F_{1, 49} = 46.81$, $P < 0.001$). Interestingly, the Bush Hill (Station BH) and the vicinity of Mississippi River mouth (Station HiPro) had the largest average animal size (Table 3.2, 27µg C $individual^{-1}$). The greater depth-decay constants for the *sensu-stricto* density (Fig. 3.3b, slope = -0.32) than for the overall density (Fig. 3.3a, slope = -0.23) suggested that the decreasing average size with depth

was associated with increasing numbers of nematodes, harpacticoids, and ostracodes at depths. The relative abundance of large meiofauna (>300μm) increased from 0.6% at the head of the Mississppi Canyon (Station MT1) to about 78.2% on the deep Mississippi Sediment Fan (Station S5) at a rate of about 10% increase every kilometer of depth (Fig. 3.4, percent meiofauna taxa in the sample = 28.75 + 10.36 *depth, $F_{1, 49} = 61.94$, $R^2 = 0.56$, $P < 0.001$). It is also worth noting that at relatively deepwater (1,572 m), Station HiPro, only had about half (23.6%) as much of the large meiofauna as other sites of similar depths (~50%, Fig. 3.4). The organic carbon biomass had higher correlation with the *sensu-stricto* density (Pearson's correlation, $\rho = 0.98$, $t = 84.5$, $df = 269$, $P < 0.001$) than with the overall density ($\rho = 0.94$, $t = 47.1$, $df = 269$, $P < 0.001$). The carbon biomass was less affected by macrofauna *sensu-stricto* because the large meiofauna comprised only ~1.8% of the total biomass.

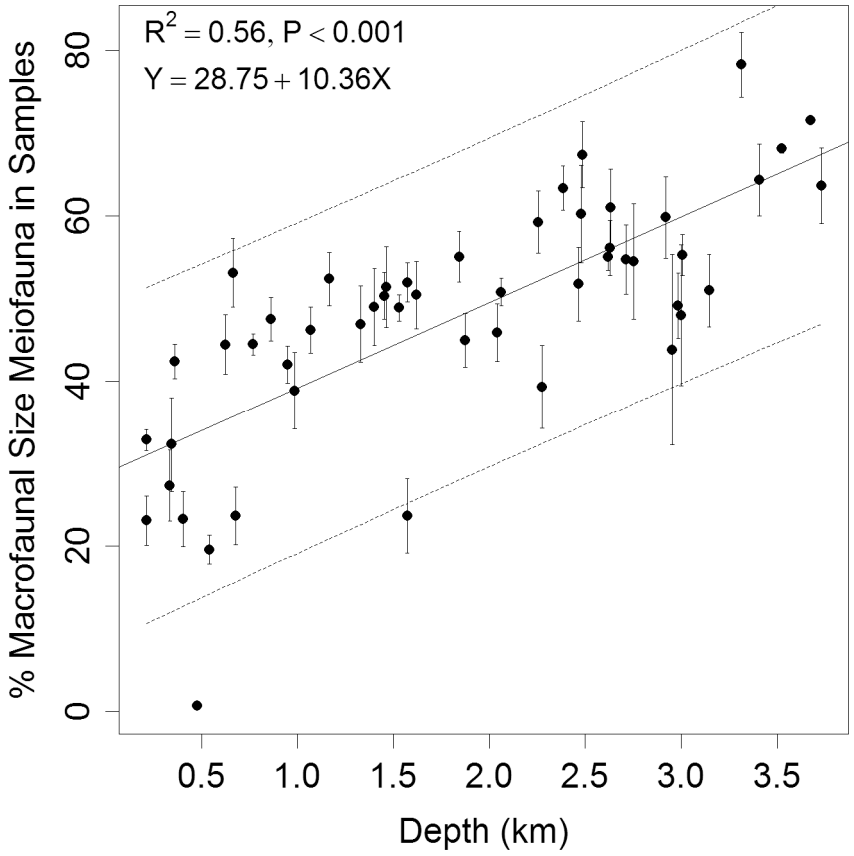

Fig. 3.4. Percent contribution of large meiofauna (>300 μm) in box core sample as a function of water depth (km) during DGoMB sampling. Linear regressions (solid line) with 95% confidence interval (between dash lines) were conducted on the station averages from 271 core replications. The standard error is shown as error bar.

3.4.2. Hypothesis testing

During DGoMB sampling, all 7 transects showed significantly log-linear decline of organic carbon biomass with depth (Table 3.3a). The regression slopes, however, differed significantly among transects (Table 3.3b, ANCOVA, slope, $F_{6, 221} = 15.01$, $P < 0.001$) with the slopes of MT (Mississippi Canyon) and C Transect (central slope) being significantly different from the rest of transects (Table 3.3c, Tukey's HSD test, $P < 0.05$). The MT Transect (Fig. 3.5, gray triangles) has the most rapid declining biomass with depth (slope = -0.57), while the C Transect (open circles) has the slowest decline (slope = -0.14). Between transects with the heterogeneous regression slopes, MT had significantly higher biomass than RW (far-west slope), W (west slope), WC (west central slope), and FL Transect (Florida slope) between depths of 0.5 and 2 km (Table 3.3c, J-N test, $P < 0.05$). The rapid declining MT Transect crisscrossed with the slow declining C Transect (Fig. 3.5); hence, the biomass was significantly higher in the MT than in the C Transect between 0.5 and 1.6-km depths but was significantly lower between 1.7 and 2.7-km depths (J-N test, $P < 0.05$).

The steep slope of the MT Transect was associated with extremely high biomass at the Mississippi Canyon head (MT1, 492.1 ± 159.88 mg C m^{-2}, mean ± s.d., n = 10, Table 3.2). At a depth of 2,712 m (MT6), MT transect converged with the RW, W, WC, and FL Transects (Fig. 3.5) to 18.8 ± 9.72 mg C m^{-2} (n = 9). The biomass of MT Transect declined sharply with depth to be significantly less than DS Transect (De Soto Canyon) between depths of 0.8 and 2.6 km and significantly less than FL Transect between 2.6

and 2.7 km (Table 3.3c, J-N test, $P < 0.05$). Despite of the increasing water depth, the C Transect maintained a relatively high level of biomass to be significantly higher than the biomass in RW and WC Transect from 0.7 to 2.9 and to 2-km depth, respectively (J-N test, $P < 0.05$).

Regression slopes of the RW, W, WC, DS, and FL Transect were not significantly different (Table 3.3d, ANCOVA, slope, $F_{4, 152} = 0.9$, $P = 0.48$); nonetheless, the elevations were significantly different (elevation, $F_{4, 152} = 25$, $P < 0.001$). Only the DS Transect (Figure 3.5, open squares) had significantly greater regression elevation than the other 4 slope transects (black symbols; Table 3.3e, Tukey's HSD test, $P < 0.001$).

Organic carbon biomass within small slope basins (B stations) declined log-linearly with depth (Table 3.4a, $F_{1, 13} = 6.5$, $P = 0.02$), while the adjacent non-basin sites (NB stations) only showed a marginal biomass-depth relationship ($F_{1, 18} = 3.5$, $P = 0.08$). The regression slopes were not significantly different (Table 3.4b, ANCOVA, slope, $F_{1, 31} = 0.3$, $P = 0.6$) and the basin biomass was only marginally higher than the non-basin biomass (elevation, $F_{1, 31} = 3.9$, $P = 0.06$).

Table 3.3. Linear regressions and ANCOVAs for organic carbon biomass against depth during DGoMB sampling. (a) Regression statistics for each transect. The dependent variable is $\log_{10}$ biomass (mg C m^{-2}). The independent variable is depth (km). (b) ANCOVA on biomass among 7 transects. (c) Transect pairs with heterogeneous slopes (based on Tukey HSD multiple comparisons, $P < 0.05$) and the depth ranges where the biomass were significantly different (Johnson-Neyman test, $P < 0.05$). Inequality sign shows the direction of the difference between transects (d) ANCOVA on biomass among transects with homogeneous slopes. (e) Tukey HSD multiple comparisons on regression elevations between transects with homogeneous slopes. Signifiance codes: ”n.s.” denotes $P \geq 0.1$, ”. ” denotes $P < 0.1$. ”*” denotes $P < 0.05$. ”**” denotes $P < 0.01$. ”***” denotes $P < 0.001$.

(a) Transect	Slope	Intercept	Df1	Df2	R2	F	P
RW	-0.33	2.14	1	33	0.68	71.7	***
W	-0.26	2.08	1	27	0.72	70.3	***
WC	-0.35	2.14	1	33	0.50	32.8	***
C	-0.14	2.08	1	28	0.36	16.0	***
MT	-0.57	2.79	1	41	0.84	214.6	***
DS	-0.28	2.52	1	25	0.40	16.8	***
FL	-0.27	2.12	1	34	0.74	94.5	***

(b) ANCOVA	Df1	Df2	SS	MS	F	P
Slope	6	221	3.0	0.5	11.9	***
Elevation	6	221	6.4	1.1	24.9	***

Table 3.3. Continued.

(c) Transects		Depths	P	Transects		Depths	P
MT >	RW	0.2-2.3	*	MT <	C	1.7-2.9	*
	W	0.4-2.0	*		DS	0.8-2.7	*
	WC	0.3-2.3	*		FL	2.6-3.0	*
	C	0.3-1.6	*	C >	RW	0.7-3.0	*
	FL	0.2-2.0	*		WC	0.7-2.7	*

(d) ANCOVA	Df1	Df2	SS	MS	F	P
Slope	4	152	0.2	0.0	0.9	n.s.
Elevation	4	152	4.4	1.1	25.0	***

(e) Transects		DF1	DF2	Q	P
DS >	RW	4	152	12.1	***
	W	4	152	10.4	***
	WC	4	152	11.0	***
	FL	4	152	9.9	***

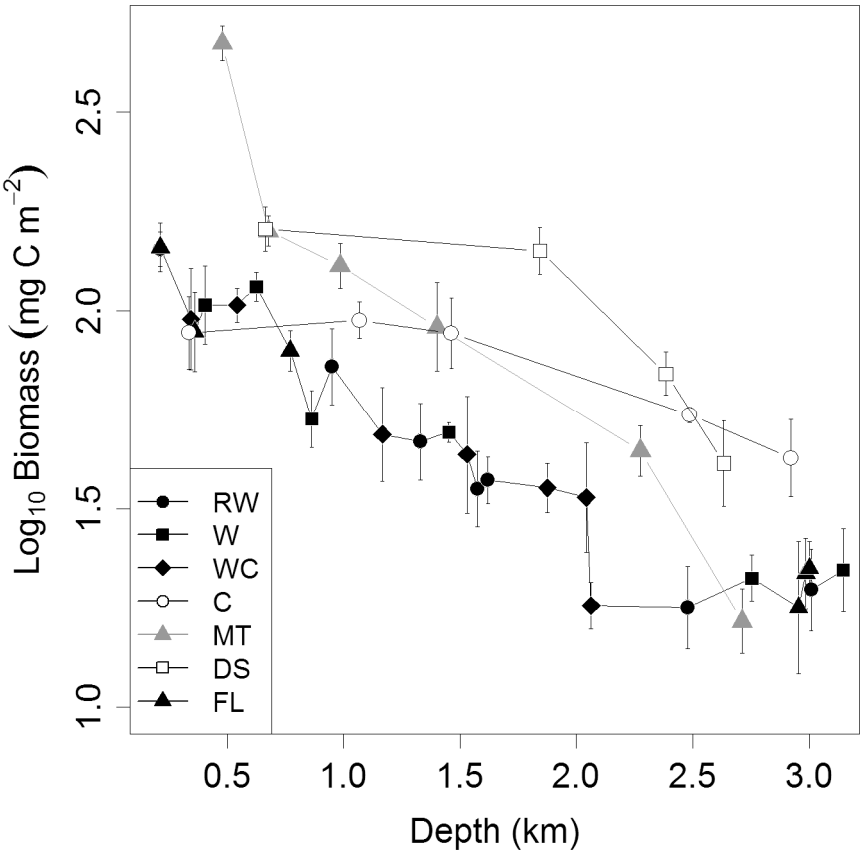

Fig. 3.5. Log_{10}-transformed organic carbon biomass against depth for each transect during DGoMB sampling. Gray triangle indicates the Mississippi Canyon (MT stations); open square indicates the De Soto Canyon (Station S35 to S38); open circle indicates the central slope (C stations); solid black symbols indicate far-west (RW stations & AC1, circle), west (W stations, squares), west central (BH and WC & NB stations, retangular), and Florida slope (Station S39 to S44, triangle). Detail locations of site can be found in Fig. 3.1. Test statistics of linear regression for each transect can be found in Table 3.3a.

Historical NGoMCS sampling showed a similar log-linear biomass-depth relationship (solid line, Fig. 3.6) with the current DGoMB sampling (dash line). Neither the regression slopes nor the regression elevations were significantly different between the two studies (Table 3.4b, ANCOVA, slope, $F_{1, 92} = 0.5$, $P = 0.48$; elevation, $F_{1, 92} = 0.6$, $P = 0.44$). Among transects being revisited, only the 3 sites on FL Transect (S41, S42, and S43) had significantly higher biomass for the NGoMCS than for the DGoMB study (Table 3.5, ANOVA, $F_{1, 46} = 10.4$, $P = 0.002$), while the biomass of the rest of transects (W, WC, and C stations) were not significantly different between the two studies (ANOVA, $P > 0.1$).

Because regression slopes and elevations were not significantly different between NGoMCS and DGoMB study, they were combined to compare with the S GoM data (Fig. 3.6). Both the N and the S GoM showed significantly log-linear declining biomass with depth (Table 3.4a, north, $F_{1, 94} = 242.7$, $P < 0.001$; south, $F_{1, 52} = 57.1$, $P < 0.001$). Regression slopes were not significantly different between the N and S GoM (Table 3.4b, ANCOVA, slope, $F_{1, 146} = 0.4$, $P = 0.53$); however, the regression elevation of the N GoM was significantly higher than the S GoM (elevation, $F_{1, 146} = 121.6$, $P < 0.001$).

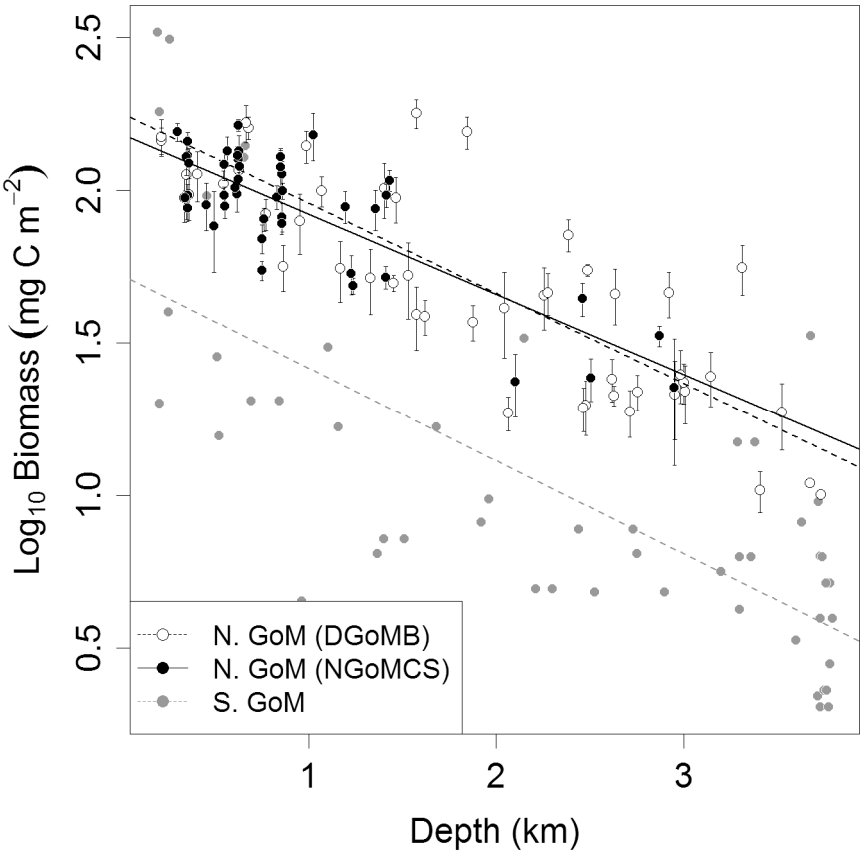

Fig. 3.6. Log_{10}-transformed organic carbon biomass as functions of water depth for the DGoMB (open circle & black dash line), NGoMCS (black circle & black line), and S GoM studies (gray circle & dray dash line). Linear regressions were conducted on the station averages from core replications. The standard error is shown as error bar. The test statistics of linear regression can be found in Table 3.4a.

Table 3.4. Linear regressions and ANCOVAs for organic carbon biomass against depth among studies. (a) Regression statistics for basins (B), non-basins (NB), NGoMCS data, DGoMB data, northern GoM (NGoMCS + DGoMB), and southern GoM. The dependent variable is $\log_{10}$ biomass (mg C m^{-2}). The independent variable is depth (km). (b) ANCOVA on biomass between basin and non-basin sampling, between historical (NGoMCS) and current (DGoMB) sampling in the northern GoM, and between northern and southern half of the GoM basin. Signifiance codes: ”n.s.” denotes P ≥ 0.1, ”. ” denotes P <0.1. ”*” denotes P < 0.05. ”**” denotes P < 0.01. ”***” denotes P < 0.001.

(a) Transect	Slope	Intercept	Df1	Df2	R2	F	P
B	-0.71	3.20	1	13	0.33	6.5	**
NB	-0.49	2.42	1	18	0.16	3.5	.
NGoMCS	-0.26	2.18	1	43	0.67	87.5	***
DGoMB	-0.29	2.25	1	49	0.69	109.8	***
N. GoM	-0.28	2.21	1	94	0.72	242.7	***
S. GoM	-0.30	1.72	1	52	0.52	57.1	***

(b) ANCOVA	Df1	Df2	SS	MS	F	P
Basin vs Non-basin (H04)						
Slope	1	31	0.01	0.01	0.3	n.s.
Elevation	1	31	0.2	0.2	3.9	.
NGoMCS vs. DGoMB (H05)						
Slope	1	92	0.02	0.02	0.5	n.s.
Elevation	1	92	0.02	0.02	0.6	n.s.
N. GoM vs. S. GoM (H06)						
Slope	1	146	0.03	0.03	0.4	n.s.
Elevation	1	146	8.7	8.7	121.6	***

Table 3.5. Randomized Complete Block ANOVA on organic carbon biomass between historical NGoMCS and current DGoMB studies. Blocking factor is different sites along the selected transects. Significance codes: ”n.s.” denotes P ≥ 0.1, ”. ” denotes P <0.1. ”*” denotes P < 0.05. ”**” denotes P < 0.01. ”***” denotes P < 0.001.

ANOVA	Df1	Df2	SS	MS	F	P
W stations						
Study	1	33	0.04	0.04	2.4	n.s
Block	4	33	2.6	0.6	43.0	***
WC5 & WC12						
Study	1	19	0.1	0.1	1.5	n.s
Block	1	19	0.9	0.9	24.1	***
C stations						
Study	1	88	0.1	0.1	2.2	n.s
Block	4	88	4.3	1.1	17.7	***
S41, S42, & S43						
Study	1	46	0.3	0.3	10.4	**
Block	2	46	3.6	1.8	73.0	***

3.4.3. Random Forest (RF) modeling and standing stock prediction

In order to minimize the effect of gear difference, a total of 652 carbon biomass and 623 abundance records from box core sampling or using similar sieve sizes (DGoMB, Table 3.2 & Appendix C Table S1; NGoMCS, Appendix C Table S3; Rowe et al. 2003, OGMEX, PROMEBIO, and SIGSBEE, Appendix C Table S4) were selected to conduct Random Forest (RF) analyses with 19 environmental predictors (Table 3.1). A total of 73% of the variance for the biomass and 59% for the density can be explained by the environmental variables. The macrofauna biomass and abundance predictions for the entire GoM basin, as well as the corresponding environmental data are provided in Appendix F File S4. When these data were permuted independently for each predictor, water depth, decadal mean of primary production (cbpm & vgpm) and phytoplankton growth (growth), as well as decadal standard deviation (SD) and mean of the sea surface temperature (sst) caused the greatest deterioration in the biomass predictions (Fig. 3.7a); however, a more subjective measure for the variable contribution would be the mean increase of prediction mean-square-error (MSE) over the entire the random forests (bar chart) normalized by the standard error (error bar). This normalized variable contribution suggested that water depth has the overwhelming importance over the decadal mean and SD of ocean color images on making the accurate biomass predictions (Fig. 3.7b).

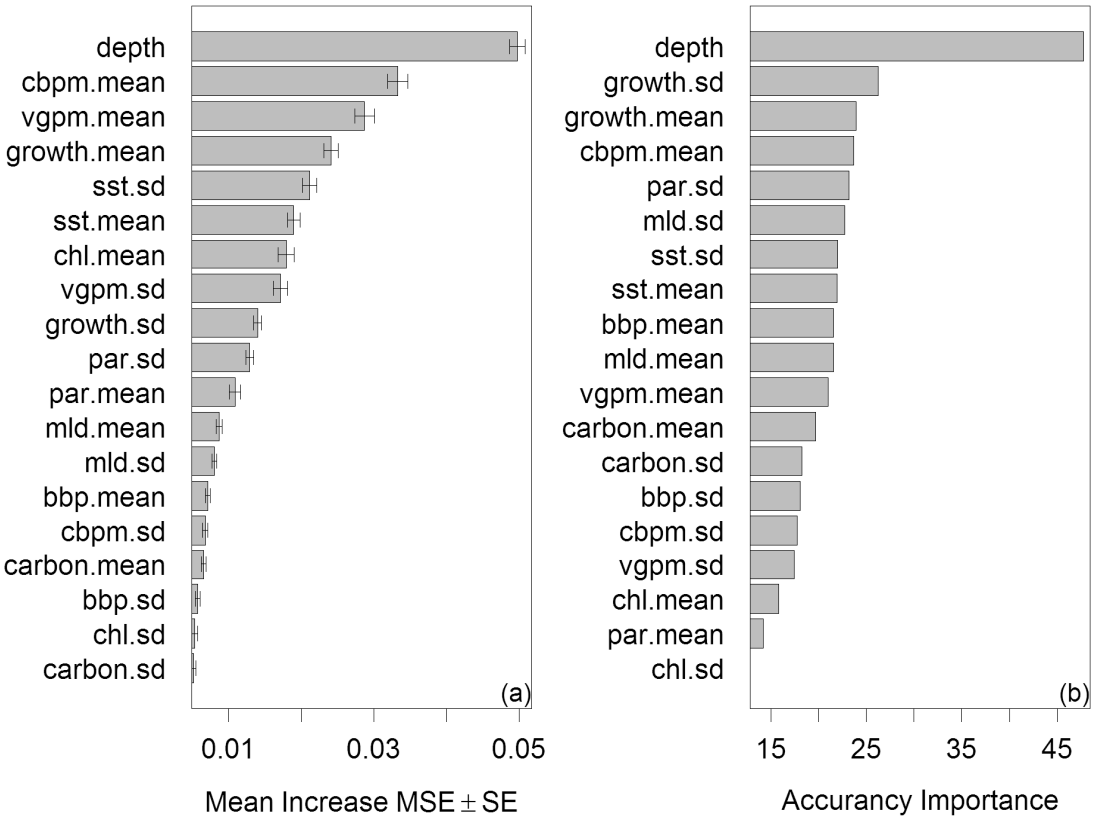

Fig. 3.7. Predictor importance based on Random Forest modeling between organic carbon biomass and water depth, as well as satellite ocean color images. (a) Increase of prediction mean-square-error (MSE) after randomly shuffling the predictor values. The purpose of permutation is to mimic the absence of that predictor; hence, the deterioration of prediction (increase of MSE) suggested the importance of predictor. Bar charts show the mean increase of MSE and standard error (error bars) across 1,000 bootstrap resampling. (b) The prediction accuracy of each predictor was estimated form the mean increase of MSE (bar charts) normalized by the standard error (error bar) in Fig. 3.7a.

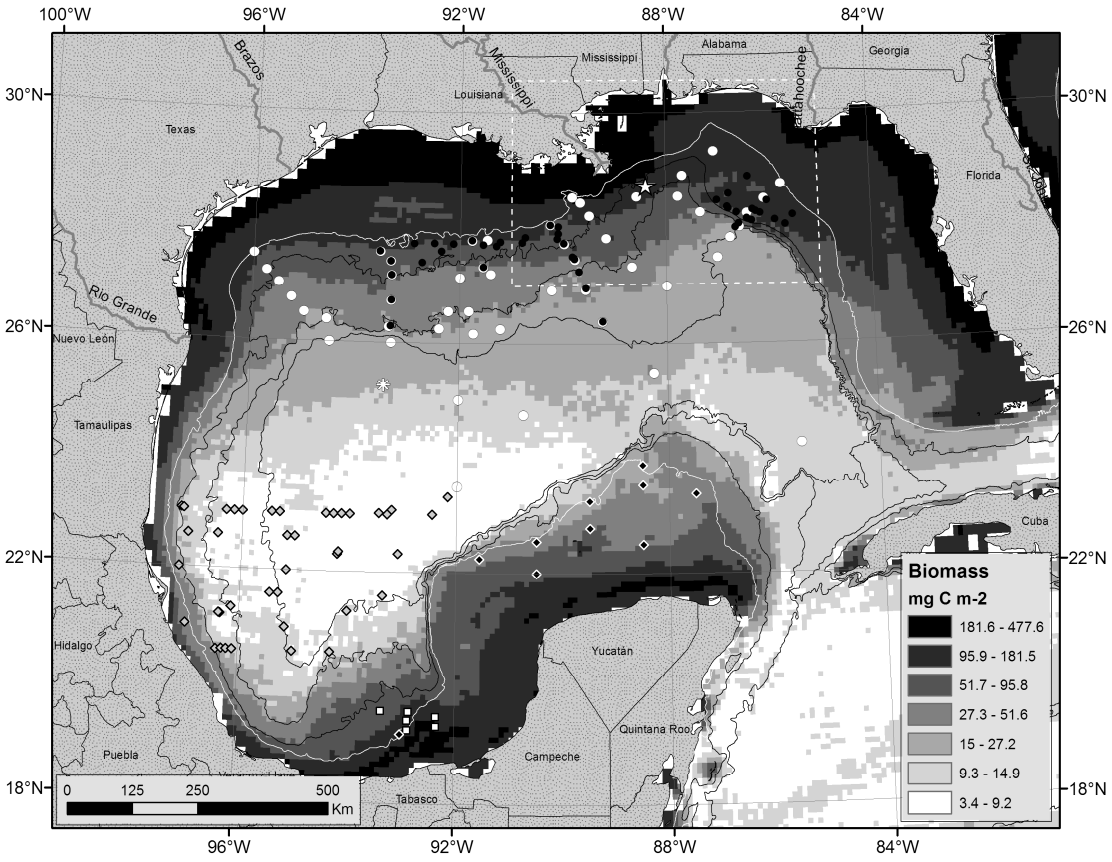

Fig. 3.8. Distribution of macrofaunal carbon biomass in the Gulf of Mexico. The biomass was predicted using Random Forest model from bathymetry and ocean color images (Table 3.1). Figure legends follow Fig. 3.1. Color gradient indicate high (black) to low carbon biomass classes (white). Fig. 3.9 shows a close-up view of the area enclosed by white dash lines.

A total of 105 kilotons of macrofaunal carbon was estimated for the GoM basin (cut off from the Yucatan Channel and Straits of Florida) based on summation of predicted cell values (carbon biomass in per unit area) * area of a 5-arcminute grid at the equator (86 km^2) * cosine of latitude for the grids. For visualization, the predictions from the RF model were classified into 7 biomass classes (Fig. 3.8). Generally, the natural classes occur in depth bands parallel to isobaths and decline toward the center of the deepest part of GoM basin. The width of biomass classes appears to correlate with seafloor topography with broad bands occurring on the gradual continental shelf. The northern half of the GoM basin shows higher biomass than the southern half of the basin. The predicted cells north of the Rio Grande River (north of Latitude 26 N) contributed ~62% of total carbon biomass in merely ~36% of GoM surface area. The highest biomass class (181.6 to 477.6 mg C m^{-2}) dominated much of the continental shelf of Louisiana and Mississippi with relatively narrow distribution on the shelves of Texas and Florida, as well as sporadic distribution on the shelf of Yucatan and Campeche. This high biomass class generally occurred shallower than 50-m depth but submerges at the head of the Mississippi Canyon (MT1) to ~500-m depth and even to ~1,000-m depth near the mouth of Mississippi River. The second highest biomass class (95.9 to 181.5 mg C m^{-2}) occurred mostly above 200-m isobath but also submerged to ~1,000-m depth on the upper Mississippi Canyon and northern part of Florida Slope. This weaker maximum reached as deep as ~2,000-m depth near the mouth of Mississippi River and the upper De Soto Canyon. The two natural classes (3.4 to 14.9 mg C m^{-2}) with the lowest carbon biomass occupied much of the Sigsbee and Florida Abyssal Plain near the center of

GoM basin, the continental slope of the SW GoM, and the Caribbean basin south of the Yucatan Channel.

A close-up view of the biomass distribution in vicinity of the *Deepwater Horizon* oil platform is provided in Fig. 3.9. The incident site (MC252, predicted biomass = 142.9 mg C m^{-2}) can be classified within the same natural class (120.5 to 192.3 mg C m^{-2}) as Stations MT2, HiPro, S35, S36, and S44, where the empirical carbon biomass ranged from 150 to 178.8 mg C m-2 (Table 3.2).

3.5. Discussion

3.5.1. Relationship between standing stocks, body size and energy constraints

This study confirmed logarithmic declines of macrofaunal abundance and biomass with depth (Rowe 1983, Rex et al. 2006, Wei et al. 2010b). Except for bacteria, this general phenomenon has occurred across all major size groups for soft-bottom communities (Rex et al. 2006, Rowe et al. 2008b, Wei et al. 2010b) and is widely accepted to be caused by an exponential decline of the particulate organic carbon (POC) flux from the euphotic zone to the seafloor (Suess 1980, Pace et al. 1987). The decline of average macrofaunal body size (biomass/abundance) with depth, however, requires careful interpretation, because the size variation in fact indicates a change of relative abundance among taxa, as the variability within taxa was not measured in this study; hence, a correct statement should be that the taxonomic composition of macrobenthos shifted to the smaller taxa with depth. This observation was supported by a shit of dominance (in

terms of abundance) from large *sensu-stricto* macrofauna on the upper slope to small macrofauna-size meiofauna on the lower slope and abyssal plain.

It has been postulated that small body size has the advantage to conserve energy and maintain viable populations in the food-limited deep sea (Thiel 1975, Rex et al. 2006, Wei et al. 2010b) as opposed to being large and benefiting from competition, resource exploitation, metabolic efficiency, and predation avoidance (McClain et al. 2009). The upper slope of the N GoM might have favored the large taxa such as polychaetes and amphipods due to the abundant resources, while the abyssal plain is more suitable for the small macrofaunal nematodes, harpacticoids, and ostrocodes as the result of low POC flux (Biggs et al. 2008, Rowe et al. 2008a), as well as the low percentage and refractory nature of organic matter in the sediments (Morse & Beazley 2008).

Evidence supporting this speculation comes from outliers in the standing stock-depth regressions (Fig. 3.3 and Fig. 3.4). The head of Mississippi Canyon (Station MT1) had extremely high abundance and biomass with almost no macrofauna-size meiofauna, presumably due to the POC input to the seafloor (77.7 mg C m^{-2} day^{-1}), the highest estimated among the DGoMB sampling sites (Biggs et al. 2008). The macrofaunal biomass only exceeded the meiofaunal (metazoan + foraminiferal) biomass at this location (Baguley et al. 2008, Rowe et al. 2008b). The dominance of amphipods, *Ampelisca mississippiana* (Soliman & Wicksten 2007), likely excluded the smaller fauna.

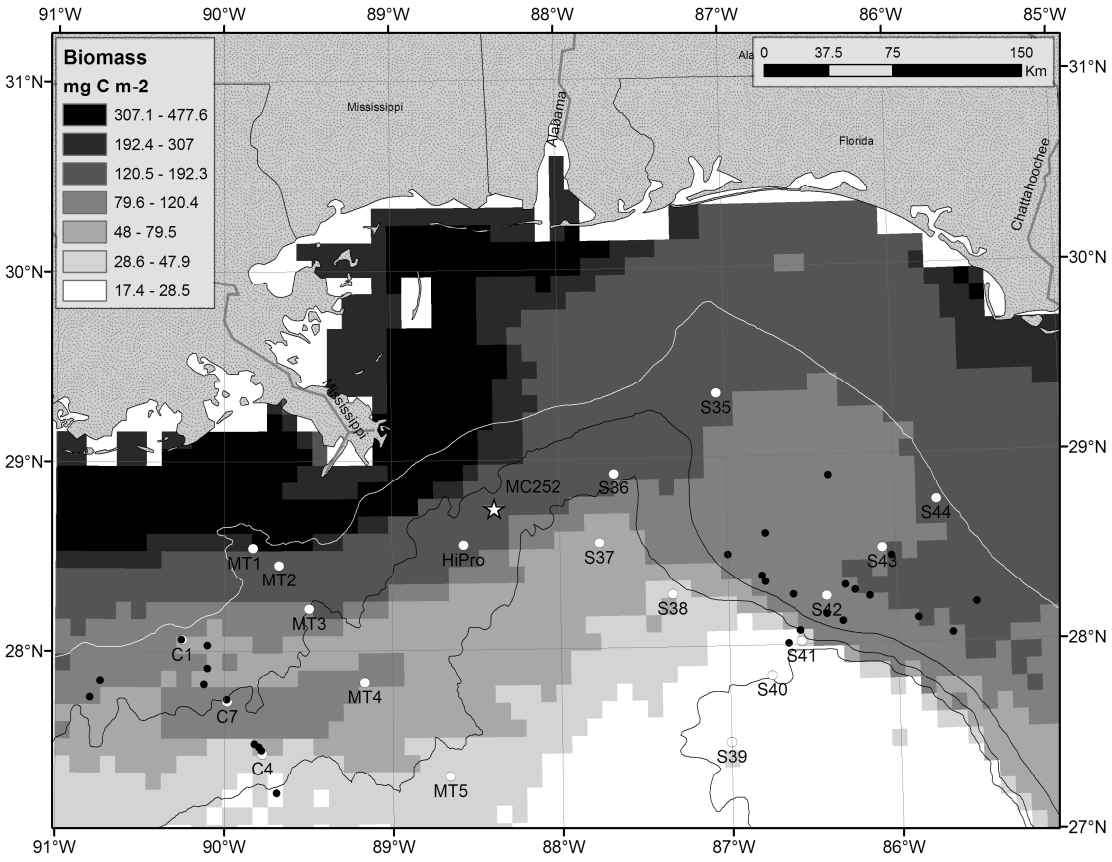

Fig. 3.9. Distribution of macrofaunal carbon biomass in the vicinity of the BP *Deepwater Horizon* oil spill site. Star symbol indicates the location of the *Deepwater Horizon* oil platform (MC252). Figure legends follow Fig. 3.1. Color gradient indicate high (black) to low carbon biomass classes (white).

Another intriguing outlier, Station HiPro, located just 27-km southwest of the BP blowout site (Fig. 3.1), also showed high biomass, large average size, and high abundance of the *sensu-stricto* macrofauna at ~1,600 m below the sea surface, presumably associated with upwelling nutrient-rich water onto the upper slope or entrained from the Mississippi River. The species composition of Station HiPro was more closely related to the shallow shelf-break communities than other stations of similar depths (Wei et al. 2010a). Elevated amounts of POC inputs via lateral advection from the surrounding shelf and slope was needed to support this benthic community, since the satellite-based estimates (Biggs et al. 2008) did not suggest excessive level of export POC flux. The signal of high surface productivity at the Station HiPro (comparable to the shelf-break sites) might have been reduced by a depth-exponential-decay equation (Pace et al. 1987) that was applied to convert surface primary production to export POC flux on the seafloor (Biggs et al. 2008).

At ~3,300 m below the sea surface, the deep Mississippi sediment fan (Station S5) was a favorable habitat for macrofaunal nematodes, hapacticoids, and ostracodes. Their abundances were 2 to 6 times more than other sites on the abyssal plain (Appendix C Table S4). It is also favored mollusk bivalves and aplacophorans with a 5 to 6-fold increase in abundance over the other abyssal sites. Similar to Station HiPro, the elevated total standing stocks with the species composition being more related to the shallower slope communities (Wei et al. 2010a) was not related to a satellite-based export POC flux (Biggs et al. 2008). Wei et al. (2010a) suggested that the macrobenthos at the Station S5 was influenced by the slumping or down-slope movements of organic-rich

sediments from the Mississippi River and surrounding shelves through the submarine canyon. Regardless of the surface versus a lateral source of organic carbon, the detritus supporting these high macrofaunal standing stocks was not likely to be fresh, labile materials, due to the extreme depth and distance from shore. It can be inferred that these taxa might better cope with potentially high quantity but low quality of food resources.

3.5.2. Summary of hypotheses testing

Based on ANCOVA results, we rejected Null Hypothesis 1. The Mississippi Canyon was unique in terms of the overall level and the rate of declining biomass with depth. Compared to the continental slopes in the NW or NE GoM, the biomass was significantly elevated on the upper and mid sections of the Mississippi Canyon. Submarine canyons are potential conduits of sediments and organic materials from the continental shelf to the deep basin. River flushing, storm surges, earthquakes, or down-slope currents can cause mass wasting of sediments along the canyon axis (Gardner 1989, Santschi & Rowe 2008). During the DGoMB trawl survey in year 2000, macrophyte debris, including the water hyacinth (*Eichhornia crassipes*), *Sargassum* spp., and wood fragments of all sizes, were found on the seafloor of the shallow head of the Mississippi Canyon. The water hyacinths (23 clumps, length ca. 15 cm) were only found at the canyon head, presumably originating from the river. High macrofaunal biomass associated with the enrichments of macrophyte debris has also been reported elsewhere in submarine canyons (Vetter & Dayton 1998, De Leo et al. 2010). It is possible that the high macrofaunal biomass was a function of rapid accumulating macrophytes and

organic materials exported from the Mississippi River and adjacent continental shelf. The extremely high biomass at the canyon head declined rapidly along the axis toward the lower section of canyon and sediment fan (Station MT6), where the biomass was equal or lower than the other continental slope transects. Interestingly, a large quantity of cobble-sized, reddish-colored sedimentary rocks, so called "iron stones", have also been found in the area from box cores, trawls, and bottom photographs (Pequegnat 1983, Rowe & Kennicutt 2009). Evidence suggests that these "iron stones" could be buried in the sediments from the upper canyon or shelves and exposed during the massive submarine slumping of unstable continental margins (Bryant et al. 1991, Rowe et al. 2008b, Santschi & Rowe 2008). Strong bottom currents below the Florida and Sigsbee Escarpment were also evident in the bottom photographs (Rowe & Kennicutt 2009) and appeared to affect the pattern of macrofaunal zonation (Wei et al. 2010a); however, it is unclear if this low biomass was linked to the "iron stones", strong bottom currents, or both.

The rate of declining biomass with depth on the Central Transect was the lowest among all transects, and thus the macrobenthic communities were able to maintain an uncommonly high level of biomass at the mid to lower slope depths. The high macrofaunal standing stocks were not first noticed in the north central GoM. During the NGoMCS sampling, the peak macrofaunal abundance occurred at 620-m and 1,400-m depths on the Central Transect. The cause was attributed to the hydrocarbon seeps in the proximity of Station C7 (~1,000-m depth, Pequegnat et al. 1990, Rowe & Kennicutt 2009). Cold seeps are known to support dense macrofaunal communities throughout the

continental margins of world's ocean (Sibuet & Olu 1998). Heterotrophic macrobenthos living in the immediate vicinity of seeps could benefit from the abundant carbon source in the food-limited deep-sea; however, the enhancement appears to be localized in the GoM and only limited to the periphery of the seep fluid (Carney 1994). During the DGoMB study, higher-than-background biomass was also found southeast off the Central Transect on the Sigsbee Abyssal Plain (Station S5, ~3,300-m depth). There was no indication of apparent enhancement of surface production or export POC flux on the Central Transect and the Station S5 (Biggs et al. 2008). It is also unlikely that such large scale enhancement of macrofaunal biomass was caused by the natural hydrocarbon seepages on the upper Louisiana continental slope. Additional sources of energy are needed to explain this anomaly, most likely the lateral transport of materials from the organic rich upper Mississippi Canyon. It may be possible that the complex interaction between the down-slope sediment transports (Balsam & Beeson 2003, Santschi & Rowe 2008) and strong westward bottom currents (Hamilton & Lugo-Fernandez 2001, Oey & Lee 2002) have shifted our expected biomass-enrichment pathway away from the axis of Mississippi Canyon.

Null Hypothesis 2 was rejected. The De Soto Canyon harbored significantly larger macrofaunal biomass than the slope transects. In contrast to the Mississippi Canyon, the De Soto Canyon does not received riverine inputs directly and has been an area of non-deposition with little evidence for recent sediment transport (Bryant et al. 1991). However, similar to the Station HiPro, the surface water of De Soto Canyon is affected by warm slope eddies (WSEs), which entrain the low salinity high chlorophyll

Mississippi River water (Jochens & DiMarco 2008). The WSEs advect the turbid "green-water" plume seaward and enhance the surface primary production and associated export flux of POC to the deepwater of NE GoM (Biggs et al. 2008). The rate of declining biomass with depth in the De Soto Canyon, however, was statistically indifferent from other slope transects, suggesting that similar processes may govern the remineralization of sinking phytodetrital carbon despite surface water being more productive over the De Soto Canyon.

Null Hypothesis 3 and 4 were accepted. Neither the steep Florida Escarpment nor the small continental slope basins on the NW GoM slope had a significant effect on macrofaunal biomass. Despite an abrupt 2,200-m depth drop along the Florida slope, the decline of biomass still followed a general depth trend similar to the NW GoM slope. It was hypothesized that the base of the Florida Escarpment (Station S41) might experience organic enrichment due to the steep escarpment and its proximity to productive continental shelf; nonetheless, our observation suggested that the water depth, not the distance away from the shelf, controlled the pattern of declining biomass. The numerous small slope basins were also hypothesized to funnel or trap organic materials during the frequent gravity slumping and density flows on the continental margin of NW GoM (Bryant et al. 1991), and thus may elevate the benthic standing stocks within the basins. In fact, after removing depth effect by ANCOVA, we did observe a slight, but not statistically significant enrichment of carbon biomass within the basins than the non-basin slope.

Null Hypothesis 5 was accepted. No significant change in macrofaunal biomass was observed between the historical and current sampling in the N GoM. Although the ANOVA test on individual transects suggested that the biomass on the Florida Transect was significantly higher during the historical NGoMCS study, the selected sites for comparison (Station S41 to S43) were not sampled at exactly the same locations between the two studies. A drastic 2,600-m depth variation among these three sites might also contribute to substantial bias in the ANOVA test. It should also be noted that our conclusion is based on the assumption that the average sizes of macrofaunal taxa were not different between the two studies.

Null Hypothesis 6 was rejected. Macrofaunal biomass on the continental margins of N GoM was significantly higher than the S GoM. This north-south variation was probably a function of the surface primary production and the associated export POC flux available to the macrobenthos. In contrast to the limited riverine influence in the S GoM, the world's third largest drainage basin, the Mississppi-Atchafalaya Rivers discharge 530 billion m^3 of freshwater and 210 megatons of sediments annually onto the continental shelf of the N GoM (Cai & Lohrenz 2010). The nutrient-laden Mississippi River plume interacts with shelf/slope eddies and contributes to some of highest measurements of primary production and export POC flux on the GoM continental margin (Lohrenz et al. 1999, Biggs et al. 2008, Cai & Lohrenz 2010). Additionally, upwelling along the edges of Loop Currents with concomitant high surface productivity is evident along the Florida Escarpment and Campeche Bank (Lohrenz et al. 1999,

Wiseman & Sturges 1999, Jochens & DiMarco 2008). The enhancement in the S GoM is relatively minor compared to the N GoM.

3.5.3. Random forest results, biomass predictions, and conclusions

Estimates of macrofaunal abundance are sensitive to artifacts such as gear design, sieve size, fragmentation of specimens, and human sorting error (Gage et al. 2002, Gage & Bett 2005, Pavithran et al. 2009). Given that most of the total macrofaunal biomass is concentrated in large, less abundant animals, biomass is often better suited and more dependable for comparing the standing stocks among studies (Rowe 1983). The same reasoning could explain the performance of Random Forest (RF) analyses on our composite GoM data, because more variability was explained for biomass than for abundance. This dichotomy also raises another interesting question of whether abundance is a suitable substitute for the measurement of biomass or production (Sanders et al. 1965, Rowe 1983). Biomass is rarely measured and thus animal density has been often used as a proxy for benthic productivity to make interferences about diversity-energy relationships in the deep sea (Rex & Etter 2010). Based on our observation, at least in the GoM, the bathymetric pattern of macrofaunal biomass did not completely follow the pattern of density due to a variation of animal size with depth. The *sensu-stricto* density, on the other hand, was probably a better representation of the biomass or benthic productivity.

Water depth is transitionally a good surrogate for benthic food supply, or utilization of energy through the mid-water food web, and thus has been widely used as a predictor to

regress against the standing stocks of macrobenthos (Rowe & Menzel 1971, Rowe et al. 1974, Rowe 1983, Rex et al. 2006). In this study, the RF analyses on the GoM macrofauna agreed with the earlier global synthesis (Wei et al. 2010b), suggesting that water depth is still the single most important predictor for modeling biomass; however, an obvious weakness, probably also contributing to the lesser importance of remote sensed data in our analyses, was the non-contemporaneous sampling between the benthic and satellite data. This problem can be solved seemingly easily for the more up-to-date DGoMB sampling, because satellite-based phytoplankton biomass and production were measured simultaneously (Biggs et al. 2008). For the older studies (NGoMCS and OGMEX), these data simply not exist. Nonetheless, besides the issue of data availability, temporal and spatial scaling are also problematic for the ocean color parameters (Johnson et al. 2007). Significant seasonal and interannual climate variations have been linked to the benthic food supply with the time-lag between the surface events and changes in macrofaunal abundance estimated to be 8 to 9 months in the abyssal NE Pacific (Ruhl et al. 2008, Smith et al. 2009). In the GoM, owing to the broad range of our sampling, as well as complex circulation and water-column processes associated with the Loop Current system (Jochens & DiMarco 2008), it is impossible to determine the precise temporal and spatial scales for extracting the satellite data and at the same time, reflect the POC supply hundreds or thousands of meters below the sea surface. Therefore, it is probably more appropriate to use a long-term average and deviation of the satellite measurements (monthly composite data from years of 1998 to 2007) to capture the overall level and interannual variability of surface ocean climate.

Besides error inherited from sample processing and predictor scaling, the unexplained variability in the macrofaunal standing stocks may also reflect energy sources not directly measureable such as the horizontal transport of carbon into or out of a benthic station (Rowe et al. 2008a), hydrocarbon inputs from the cold seeps (Cordes et al. 2009), and accumulation of macrophytes in the submarine canyon (Vetter & Dayton 1998). Other factors that are physiologically important such as bottom water temperature (Narayanaswamy et al. 2010), dissolved oxygen (Quiroga et al. 2005), and export POC flux (Johnson et al. 2007) were not included as predictors, because the available global data (Levitus 2010) or models (Dunne et al. 2007, Yool et al. 2009) were not of sufficient resolution (1 degree grids) to reveal the spatial heterogeneity and details needed for our local prediction. The global scale analyses, however, showed that the ocean color data and bathymetry were among the most important predictors for modeling the distribution of benthic standing stocks and these predictors alone have great utility on local-scale modeling and high resolution predictions (Wei et al. 2010b).

In general, the biomass prediction based on RF model agrees with the observations, showing a depth related pattern with apparent enhancements on the N GoM shelf near the major rivers, in the NE GoM close to the Mississippi, De Soto Canyon and upper Florida slope, and on the S GoM shelf along the Campeche Banks. These prominent features are related to complex biophysical interactions among the riverine influence (Cai & Lohrenz 2010), seafloor geomorphology (Bryant et al. 1991, Bianchi et al. 2006), and the Loop Current associated eddies and upwelling (Lohrenz et al. 1999, Biggs et al. 2008), which regulate the phytoplankton production and food supply to the benthos.

Even though we did not include biomass observations from the Caribbean Basin, our predictions of the area fall within the range of empirical values (2.6 to 15.2 mg C m^{-2}) published by Richardson and Young (1987). This low level of benthic biomass extends northward and westward to the S GoM, presumably associated with the low productivity water from the offshore Caribbean that enters the GoM with the Loop Current (Jochens & DiMarco 2008). These water masses may conserve their hydrographic property for a prolonged period of time and contribute to the low benthic biomass on the Mexican margin (Wiseman & Sturges 1999).

The hydrocarbon released by the BP oil spill is also an energy source and eventually will be degraded and assimilated into the aquatic food web. If we assume that everything ultimately falls to the seafloor, can we see a surge of benthic biomass similar to what has been observed at the head of the Mississippi Canyon? The amount of hydrocarbons released during the spill (up to 500 kilotons, Joye et al. 2011), however, was relatively small compared to the annual organic carbon export from the Mississippi River (on the order of megatons per years, Cai & Lohrenz 2010). Another possibility could be the loss of environmentally sensitive species during the initial spill followed by succession of opportunistic, pollution resilient species during the recovery stage (Kingston 2002). Our results provide a baseline condition of the sediment-dwelling macrobenthos that may be under immediate or long-term impacts of the BP oil spill. It is necessary to revisit these historical sites using similar sampling methods (e.g. GOMEX Box Core, 300-μm sieve) to make sensible comparison for post-spill effect assessment.

CHAPTER IV

FAUNAL ZONATION OF LARGE EPIBENTHIC INVERTEBRATES OFF NORTH CAROLINA REVISITED

4.1. Overview

The dominant populations of large epibenthic megafauna off North Carolina were mapped in the 1960's from the upper continental slope out to the Hatteras Abyssal Plain using multi-shot sea floor photography. The present re-analysis of the original data using contemporary computer-based methods and geo-referenced mapping (GIS) reveal that the overall patterns inferred initially can be substantiated. Individual species occurred in narrow depth bands that hugged the topography along the entire sampling area, but multi-species assemblages emerge with the modern, more formal quantitative methods.

4.2. Introduction

The Census of Marine Life (CoML) has expectations that the Ocean Biological Information System (OBIS) will archive the locations where all species of marine life are encountered, thus eventually allowing maps of all species distributions to be mapped world-wide, a broad vision attributed to J. Frederick Grassle, for whom we are contributing these papers, This short note is an attempt to assemble a small subset of earlier data into the context of the Continental Margins Ecosystem (COMARGE) project, which is one of many components of CoML initiatives. Most importantly, this area in the NW Atlantic off North Carolina is familiar to Fred Grassle and the 2nd author, as

they worked there, between touch football games, contemporaneously on the R/V EASTWARD, memories perhaps best forgotten.

The data involved were collected from the R/V EASTWARD using a multishot bottom pogo-camera which captured 25 to 50 exposures, covering 6.3 square meters of sea floor with each shot. The advantage of the pogo camera is that every picture was taken at the same height and angle above the sea floor, thus exposing a well-defined area, which allowed quantitative estimates of the densities of visible abundant organisms. By capturing dominant animals in bottom trawls at the same locations as the camera lowerings, the dominant animals in the photos could be identified to species. [Specific details on the methods are available in Rowe and Menzies (1969)] A total of 157 camera lowerings were accomplished, with 27 species identified over the area surveyed. The mapping extended from 32˚ N and 34˚ N latitude and 77˚ and 71˚W longitude.The original analyses were presented in the 2nd author's PhD thesis at Duke (1968), Rowe and Menzies (1969) ands Menzies, George and Rowe (1973). The patterns were also compared closely with those described by Grassle et al (1975) off New England using DSRV ALVIN. The photographs provided accurate counts of the abundant species as a function of depth and latitude. Multi-species assemblages were defined as depth ranges with a minimum of change in species, whereas boundaries between assemblages were locations where the rate of change in species composition was a maximum (Menzies et al. 1973). This use of 'overlap frequencies' or numbers of first and last entries on the depth gradient has been a traditional approach to defining zonation (Carney 2005). The

depth bands of species which occurred together in high frequency were considered to be faunal zones (Rowe & Menzies 1969).

The objective of the present paper is to reexamine the 40-year-old data set with the new multivariate analytic methods now available in commercial statistical packages. The natural grouping of samples was identified based on the similarity of the multi-species database. A geo-referenced map was constructed to make the information more readily available through CoML and subject the earlier conclusions to an objective re-assessment.

4.3. Data Analyses

For our re-assessment, species abundances (the number of individuals) at each location were 4th root transformed to construct a matrix of intra-sample similarities (Bray-Curtis similarity) to be analyzed using the package PRIMER version 6. At the same time, a modified Normalized Expected Shared Species (NNESS) index (Grassle & Smith 1976, Gallagher 1996) was computed using COMPAH96 to compare with Bray-Curtis similarity. Cluster analysis (group-average linkage) was done with SIMPROF testing the null hypothesis that a sub-cluster within the dendrogram can be recreated by permuting the entry species and locations. Sub-clusters confirmed by SIMPROF ($P<0.05$) were considered to be natural faunal groups. The intra-sample similarities were used to compute non-metric multi-dimensional scaling (MDS) in which the faunal similarities between sites were represented by distances. The species in each faunal zone were broken down to percent contribution (SIMPER) to the average faunal similarity

within the zone. Bathymetric data were derived from the NOAA National Geophysical Data Center and the map was produced using ArcGIS® 9.0.

4.4. Results

The original analysis of 40 years ago considered faunal discontinuities to be located at depths where the fewest species overlaps. These minima were encountered at the outer margin of Blake Plateau (1000 m), upper continental rise (3600 m), and the lower rise and abyssal plain (Rowe 1968, Rowe & Menzies 1969). The highest densities were encountered along abrupt boundaries at the shallow end of distributions, tapering out with depth. Several species were thought to‘re-appear’ in a second band in deeper water, after a hiatus at intermediate depths.

The current analysis with PRIMER identified 9 significant faunal zones, assigned alphabetical labels from shallow to deep (Fig. 4.1). The shallow Zones A, B and C have very low within-zone faunal similarity (< 30%); the intermediate Zones D and G have faunal similarity of about 40%; the deeper Zones E and F have faunal similarity of about 60%; and the deepest Zones I and H have faunal similarity of about 90%. Separated clustering based on NNESS (m=1) generally agree with results of the Bray-Curtis similarity (Fig. 4.1), where Zones B, C, D and part of Zones E, F, G are lumped together (Fig. 4.2). The same symbols were used in the Map (Fig. 4.3) and MDS plot (Fig. 4.4) to see the relationships between the data and the geographic location of the populations under scrutiny.

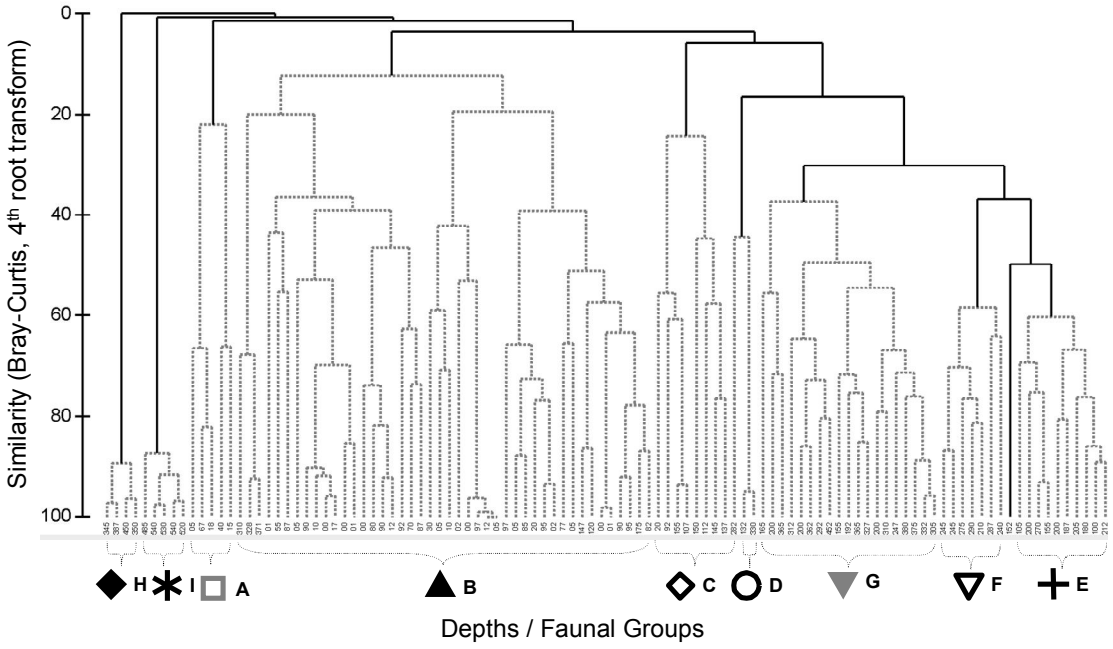

Fig. 4.1. Group-average clustering based on faunal similarity. The species abundances were 4th root transformed before converting to Bray-Curtis similarities. X axis represents the sampling depth (m) and faunal zones. Y axis represents the similarity (%). Solid lines indicate significant evidence of structure (SIMPROF test, $P<0.05$). Dotted lines indicate no evidence of structure.

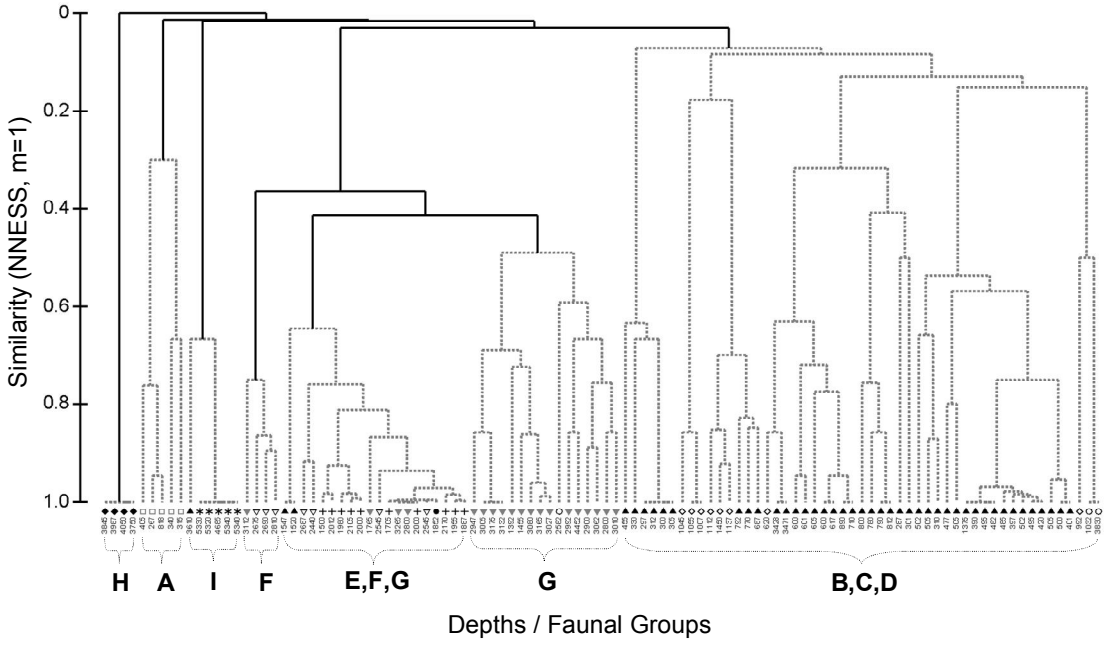

Fig. 4.2. Group-average clustering based on the modified Normalized Expected Shared Species (NNESS) at a random sample size (m) of 1. X axis represents the sampling depth (m) and faunal zones. The symbols indicate significant faunal zones based on Fig. 4.1. Y axis represents the NNESS coefficient. Solid lines indicate significant evidence of structure (SIMPROF test, $P<0.05$). Dotted lines indicate no evidence of structure.

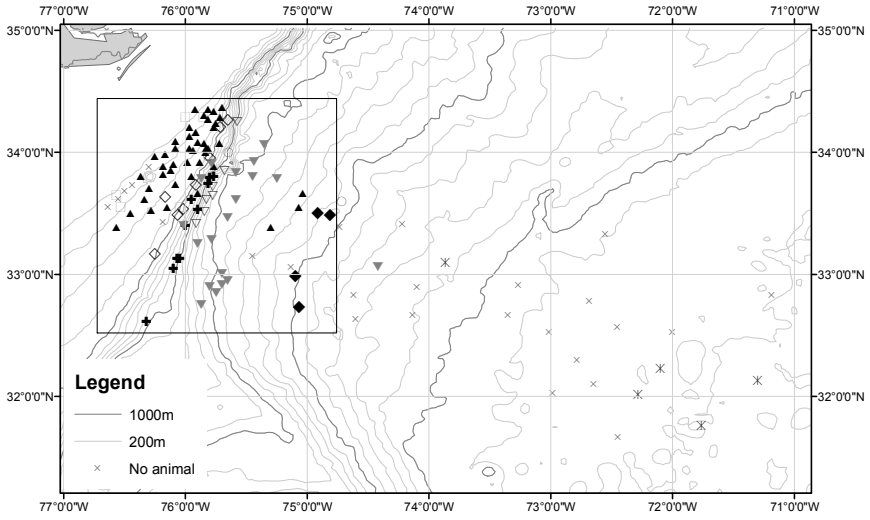

(a)

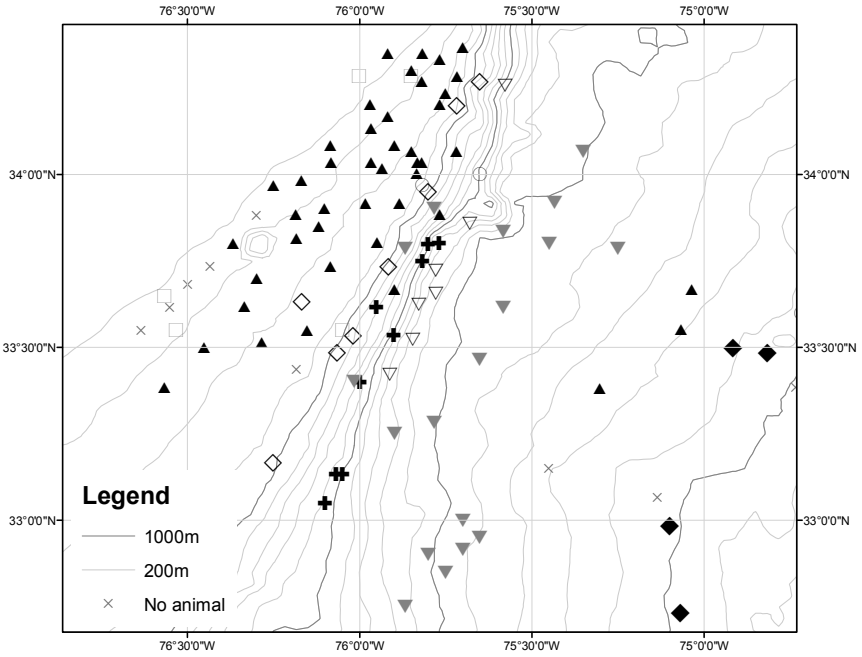

(b)

Fig. 4.3. Sampling area and distribution of significant faunal groups based on cluster analysis. Group symbols are identical to Fig. 4.1. The second figure is a close-up view of the square area in the first figure.

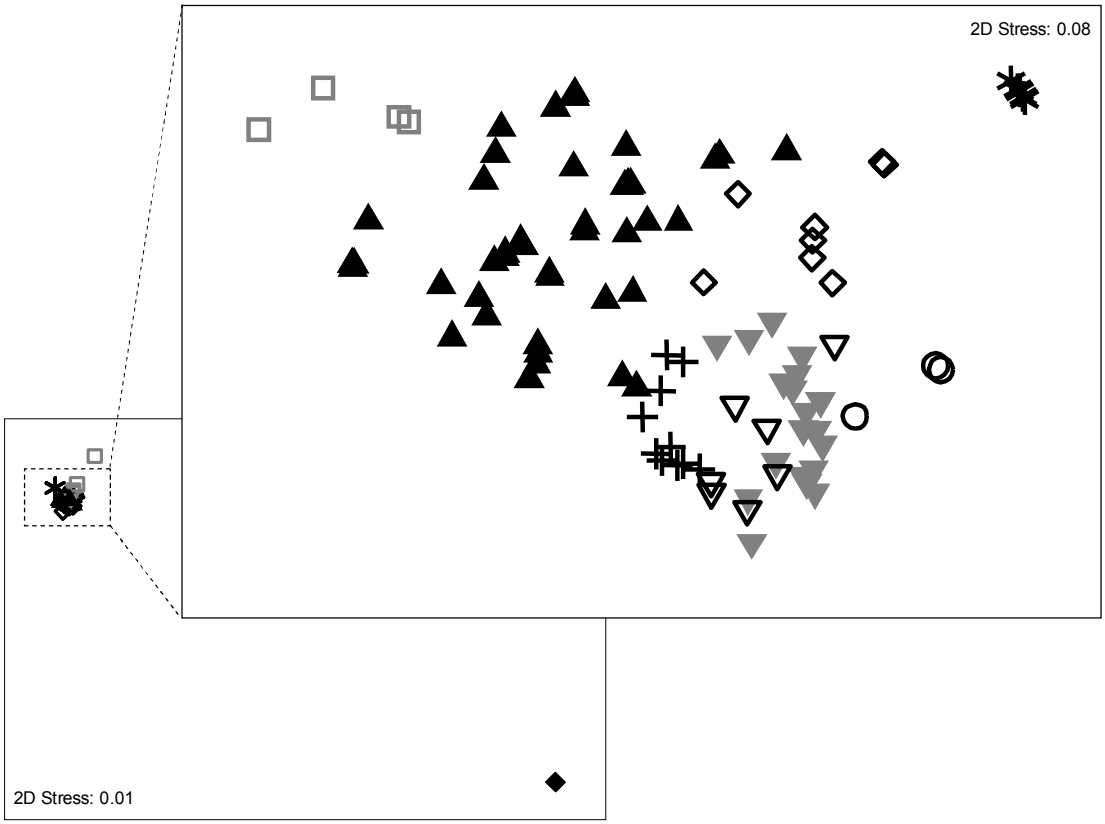

Fig. 4.4. Non-metric MDS plot for species abundance data. Group symbols are identical to Fig. 4.1. The analysis is based on 4th root transformed data and Bray-Curtis similarity. The bottom left figure is the MDS for all the samples. The upper right is a separate MDS that excluded outliers.

The faunal zones were distributed in narrow ribbons along the depth contours. Dense and narrow zones occurred at the area with the steepest topography (1000-3000m). Zone B and G occurred in bands at several depth ranges (expatriate/recurrent population). Large animals were absent between 4100 and 5300m, separating the Umbellula lindahli population in Zone H from Amphiophiura bullata population in Zone I.

Non-metric MDS (Fig. 4.4) illustrates that the faunal composition in Zone H was very different from the rest of the zones that cluster together (faunal discontinuity). There was also one station in Zone A outside of that cluster. Faunal zones were generally distinct with little overlap. The faunal composition in Zone B, C, D, E, F and G are close, while Zone A and I appear to be more different from the subgroup mentioned above. Zone E, F and G overlap to some degree. Based on the MDS plot, nine faunal zones can be lumped into 4 major depth zones with more similar faunal compositions, including a 1)shelf-transition (Zone A), 2) a continental slope & upper rise (Zone B,C, D, E, F and G), 3) the lower continental rise (Zone H) and 4) the abyssal plain (Zone I).

Table 4.1. Species contributing the most to average similarity within faunal zones. Sim% is the average Bray-Curtis similarity within a faunal zone. Abund. is the animal abundance per photo within the faunal zones. Contrib% is the percent contribution of species to the average similarity within a faunal zone. Cum% is the cumulative percent contribution.

Group	Sim%.	Species	Abund	Contrib%	Cum.%
A	41.32	*Catapagurus sharreri*	0.64	75.45	75.45
		Cidaris abyssicola	0.27	16.01	91.46
		Actinauge longicornis	0.25	8.54	100
B	25.17	*Hyalinoecia tubicola*	0.48	33.97	33.97
		Munida valida	0.42	32.9	66.87
		Parapagurus pilosimanus	0.28	14.38	81.25
		Cancer borealis	0.18	12.38	93.63
C	39.18	*Flabellum goodei*	0.68	70.52	70.52
		Cerianthis sp.	0.48	27.11	97.63
D	61.26	*Pennatula aculeata*	0.46	100	100
E	66.77	*Ophiomusium lymani*	2.09	67.11	67.11
		Ophiacanatha simulans	1.31	29.04	96.15
F	66.29	*Ophiomusium lymani*	1.32	48.56	48.56
		Anthomastus grandiflorus	1.06	48.49	97.06
G	52.16	*Ophiomusium lymani*	0.75	54.85	54.85
		Hyalonema boreale	0.73	29.36	84.2
		Pennatula aculeata	0.34	10.48	94.69
H	91.94	*Umbellula lindahli*	0.51	100	100
I	91.08	*Amphiophiura bullata*	0.55	100	100

4.5. Characteristics of Each Depth Zone

The shelf-transition communities of Zone A (267-405m), plus one outlier at 818m, are composed of the hermit crab Catapagurus sharreri, and the anemones Cidaris abyssicola and Actinauge logicornis . These three species contributed more than 90% to the within-zone faunal similarity (Table 4.1). The continental slope & upper rise communities (287-3265m), Zone B, covered most of the upper slope (287-890m), but there were two reoccurring patches at mid slope (1375-1547m) and upper rise (3428-3610m). The large tubiculous polychaete Hyalinoecia tubicola, the squat lobster Munida valida, the hermit crab Parapagurus pilosimanus and the crab Cancer borealis were the most important species. Zone C occurred on the mid slope (992-1450m), but there was one station at 620m. The cnidarians Flabellum Goodei and Cerianthis sp. explained more than 90% of average similarity within Zone C. Zone E (1500-2170m), Zone F (2440-2810m) and Zone G (2800-3265m) stretched along the lower slope to upper rise. However, Zone G had another patch which reoccurred between 1392 to 1765m, as well as one station at 4452m. The brittle star Ophiomusium lymani was the most important species in these areas, contributing about 50% or more of the average within zone similarities. Zone D was patchily distributed at three different depths (1032m, 2582m, and 3830m) where only one species (the stalked sea pen Pennatula aculeate) had been photographed. The lower rise community (3750-4050m), Zone H, was broadly distributed with only the stalked anthozoan Umbellula lindahli present in the photos. The abyssal plain community (5320-5340m), Zone I, only had a single species, the large brittle star Amphiophiura bullata. This species was also sampled at 4685 m.

4.6. Discussion

The general patterns of distributions of individual species in narrow depth bands remain the same, but the multivariate analyses reveal more nuanced information with greater confidence. Multiple sub-zones were defined with the new methods, accompanied by 'outliers', much of which was not recognized in Rowe and Menzies (1969). However, what had been called "recurrent zones" on the upper slope (majority), with repeats at mid slope and upper rise (Zone G), were confirmed in the re-assessment, as was Zone H on the mid slope and upper rise.

The new analyses illustrate that 'depth' rarely forms an immutable boundary, especially on the lower end of distributions of individual species. or of groups of species. because the assemblages in several instances appear 'out of place (depth)'. If the fauna is particularly sparse, with only one or two species occurring at frequencies of only one or two per hectare, then machine-based analyses are hardly worthwhile.

What were called "recurrent zones" on the upper slope (the 'main' population), with repeats at mid slope and upper rise (Zone G), were confirmed, as was Zone H on the mid slope and upper rise (main population). The original study was based on the distribution of individual species. The current analyses suggested the assemblages may recur as outliers at deeper depths.

CHAPTER V

BATHYMETRIC ZONATION OF DEEP-SEA MACROFAUNA IN RELATION TO EXPORT OF SURFACE PHYTOPLANKTON PRODUCTION

5.1. Overview

Macrobenthos of the deep, northern Gulf of Mexico (GoM) was sampled with box cores (0.2 m^2) along multiple cross-depth transects extending from depths of 200 m to the maximum depth of the basin at 3700 m. Bathymetric (depth) zonation of the macrofaunal community was documented for 6 major taxa (a total of 957 species) on the basis of shared species among geographic locations; 4 major depth zones were identified, with the 2 intermediate-depth zones being divided horizontally. Faunal turnover with increasing depth reflects an underlying continuum of species replacements without distinct boundaries. The zonal patterns correlated with depth and detrital particulate organic carbon (POC) export flux estimated from remotely-sensed phytoplankton pigment concentrations in the surface water. The Mississippi River and its associated mesoscale eddies, submarine canyon, and deep sediment fan appear to influence the horizontal zonation pattern through export of organic carbon from the ocean surface and the adjacent continental margin. On the local scale, near-bottom currents may shape the zonation pattern by altering sediment grain size, food availability, and larval dispersal. This study suggests a macroecological relationship between depth, export POC flux, and zonation; parsimonious zonal thresholds need to be tested independently for other continental margin ecosystems.

5.2. Introduction

The steep slopes of continental margins are among the largest environmental gradients on the planet. The rapid change of faunal composition down the continental margin has fascinated deep-sea ecologists for over a century and remains a difficult and elusive pattern to explain. Depth zonation was first noticed during the 'Challenger Expedition,' with a distinct biota on the shelves and in the abyss, and a zone of transition in between. The boundary of the faunal zone has been defined as the depth of maximum faunal change (Ekman 1953, Menzies et al. 1973). In order to distinguish boundaries between zones, as opposed to continuous replacement of species with depth, 'zonation' should be described as a non-repeating, sequential species replacement, in which all or some of the species have restricted ranges of distribution (Rex 1981, Carney et al. 1983, Carney 2005). A faunal boundary is best described as areas of rapid faunal change encompassing an area of slow faunal change across depths (Hecker 1990, Gage & Tyler 1991).

Studies of zonation in the deep sea have focused primarily on the general patterns of megafaunal assemblages (Hecker 1990, Cartes & Carrasson 2004, Wei & Rowe 2009) or distribution and abundance of a particular taxon, such as fishes (Jacob et al. 1998, Powell et al. 2003), decapod crustaceans (Cartes & Sardà 1993, Wicksten & Packard 2005), echinoderms (Howell et al. 2002), and holothurians (Billett 1991). Zonation studies on macrofaunal assemblages are relatively sparse (Grassle et al. 1979, Rowe et al. 1982, Gage et al. 2000) and have mostly dealt with individual taxa (Rex 1977, Cartes &

Sorbe 1997, Pérez-Mendoza et al. 2003, Olabarria 2005, Aldea et al. 2008). Most previous investigations were carried out along a single narrow depth transect and reported a vertical zonation across isobaths. Horizontal zonation has also been suggested, presumably due to changes in physical or chemical conditions within geographical areas (Hecker 1990).

In the Gulf of Mexico (GoM), deep-sea zonation studies have focused on the depth distribution of benthic foraminifera and megafauna trawling, with sporadic studies on benthic macrofauna. Culver & Buzas (1981, 1983) compiled published foraminifera data from 1918 to 1978 in the GoM and established Upper-Bathyal (200 to 500 m), Middle-Bathyal (500 to 1000 m), and Lower-Bathyal (1000 to 2000 m) Zones on the continental slope (Culver 1988). The prominent foraminiferan zones have been related to water masses (Culver & Buzas 1981, Denne & Sen Gupta 1991) in which the Upper-Bathyal Zone was associated with the temperature gradient, oxygen supply, and organic flux, and the Middle and Lower-Bathyal Zone were correlated with organic flux to the seafloor (Loubere et al. 1993).

Pequegnat et al. (1983) proposed 5 megafauna zones in the northern GoM, including Shelf/Slope-Transition (150 to 450 m), Archibenthal (475 to 950 m), Upper-Abyssal (975 to 2250 m), Meso-Abyssal (2275 to 3200 m), and Lower-Abyssal Zone (3225 to 3850 m). The highest faunal turnover was at 1000 m (Pequegnat et al. 1990). Gallaway (1988) merged the Abyssal Zones and then extended the Archibenthal Zone to a deeper depth of about 1350 m. The distribution pattern of macrofauna was different from the

megafauna. Both the Shelf/Slope-Transition (300 to 700 m) and Archibenthal Zone (700 to 1650 m) for macrofauna extended to deeper depths than those for megafauna, while the Abyssal Zone (2000 to 3000 m) was limited by lack of samples on the abyssal plain. A comparison between principal component analysis (PCA) classification on physico-chemical parameters and the biological classification suggested that bottom temperature, salinity, hydrocarbon level, and sediment characteristics were important factors relating to the zonation pattern of macrofauna.

The cause of depth zonation has been attributed to sunlight (or absence of), temperature, pressure, water masses, and most importantly availability of food (Carney et al. 1983, Carney 2005). The seafloor community relies on the sinking detrital carbon from the euphotic zone (Gage & Tyler 1991). The downward flux of fecal pellets or marine snow is consumed by the mid-water community and declines exponentially with depth (Suess 1980, Pace et al. 1987, Rex et al. 2006). In the northern GoM, the flux of particulate organic carbon (POC) not only declines with depth, but is 2 times higher in the northeast than in the northwest GoM (Biggs et al. 2008). The depth-dependent detritus flux from surface production has been linked to benthic standing stocks (Johnson et al. 2007) and taxon composition (Ruhl et al. 2008). However, the relationship between the export POC flux and species composition or faunal zonation is still poorly understood.

In this study, we used a broad, systematic survey to examine the zonation pattern of the entire macrofaunal assemblage with several potentially interacting communities. We propose that faunal zonation is not only taking place across isobaths, but also

horizontally from the northeast to the northwest GoM due to the influence of the Mississippi River. The horizontal productivity gradient in the northern GoM provides a unique opportunity to tease out the potential effects of food supply on zonation independent of depth by examining the relationship between zonation (species composition) and the remotely sensed export POC flux (Biggs et al. 2008), coupled with new information on bottom water properties (Jochens & DiMarco 2008), sediment geochemistry (Morse & Beazley 2008), and anthropogenic contaminants (Wade et al. 2008).

5.3. Materials and Methods

5.3.1. Sampling program

As part of the Deep Gulf of Mexico Benthos (DGoMB) study, benthic macrofauna was sampled from 2000 to 2002 (Rowe & Kennicutt 2008). A total of 51 locations from depths of 200 to 3700 m (Fig. 5.1; Appendix D Table S1) were sampled with GOMEX box cores (sampling area = 0.17 m^2; Boland & Rowe 1991). At least 5 cores were deployed at each station, and overall 271 cores were taken, which equals over 46 m^2 of seafloor sampled. The top 15 cm of sediments were sieved on a 300 μm screen. The retained material was fixed in 10% buffered formalin diluted with filtered seawater. Samples were stained with 5% Rose Bengal for at least 24 h, and then rinsed with fresh water. The stained samples were sorted into major taxonomic groups and transferred to 70% ethyl alcohol for permanent preservation. Six major macrofaunal taxa, including amphipods (analyzed by J.M.F. and Y.S.), aplacophorans (A.H.S.), bivalves (M.K.W.,

R.D., and M.C.), cumaceans (I.P.), isopods (G.D.F.W.), and polychaetes (G.F.H. and Y.W.), were separated into 957 putative species (27% named species and 73% undescribed species) by the named taxonomists.

5.3.2. Environmental data selection

Not all environmental data had complete coverage in our study area. Only the data that covered more than 90% of the sites and were not auto-correlated (Pearson's correlation, $\rho < 0.9$) were retained for the analysis. A total of 12 variables including depth, export POC, temperature, salinity, dissolved oxygen, fluorescence, backscatter, particulate material, percent sand, percent silt, percent clay, total polycyclic aromatic hydrocarbons (PAHs; Table 5.1) and 16 trace metals (Al, Ba, Be, Ca, Cr, Cu, Fe, Mg, Mn, Na, Ni, Si, Sr, Ti, V, and Zn) were retained. Export POC flux to the seafloor was calculated using an exponential decay model (flux [z] = $3.523 \times \text{NPP} \times z^{-0.734}$), where z = depth and NPP = satellite-based net primary production (Pace et al. 1987). Detailed methodology can be found in Biggs et al. (2008). The complete list of environmental and macrofauna data are archived in the U.S. Department of the Interior, Minerals Management Service and the Ocean Biogeographic Information System (OBIS).

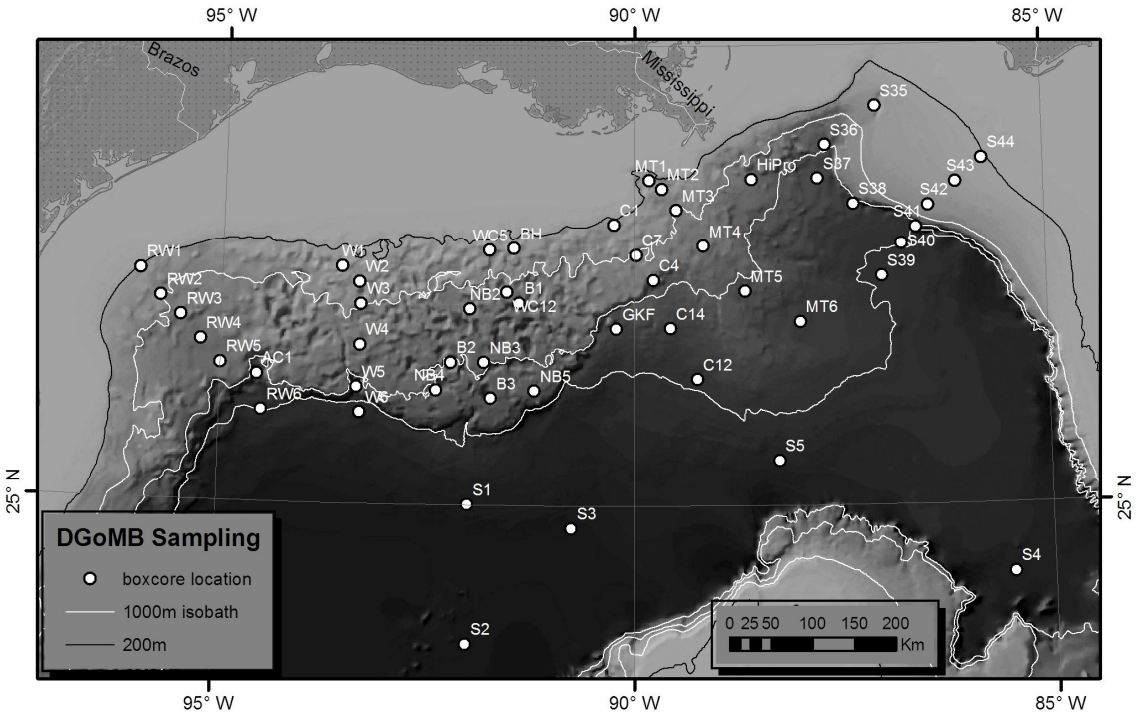

Fig. 5.1. Box core locations during the Deep Gulf of Mexico Benthos (DGoMB) study. Black line: 200 m, white lines: 1000 m isobaths. Abyssal plain sites (S1 to S5) sampled in summer 2002. Other slope sites sampled in summer 2000 and partially re-visited in summer 2001. Derived from French & Schenk (2006).

5.3.3. Data analysis

Bray-Curtis similarity (Bray & Curtis 1957) was calculated on 4th-root transformation of average species abundance per box core to define relationships of the faunal composition between all sites (Clarke & Warwick 2001). The purpose of this transformation is to accentuate the effect of rare species. The intra-location resemblance was subjected to group-average linkage cluster analysis. A similarity profile test (SIMPROF) was performed on a null hypothesis that a specific sub-cluster can be recreated by permuting the entry species and samples. The significant branch (SIMPROF, $p < 0.05$) was used as a prerequisite for defining the faunal zones.

Non-metric multidimensional scaling (MDS) was conducted on the resemblance matrix to examine the sample relationship on a 2-dimensional plane. The average similarities within a faunal zone and dissimilarity between faunal zones were broken down to similarity percent contribution (SIMPER) of each species. The species that contributed the most within the zone and species that discriminate 1 zone from another were examined as characteristics of the faunal zones.

The environmental data were logarithm transformed, normalized (divided by standard deviation), and computed for Euclidean distances. The intra-location distances were used as a proxy to characterize the seafloor environment and correlated with the intra-location faunal resemblance using Spearman's rank correlation (RELATE). A principal component analysis (PCA) was conducted on the environment distance matrix to examine the relationship of the seafloor properties among the biotic zones. The 10 best

subsets of environmental variables (highest correlations with faunal resemblance) were selected from all possible combinations (BIO-ENV).

One-way ANOSIM was performed on the same distance matrix to test the null hypothesis that the multivariate environmental data were not different in the pre-defined faunal zones. The test statistic R (usually between 0 and 1) is a measurement of the degree of group separation. To avoid a Type 1 error, the ANOSIM pairwise comparisons between faunal zones employed a high level of significance (p value = 1%).

The best subset of variables determined by BIO-ENV was subjected to a constrained type of cluster analysis (LINKTREE) on the same set of faunal resemblance. The dendrogram was constructed by successive binary partitions of biotic community samples. Each division was determined by a threshold on 1 of the environmental variables that maximized the between-group variance (largest ANOSIM R statistic). The binary split was continued until SIMPROF suggested the new branch was not significant ($p > 0.05$).

The multivariate zonation and environmental analyses were conducted using PRIMER v6 (Clarke & Warwick 2001, Clarke et al. 2008). Bathymetric maps were generated using ArcGIS 9.0.

5.4. Results

5.4.1. Zonation pattern and faunal distribution

Hierarchical cluster analysis and SIMPROF revealed 13 significant groups (Fig. 5.2, $p < 0.05$), which can be categorized as 6 faunal zones (Zones 1, 2E, 2W, 3E, 3W, 4) and 2 independent locations (GKF and WC5). Zones 1, 2 (including 2E and 2W), 3 (including 3E and 3W), and 4 were separated at the 25% similarity level; Zones 2E and 2W were separated at the 30% similarity level; and Zones 3E and 3W were separated at the 29% similarity level. Due to the low faunal similarities with other stations (20.1 to 22.6%), the independent stations were not included in any faunal zone. The MDS ordination (Fig. 5.3, stress = 0.17) reflects an underlying continuum without distinct zonal boundaries along the depth gradient. The negative direction of the x-axis follows from the shallow toward the deeper faunal zones. The y-axis separates Zone 2E from 2W and Zone 3E from 3W. Zones 2E, 3E, and the east side of Zone 4 (sites S39, S40, and S4) were closer to Zone 1 than their western counterparts, indicating that the species composition of the eastern faunal zones, or the east side of Zone 4, was shifted to resemble Zone 1. The assignment of Hipro to Zone 1, MT3 to Zone 2E, and S39 to Zone 4 may seem somewhat arbitrary in the 2D MDS ordination (Fig. 5.3). However, a more detailed 3D MDS ordination (3D stress = 0.13) confirmed that the cluster analysis (Fig. 5.2) allocated the faunal zones properly. Based on the results of cluster analysis and MDS, a map of deep-sea macrofaunal zones in the northern GoM can be generated (Fig. 5.4) in

which the zones are separated by proposed boundaries. Note that WC5 and GKF are independent and do not belong to any zones.

Zone 1 was a narrow ribbon extending from 213 to 542 m with an apparent submergence to 1572 m at Hipro. Zone 2 was separated into an east (Zone 2E, 625 to 1828 m) and west subzone (Zone 2W, 863 to 1620 m). Zone 3 was separated into 2 subzones with the east zones (Zone 3E, 2275 to 3314 m) extending deeper than the west zone (Zone 3W, 2042 to 3008 m). Zone 3W covered the most complex bathymetric features in northern GoM, including the Alaminos Canyon (AC1), basins (B1-2), non-basins (W5, NB3-5), and the base of the Sigsbee Escarpment (RW6). However, these sites showed no indication that they affected the zonal distribution (no significant groups). Zone 4 (2954 to 3732 m) occupied the abyssal plain (S1–S4) and the base of the Florida Escarpment (S39, S40).

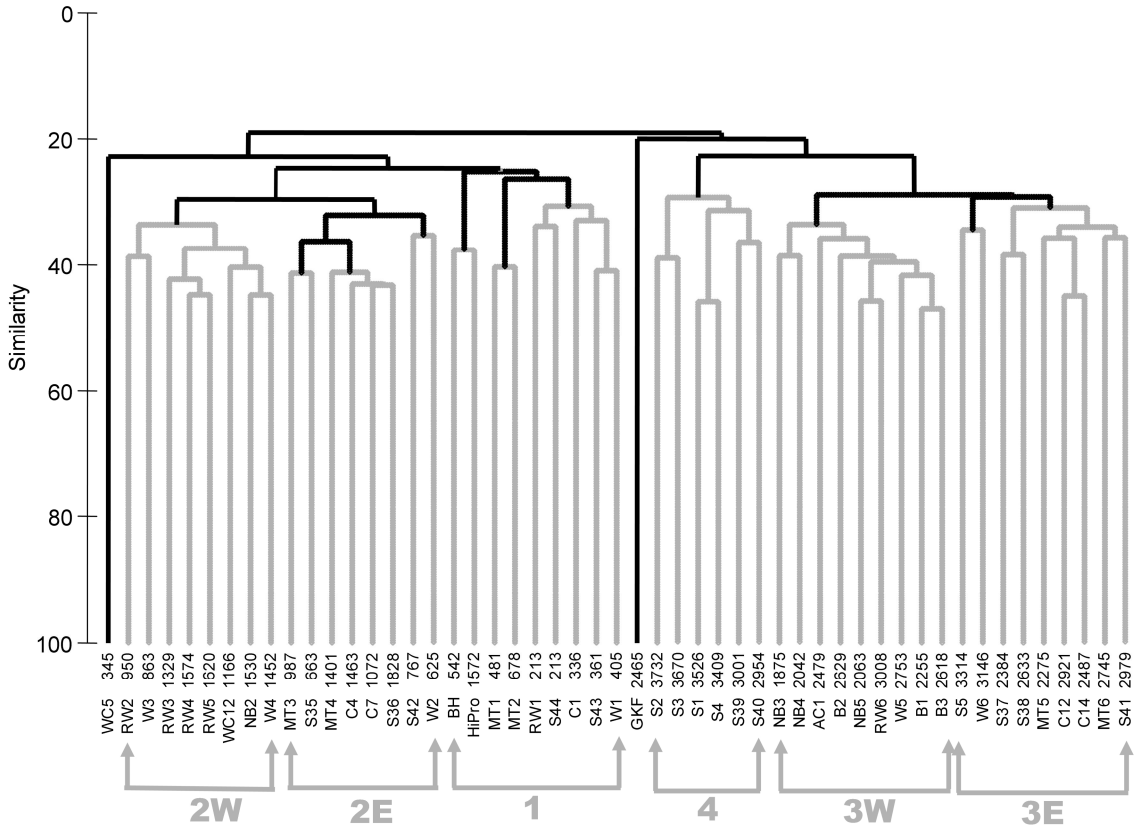

Fig. 5.2. Group-average cluster analysis on faunal resemblance. The abundance of each species was 4th-root transformed before calculating Bray-Curtis similarity. Black branches indicate significant faunal groups where the similarity profile (SIMPROF) test ($p < 0.05$) suggested that the structure is not random. The x-axis shows faunal zones, station name, and sampling depth (m). The y-axis shows Bray-Curtis similarity (%).

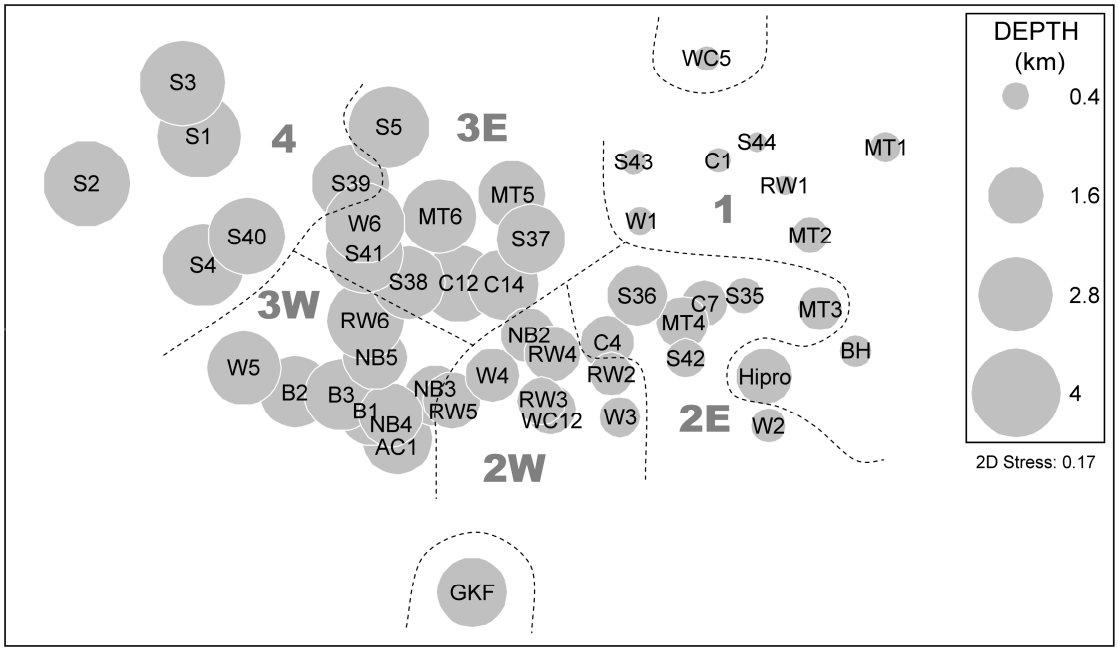

Fig. 5.3. Non-metric multidimensional scaling (MDS) ordination of Bray-Curtis faunal similarity. The faunal similarity between sites is represented by the relative distance. Bubble size shows relative water depths. Faunal zones are separated by dotted lines.

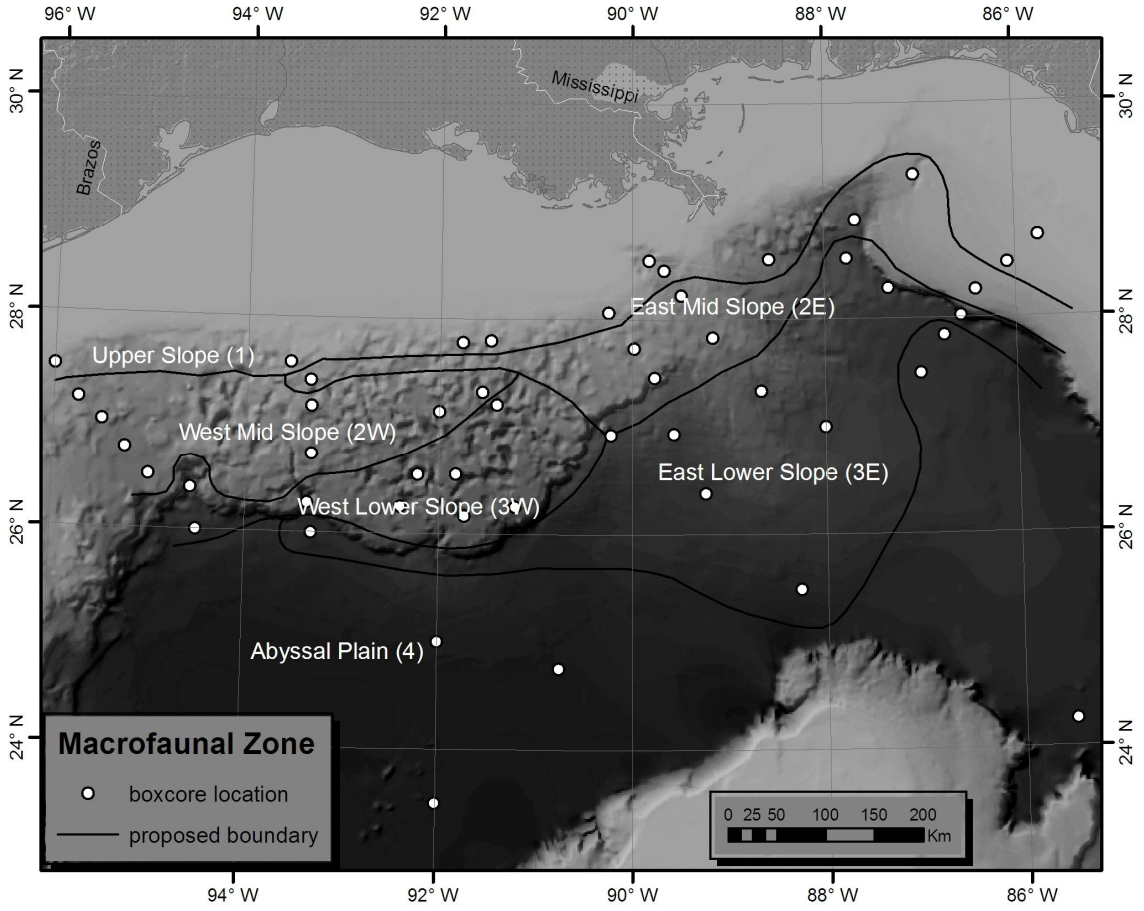

Fig. 5.4. Locations and extent of macrofaunal zones determined by cluster analysis (see Fig. 5.2). The proposed boundaries (thick black lines) follow the midpoints between 2 adjacent zones. WC5 and GKF are not included in any faunal zone. Maps derived from French & Schenk (2006).

The 5 species contributing the most to each faunal zone are shown in Appendix D Table S2, based on SIMPER, and Appendix D Table S3, based on abundance. In Zone 1, the 5 most dominant species that accounted for 53.9% of abundance contributed only a total of 5% to the average similarity. For example, the most abundant species of amphipod, *Ampelisca mississippiana*, occurred mostly in Zone 1 and was relatively sparse in Zones 2W, 2E, and 3. However, 99% of the specimens (15851 individuals m^{-2}) were only found at the head of the Mississippi Canyon (MT1), suggesting a patchy distribution (Soliman & Wicksten 2007). In Zones 2E, 2W, 3E, 3W, and 4, the species that contributed the most to the average similarities and to abundance were largely repeated; thus, the dominant species were more evenly distributed. Some species made large contributions to average faunal similarities in more than 1 faunal zone. In other words, zonation was less obvious. For example, the polychaete *Tharyx marioni* was important to Zones 1, 2W, and 3E; the bivalve Heterodonta sp. B contributed largely to Zones 3E, 3W, and 4; and the polychaete *Aricidea suecia* contributed significantly to Zones 1, 2E, and 2W. Two polychaetes (*Levinsenia uncinata*, *Paraonella monilaris*) were important species in the most faunal zones, with the former contributing to Zones 1, 2E, 2W, and 3W and the latter to Zones 2W, 3W, 3E, and 4. One of the characteristic species in Zone 4, the bivalve *Vesicomya vesica*, has been considered an indicator for cold-seep communities (Sibuet & Olu 1998). To our surprise, this species was distributed throughout our sampling area (in 29 out of 51 locations), even on the abyssal plain.

SIMPER was also performed to break down the average dissimilarity between independent stations and their adjacent faunal zones (Appendix D Table S4). The species

that only appeared in GKF but not in Zones 3W or 3E seemed to contribute extensively to the dissimilarity between GKF and the adjacent zones. Between Zone 1 and WC5, 2 polychaete Prionospio species had the highest contributions to the average dissimilarity. Most species that had high contributions to the dissimilarities were more abundant in WC5 than in Zone 1.

In the SIMPER analysis, polychaete species appeared to be the most important taxon. The importance of bivalve species, however, increased from Zones 3E and 3W toward the deeper Zone 4 (Appendix D Table S2, Fig. 5.5). The isopods were the third most important taxon, with the contribution increasing slightly across Zone 1 to Zone 4.

The species can also be categorized based on the breadth of their distribution with depth, with ‘stenozonal’ species occupying narrow ranges and ‘euryzonal’ species occupying broad ranges. The stenozonal species restricted to a single zone can then be compared to the euryzonal species that co-occurred throughout all zones, and the slope species that co-occurred in Zones 1, 2E, 2W, 3E, and 3W (Fig. 5.6). Zones 1 and 2E had the most stenozonal species and the fewest euryzonal species, whereas Zones 3W and 4 had the most euryzonal species and fewest stenozonal species. The combination of the slope and euryzonal species accounted for 26% to 40% of the species in Zones 3E, 3W, and 4, suggesting that species with wide ranges dominated the lower slope and abyssal plain.

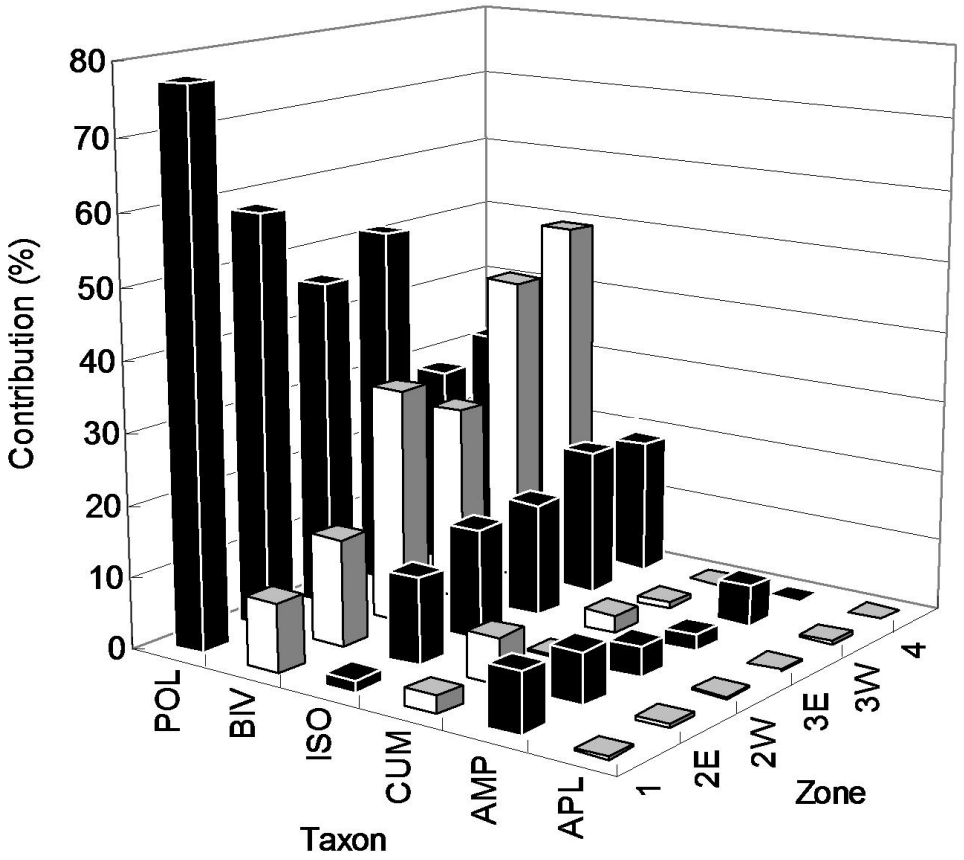

Fig. 5.5. Percent taxon contribution to faunal zonation based on similarity percent contribution (SIMPER) analysis. The average Bray-Curtis similarities within faunal zones were broken down to percent contributions for polychaetes (POL), bivalves (BIV), isopods (ISO), cumaceans (CUM), amphipods (AMP), and aplacophorans (APL).

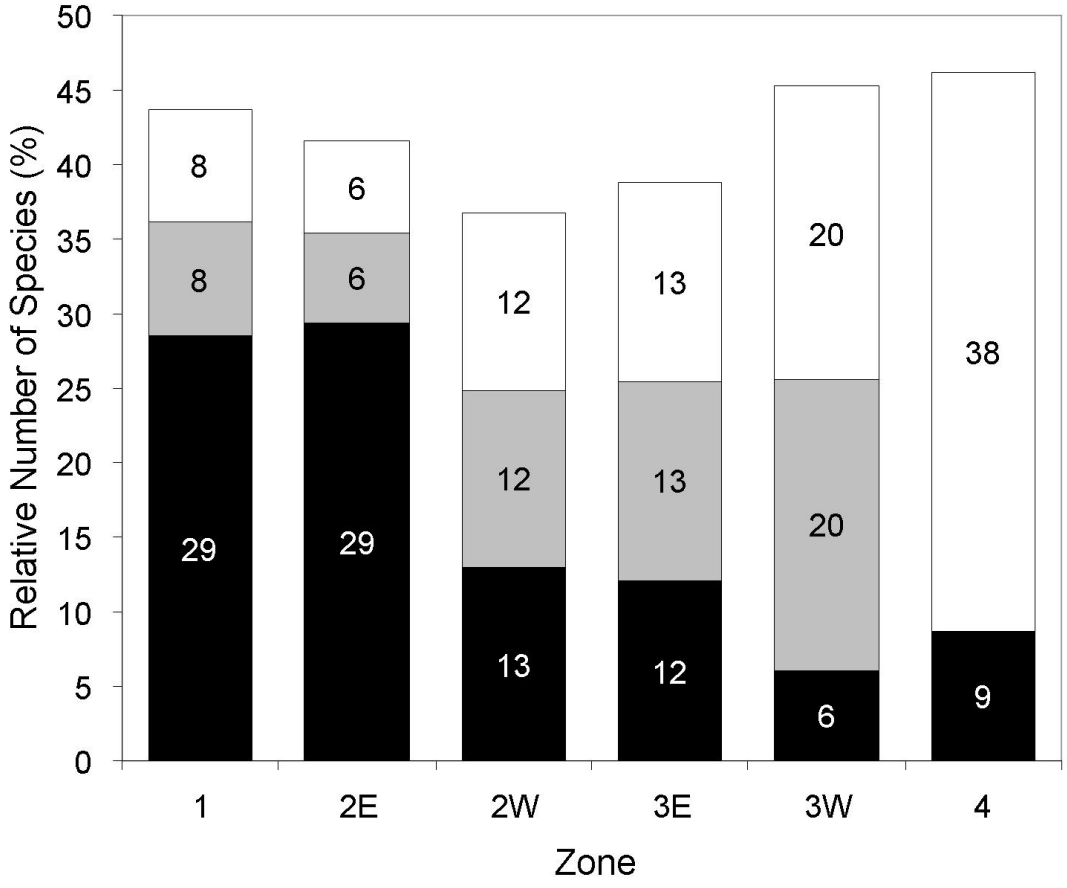

Fig. 5.6. Number of euryzonal, slope, and stenozonal species relative to the total numbers of species in each zone. Black, gray, and white bars indicate the percentages of stenozonal, slope, and euryzonal species, respectively.

5.4.2. Linking environmental variables to faunal zonation

The trace metals were reduced by PCA to 2 principal component (PC) axes (78.5% of total variance explained). PC1 had roughly equal contributions from Ca, Be, Al, Ti, Zn, Fe, V, Cr, Si, Ba, Mg, Mn, and Ni. PC2 was dominated by Cu and Sr, as well as other lesser important elements, including Na, Ni, Ca, Ba, and Mg. The trace metal PC1 (MET1) and PC2 (MET2) were then combined with the other 12 variables (Table 5.1). One-way ANOSIM suggested that the multivariate environmental data were significantly different among the faunal zones ($R = 0.33$, $p < 0.001$) and the pairwise tests were significant between most pairs of zones ($p < 0.01$). A PCA of the 14 environmental variables showed a continuous change of seabed properties with slightly overlapping stations between the adjacent zones (Fig. 5.7). The first 2 PC axes explained 72.1% of the total variance. MET1 dominated the PC1 axis. MET2, depth, and dissolved oxygen had the highest positive loading on the PC2 axis, while export POC flux and temperature had the largest negative loadings.

The intra-location distance of 14 environmental variables had a significant correlation with faunal resemblance (RELATE, $\rho = 0.44$, $p < 0.001$). The individual correlation (RELATE) on each variable suggested that the export POC flux had the highest correlation with the faunal resemblance matrix ($\rho = 0.70$, $p < 0.001$), followed by water depth ($\rho = 0.67$, $p < 0.001$) and the other 8 variables (Table 5.1). The total PAH concentration, relative backscatter, particulate material concentration, and percent clay content were not significantly correlated with the faunal resemblance ($p > 0.05$). The

best subsets of environmental variables were combinations of export POC flux, depth, relative fluorescence, dissolved oxygen, MET2, percent sand, and temperature (Table 5.2).

When the RELATE analysis was restricted to the zones of similar depths, such as the subzones of Zones 2 or 3 (Table 5.3), the export POC flux remained the most important correlate of faunal resemblance for Zone 2 ($\rho = 0.51$, $p < 0.001$) and for Zone 3 ($\rho = 0.27$, $p = 0.01$), while depth fell to the 4th best correlate for Zone 2 ($\rho = 0.38$, $p = 0.02$) and the 6th best correlate for Zone 3 ($\rho = 0.18$, $p = 0.04$). The top 6 environmental variables for Zones 2 and 3 (Table 5.3) were plotted against the respective subzones (Fig. 5.8). A Student's t-test suggested that out of 6 variables, only the export POC flux ($t = 2.60$, $df = 9.03$, $p = 0.03$) was significantly different between Zones 2E and 2W (Fig. 5.8a). Between Zones 3E and 3W, percent sand content ($t = 2.29$, $df = 8.37$, $p < 0.05$) and MET1 ($t = 2.24$, $df = 12.25$, $p = 0.04$) were significantly different (Fig. 5.8i & k). The concentration of Ca was significantly higher in Zone 3E than in Zone 3W ($t = 2.30$, $df = 13.63$, $p = 0.04$). The concentrations of Al, Ba, Be, Cr, and Mg were significantly lower in Zone 3E than in Zone 3W (t-test, $p < 0.05$). However, none of the trace metals was considered to be in high enough concentration to adversely affect the benthic biota (Wade et al. 2008). The high correlation of trace metals to faunal resemblance might be a result of collinearity between trace metals and the silt-clay fraction nearshore.

Table 5.1. RELATE tests on the selected environmental data. A Spearman rank correlation coefficient was calculated between individual variables and faunal similarity. POC: particulate organic carbon, PAH: polycyclic aromatic hydrocarbon, PDR: precision depth recorder.

Variable	ρ	p	Description	Gear
POC	0.697	<0.001	Export POC flux (mg-C $m^{-1}d^{-1}$)	SeaWifs satellite
DEP	0.671	<0.001	Water depth (km)	PDR
SAL	0.451	<0.001	Salinity (psu)	CTD
MET2	0.446	<0.001	Trace metal principal component 2	Box core
DO	0.415	<0.001	Dissolved oxygen (ml l^{-1})	CTD
TEM	0.394	<0.001	Potential temperature (°C)	CTD
MET1	0.262	<0.001	Trace metal principal component 1	Box core
FLU	0.232	<0.001	Relative fluorescence (volts)	CTD
SAN	0.177	0.003	Percent sand (%)	Box core
SIL	0.12	0.019	Percent silt (%)	Box core
PAHs	0.062	0.14	Total PAH with perylene (μg g^{-1})	Box core
BAC	0.039	0.23	Relative backscatter (mg l^{-1})	CTD
PM	-0.002	0.482	Particulate material (mg l^{-1})	Niskin bottle
CLA	-0.025	0.635	Percent clay (%)	Box core

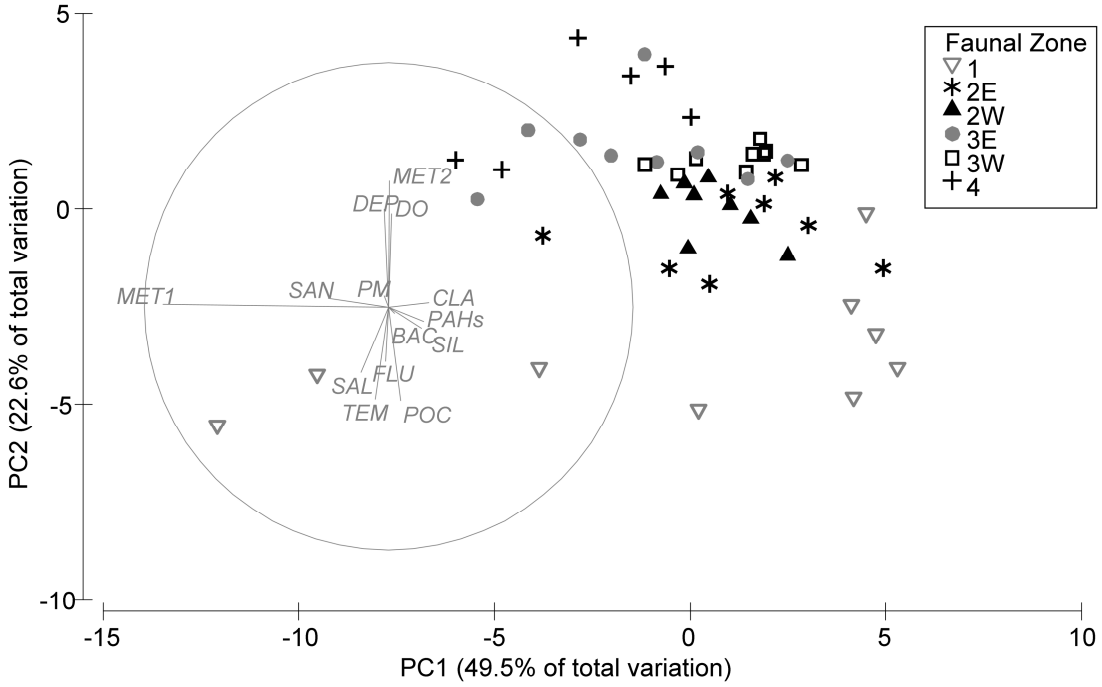

Fig. 5.7. Principal component analysis (PCA) of all 14 environmental variables. The environmental data were logarithm transformed and normalized before computing Euclidean distances. The symbols indicate the faunal zones indentified by cluster analysis (see Fig. 5.2).

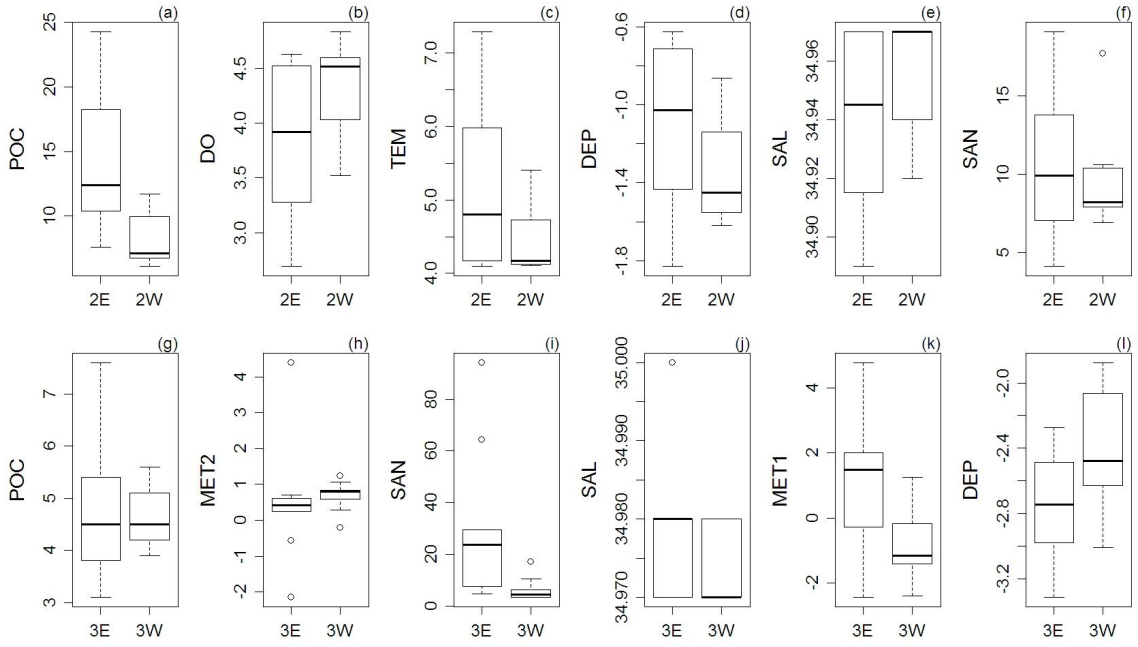

Fig. 5.8. Zones 2E and 2W for (a) export POC flux, (b) dissolved oxygen, (c) temperature, (d) depth, (e) salinity, and (f) percent sand; and Zones 3E and 3W for (g) export POC flux, (h) trace metal PC2, (i) percent sand, (j) salinity, (k) trace metal PC1, and (l) depth. The thick line indicates median; lower and upper hinges indicate 25% and 75% quartiles; whiskers indicate the minimum and maximum values; open circles indicate outliers.

The water depth and export POC flux were selected by BIO-ENV as the optimal subset of variables that gave the best match to faunal resemblance ($\rho = 0.722$). LINKTREE analysis was conducted for 49 sites (Fig. 5.9). Even though the export POC flux was selected as the best individual variable by RELATE (Table 5.1), water depth occupied more divisions (11 times) than export POC flux (8 times) in LINKTREE. Generally, the natural grouping in the LINKTREE matched the pre-defined zones (Fig. 5.2). In Fig. 5.9, the matched sites are highlighted (bold letters) and the names of the respective faunal zones (gray text boxes) are underneath each group. The first split (A) was explained by depth, separating the Sigsbee Abyssal Plain (S1, S2, S3, depth ≥ 3.51 km) from the rest of the sites (depth ≤ 3.41 km). It is also a natural division on the MDS ordination (Fig. 5.3). The export POC flux determined the second split (B) and obliquely divided the northern GoM in half. The right partition (POC flux ≥ 10.3 mg C m^{-2} d^{-1}) includes the upper and east mid-slope (Zones 1 and 2E). The left partition (POC flux ≤ 9.5 mg C m^{-2} d^{-1}) includes the lower and west mid-slope (Zones 2W, 3E, and 3W) as well as 2 deep sites at the central (S5) and the southeast GoM (S4). The third split (C) suggests that the abyssal plain community (Zone 4) is best defined by depth ≥ 3.31 km or POC flux ≤ 3.1 mg C m^{-2} d^{-1}. The communities on the lower and west mid-slope (Zones 2W, 3E, and 3W) fell within the POC flux range between 3.7 and 9.5 mg C m^{-2} d^{-1}. A range of characteristic environmental variables can be generated for each zone as the binary division proceeds (Table 5.4). However, the natural grouping in LINKTREE is not identical to the original dendrogram (Fig. 5.2). The detailed environmental threshold in each zone should be considered a parsimonious explanation.

Table 5.2. BIO-ENV analysis, showing that the 10 best subsets of environmental variables give the highest correlations in the RELATE test. The Spearman rank correlation coefficient was calculated between the subset of variables and faunal similarity. Variables are defined in Table 5.1.

Correlation (ρ)	Variables
0.722	DEP, POC
0.715	DEP, POC, FLU
0.697	POC
0.687	DEP, POC, DO, FLU
0.681	DEP, POC, FLU, MET2
0.68	DEP, POC, MET2
0.679	DEP, POC, DO, FLU, MET2
0.679	DEP, POC, FLU, SAN
0.676	DEP, POC, TEM, FLU
0.674	DEP, POC, DO, FLU, SAN

Table 5.3. RELATE tests restricted to Zone 2 (E and W) or Zone 3 (E and W) on the selected environmental data. A Spearman rank correlation coefficient was calculated between individual variables and faunal similarity of Zone 2 or Zone 3. Variables are defined in Table 5.1.

Zones 2E & W			Zones 3E & W		
Variable	ρ	p	Variable	ρ	p
POC	0.511	<0.001	POC	0.27	0.008
DO	0.437	<0.001	MET2	0.257	0.024
TEM	0.437	<0.001	SAN	0.25	0.012
DEP	0.38	0.002	SAL	0.232	0.037
SAL	0.283	0.011	MET1	0.195	0.034
SAN	0.24	0.026	DEP	0.178	0.043
BAC	0.223	0.020	FLU	0.173	0.059
CLA	0.216	0.023	BAC	0.109	0.182
SLT	0.168	0.058	CLA	0.095	0.237
MET1	0.134	0.144	PM	0.08	0.259
PAHs	0.107	0.158	SLT	0.047	0.355
MET2	0.068	0.286	TEM	-0.041	0.650
PM	0.047	0.339	PAHs	-0.068	0.702
FLU	0.025	0.375	DO	-0.116	0.882

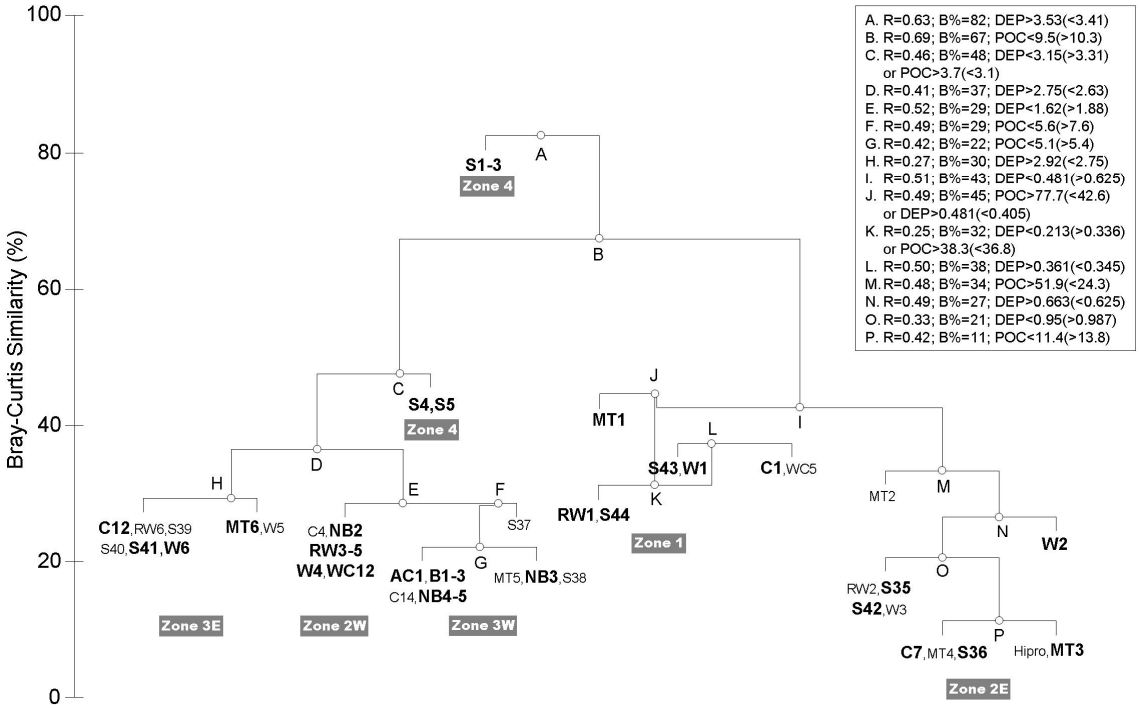

Fig. 5.9. Linkage tree analysis (LINKTREE), showing binary clustering of sites based on species composition and constrained by the threshold of water depths (km) or export particulate organic carbon (POC) fluxes (mg C m^{-1} day^{-1}). An optimal ANOSIM R value (largest group separation) was selected from all possible divisions between any 2 environmental values. The successive division stopped when a similarity profile (SIMPROF) test suggested that the branch was not significant ($p > 0.05$). The stations matched to the pre-defined faunal zones (gray text boxes) are highlighted in bold. In the text box key, each division (A, B, C...) is followed by an ANOSIM R value, Bray-Curtis similarity (B%), and a range of environmental values explaining the division. The first inequality defines the branch to the left and the second inequality (in brackets) indicates the branch to the right.

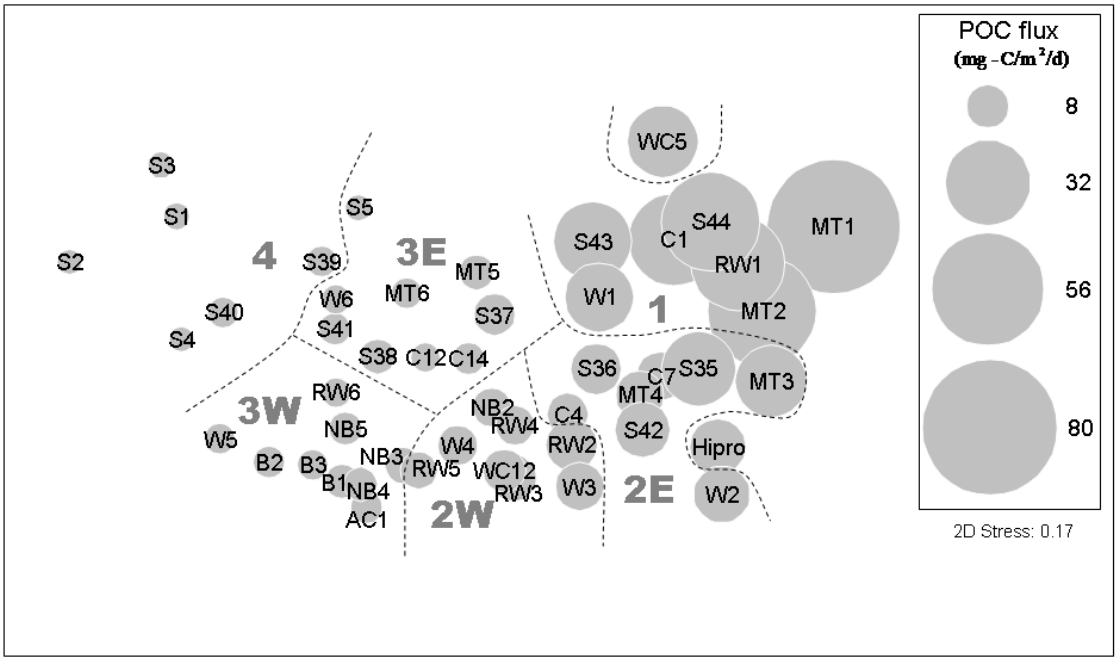

Fig. 5.10. Non-metric multidimensional scaling (MDS) ordination of the Bray-Curtis faunal similarity. The faunal similarity between sites is represented by the relative distance. Bubble size shows the relative export particulate organic carbon (POC) flux. Faunal zones are separated by dotted lines.

Table 5.4. Thresholds of water depths (km) or export particulate organic carbon (POC) flux (mg C m^{-1} d^{-1}) in each faunal zone based on LINKTREE analysis. DEP: water depth (km).

Faunal zones	Environmental thresholds	Division
Upper slope (Zone 1)	POC ≥10.3 and DEP ≤0.481	Split I to left
East mid-slope (Zone 2E)	10.3≤ POC ≤24.3	Split M to right
West mid-slope (Zone 2W)	3.7≤ POC ≤9.5 and DEP ≤1.62	Split E to left
West lower slope (Zone 3W)	3.7≤ POC ≤5.6	Split F to left
East mid-slope (Zone 3E)	3.7≤ POC ≤9.5 and DEP ≥2.75	Split D to left
Abyssal plain (Zone 4)	DEP ≥3.31 or POC ≤3.1	Split C to right

The environmental variables were superimposed on the MDS ordination with the size of the bubble denoting the magnitude of a given environmental value. A distinct zonal pattern was observed for the export POC flux, with clear between-zone and small within-zone variation (Fig. 5.10). Water depth was highly correlated ($\rho = 0.67$, $p < 0.001$) with faunal resemblance, but no difference was apparent between the east zones (2E, 3E) versus west zones (2W, 3W). The higher export POC flux to Zone 2E than to 2W may be important in explaining horizontal zonation.

5.5. Discussion

The separation of east and west zones on the mid- and lower slope suggested a horizontal zonation caused by an east-west environmental gradient. Evidence that included a significantly distinct faunal group at the head of the Mississippi Trough (MT1 and MT2), a submergence zone on the eastern, upper slope (Hipro) and central GoM (S5), as well as a shift in faunal composition in the east faunal zones toward one that more closely resembled the upper-slope community, also suggests a potential influence of the Mississippi River and the adjacent canyon. In the summers, mesoscale eddies can generate cross-margin flows and move low-salinity, high-chlorophyll Mississippi River water off the shelf into the deep eastern GoM, which can lead to high POC input to the seabed (Biggs et al. 2008, Jochens & DiMarco 2008). This input was evident for the mid-slope zones, where the export POC flux was significantly higher in Zone 2E than in Zone 2W. On the lower slope zones, the east-west difference of export POC flux was not evident. The satellite-based export POC, however, only estimated the pelagic source of

sinking POC from plankton. The labile sedimentary organic matter originating from the Mississippi River plume can also be rapidly transported through the upper Mississippi Canyon via turbidity flows or mass wasting processes (Bianchi et al. 2006) and potentially to the lower part of the Mississippi Canyon and sediment fan (Balsam & Beeson 2003, Morse & Beazley 2008). This lateral or down-slope transport of organic carbon can contribute a substantial fraction of the total POC input to the deep GoM basin (Rowe et al. 2008a). In fact, on the lower part of the Mississippi Sediment Fan (S5), macrofaunal biomass was more than 5 times higher than the adjacent abyssal sites at similar depths (Rowe et al. 2008b), while the export POC flux (Biggs et al. 2008) did not indicate any difference. The submergence of Zone 3E on the lower Mississippi Sediment Fan suggests that the depth-dependent decay model (Pace et al. 1987) may underestimate export POC flux. Lateral down-slope transport of material can be added to the estimate of export POC flux as suggested by Rowe et al. (2008a), and this addition would influence the east-west difference observed on the lower slope.

An unusual feature of Zones 2E and 3E is a narrow extension to the western GoM (Fig. 5.4). The extension of Zone 2E coincides with a continuous band of fine-grained Mississippi sediment extending west along the outer shelf and upper slope (Balsam & Beeson 2003). The extension of Zone 3E coincides with intensified bottom currents that propagate westward along the base of the Sigsbee Escarpments (Hamilton & Lugo-Fernandez 2001, Oey & Lee 2002). These are high-speed (9 km d–1) and short-period (peak spectra lasting 10 to 14 d) continuous bottom currents that may transport organic material in the deep GoM basin (Jochens & DiMarco 2008), potentially from the lower

Mississippi Canyon and sediment fan to the western GoM along the escarpment. Likewise, such near-bottom currents can support larval transport and recruitment. This transport may also affect sediment dispersal along the Sigsbee Escarpment (Balsam & Beeson 2003).

The low faunal association (similarity < 50%, Fig. 5.2) may reflect an inevitable sampling error and underestimation of diversity inherent in box coring. However, unlike earlier studies of single taxa or which included only the more common species in the analysis, we analyzed the complete macrofaunal community.

WC5 and GKF were not included in our defined faunal zones. Nonetheless, these distinct sites may contain important information on the linkage between the environment and the faunal composition. The polychaete *Prionospio cristata* dominated WC5 (48.3% of total abundance) and contributed the most difference between WC5 and the adjacent Upper-Slope Zone (Appendix D Table S4). All sites with *P. cristata* had high silt (>33.9%) and clay (>47.1%) material, which supports the previous observations that the genus *Prionospio* is a suspension/deposit feeder that occurs in soft muddy sediments (Jumars & Fauchald 1977, Fauchald & Jumars 1979). In fact, WC5 had 1 of the highest silt (44.5%) and clay contents (49.9%) of the sites sampled. However, several sites (MT4, Hipro, and GKF) with similar silt (44.5~45.5%) and clay (45.5~52.9%) contents did not include any P. cristata, probably due to the greater depth and potentially lower POC input. P. cristata was not encountered at WC5 during a previous study (Gallaway 1988). Three Prionospio species contributed only 0.9% of the total abundance in WC5. The

dominant species in the previous study was *Litocorsa antennata* (18.2% of the total abundance). In contrast, L. antennata was not encountered at WC5 in the current study. A dramatic change of sediment content might explain the difference, because the silt content at WC5 was only 18.6% in the previous study (Gallaway 1988).

The furrow formations in GKF were recently discovered on the sea floor at the base of Green Knoll. These mega-furrows are 5 to 10 m deep and 10 to 30 m wide, oriented parallel to the Sigsbee Escarpment, and are believed to be associated with strong near-bottom currents (Bean et al. 2002). The distinct species composition is possibly related to the unique geological feature and high-energy environment.

The presence of relatively few stenozonal species and more euryzonal species on the West Lower-Slope (Zone 3W) and Abyssal Plain Zone (Zone 4) suggests that the benthic community in the Abyssal Plain Zone represents an extension of a subset of the slope species. Similar patterns were also reported for isopods with large depth ranges cutting across zones (Wilson 2008). Rex et al. (2005) proposed a source-sink dynamics model to explain abyssal plain diversity, in which the populations are regulated and sustained by energy constraints and immigration from the continental margin. This hypothesis may explain the high contribution of bivalve species to the average faunal similarity in the Abyssal Plain Zone, since their planktonic, lecithotrophic larvae (Zardus 2002) would provide a dispersal advantage over the slope-dominated polychaete species, which are mostly brooders (Young 2003). The success of bivalves may also be due to the deposit feeding mode and the high gut to body volume ratio, which increases the

sediment retention time and thus allows more complete conversion and absorption of sparse labile organic materials (Gage & Tyler 1991). Wilson (2008) proposed that the semi-enclosed GoM basin may have experienced a Holocene extinction event that exterminated the deeper living fauna below the sill depth of 2000 m. Under this scenario, the fauna of the Caribbean Basin would have repopulated the GoM from above the sill depth to the south. This is consistent with the observation that the midpoints of most isopod depth ranges (79.4%) are above 2000 m (80.9% to 93.3% for the other taxa). The observed broad depth ranges of much of the fauna could then be related to ongoing process of migration to the deeper sections of the GoM.

Negative branches were observed at Split J and Split L in the LINKTREE analysis (Fig. 5.9). Clarke et al. (2008) explained the reversal as an indication that some needed explanatory variable is lacking. For example, based on a natural, non-constrained split, MT1 should be separated at Split I from the rest of the samples, due to its unique faunal composition. However, the only 2 variables included in the LINKTREE, depth and POC flux, were not able to explain this split. As a result, a less natural split (lower B%) was made prior to the more natural split (higher B%).

The calculation of export POC flux incorporates surface production with a depth-dependent function (Pace et al. 1987). This method creates a spurious relationship between the export POC flux and any variable that is correlated with depth. However, our study suggests that the export POC flux is not only significantly correlated with the overall zonation pattern, but is the best correlate of faunal resemblance for mid- or lower

slope at similar depths. For the first time, the relationship between the export POC flux and faunal zonation is distinguished independent of the depth effect.

The macroecological relationship between POC flux, water depth, and zonation presented here is a correlative approach. Causality can only be confirmed unambiguously by testing the relationship independently at other locations, such as the southern GoM or other continental margins (Kerr et al. 2007). In 2008, approximately 72% of GoM's oil production came from wells at depths greater than 300 m, and the numbers of ultra-deep platforms (1500 to 3700 m) are increasing (Richardson et al. 2008). In addition, the community structure of deep-sea macrofauna can change over contemporary timescales with surface-ocean climate (Ruhl et al. 2008). An increase in anthropogenic activity in the deep water of the GoM and concurrent global climate change may affect benthic community structure and at the same time provide a natural experimental opportunity to test the existing pattern of faunal zonation and the underlying macroecological relationship on temporal scales.

CHAPTER VI

LONG-TERM OBSERVATIONS OF EPIBENTHIC FISH ZONATION IN THE DEEP NORTHERN GULF OF MEXICO

6.1. Overview

Three deep-sea studies (from years 1964 to 2002) in the northern Gulf of Mexico (GoM) were contrasted to identify temporal and spatial changes in epibenthic fish species composition. The consistent pattern of faunal zonation over different sampling times suggested that there has been no large-scale temporal change on the upper slope. However, at local scales, the most current data suggested a potential shift in species composition of west central upper-slope assemblages toward resembling lower slope assemblages. The zonation of the deepest stations was inconsistent among different sampling times, but it is not clear that the difference was a result of temporal change, spatial heterogeneity in species composition or evolution of sampling gear. Analyses based on the pooled data suggest a continuum of species replacement with depth or macrobenthos biomass. The species composition changed more rapidly with depth above ~1,000 m but was decoupled from the macrofauna biomass of more than ~100 mg C m^{-2}, suggesting that the demersal fishes may be less dependent on macrobenthos due to their wide selection of both benthic and pelagic prey on the upper slope. Rapid demersal fish species turnover with depauperate macrobenthos (< ~100 mg C m^{-2}) may indicate intensified competition for limited quantity and choice of prey.

6.2. Introduction

6.2.1. Rationale

Rapid changes of faunal composition down the continental margin, or bathymetric faunal zonation, has been postulated to result from declining availability of phytodetritus delivered to the benthos (Rex et al. 2005, Rex & Etter 2010, Wei et al. 2010a). Multiple biological and physical factors contribute to the zonation pattern; however, they are often coupled to each other and correlated with water depth (Carney et al. 1983, Carney 2005, Rex & Etter 2010). It has been well established that the distribution of soft-bottom assemblages are zoned with depth in the deep ocean, usually as distinct narrow bands parallel to the isobaths (Rowe & Menzies 1969, Menzies et al. 1973, Haedrich et al. 1975, Cartes & Carrasson 2004, Wei & Rowe 2009). The changes of faunal constituents or zonal boundaries, on the other hand, can also occur along isobaths, presumably related to the horizontal variability in physical parameters or productivity gradients within a geographic area (Markle & Musick 1974, Hecker 1990, Wei et al. 2010a). While the spatial distribution and composition of benthic assemblages has been widely studied, large-scale temporal changes in presence or absence of the non-commercial, deep-sea species are not so clear, largely due to the scarcity of long-term data and potential bias associated with the evolution of sampling techniques. Nevertheless, the best available data are probably from the long time-series stations in the abyssal NE Pacific (Station M, Smith & Druffel 1998) and in the NE Atlantic (Procupine Abyssal Plain, Lampitt et al. 2010), where apparent temporal changes in taxa

or species composition have been observed and linked to long-term, climate-driven variations in surface production and the export flux of particulate organic carbon (POC) to the seafloor (Ruhl 2008, Ruhl et al. 2008, Smith et al. 2009, Billett et al. 2010, Kalogeropoulou et al. 2010). Based on these observations, it might be possible to infer that the temporal faunal changes may extend to areas experiencing the same climate forcing or with similar oceanographic conditions, and thus the pattern of faunal zonation may be altered at contemporary time scales. Unfortunately, large-scale studies to test this speculation have not existed yet due to the expense of long-term research. Problems associated with consistent taxonomic identifications between historical studies also impede temporal comparisons of species composition for the small, diverse metazoan infauna.

6.2.2. Study objective

In this study, we compared the zonation pattern of epibenthic fish communities from three large deep-sea surveys in the northern Gulf of Mexico (GoM): 1) R/V Alaminos study from year 1964 to 1973 (Pequegnat 1983), 2) North Gulf of Mexico Continental Slope (NGoMCS) study from year 1983 to 1985 (Gallaway 1988, Pequegnat et al. 1990), and 3) Deep Gulf of Mexico Benthos (DGoMB) program from year 2000 to 2002 (Powell et al. 2003, Rowe & Kennicutt 2009). A direct comparison of the fish zonation among the three studies is difficult due to numerous spatial and temporal "gaps" across the database; hence, alternative approaches were utilized in this analysis. First, the zonation pattern was examined for each dataset of different sampling time as well as for

the pooled data based on the same criteria. The purpose is to look for large-scale patterns (such as depth zonation) to determine whether these patterns are consistent among studies and, at the same time, in accord with the zonal patterns from the pooled data. This approach, however, requires extrapolations of the observed patterns and thus results were not statistically comparable among studies. Second, in a limited number of areas and sampling sites, the historical sampling was roughly revisited in close proximity or repeated at the exact locations. These samples can be compared statistically at the regional scale. Both approaches were employed to cross-verify the zonation patterns among studies and examine potential temporal variation of fish species composition. The large-scale faunal turnover or species replacement pattern was also examined using water depth and metazoan macrofauna biomass in the sediments (Wei et al. In preparation), as surrogates for export POC flux (Smith et al. 1997, Johnson et al. 2007) and potential food sources for the epibenthic fish communities.

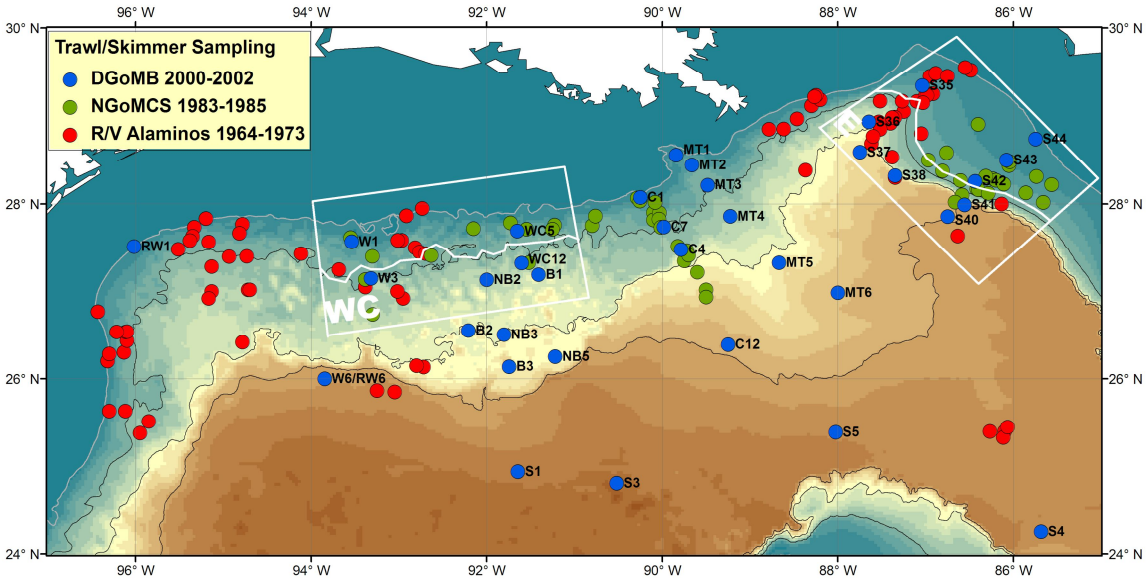

Fig. 6.1. Historical sampling of deep-sea epibenthic fishes in the northern GoM. The selected areas, WC and E, were used to test the null hypotheses across three studies (colored symbols) and two different depth intervals (separated by white lines in middle of the boxes). The color gradients reflect the depth change from shallow (blue green) to deep (brown). The gray line indicates 200-m isobath. The black lines indicate 1000-m isobaths. The station names give the DGoMB sampling sites.

6.3. Materials and Methods

6.3.1. Field sampling

Species presence/absence data for epibenthic fishes were obtained from the R/V Alaminos, NGoMCS, and DGoMB databases (Fig. 6.1, Appendix C Table S1). A 20-m otter trawl with 76-mm stretch mesh and 25-mm cod-end mesh was used during the Alaminos curises. The towing time varied from 30 minuties at shallow depths to 3 hours at depths below 3,000 m. In addition to the trawl net, a 3-m gap benthic skimmer (Pequegnat et al. 1970) was also employed on the seafloor at a speed between 2 to 4 knots for approximately 1 hour. The skimmer is a combination of dredge and trawl, and it is capable of semi-quantitatively sampling a wide variety of bottom organisms (including demersal fishes). A total of 136 species was recorded in 80 trawls/skimmers spanning 183 to 3,365-m depth. The NGoMCS study used a 9-m swept width semi-balloon otter trawl with 38-mm stretch mesh and 13-mm cod-end mesh. The trawl was towed at a speed of 1 to 3 knots for approximately 1 hour at stations shallower than 1,300-m depth and two or more hours at deeper stations. A total of 123 species was recorded in 55 trawls from depths of 329 to 2,858 m. During the DGoMB study, a 10-m swept width semi-balloon otter trawl with 64-mm stretch mesh and 25-mm cod-end mesh was used to sample 37 trawls between depths of 188 to 3,655 m. A total of 152 species was generated from the study.

6.3.2. Data analyses

Occurrences of fish species from three deep-sea surveys were cross-verified with the scientific names in FishBase (Froese & Pauly 2000) and then compiled into a single table including 274 species and 172 bottom trawl/skimmer samples (Appendix C Table S2, Table S3). The sample-by-species table was converted to Sørensen's similarity matrix using the formula, $QS = 2C / (A + B)$, where A and B are the number of species in the 2 compared samples and C is the number of species shared by the 2 samples (Sørensen 1948). With presence/absence data, the Sørensen's index is equivalent to the commonly-used Bray-Curtis similarity (Bray & Curtis 1957) for quantitative data (Clarke & Warwick 2001). In order to obtain a clear picture on the structure of faunal composition, a subset of 165 species with > 1 occurrence was retained to calculate intra-sample Sørensen's similarities and then subjected to group-average cluster analysis (Clarke & Warwick 2001). The fish faunal zones (with relatively homogeneous species composition) were identified based on the prerequisite of significant clusters (SIMPROF test, $P < 0.05$, Clarke & Gorley 2006) with at least 10% of the Sørensen's similarity shared among the samples. Characteristic species were identified as those with the highest occurrence within each zone. Besides the cluster analysis, all multivariate analyses throughout this paper were based on the Sørensen's similarity matrix converted from the full species list. The faunal affinity between the samples was examined by non-metric multi-dimensional scaling (MDS) represented by relative distances on a two dimenional plane (Clarke & Warwick 2001). Spearman's rank correlations of the fish resemblance matrix with sampling depth or metazoan macrofauna biomass in the

sediments were examined using RELATE (Clarke & Warwick 2001). The macrofauna biomass measurements for the NGoMCS and DGoMB studies were derived from Wei et al. (2010b, In preparation).

During the course of the GoM deepwater sampling, few locations have been re-visited across the studies. Only the west central (WC) and east (E) of the northern GoM have been sampled roughly in proximity across all 3 studies (enclosed by white boxes in Fig. 6.1); therefore, permutational multivariate analysis of variance (PERMANOVA) based on randomized completed block (RCB) design (Anderson et al. 2008) were conducted on these areas to test the null hypotheses that there was no change in fish species composition across the three different sampling times. The blocking factor used two depth intervals separated by 900 and 840-m isobaths in the WC and E areas, respectively (solid lines within the boxes, Fig. 6.1). One way analysis of similarity (ANOSIM, Clarke & Warwick 2001) was also conducted to double-check the result of PERMANOVA. The multiple comparisons employed a low alpha level to avoid the Type 1 error ($\alpha = 2\%$, Bonfferoni correction, Clarke & Warwick 2001). The DGoMB study repeated the NGoMCS sampling at Stations W1, W2, WC5, WC12, C1, C7 and C4 (Fig. 6.1). The DGoMB program also sampled in the proximity of the NGoMCS and Alaminos sites at Stations S41, S42 and S43, as well as Stations S35, S36, S37 and S38, respectively (Fig. 6.1). For these locations, the PERMANOVA (or ANOSIM) was employed to test for temporal variation in species composition. The depth block, however, was replaced by different sampling sites along the selected transect. To increase sample size for

PERMANOVA (or ANOSIM) tests, Stations W1, W2, WC5 and WC12 were combined as a single transect before conducting the analysis.

The multivariate and GIS analyses used PRIMER 6 & PERMANOVA+ and ESRI® ArcMap™ 9.2.

6.4. Results

6.4.1. R/V Alaminos sampling from years 1964 to 1973

Group-average cluster analysis and SIMPROF test on intra-sample Sørensen's similarities suggested 5 significant groups ($P < 0.05$). These natural groups were listed from shallow to deep according to their minimum sampling depths (Fig. 6.2a & b). The same arrangements were employed for the other two studies and the pooled data. Trawl no. 81 and 99 were not shown in the dendrogram due to no similarity with the rest of samples and to one another (Appendix C Table S1). Except for the two shallowest sites sharing 66.7% of Sørensen's similarity, the rest of the groups shared similarities of 10.3 to 23.3 % (Fig. 6.2a). Shelf-Break (SB) and Upper-Slope (US) Groups extended from depths of 183 to 210 m and 183 to 538 m, respectively (Fig. 6.2b). Upper-to-Mid-Slope (U-MS) Group occupied part of the upper slope and most of the mid slope from depths of 379 to 1,829 m. Lower-Slope (LS) Group had one station on the mid slope at 1,134-m depth and covered the lower slope between depths of 1,829 and 2,140 m. Low-Slope-to-Abyssal (LS-A) Group represented the deepest sampling from 2,103 to 3,267-m depth.

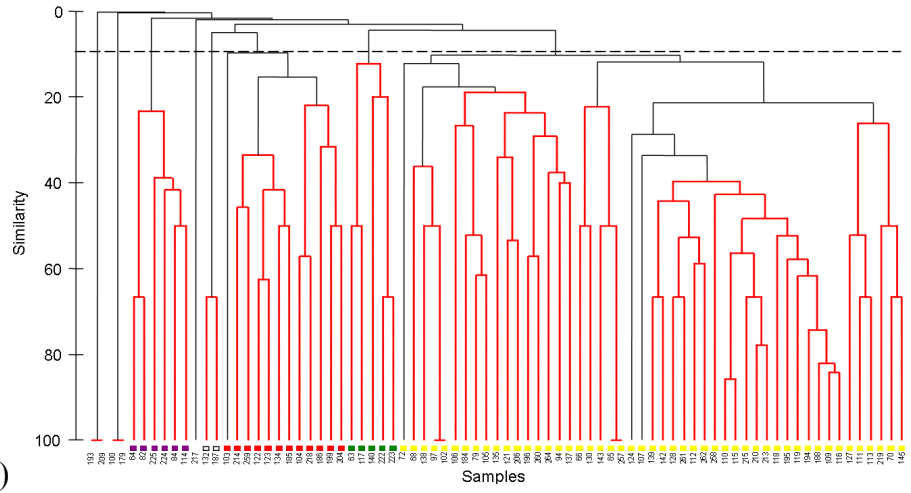

(a)

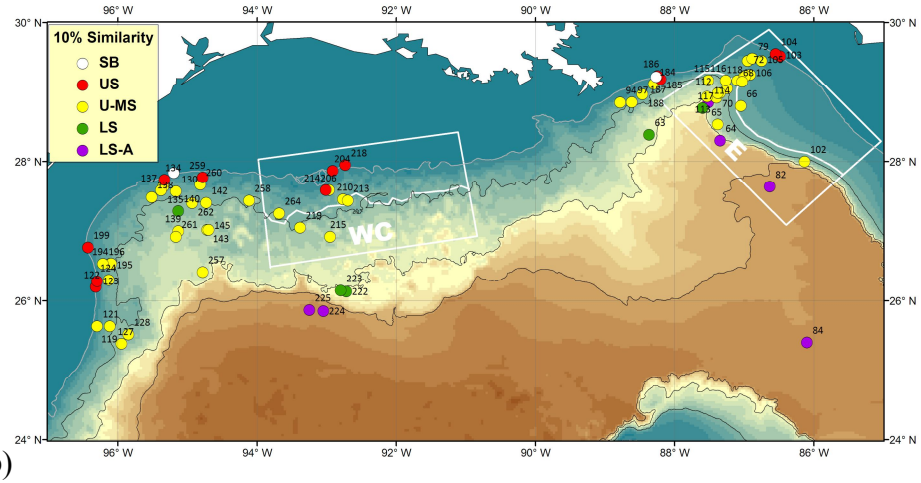

(b)

Fig. 6.2. Epibenthic fish species composition and faunal zonation during the R/V Alaminos cruises from year 1964 to 1973. (a) Group-average cluster analysis on intra-sample Sørensen's similarities. The black solid lines indicate significant structure (SIMPROF test, P < 5%). The dash line shows 10% similarity. (b) Distribution of the fish faunal zones with at least 10% of faunal similarity. Color scheme follows the Fig. 6.2a. The independent samples in the dendrogram (Fig. 6.2a), Trawl No. 193, 209, 100, 179 and 217, were not plotted.

6.4.2. North Gulf of Mexico Continental Slope (NGoMCS) Study from years 1983 to 1985

A total of 4 significant groups ($P < 0.05$) were indentified by cluster analysis and SIMPROF (Fig. 6.3a). Upper-Slope (US) and Upper-to-Mid Slope (U-MS) Groups were separated at 10% of Sørensen's similarity with the sampling depths extending from 329 to 552 m and 603 to 1,510 m, respectively (Fig. 6.3b). The 2 deepest groups, Lower-Slope 1 (LS1) and Low-Slope 2 (LS2), occupied depths from 2,074 to 2,504 m and from 2,401 to 2,858 m, respectively.

6.4.3. Deep Gulf of Mexico Benthos (DGoMB) program from years 2000 to 2002

Cluster analysis with SIMPROF suggested 5 significant groups ($P < 0.05$) sharing at least 10% to 36.6% of Sørensen's similarity (Fig. 6.4a). Station S3 was not included in the dendrogram due to no similarity with the other sites (Appendix C Table S1). Shelf-Break (SB) Group included the two shallowest sites at depths of 188 and 213 m (Fig. 6.4b). Upper-Slope (US) Group occurred between 325 and 461-m depth. Upper-to-Mid-Slope (U-MS) Group extended from depths of 670 m to 1,369 m. Mid-to-Lower-Slope (M-LS) Group covered the largest sampling area, including shallower distribution at Station WC5, WC12 and C7 between depth of 758 to 1,100 m and the other deep sites extending from 1,784 to 3,010-m depth. Lower-to-Abyssal (LS-A) Group showed an exclusive deepwater distribution from 2,608 to 3,590-m depth.

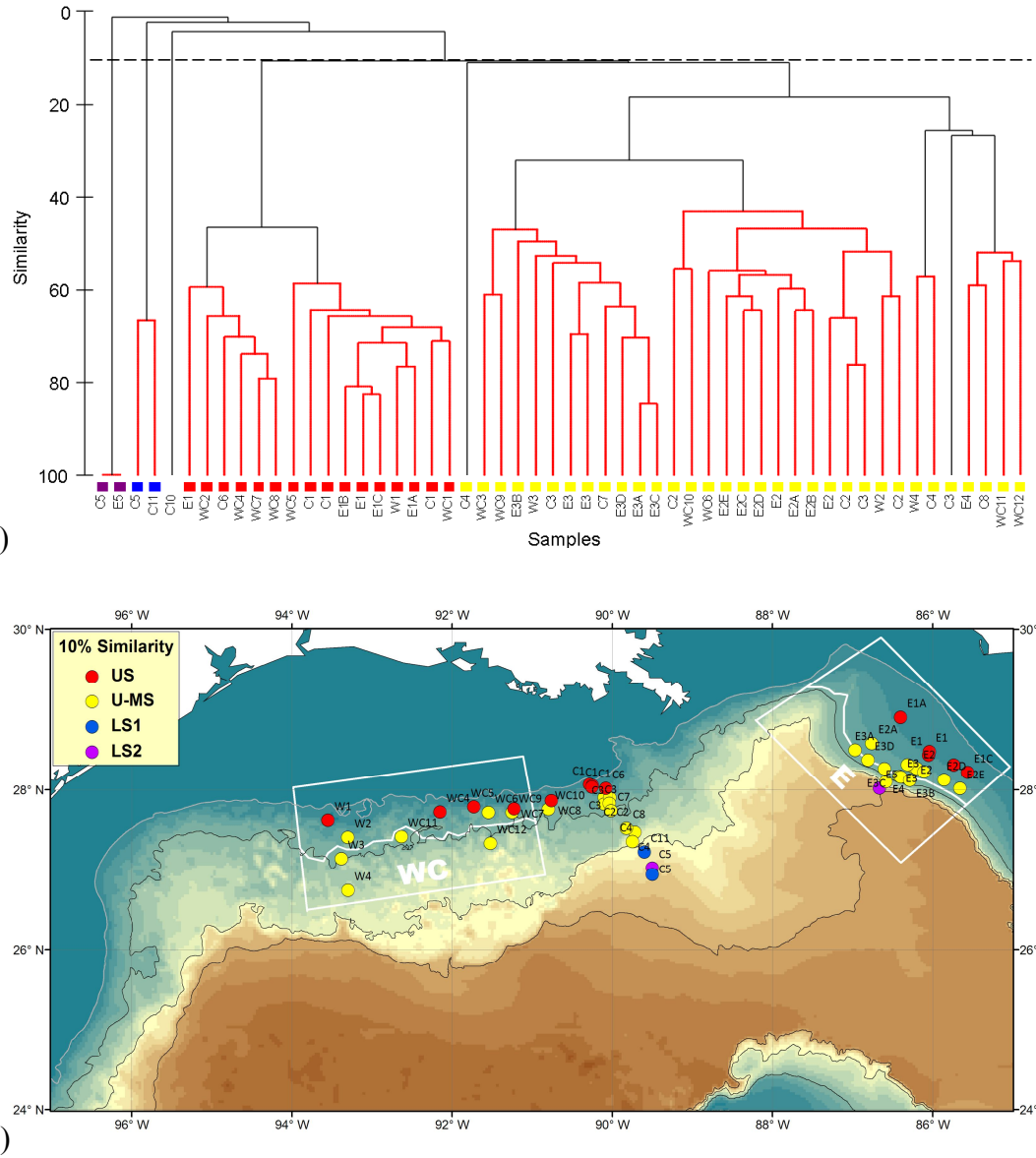

Fig. 6.3. Epibenthic fish species composition and faunal zonation during the NGoMCS study from year 1983 to 1985. (a) Group-average cluster analysis on intra-sample Sørensen's similarities. The black solid lines indicate significant structure (SIMPROF test, $P < 5\%$). The dash line shows 10% similarity. (b) Distribution of the fish faunal zones with at least 10% of faunal similarity. The same color scheme is used in Fig. 6.3a.

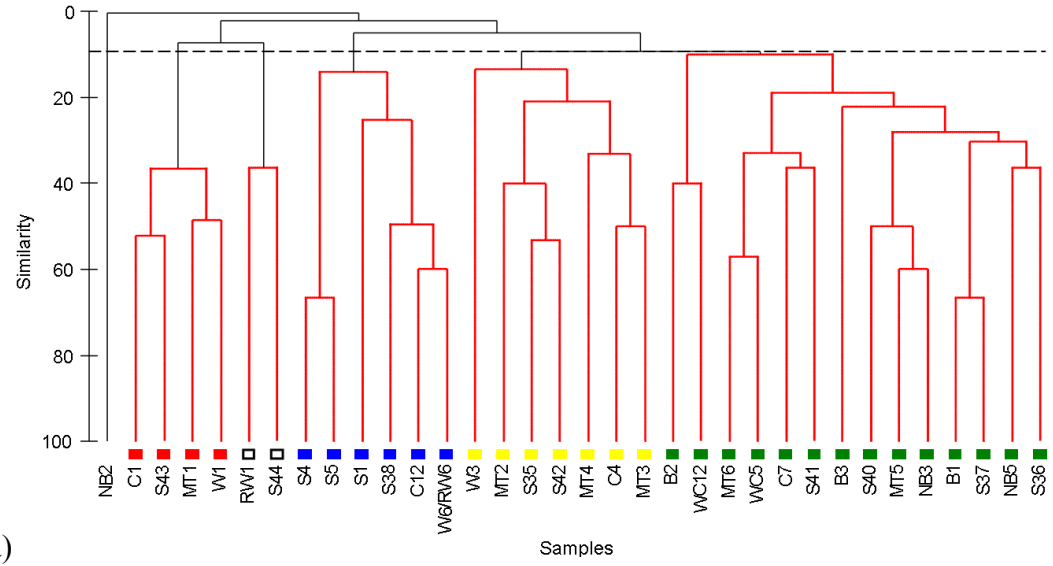

(a)

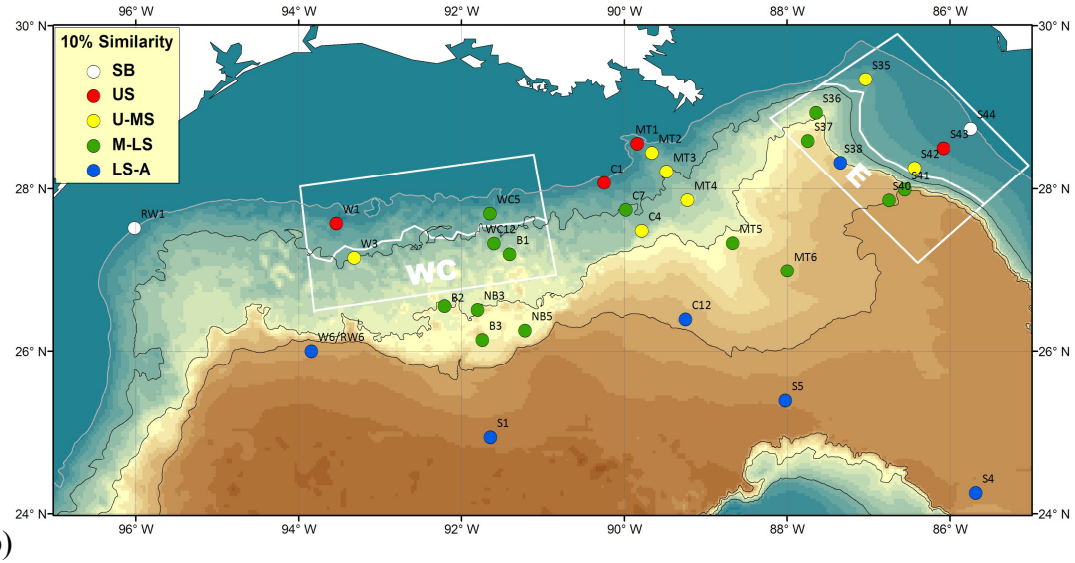

(b)

Fig. 6.4. Epibenthic fish species composition and faunal zonation during the DGoMB study from year 2000 to 2002. (a) Group-average cluster analysis on intra-sample Sørensen's similarities. The black solid lines indicate significant structure (SIMPROF test, $P < 5\%$). The dash line shows 10% similarity. (b) Distribution of the fish faunal zones with at least 10% of faunal similarity. The same color scheme is used in Fig. 6.4a.

6.4.4. Pooled data from year 1964 to 2002

A total of 7 significant groups ($P < 0.05$) were indentified from the pooled data based on cluster analysis and SIMPROF (Fig. 6.5a). Station S3 was not included in the dendrogram due to no similarity with the other sites (Appendix C Table S1). The majority of the natural groups shared at least 10 to 17.1% of Sørensen's similarity; however, in order to meet the prerequisite of significant cluster structure (SIMPROF test, $P < 0.05$), Lower-Slope-to-Abyssal 1 (LS-A1) and Lower-Slope-to-Abyssal 2 (LS-A2) Groups shared only 2.4 and 8.1% of the Sørensen's similarities, respectively (Fig. 6.5a & b). The top 10 species with highest occurrence for each natural group were listed as characteristics species in Appendix C Table S4. Non-metric multi-dimensional scaling (MDS) illustrates a continuum of changes from the shelf break to the abyssal plain without distinct boundaries along the depth gradient (Fig. 6.6). The first axis (MDS1) appear to explain most of the variation in the MDS plot. The rate of change for the MDS1 with depth was more rapid on the upper slope (< 1,000-m depth) than the lower slope and abyssal plain (Fig. 6.7a). Nevertheless, the MDS1 changed more rapidly at the lower end (< 100 mg C m^{-2}) than the higher end of the macrofauna biomass (Fig. 6.7b, red symbols and red line). It has been suggested that macrofauna biomass declines exponentially with depths (Rowe 1983, Rex et al. 2006, Wei et al. 2010b); hence the depth-MDS1 relationship (Fig. 6.7a, blue symbols) was converted to macrofauna biomass-MDS1 plot (Fig. 6.7b, blue symbols) using an empirical equation from the northern GoM, Log_{10} biomass in mg C m^{-2} = 2.21 – 0.28 * depth in km ($R^2 = 0.72$, $F_{1, 94} = 242.7$, $P < 0.001$, Wei et al. In preparation). At the lower macrofauna biomass (<~100

mg C m-^{2}), the synthetic trend (Fig. 6.7b, blue line) was comparable to the observation (red line) but they are in discord at the high biomass (> ~100 mg C m^{-2}). The fish Sørensen's similarity matrix, however, was more tightly correlated to the water depth (RELATE, $\rho = 0.673$, $P < 0.001$) than to the macrofauna biomass in the sediments (RELATE, $\rho = 0.233$, $P < 0.001$).

Shelf-Break (SB) Group covered depths from 183 to 237 m (Fig. 6.5b). The duckbill flathead (*Bembrops anatirostris*) and longspine scorpionfish (*Pontinus longispinis*) had the highest occurrences accounting for 60% of the sampling sites in this group. Three-eye flounder (*Ancylopsetta dilecta*), sash flounder (*Trichopsetta ventralis*) and wenchman (*Pristipomoides aquilonaris*) also occurred in 30 to 40 % of sampling sites in this area.

Upper-Slope (US) Group occupied depths from 274 m to 696 m with sporadic distributions at deeper depths between 853 and 1,097 m (Fig. 6.5b). The goby flathead (*Bembrops gobioides*), western softhead grenadier (*Malacocephalus occidentalis*) and Atlantic batfish (*Dibranchus atlanticus*) were the most common species occurring at 62 to 73% of the sampling sites in this group.

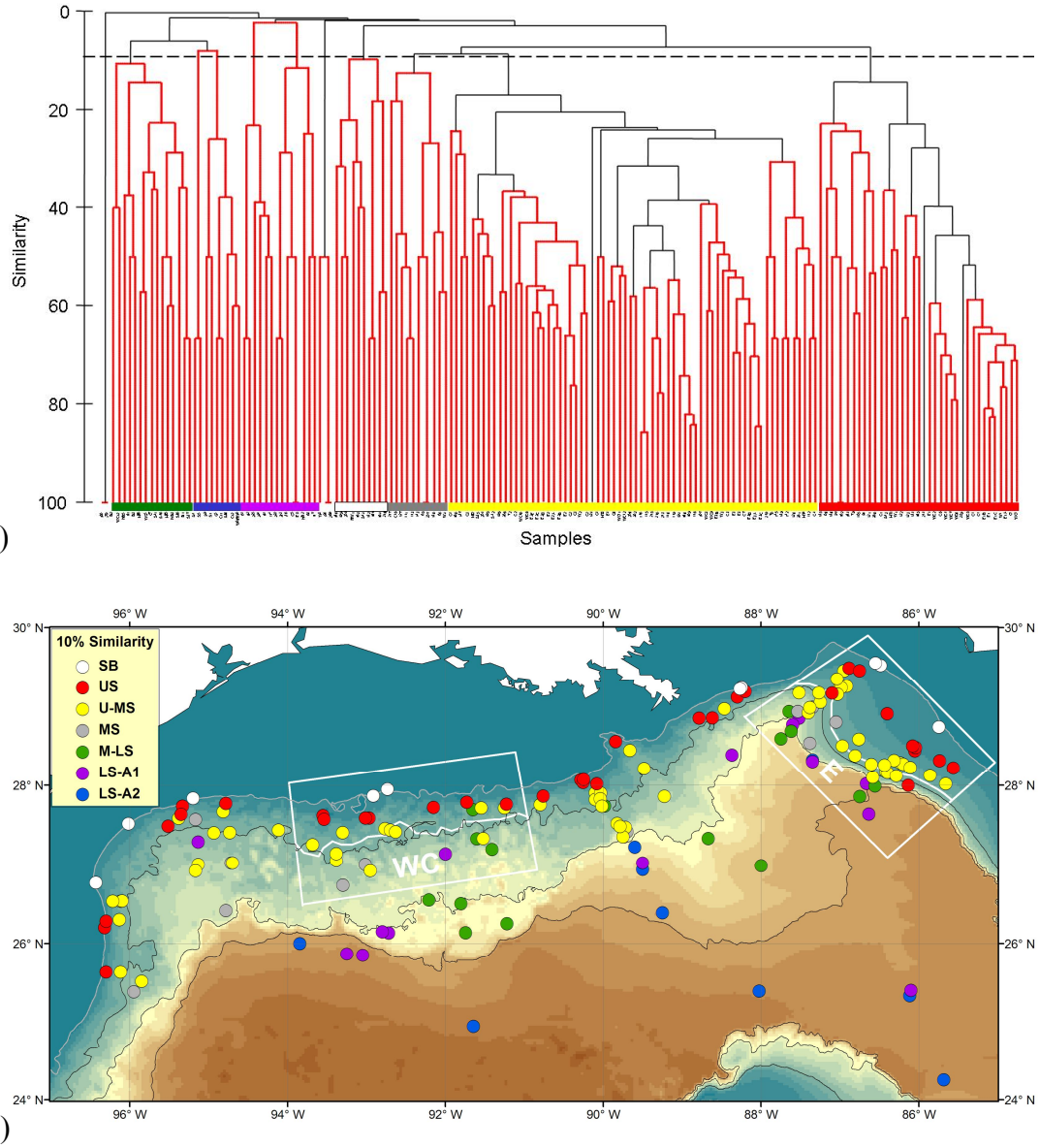

Fig. 6.5. Epibenthic fish species composition and faunal zonation for the pooled data from year 1964 to 2002. (a) Group-average cluster analysis on intra-sample Sørensen's similarities. The black solid lines indicate significant structure (SIMPROF test, $P < 5\%$). The dash line shows 10% similarity. (b) Distribution of the fish faunal zones with at least 10% of faunal similarity. The same color scheme is used in Fig. 6.5a.

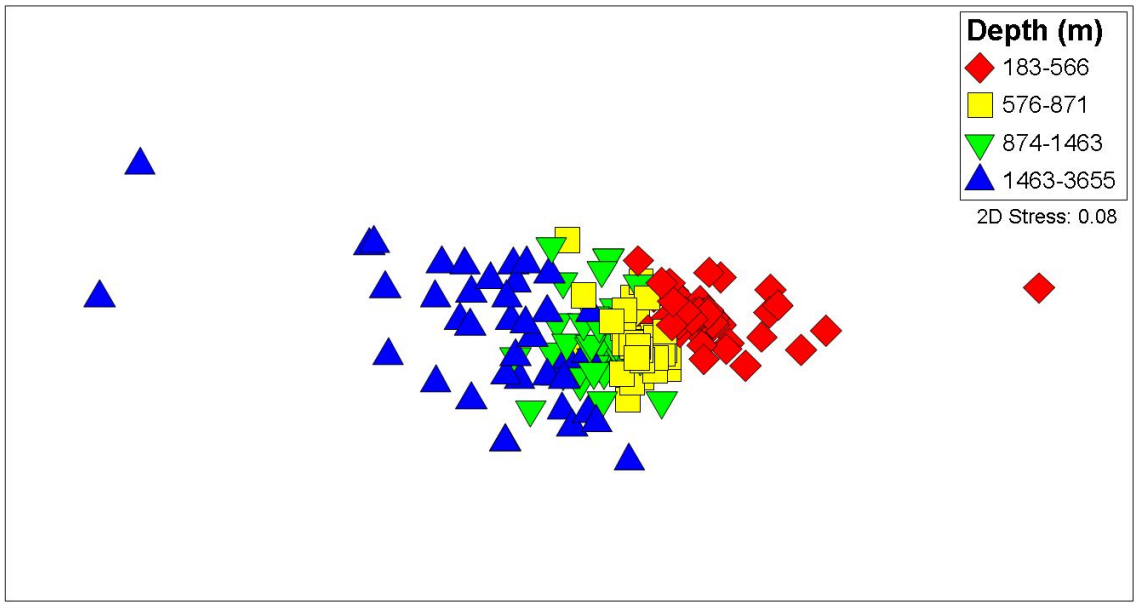

Fig. 6.6. Non-metric multi-dimensional scaling (MDS) on intra-sample Sørensen's similarities of pooled data. The distances between samples represent dissimilarities in species composition. Color schemes show four depth intervals with equivalent numbers of samples.

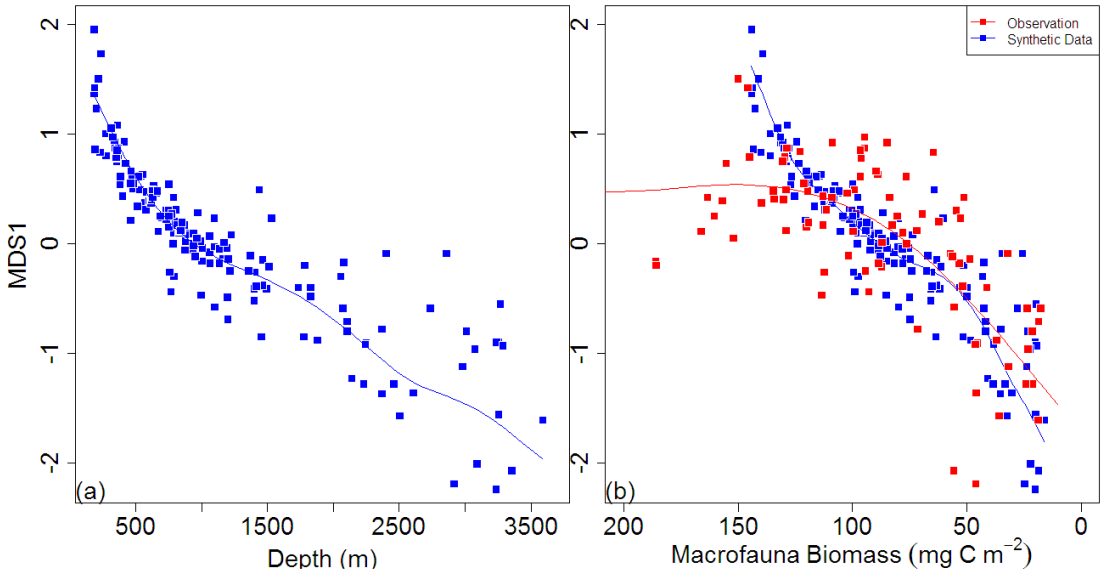

Fig. 6.7. First axis of the non-metric multi-dimensional scaling (MDS) plotted against (a) depth (blue square) and (b) total macrofauna biomass in the sediments (red square). The MDS axis represents species composition of epibenthic fishes in multivariate space. The macrofauna biomass for the NGoMCS and DGoMB studies were derived from Wei et al. (In preparation). The trend lines show the MDS1 as smooth spline functions of depth and macrofauna biomass. The depth values in Fig. 6.7a were coverted to macrofauna biomass using an empirical equation from the northern GoM, Log_{10} biomass (mg C m^{-2}) = 2.21 – 0.28 * depth (km) (R^2 = 0.72, P < 0.001, Wei et al. In preparation) and then plotted against the MDS1 (Fig. 6.7b, blue symbols).

Upper-to-Mid-Slope (U-MS) Group extended from the lower section of upper slope to the upper section of mid slope between 566 and 1,510-m depth (Fig. 6.5b). In this zone, 7 out of the top 10 highest occurring species were macrourids (in 35 to 68% of the sampling sites). The most common were the cutthroat eel (*Synaphobranchus oregoni*) at 76% of the sites. The Atlantic batfish (*Dibranchus atlanticus*) was found at 59% of the sites. This was also one of the most common species in the Shelf-Break (SB) and Upper-Slope (US) Groups.

Except for two samples occurring at ~800-m depth, Mid-Slope (MS) Group covered depths from 1,198 to 1,829 m (Fig. 6.5b). The Gilbert's halosaurid (*Aldrovandia affinis*) was the most common species being in 64% of the sampling sites. This group shared most of its characteristic species with other natural groups such as Mid-to-Lower-Slope (M-LS) and LS-A1 (*Aldrovandia gracilis*), LS-A1 (*Bathypterois quadrifilis* and *Barathronus bicolor*), U-MS (*Synaphobranchus oregoni* and *Gadomus longifilis*), and M-LS and LS-A2 (*Ipnops murrayi*). It is possible that this group represented a transition between upper slope and the deeper water assemblages. It is also worth noting that this group was arbitrarily cut off from U-MS Group based on the criteria of 10% similarity (Fig. 6.5a). The two groups shared around 8.7% of the similarity.

Mid-to-Lower-Slope (M-LS) Group occurred between 1,784-m and 3,010-m depth with a few sites extending to the upper slope of the west central northern GoM between 758 and 1,100-m depth (Fig. 6.5b). The elongated bristlemouth (*Gonostoma elongatum*) was the characteristic species, occurring in 67 % of the sampling sites.

Table 6.1. Permutational multivariate analysis of variance (PERMANOVA) on epibenthic fish species composition among 3 deep-sea surveys conducted between years 1964 and 2002 in the northern GoM. The randomized completed block (RCB) PERMANOVA were employed for (a) the east and (b) the west central areas roughly overlap by all 3 surveys (Fig. 6.1). The blocking factor used two depth intervals separated by 840-m depth in the east area and 900-m depth in the west central area. For a limited number of sites, the most current DGoMB study repeated the historical NGoMCS or R/V Alaminos sampling; hence, the PERMANOVA was also conducted on (c) Station W1, W3, WC5 and WC12, (d) Station C1, C7 and C4, (e) Station S41, S42 and S43, and (f) S35, S36, S37 and S38 to examine the temporal variation on fish species composition. The blocking factor for PERMANOVA on these repeated sampling used different sites along the selected transects.

Source	df	SS	MS	Pseudo-F	P
(a) E area (across 3 studies)					
Time	2	19662	9831	1.99	0.079
Block	1	10886	10886	2.99	<0.001
Error	46	167260	3636		
(b) WC area (across 3 studies)					
Time	2	12753	6376	1.26	0.302
Block	1	10392	10392	3.25	0.001
Error	20	64040	3202		
(c) W1, W3, WC5 & WC12 (NGoMCS vs. DGoMB)					
Time	1	5576	5576	1.51	0.510
Block	1	5447	5447	1.42	0.220
Error	4	15373	3843		

Table 6.1. Continued.

Source	df	SS	MS	Pseudo-F	P
(d) C1, C7 & C4 (NGoMCS vs. DGoMB)					
Time	1	4537	4537	1.10	0.403
Block	2	12635	6318	2.99	0.026
Error	3	6341	2114		
(e) S41, S42 & S43 (NGoMCS vs. DGoMB)					
Time	1	5531	5531	1.43	0.287
Block	2	13939	6969	3.17	0.023
Error	3	6597	2199		
(f) S35, S36, S37 & S38 (Alaminos vs. DGoMB)					
Time	1	5229	5229	1.76	0.174
Block	3	16502	5501	2.82	0.020
Error	1	1953	1953		

Except for a few samples on the mid slope, two Lower-Slope-to-Abyssal Group (LS-A1 and LS-A2) occurred between 2,057 and 3,287 m, as well as 2,074 and 3,590 m, respectively (Fig. 6.5b). Although these two groups seem to cover similar depth ranges, they do not share any characteristic species. *Bassozetus normalis* and *Venefica procera* were the most common species in the LS-A1 Group (36% occurrence), while bony-eared assfish (*Acanthonus armatus*) and tripodfish (*Bathypterois grallator*) had the highest occurrence in the LS-A2 Group (in 56 to 67% of the sites). It is also apparent that the distribution pattern of the M-LS and LS-A2 Groups derived mostly from the DGoMB sampling (M-LS and LS-A in Fig. 6.4b, respectively), while the distribution of the LA-A1 Group seems to be derived from the R/V Alaminos sampling (LS + LS-A Groups in Fig. 6.2b).

6.4.5. Hypothesis testing

Depth block had significant effects on fish species composition of E (PERMANOVA, block, $F_{1, 46} = 2.99$, $P < 0.001$, Table 6.1a) and WC areas (block, $F_{1, 20} = 3.25$, $P = 0.001$, Table 6.1b); however, only a marginal temporal effect was detected in the E area (PERMANOVA, time, $F_{2, 46} = 1.99$, $P = 0.079$, Table 6.1a). On the other hand, ANOSIM suggested significant temporal effects on both E and WC areas (east, $R = 0.151$, $P = 0.003$; west central, $R = 0.204$, $P = 0.002$). In area E, only the NGoMCS study was significantly different from the DGoMB study (multiple comparisons, $R = 0.494$, $P < 0.001$). None of the pair-wise comparisons in the WC area was significantly different ($P > 0.02$). Except for the Station W1, W3, WC5 and WC12 (PERMANOVA,

block, $F_{1,4} = 1.42$, P = 0.22, Table 6.1c), depth block had significant effects on species composition between the historical and revisited transects (block, P = 0.02 to 0.03, Table 6.1d to f). No significant temporal effect was detected for the repeated sampling (PERMANOVA, time, P = 0.17 to 0.51, Table 6.1c to f). The ANOSIM tests on repeated transects also confirmed no evidence of temporal changes in composition (R = 0.068 to 0.271, P = 0.114 to 0.214)

6.5. Discussion

6.5.1. Temporal comparison of zonation patterns

Our analyses of individual studies and the pooled data agreed with previous investigations showing distinct depth zonation without horizontal faunal changes along isobaths (Pequegnat 1983, Pequegnat et al. 1990, Powell et al. 2003). The distribution of the shelf-break zone (~200-m depth), upper-slope zone (~300 to 500-m depth) and upper-to-mid slope zone (~600 to 1600-m depth) were consistent across different sampling times. This re-occurring pattern also matched depth zones based on the cluster analysis of pooled data, suggesting no discernable large-scale temporal change of depth zonation on the upper section of the continental slope. Nevertheless, at a local scale, it appears that in the WC area (WC5 and WC12, Fig. 6.4b) species composition of the most current DGoMB sampling more closely resembles the deeper assemblages from the lower slope, as opposed to the typical upper slope assemblages at the other two sites to the west (W1 and W3), and at the same locations during the historical NGoMCS sampling (WC5 and WC12, Fig. 6.3b). This potential temporal change was also

supported by cluster analyses of pooled data when the same locations (WC5 and WC12) from the NGoMCS and DGoMB sampling were assigned to the shallow and deep groups, respectively; however, a direct comparison by PERMANOVA and ANOSIM did not find a significant difference between the studies. This is probably because we included two additional repeated sites on the west transect (W1 and W2) in order to have enough values for sample permutation (at least 20) for any significant result ($\alpha = 0.05$) in the PERMANOVA and ANOSIM, and this reduced the statistical power of these tests. On the other side of the northern GoM, the statistical difference between the DGoMB and NGoMCS sampling in the E area (based on ANOSIM) is probably because the DGoMB sampled a wider depth range than the NGoMCS study, since the individual transect comparison of the revisited sites did not suggest a significant temporal effect and the zonal patterns were consistent among 3 studies and the pooled data.

Even though the lower-slope and lower-slope-to-abyssal zones re-occurred across three studies, these similar depth zones did not fall into the same natural groups in clustering of the pooled data. The observed pattern usually reflected the faunal zones from either the R/V Alaminos or the DGoMB studies, because the NGoMCS study only had two sampling sites below 2,000-m depth. Sampling in these areas was generally scattered and the majority of the sites was only visited once during the three studies; hence, it is difficult to discern whether this inconsistency is due to spatial heterogeneity in species composition, temporal changes in faunal zonation, or simply the sampling gear difference. The R/V Alaminos studies used a combination of benthic skimmer and trawl while the NGoMCS and DGoMB were sampled exclusively by semi-balloon otter trawl.

Mixing the skimmer and otter trawl samples does not seem to affect the consistency of zonal pattern on the upper and mid slope, presumably due to the higher sampling effort and larger sample size (numbers of recovered specimens) in the shallower water; however, when the fish abundance declined with depth (Pequegnat et al. 1990, Powell et al. 2003), the gear effect could be magnified because the skimmer sampled a smaller area than the otter trawl and might have been less effective in recovering large mobile megafauna.

6.5.2. Productivity-β diversity relationship

Since no apparent change of zonal pattern was evident among studies of different sampling times, we combined the three datasets in order to examine the large-scale species turnover in the northern GoM. Our analyses on epibenthic fish communities confirmed a gradual, continuum change of species composition along a depth gradient (Howell et al. 2002, Wei & Rowe 2009, Wei et al. 2010a). The term "zonation" in this paper was adopted to conveniently explain and visualize the large-scale and potentially long-term pattern. Unlike the rocky intertidal shore with sequential, delineated bands of species distribution (Stephenson & Stephenson 1949), the faunal turnover in the deep-sea soft-sediment habitats rarely formed immutable boundaries with many species occupying overlapping ranges (Rowe & Menzies 1969, Wei & Rowe 2009); hence, the zonal pattern observed here is better described as the rate of species replacement along a habitat gradient (Rex & Etter 2010), or β diversity (Whittaker 1960, 1972).

Based on Terborgh's (1971) theory of species distribution on environmental gradients, the continuum turnover of species in this study is more likely to be related to resources that vary continuously with depth, such as temperature, pressure (Somero 1992) or decline of POC flux (Wei et al. 2010a), rather than factors implying discontinuity such as an abrupt shift of water mass structure (Bett 2001, Narayanaswamy et al. 2010) or the oxygen minimum zone (Levin et al. 2000). In the northern GoM, the variability of hydrographic properties becomes greatly reduced below ~800-m depth and their horizontal distribution was approximately uniform below the depth of the Yucatan sill (~1,500-m depth) (McLellan & Nowlin 1963, Jochens & DiMarco 2008). This homogeneity may contribute to the slightly slower rate of change in faunal composition (or lower β diversity) on the lower-slope and abyssal plain compared to the upper-slope depths. In deep water, the exponential decline of export POC flux with depth was probably the main physical driving force for the pattern of β diversity (Rex & Etter 2010), because the selection for pressure-resistant species occurs at relatively shallow depths (500 to 1,000 m, Somero 1992).

Interestingly, the rate of change in demersal fish species composition with macrofauna biomass seemed to contradict its relationship with depth. The disparity, however, can not simply be explained by an exponential relationship between the macrofauna biomass and depth (Rowe 1983, Rex et al. 2006, Wei et al. 2010b). In contrast with the rapid species replacement above 1,000-m depths, the rate of change was surprisingly low when the macrofauna biomass was the highest on the shelf edge and upper slope (> 100 mg C m^{-2}). This suggests that the changes of demersal fish composition, although continuous, were

decoupled from the variation at the higher end of macrofauna biomass, presumably because supplies of food resources were substantially larger and more variable on the shelf edge and upper slope. The motile demersal fishes can feed on a broad spectrum of benthic and pelagic prey (Crabtree et al. 1991, Gartner et al. 1997) and thus might have wide distributions and slow rate of species turnover (Haedrich et al. 1980, Rex 1981). On the shelf edge and upper slope, demersal fishes can also feed directly on the mesopelagic fauna (Stefanescu et al. 1993, Gordon et al. 1995, Gartner et al. 1997, McClatchie et al. 1997); hence, they may rely less on sediment-dewelling macrofauna.

Rex (1977) hypothesized that at high trophic levels, such as demersal fishes, the assemblage structure would be influenced more by competition, as opposed to lower trophic-level macrofauna, being affected more by predation (Menge & Sutherland, 1976). He proposed that when competition is strong, species may repulse one another, giving rise to fewer overlapping ranges of distribution and thus more pronounced zonation along a resource gradient (Terborgh 1971, Rex & Etter 2010). This hypothesis poses another interesting explanation for the relationship between macrofauna biomass (productivity) and rates of change in demersal fish species composition (β diversity). The macrofauna, per se, is not the only diet for the demersal fishes but it might shed some light on the overall level of POC flux delivered to the benthos (Smith et al. 1997, Johnson et al. 2007, Sweetman & Witte 2008). Conventionally, intra- or inter-specific competition is assumed to be higher when resources are abundant, such as high macrofauna biomass or export POC flux on the shelf edge and upper slope. This may be to some degrees be true for the less motile, deposit-feeding megafauna invertebrates;

however, the search of food for the demersal fishes is likely to cover broad ranges and not be limited to their local ambit and specific prey items (Haedrich et al. 1980). On the upper slope, direct predation from mesopelagic predators (Gartner et al. 1997) and biochemical stresses associated with changing temperature and pressure (Somero 1992) may relax the competition among demersal fishes. In deep water, the competition for prey may intensify when the quantity and choices of diets decline with increasing depth; hence, the shift to rapid species replacement with depauperate macrofauna biomass may be a function of enhanced competition.

6.5.3. Weakness of analyses and conclusions

Obviously, our interpretations on the observed productivity-β diversity relationship are bold conjectures based on a few snapshots of fish assemblage structure (MDS plot). If the species turnover does imply competition, our analyses based on presence/absence data should be independent of any variation within species and thus likely to reflect only intra-specific rather than inter-specific competition. Biological interactions such as life history tactics, competition, and predation are much more complicated and likely to act together with the environmental heterogeneity to shape the pattern of faunal zonation (Rex 1981). By accessing the outcomes of these elusive and hard-to-quantify processes, it might be possible to gain some insights and make inference about how the biological interactions are functioning with the environmental gradients. In contrast to strong seasonal and inter-annual climate forcing at the long-term sites of the NE Pacific and NE Atlantic (Smith et al. 2009), the GoM receives relatively constant energy supplies

(Lohrenz et al. 1999, Cai & Lohrenz 2010), with hydrographic properties in the deepwater being constant in the past 30 to 40 years (Jochens & DiMarco 2008). The surface phytoplankton biomass on the continental slope displays well-define seasonal cycles (Müller-Karger et al. 1991) with little inter-annual variability observed within the N GoM (Biggs et al. 2008). On the seafloor, the overall levels and the rates of declining benthic macrofauna biomass with depth were also comparable between the NGoMCS sampling in the 1980's and DGoMB sampling in the 2000's (Wei et al. In preparation). It is also possible that the pattern of zonation (or β diversity) was heavily influenced by the declining food supply with depth and thus any temporal climatic effects were overwhelmed by the immense depth variation in our large-scale analyses. Nevertheless, we feel confident that the deep-sea demersal fishes in the northern GoM, at least on the upper slope, did not undergone major changes in the past 40 years.

CHAPTER VII

CONCLUSIONS

Based on our global analyses, multivariate predictors indicating upper ocean climate, phytoplankton biomass, export POC flux, and water depth explained 63% to 88% of stock variability among major benthic size groups. Integrated biomass predictions illustrates that total seafloor stocks are highest at the poles, on continental margins associated with coastal upwelling and with broad zones associated with equatorial divergence. Lowest predictions are consistently encountered on the central abyssal plains of major ocean basins. In the northeastern GoM, macrofauna standing stocks were enhanced on the productive continental slope associated with the nutrient-laden Mississippi River outflows, eddy transport of the river plumes, and upwelling of nutrients along the Loop Current edges. The meager biomass of the Mexican margin reflects the characteristic low productivity Caribbean water that enters the gulf with the Loop Currents. These syntheses suggest that the amount of energy escaping the upper ocean to support the seafloor organisms are positive functions of surface primary production and delivery of the particulate organic carbon (POC) flux at depths. The enhancement of macrofauna standing stocks at the Mississippi and De Soto Submarine Canyon and deep sediment fan is presumed to be caused by lateral advections of organic carbon from the surrounding continental shelf and slope that is independent of satellite estimate of phytoplankton biomass and may contribute the unexplained variability in our

predicted models. In addition to the declining standing stocks, the decrease in quantity and quality of POC flux may explain the decrease of average animal size and shift of biomass hierarchy toward the smaller size groups with depth. Within a benthic size group (e.g. macrofauna), the decline of average size with depth was a function of a shift numerical dominance from large to smal taxa. These evidences suggest that small body size may have the advantage to conserve energy and maintain viable population in the food-limited deep sea (Thiel 1975, Rex et al. 2006, Wei et al. 2010b).

Re-analysis of the Rowe and Menzies' data (1969) revealed that individual epibenthic invertebrate species and multi-species assemblages occurred in narrow depth bands that hugged the topography from the upper slope to Abyssal Plain. Similar to the cause of declining standing stocks with depth, the continuum of species replacement with depth is likely to be driven by a continuous decrease in quantity and quality of food resources in the deep sea. Nevertheless, large-scale analyses in the northern GoM revealed not only vertical (depth) but horizontal (east vs. west) macrofauna zonation, suggesting that the faunal turnover can occur independent of depth variation and followed an east-west productivity gradient due to the influence of the Mississippi River and Canyon in the northeastern GoM. On the upper section of the continental slope, no discernable large-scale temporal change of demersal fish zonation was evident across surveys between years 1964 and 2002 in the northern GoM. The changes in demersal fish species composition along the depth gradient, again, were continuum without distinct boundaries; however, no horizontal variability was evident, presumably due to the mobility of demersal fish that is capable to explore wide spectrum of prays as opposed to the

relatively sessile macrofauna mainly feeding on the deposits. An apparent shift in rates of fish species replacement at ~1,000-m depth or when macrofauna biomass was ~100 mg C m^{-2} suggests both environmental heterogeneity and complex biological interactions likely to shape the pattern of faunal zonation.

LITERATURE CITED

Adcroft A, Hallberg R, Dunne JP, Samuels BL, Galt JA, Barker CH, Payton D (2010) Simulations of underwater plumes of dissolved oil in the Gulf of Mexico. Geophysical Research Letters 37:L18605

Aldea C, Olabarria C, Troncoso JS (2008) Bathymetric zonation and diversity gradient of gastropods and bivalves in West Antarctica from the South Shetland Islands to the Bellingshausen Sea. Deep Sea Research Part I: Oceanographic Research Papers 55:350-368

Amante C, Eakins BW (2009) ETOPO1 1 Arc-Minute Global Relief Model: Procedures, Data Sources and Analysis NOAA Technical Memorandum NESDIS NGDC-24, p 19

Anderson MJ, Gorley RN, Clarke KR (2008) PERMANOVA+ for PRIMER: Guide to software and statistical methods, PRIMER-E, Plymouth

Baguley JG, Montagna PA, Hyde LJ, Rowe GT (2008) Metazoan meiofauna biomass, grazing, and weight-dependent respiration in the Northern Gulf of Mexico deep sea. Deep Sea Research Part II: Topical Studies in Oceanography 55:2607-2616

Balsam WL, Beeson JP (2003) Sea-floor sediment distribution in the Gulf of Mexico. Deep Sea Research Part I: Oceanographic Research Papers 50:1421-1444

Bean DA, Bryant WR, Slowey NC, Scott E, Whitehead MA (2002) Past and present furrow development in the Green Knoll area determined from 3D seismic data AAPG Annual Meeting, Houston, TX

Behrenfeld MJ, Falkowski PG (1997) Photosynthetic rates derived from satellite-based chlorophyll concentration. Limnology and Oceanography 42:1-20

Bett B, Vanreusel A, Vincx M, Soltwedel T, Pfannkuche O, Lambshead P, Gooday A, Ferrero T, Dinet A (1994) Sampler bias in the quantitative study of deep-sea meiobenthos. Marine Ecology Progress Series 104:197-197

Bett BJ (2001) UK Atlantic Margin Environmental Survey: Introduction and overview of bathyal benthic ecology. Continental Shelf Research 21:917-956

Bianchi TS, Allison MA, Canuel EA, Corbett DR, McKee BA, Sampere TP, Wakeham SG, Waterson E (2006) Rapid export of organic matter to the Mississippi Canyon. Eos, Transactions, American Geophysical Union 87(50), doi:10.1029/2006EO500002

Biggs DC, Hu C, Müller-Karger FE (2008) Remotely sensed sea-surface chlorophyll and POC flux at Deep Gulf of Mexico Benthos sampling stations. Deep Sea Research Part II: Topical Studies in Oceanography 55:2555-2562

Billett DSM (1991) Deep-sea holothurians. Oceanography and Marine Biology: An Annual Review 29:259-317

Billett DSM, Bett BJ, Reid WDK, Boorman B, Priede IG (2010) Long-term change in the abyssal NE Atlantic: The 'Amperima Event' revisited. Deep Sea Research Part II: Topical Studies in Oceanography 57:1406-1417

Bivand RS, Pebesma EJ, Gomez-Rubio V (2008) Applied spatial data analysis with R, Springer, New York

Boehlert G, Genin A (1987) A review of the effects of seamounts on biological processes. In: Keating BH (ed) Seamounts, islands and atolls. American Geophysical Union, p 319–334

Boetius A, Lochte K (1994) Regulation of microbial enzymatic degradation of organic matter in deep-sea sediments. Marine Ecology-Progress Series 104:299-299

Boland GS, Rowe GT (1991) Deep-sea benthic sampling with the GOMEX box corer. Limnology and Oceanography 36:1015-1020

Bray JR, Curtis JT (1957) An ordination of the upland forest communities of southern Wisconsin. Ecological Monographs 27:326-349

Breiman L (2001) Random forests. Machine Learning 45:5-32

Breiman L, Freidman J, Olshen R, Stone C (1984) Classification and regression trees, Wadsworth, Belmont, CA

Brooks J, Kennicutt M (1987) Deep-sea hydrocarbon seep communities: Evidence for energy and nutritional carbon sources. Science 238:1138

Bryant WR, Lugo J, Cordova C, Salvador A (1991) Physiography and bathymetry. In: Salvador A (ed) The Gulf of Mexico Basin, Vol J. Geological Society of America, Boulder, CO, p 13-30

Cai W-J, Lohrenz SE (2010) The Mississippi River plume and adjacent margin in the Gulf of Mexico. In: Liu K-K, Atkinson L, Quiñones RA, Talaue-McManus L (eds) Carbon and nutrient fluxes in continental margins: A global synthesis. Springer, Berlin, Germany, p 406-423

Camilli R, Reddy CM, Yoerger DR, Van Mooy BAS, Jakuba MV, Kinsey JC, McIntyre CP, Sylva SP, Maloney JV (2010) Tracking hydrocarbon plume transport and biodegradation at Deepwater Horizon. Science 330:201-204

Carney RS (1994) Consideration of the oasis analogy for chemosynthetic communities at Gulf of Mexico hydrocarbon vents. Geo-Marine Letters 14:149-159

Carney RS (2005) Zonation of deep-sea biota on continental margins. Oceanography and Marine Biology An Annual Review 43:211-279

Carney RS, Haedrich RL, Rowe GT (1983) Zonation of fauna in the deep sea. In: Rowe GT (ed) Deep-Sea biology, Vol 8. Wily-Interscience, New York, p 371-398

Cartes JE, Carrasson M (2004) Influence of trophic variables on the depth-range distributions and zonation rates of deep-sea megafauna: The case of the Western Mediterranean assemblages. Deep Sea Research Part I: Oceanographic Research Papers 51:263-279

Cartes JE, Sardà F (1993) Zonation of deep-sea decapod fauna in the Catalan Sea (Western Mediterranean). Marine Ecology Progress Series 94:27-34

Cartes JE, Sorbe JC (1997) Bathyal cumaceans of the Catalan Sea (North-western Mediterranean): Faunistic composition, diversity and near-bottom distribution along the slope (between 389 and 1859 m). Journal of Natural History 31:1041-1054

Clarke KR, Gorley RN (2006) PRIMER v6: user manual/tutorial., PRIMER-E, Plymouth, UK

Clarke KR, Somerfield PJ, Gorley RN (2008) Testing of null hypotheses in exploratory community analyses: similarity profiles and biota-environment linkage. Journal of Experimental Marine Biology and Ecology 366:56-69

Clarke KR, Warwick RM (2001) Change in marine communities: An approach to statistical analysis and interpretation, Primer-e, Polymouth

Clough L, Ambrose W (1997) Infaunal density, biomass and bioturbation in the sediments of the Arctic Ocean. Deep Sea Research Part II: Topical Studies in Oceanography 44:1683-1704

Clough L, Renaud P, Ambrose Jr W (2005) Impacts of water depth, sediment pigment concentration, and benthic macrofaunal biomass on sediment oxygen demand in the western Arctic Ocean. Canadian Journal of Fisheries and Aquatic Sciences 62:1756-1765

Cordes EE, Bergquist DC, Fisher CR (2009) Macro-ecology of Gulf of Mexico cold seeps. Annual Review of Marine Science 1:143-168

Crabtree RE, Carter J, Musick JA (1991) The comparative feeding ecology of temperate and tropical deep-sea fishes from the western North Atlantic. Deep Sea Research Part A Oceanographic Research Papers 38:1277-1298

Crone TJ, Tolstoy M (2010) Magnitude of the 2010 Gulf of Mexico oil leak. Science 330:634

Culver SJ (1988) New foraminiferal depth zonation of the northwestern Gulf of Mexico. PALAIOS 3:69-85

Culver SJ, Buzas MA (1981) Foraminifera distribution of provinces in the Gulf of Mexico. Nature 290:328-329

Culver SJ, Buzas MA (1983) Recent benthic foraminiferal provinces in the Gulf of Mexico. Journal of Foraminiferal Research 13:21-31

Cutler A, Stevens JR (2006) Random forests for microarrays. In: Alan K, Brian O (eds) Methods in enzymology, Vol 411. Academic Press, San Diego, CA, p 422-432

Cutler DR, Edwards TC, Beard KH, Cutler A, Hess KT, Gibson J, Lawler JJ (2007) Random forests for classification in ecology. Ecology 88:2783-2792

Danovaro R, Croce ND, Eleftheriou A, Fabiano M, Papadopoulou N, Smith C, Tselepides A (1995) Meiofauna of the deep Eastern Mediterranean Sea: Distribution and abundance in relation to bacterial biomass, organic matter composition and other environmental factors. Progress in Oceanography 36:329-341

Danovaro R, Dell'Anno A, Corinaldesi C, Magagnini M, Noble R, Tamburini C, Weinbauer M (2008) Major viral impact on the functioning of benthic deep-sea ecosystems. Nature 454:1084-1087

Danovaro R, Gambi C, Della Croce N (2002) Meiofauna hotspot in the Atacama Trench, eastern South Pacific Ocean. Deep Sea Research Part I: Oceanographic Research Papers 49:843-857

De Leo FC, Smith CR, Rowden AA, Bowden DA, Clark MR (2010) Submarine canyons: Hotspots of benthic biomass and productivity in the deep sea. Proceedings of the Royal Society B: Biological Sciences 277(1695):2783-2792

Dean H (2008) The use of polychaetes (Annelida) as indicator species of marine pollution: A review. Revista de Biología Tropical 56:11-38

De'ath G (2007) Boosted trees for ecological modeling and prediction. Ecology 88:243-251

Deming J, Baross J (1993) The early diagenesis of organic matter: Bacterial activity. In: Engel MH, Macko SA (eds) Organic geochemistry. Plenum Press, New York, p 119-144

Deming J, Baross J (2000) Survival, dormancy, and nonculturable cells in extreme deep-sea environments. In: Colwell RR, Grimes DJ (eds) Nonculturable microorganisms in the environments. American Society for Microbiology Press, Washington, DC, p 147–197

Deming J, Yager P (1992) Natural bacterial assemblages in deep-sea sediments: Towards a global view. In: Rowe GT, Pariente V (eds) Deep-sea food chains and the global carbon cycle. Kluwer, Dordrecht, The Netherlands, p 11-27

Deming JW, Carpenter SD (2008) Factors influencing benthic bacterial abundance, biomass, and activity on the northern continental margin and deep basin of the Gulf of Mexico. Deep Sea Research Part II: Topical Studies in Oceanography 55:2597-2606

Deming JW, Colwell RR (1985) Observations of barophilic microbial activity in samples of sediment and intercepted particulates from the Demerara Abyssal Plain. Appl Environ Microbiol 50:1002-1006

Denne RA, Sen Gupta BK (1991) Association of bathyal foraminifera with water masses in the northwestern Gulf of Mexico. Marine Micropaleontology 17:173-193

Dixon JL, Turley CM (2000) The effect of water depth on bacterial numbers, thymidine incorporation rates and C:N ratios in northeast Atlantic surficial sediments. Hydrobiologia 440:217-225

Dunne J, Sarmiento J, Gnanadesikan A (2007) A synthesis of global particle export from the surface ocean and cycling through the ocean interior and on the seafloor. Global Biogeochemical Cycles 21:GB4006

Ekman S (1953) Zoogeography of the sea, Sidgwick and Jackson, London

Escobar-Briones E, Estrada Santillán EL, Legendre P (2008a) Macrofaunal density and biomass in the Campeche Canyon, Southwestern Gulf of Mexico. Deep Sea Research Part II: Topical Studies in Oceanography 55:2679-2685

Escobar-Briones EG, Díaz C, Legendre P (2008b) Meiofaunal community structure of the deep-sea Gulf of Mexico: Variability due to the sorting methods. Deep Sea Research Part II: Topical Studies in Oceanography 55:2627-2633

Escobar-Briones EG, Soto LA (1997) Continental shelf benthic biomass in the western Gulf of Mexico. Continental Shelf Research 17:585-604

Fauchald K, Jumars PA (1979) Diet of worms: A study of polychaete feeding guilds. Annual Review of Oceanography and Marine Biology 17:193-284

Flach E, Muthumbi A, Heip C (2002) Meiofauna and macrofauna community structure in relation to sediment composition at the Iberian margin compared to the Goban Spur (NE Atlantic). Progress in Oceanography 52:433-457

French CD, Schenk CJ (2006) Map showing geology, oil and gas fields, and geologic provinces of the Gulf of Mexico region. World Energy Assessment Team, USGS, URL: http://pubs.usgs.gov/of/1997/ofr-97-470/OF97-470L/

Froese R, Pauly D (eds) (2000) FishBase 2000: Concepts, design and data sources, Vol 1594. ICLARM, Los Baños, Laguna, Philippines.

Gage J, Bett B (2005) Deep-sea benthic sampling. In: Eleftheriou A, McIntyre A (eds) Methods for the study of the marine benthos. Blackwell, Oxford, UK, p 273-325

Gage JD, Hughes DJ, Vecino JLG (2002) Sieve size influence in estimating biomass, abundance and diversity in samples of deep-sea macrobenthos. Marine Ecology Progress Series 225:97-107

Gage JD, Lamont PA, Kroeger K, Paterson GLJ, Gonzalez Vecino JL (2000) Patterns in deep-sea macrobenthos at the continental margin: standing crop, diversity and faunal change on the continental slope off Scotland. Hydrobiologia 440:261-271

Gage JD, Tyler PA (1991) Deep-sea biology: A natural history of organisms at the deep-sea floor, Cambridge University Press, Cambridge

Gallagher ED (1996) COMPAH 96 documentation. University of Massachusetts at Boston, Boston, MA, p 59

Gallaway BJ (1988) Northern Gulf of Mexico continental slope study, final report: Year 4. Volume II: Synthesis report., U.S. Department of the Interior, Minerals Management Service, Gulf of Mexico OCS Regional Office, New Orleans, LA.

Gardner WD (1989) Baltimore Canyon as a modern conduit of sediment to the deep sea. Deep Sea Research Part A Oceanographic Research Papers 36:323-358

Gartner JV, Crabtree RE, Sulak KJ (1997) Feeding at depth. In: David JR, Anthony PF (eds) Fish physiology, Vol 16. Academic Press, San Diego, CA, p 115-193

Gesteira JLG, Dauvin JC (2000) Amphipods are good bioindicators of the impact of oil spills on soft-bottom macrobenthic communities. Marine Pollution Bulletin 40:1017-1027

Gettleson DA (1976) An ecological study of the benthic meiofauna and macroinfauna of a soft bottom area on the Texas outer continental shelf. Ph.D dissertation, Texas A&M University, College Station, TX

Gooday A, Levin L, Linke P, Heeger T (1992) The role of benthic foraminifera in deep-sea food webs and carbon cycling. In: Rowe G, Pariente V (eds) Deep-sea food chains and the global carbon cycle. Kluwer, Dordrecht, The Netherlands, p 63-91

Gordon JDM, Merrett NR, Haedrich RL (1995) Environmental and biological aspects of slope-dwelling fishes. In: Hopper AG (ed) Deep-water fisheries of the North Atlantic Oceanic slope. Kluwer Academic Publishers, Dordrecht, the Netherlands, p 1–30

Graham WM, Condon RH, Carmichael RH, D'Ambra I, Patterson HK, Linn LJ, Hernandez FJ (2010) Oil carbon entered the coastal planktonic food web during the Deepwater Horizon oil spill. Environmental Research Letters 5:045301

Grassle JF, Elmgren R, Grassle JP (1981) Response of benthic communities in merl experimental ecosystems to low level, chronic additions of No. 2 fuel oil. Marine Environmental Research 4:279-297

Grassle JF, Sanders HL, Smith WK (1979) Faunal changes with depth in the deep-sea benthos. Ambio Special Report 6:47-50

Grassle JF, Smith W (1976) A similarity measure sensitive to the contribution of rare species and its use in investigation of variation in marine benthic communities. Oecologia 25:13-22

Grebmeier JM, Barry JP (2007) Chapter 11 benthic processes in polynyas. In: Smith WO, Barber DG (eds) Elsevier oceanography series, Vol 74. Elsevier, Netherlands, p 363-390

Grebmeier JM, Cooper LW, Feder HM, Sirenko BI (2006) Ecosystem dynamics of the Pacific-influenced Northern Bering and Chukchi Seas in the Amerasian Arctic. Progress in Oceanography 71:331-361

Haedrich RL, Rowe GT, Polloni PT (1975) Zonation and faunal composition of epibenthic populations on the continental slope south of New England. Journal of Marine Research 33:191-212

Haedrich RL, Rowe GT, Polloni PT (1980) The megabenthic fauna in the deep sea south of New England, USA. Marine Biology 57:165-179

Hamilton P, Lugo-Fernandez A (2001) Observations of high speed deep currents in the northern Gulf of Mexico. Geophysical Research Letters 28:2867-2870

Hazen TC, Dubinsky EA, DeSantis TZ, Andersen GL, Piceno YM, Singh N, Jansson JK, Probst A, Borglin SE, Fortney JL, Stringfellow WT, Bill M, Conrad ME, Tom LM, Chavarria KL, Alusi TR, Lamendella R, Joyner DC, Spier C, Baelum J, Auer M, Zemla ML, Chakraborty R, Sonnenthal EL, D'haeseleer P, Holman H-

YN, Osman S, Lu Z, Van Nostrand JD, Deng Y, Zhou J, Mason OU (2010) Deep-sea oil plume enriches indigenous oil-degrading bacteria. Science 330:204-208

Hecker B (1990) Variation in megafaunal assemblages on the continental margin south of New England. Deep Sea Research Part A Oceanographic Research Papers 37:37-57

Heip CHR, Duineveld G, Flach E, Graf G, Helder W, Herman PMJ, Lavaleye M, Middelburg JJ, Pfannkuche O, Soetaert K, Soltwedel T, de Stigter H, Thomsen L, Vanaverbeke J, de Wilde P (2001) The role of the benthic biota in sedimentary metabolism and sediment-water exchange processes in the Goban Spur area (NE Atlantic). Deep Sea Research Part II: Topical Studies in Oceanography 48:3223-3243

Ho CK, Pennings SC, Carefoot TH (2010) Is diet quality an overlooked mechanism for Bergmann's rule? The American Naturalist 175:269-276

Holme N, McIntyre A (1971) Methods for the study of marine benthos. IBP Handbook No. 16, Blackwell, Oxford, UK

Howell KL, Billett DSM, Tyler PA (2002) Depth-related distribution and abundance of seastars (Echinodermata: Asteroidea) in the Porcupine Seabight and Porcupine Abyssal Plain, N.E. Atlantic. Deep Sea Research Part I: Oceanographic Research Papers 49:1901-1920

Huitema BE (1980) Chapter 13 analysis of heterogeneous regression case: Johnson-Neyman technique. In: The analysis of covariance and alternatives, Wiley-Interscience, New York, p 271-296

Ingels J, Van den Driessche P, De Mesel I, Vanhove S, Moens T, Vanreusel A (2010) Preferred use of bacteria over phytoplankton by deep-sea nematodes in polar regions. Mar Ecol Prog Ser 406:121-133

IPCC 2007 Climate Change (ed) (2007) The Physical Science Basis. Contribution of Working Group I to the Fourth Assessment Report of the Intergovernmental Panel on Climate Change Cambridge University Press, Cambridge, UK and New York, USA

Jacob W, McClatchie S, Probert PK, Hurst RJ (1998) Demersal fish assemblages off southern New Zealand in relation to depth and temperature. Deep Sea Research Part I: Oceanographic Research Papers 45:2119-2155

Jochens AE, DiMarco SF (2008) Physical oceanographic conditions in the deepwater Gulf of Mexico in summer 2000-2002. Deep Sea Research Part II: Topical Studies in Oceanography 55:2541-2554

Johnson NA, Campbell JW, Moore TS, Rex MA, Etter RJ, McClain CR, Dowell MD (2007) The relationship between the standing stock of deep-sea macrobenthos and surface production in the western North Atlantic. Deep Sea Research Part I: Oceanographic Research Papers 54:1350-1360

Joye S, MacDonald I (2010) Offshore oceanic impacts from the BP oil spill. Nature Geoscience 3:446-446

Joye SB, MacDonald IR, Leifer I, Asper V (2011) Magnitude and oxidation potential of hydrocarbon gases released from the BP oil well blowout. Nature Geoscience advance online publication

Judson RS, Martin MT, Reif DM, Houck KA, Knudsen TB, Rotroff DM, Xia M, Sakamuru S, Huang R, Shinn P, Austin CP, Kavlock RJ, Dix DJ (2010) Analysis of eight oil spill dispersants using rapid, in vitro tests for endocrine and other biological activity. Environmental Science & Technology 44:5979-5985

Jumars PA, Fauchald K (1977) Between-community contrasts in successful polychaete feeding strategies. In: Coull BC (ed) Ecology of Marine Benthos. University of South Carolina Press, Columbia, South Carolina, p 1-20

Kalogeropoulou V, Bett BJ, Gooday AJ, Lampadariou N, Martinez Arbizu P, Vanreusel A (2010) Temporal changes (1989-1999) in deep-sea metazoan meiofaunal assemblages on the Porcupine Abyssal Plain, NE Atlantic. Deep Sea Research Part II: Topical Studies in Oceanography 57:1383-1395

Kerr JT, Kharouba HM, Currie DJ (2007) The macroecological contribution to global change solutions. Science 316:1581-1584

Kessler JD, Valentine DL, Redmond MC, Du M, Chan EW, Mendes SD, Quiroz EW, Villanueva CJ, Shusta SS, Werra LM, Yvon-Lewis SA, Weber TC (2011) A persistent oxygen anomaly reveals the fate of spilled methane in the deep Gulf of Mexico. Science 331(6015):312-315

Kingston PF (2002) Long-term environmental impact of oil spills. Spill Science & Technology Bulletin 7:53-61

Kirchman DL, Moran XAG, Ducklow H (2009) Microbial growth in the polar oceans - role of temperature and potential impact of climate change. Nature Reviews Microbiology 7:451-459

Kujawinski EB, Kido Soule MC, Valentine DL, Boysen AK, Longnecker K, Redmond MC (2011) Fate of dispersants associated with the Deepwater Horizon oil spill. Environmental Science & Technology 45:1298–1306

Lampitt RS, Billett DSM, Martin AP (2010) The sustained observatory over the Porcupine Abyssal Plain (PAP): Insights from time series observations and process studies. Deep Sea Research Part II: Topical Studies in Oceanography 57:1267-1271

Lehr W, Bristol S, Possolo A (2010) Oil budget calculator Deepwater Horizon. The Federal Interagency Solutions Group, Oil Budget Calculator Science and Engineering Team, National Incident Command, p 217

Levin L, Gage J, Martin C, Lamont P (2000) Macrobenthic community structure within and beneath the oxygen minimum zone, NW Arabian Sea. Deep Sea Research Part II: Topical Studies in Oceanography 47:189-226

Levitus S (ed) (2010) World Ocean Atlas 2009, Vol 1-4. NOAA Atlas NESDIS 68-71, U.S. Government Printing Office, Washington, D.C., US

Liaw A, Wiener M (2002) Classification and regression by randomForest. R News 2:18-22

Lochte K (1992) Bacterial standing stock and consumption of organic carbon in the benthic boundary layer of the abyssal North Atlantic. In: Rowe GT, Pariente V

(eds) Deep-sea food chains and the global carbon cycle. Kluwer, Dordrecht, The Netherlands, p 1-10

Lochte K, Turley CM (1988) Bacteria and cyanobacteria associated with phytodetritus in the deep sea. Nature 333:67-69

Lohrenz SE, Wiesenburg DA, Arnone RA, Chen X (1999) What controls primary production in the Gulf of Mexico. In: Kumpf H, Steidinger K, Sherman K (eds) The Gulf of Mexico large marine ecosystem: Assessment, sustainability and management. Blackwell Science, Malden, MA, p 151–170

Loubere P, Gary A, Lagoe M (1993) Sea-bed biogeochemistry and benthic foraminiferal bathymetric zonation on the slope of the Northwest Gulf of Mexico. PALAIOS 8:439-449

Markle DF, Musick JA (1974) Benthic-slope fishes found at 900m depth along a transect in the western N. Atlantic Ocean. Marine Biology 26:225-233

McClain C, Rex M, Etter R (2009) Patterns in deep-sea macroecology In: Witman JD, Roy K (eds) Marine macroecology. The University of Chicago Press, Chicago, p 440

McClatchie S, Millar RB, Webster F, Lester PJ, Hurst R, Bagley N (1997) Demersal fish community diversity off New Zealand: Is it related to depth, latitude and regional surface phytoplankton? Deep Sea Research Part I: Oceanographic Research Papers 44:647-667

McIntyre AD (ed) (2010) Life in the world's oceans: Diversity, distribution and abundance, Wiley-Blackwell, Oxford, UK

McLellan H, Nowlin W (1963) Some features of the deep water in the Gulf of Mexico. Journal of Marine Research 21:233-245

Menge BA, Sutherland JP (1976) Species diversity gradients: Synthesis of the roles of predation, competition, and temporal heterogeneity. The American Naturalist 110:351-369

Menzies RJ, George RY, Rowe GT (1973) Abyssal environment and ecology of the world ocean. Wiley, New York, p 488

Morse JW, Beazley MJ (2008) Organic matter in deepwater sediments of the Northern Gulf of Mexico and its relationship to the distribution of benthic organisms. Deep Sea Research Part II: Topical Studies in Oceanography 55:2563-2571

Müller-Karger FE, Walsh JJ, Evans RH, Meyers MB (1991) On the seasonal phytoplankton concentration and sea surface temperature cycles of the Gulf of Mexico as determined by satellites. Journal Geophysical Research 96:12645-12665

Narayanaswamy BE, Bett BJ, Hughes DJ (2010) Deep-water macrofaunal diversity in the Faroe-Shetland region (NE Atlantic): A margin subject to an unusual thermal regime. Marine Ecology 31:237-246

Oey L-Y, Lee H-C (2002) Deep eddy energy and topographic rossby waves in the Gulf of Mexico. Journal of Physical Oceanography 32:3499-3527

Olabarria C (2005) Patterns of bathymetric zonation of bivalves in the Porcupine Seabight and adjacent Abyssal plain, NE Atlantic. Deep Sea Research Part I: Oceanographic Research Papers 52:15-31

Oppel S, Huettmann F (2010) Using a Random Forest model and public data to predict the distribution of prey for marine wildlife management. In: Cushman SA, Huettmann F (eds) Spatial complexity, informatics, and wildlife conservation, Springer, New York, p 151-163

Pace ML, Knauer GA, Karl DM, Martin JH (1987) Primary production, new production and vertical flux in the eastern Pacific Ocean. Nature 325:803-804

Patching JW, Eardly D (1997) Bacterial biomass and activity in the deep waters of the eastern Atlantic--evidence of a barophilic community. Deep Sea Research Part I: Oceanographic Research Papers 44:1655-1670

Pavithran S, Ingole B, Nanajkar M, Goltekar R (2009) Importance of sieve size in deep-sea macrobenthic studies. Marine Biology Research 5:391-398

Pequegnat WE (1983) The ecological communities of the continental slope and adjacent regimes of the northern Gulf Of Mexico., A final report by TerEco Corporation for the U.S. Department of the Interior, Minerals Management Service Gulf of Mexico OCS Office Metairie, LA

Pequegnat WE, Bright T, James BM (1970) The benthic skimmer, a new biological sampler for deep-sea studies. In: Pequegnat WE, Chace FA (eds) Texas A&M University Oceanographic Studies, Vol 1: Contributions on the biology of the Gulf of Mexico Gulf Publishing Company, Houston, USA, p 17-20

Pequegnat WE, Gallaway BJ, Pequegnat LH (1990) Aspects of the ecology of the deep-water fauna of the Gulf of Mexico. American Zoologist 30:45-64

Pérez-Mendoza AY, Hernández-Alcántara P, Solís-Weiss V (2003) Bathymetric distribution and diversity of deep water polychaetous annelids in the Sigsbee Basin, northwestern Gulf of Mexico. Hydrobiologia 496:361-370

Petersen CGJ (1913) Valuation of the sea, Part 2. The animal communities of the sea-bottom and their importance for marine zoogeography. Report of the Danish Biological Station 21:1-43

Petersen CGJ (1918) The sea-bottom and its production of fish-food. Report of the Danish Biological Station 25:1-62

Pfannkuche O, Lochte K (2000) The biogeochemistry of the deep Arabian Sea: Overview. Deep Sea Research Part II: Topical Studies in Oceanography 47:2615-2628

Pikitch EK, Santora C, Babcock EA, Bakun A, Bonfil R, Conover DO, Dayton P, Doukakis P, Fluharty D, Heneman B, Houde ED, Link J, Livingston PA, Mangel M, McAllister MK, Pope J, Sainsbury KJ (2004) Ecosystem-Based Fishery Management. Science 305:346-347

Pitcher CR, Lawton P, Ellis N, Smith SJ, Incze LS, Wei C-L, Greenlaw ME, Wolff NH, Sameoto JA, Snelgrove PVR (In preparation) Exploring the role of environmental variables in shaping patterns of biodiversity composition in seabed assemblages.

Powell SM, Haedrich RL, McEachran JD (2003) The deep-sea demersal fish fauna of the northern Gulf of Mexico. Journal of Northwest Atlantic Fishery Science 31:19-33

Prasad A, Iverson L, Liaw A (2006) Newer classification and regression tree techniques: Bagging and random forests for ecological prediction. Ecosystems 9:181-199

Quéric N-V, Soltwedel T, Arntz WE (2004) Application of a rapid direct viable count method to deep-sea sediment bacteria. Journal of Microbiological Methods 57:351-367

Quiroga E, Quiñones R, Palma M, Sellanes J, Gallardo VA, Gerdes D, Rowe G (2005) Biomass size-spectra of macrobenthic communities in the oxygen minimum zone off Chile. Estuarine, Coastal and Shelf Science 62:217-231

R Development Core Team (2010) R: A language and environment for statistical computing R Foundation for Statistical Computing, Vienna, Austria

Rex M, Etter R (2010) Deep-sea biodiversity: Pattern and scale, Harvard University Press, Cambridge, MA

Rex MA (1977) Zonation in deep-sea gastropods: The importance of biological interactions to rates of zonation. In: Keegan BF, Ceidigh, P. O., Boaden, P. J. S. (ed) Biology of benthic organism. Pergamon Press, New York, p 521-530

Rex MA (1981) Community structure in the deep-Sea benthos. Annual Review of Ecology and Systematics 12:331-353

Rex MA, Etter RJ, Morris JS, Crouse J, McClain CR, Johnson NA, Stuart CT, Deming JW, Thies R, Avery R (2006) Global bathymetric patterns of standing stock and body size in the deep-sea benthos. Marine Ecology Progress Series 317:1-8

Rex MA, McClain CR, Johnson NA, Etter RJ, Allen JA, Bouchet P, Warén A (2005) A source-sink hypothesis for abyssal biodiversity. The American Naturalist 165:163-178

Richardson GE, Nixon LD, Bohannon CM, Kazanis EG, Montgomery TM, Gravois MP (2008) Deepwater Gulf of Mexico 2008: America's offshore energy future, U.S. Department of the Interior, Minerals Management Service, Gulf of Mexico OCS Region, New Orleans, LA

Richardson MD, Young DK (1987) Abyssal benthos of the Venezuela Basin, Caribbean Sea: standing stock considerations. Deep Sea Research Part A Oceanographic Research Papers 34:145-164

Rowe GT (1968) Distribution patterns in populations of large, deep-sea benthic invertebrates off North Carolina. Ph.D. dissertation, Duke University, Durham, NC

Rowe GT (1983) Biomass and production of deep-sea macrobenthos. In: Rowe GT (ed) Deep-sea biology, Vol 8. Wily-Interscience, New York, p 97-121

Rowe GT, Boland GS, Escobar Briones EG, Cruz-Kaegi ME, Newton A, Piepenburg D, Walsh I, Deming J (1997) Sediment community biomass and respiration in the Northeast water polynya, Greenland: A numerical simulation of benthic lander and spade core data. Journal of Marine Systems 10:497-515

Rowe GT, Boland GS, Phoel WC, Anderson RF, Biscaye PE (1994) Deep-sea floor respiration as an indication of lateral input of biogenic detritus from continental

margins. Deep Sea Research Part II: Topical Studies in Oceanography 41:657-668

Rowe GT, Deming JW (In Press) An alternative view of the role of bacteria in the cycling of organic matter in deep-sea sediments. Marine Biology Research

Rowe GT, Kennicutt MC (2008) Introduction to the Deep Gulf of Mexico Benthos program. Deep Sea Research Part II: Topical Studies in Oceanography 55:2536-2540

Rowe GT, Kennicutt MC (2009) Northern Gulf of Mexico continental slope habitats and benthic ecology study, final report. U.S. Dept. of the Interior, Minerals Management Service, Gulf of Mexico OCS Region Regional Office, New Orleans, LA.

Rowe GT, Lohse A, Hubbard F, Boland GS, Escobar Briones E, Deming J (2003) Preliminary trophodynamic carbon budget for the Sigsbee Deep benthos, Northern Gulf of Mexico. American Fisheries Society Symposium 36:225-238

Rowe GT, Menzel D (1971) Quantitative benthic samples from the deep Gulf of Mexico with some comments on the measurement of deep-sea biomass. Bulletin of Marine Science 21:556-566

Rowe GT, Menzies RJ (1969) Zonation of large benthic invertebrates in the deep-sea off the Carolinas. Deep Sea Research and Oceanographic Abstracts 16:531-532

Rowe GT, Morse J, Nunnally C, Boland GS (2008) Sediment community oxygen consumption in the deep Gulf of Mexico. Deep Sea Research Part II: Topical Studies in Oceanography 55:2686-2691

Rowe GT, Pariente V (eds) (1992) Deep-sea food chains and the global carbon cycle, Kluwer, Dordrecht, The Netherlands

Rowe GT, Polloni PT, Haedrich RL (1982) The deep-sea macrobenthos on the continental margin of the northwest Atlantic Ocean. Deep Sea Research Part A Oceanographic Research Papers 29:257-278

Rowe GT, Polloni PT, Horner SG (1974) Benthic biomass estimates from the northwestern atlantic ocean and the northern Gulf of Mexico. Deep Sea Research and Oceanographic Abstracts 21:641-650

Rowe GT, Sibuet M, Deming JW, Khripounoff A, Tietjen J, Macko S, Theroux R (1991) "Total" sediment biomass and preliminary estimates of organic carbon residence time in deep-sea benthos. Marine Ecology Progress Series 79:99-114

Rowe GT, Staresinic N (1979) Sources of organic matter to the deep-sea benthos. Ambio Special Report:19-23

Rowe GT, Wei C-L (In preparation) Biodiversity of deep-sea macrofauna as a function of food supply.

Rowe GT, Wei C-L, Nunnally C, Haedrich R, Montagna P, Baguley JG, Bernhard JM, Wicksten M, Ammons A, Briones EE, Soliman Y, Deming JW (2008) Comparative biomass structure and estimated carbon flow in food webs in the deep Gulf of Mexico. Deep Sea Research Part II: Topical Studies in Oceanography 55:2699-2711

Ruhl HA (2008) Community change in the variable resource habitat of the abyssal northeast Pacific. Ecology 89:991-1000

Ruhl HA, Ellena JA, Smith KL (2008) Connections between climate, food limitation, and carbon cycling in abyssal sediment communities. Proceedings of the National Academy of Sciences 105:17006-17011

Sanders HL, Hessler RR, Hampson GR (1965) An introduction to the study of deep-sea benthic faunal assemblages along the Gay Head-Bermuda transect. Deep Sea Research and Oceanographic Abstracts 12:845-848

Santschi PH, Rowe GT (2008) Radiocarbon-derived sedimentation rates in the Gulf of Mexico. Deep Sea Research Part II: Topical Studies in Oceanography 55:2572-2576

Sibuet M, Olu K (1998) Biogeography, biodiversity and fluid dependence of deep-sea cold-seep communities at active and passive margins. Deep Sea Research Part II: Topical Studies in Oceanography 45:517-567

Smith C (1992) Factors controlling bioturbation in deep-sea sediments and their relation to models of carbon diagenesis. In: Rowe GT, Pariente V (eds) Deep-sea food chains and the global carbon cycle. Kluwer, Dordrecht, The Netherlands, p 375-393

Smith CR, Berelson W, Demaster DJ, Dobbs FC, Hammond D, Hoover DJ, Pope RH, Stephens M (1997) Latitudinal variations in benthic processes in the abyssal equatorial Pacific: control by biogenic particle flux. Deep Sea Research Part II: Topical Studies in Oceanography 44:2295-2317

Smith CR, Maybaum HL, Baco AR, Pope RH, Carpenter SD, Yager PL, Macko SA, Deming JW (1998) Sediment community structure around a whale skeleton in

the deep Northeast Pacific: Macrofaunal, microbial and bioturbation effects. Deep Sea Research Part II: Topical Studies in Oceanography 45:335-364

Smith JKL, Druffel ERM (1998) Long time-series monitoring of an abyssal site in the NE Pacific: An introduction. Deep Sea Research Part II: Topical Studies in Oceanography 45:573-586

Smith K, Hinga K (1983) Sediment community respiration in the deep sea. In: GT R (ed) Deep-sea biology. Wily-Interscience, New York, p 331–370

Smith KL, Ruhl HA, Bett BJ, Billett DSM, Lampitt RS, Kaufmann RS (2009) Climate, carbon cycling, and deep-ocean ecosystems. Proceedings of the National Academy of Sciences 106:19211-19218

Snelgrove P (2010) Discoveries of the census of marine life: Making ocean life count, Cambridge University Press, Cambridge, UK

Soliman Y, Wicksten M (2007) Ampelisca mississippiana: A new species (Crustacea: Amphipoda: Gammaridea) from the Mississippi Canyon (Northern Gulf of Mexico). Zootaxa 1389:45-54

Soliman YS, Wade TL (2008) Estimates of PAHs burdens in a population of ampeliscid amphipods at the head of the Mississippi Canyon (N. Gulf of Mexico). Deep Sea Research Part II: Topical Studies in Oceanography 55:2577-2584

Soltwedel T (2000) Metazoan meiobenthos along continental margins: A review. Progress in Oceanography 46:59-84

Somero GN (1992) Biochemical ecology of deep-sea animals. Cellular and Molecular Life Sciences 48:537-543

Sørensen TA (1948) A method of establishing groups of equal amplitude in plant sociology based on similarity of species content, and its application to analyses of the vegetation on Danish commons. Kongelige Danske Videnskabernes Selskabs Biologiske Skrifter 5:1-34

Stefanescu C, Lloris D, Rucabado J (1993) Deep-sea fish assemblages in the Catalan Sea (western Mediterranean) below a depth of 1000 m. Deep Sea Research Part I: Oceanographic Research Papers 40:695-707

Stephenson TA, Stephenson A (1949) The universal features of zonation between tide-marks on rocky coasts. Journal of Ecology 37:289-305

Strobl C, Boulesteix A-L, Kneib T, Augustin T, Zeileis A (2008) Conditional variable importance for random forests. BMC Bioinformatics 9:307

Suess E (1980) Particulate organic carbon flux in the oceans-surface productivity and oxygen utilization. Nature 288:260-263

Svetnik V, Liaw A, Tong C, Culberson JC, Sheridan RP, Feuston BP (2003) Random Forest: A Classification and Regression Tool for Compound Classification and QSAR Modeling. Journal of Chemical Information and Computer Sciences 43:1947-1958

Sweetman A, Witte U (2008) Response of an abyssal macrofaunal community to a phytodetrital pulse. Marine Ecology Progress Series 355:73-84

Terborgh J (1971) Distribution on environmental gradients: Theory and a preliminary interpretation of distributional patterns in the avifauna of the Cordillera Vilcabamba, Peru. Ecology 52:23-40

Thiel H (1975) The size structure of the deep-sea benthos. Internationale Revue der gesamten Hydrobiologie und Hydrographie 60:575-606

Valentine DL, Kessler JD, Redmond MC, Mendes SD, Heintz MB, Farwell C, Hu L, Kinnaman FS, Yvon-Lewis S, Du M, Chan EW, Tigreros FG, Villanueva CJ (2010) Propane respiration jump-starts microbial response to a deep oil spill. Science 330:208-211

Van Dover C (2000) The ecology of deep-sea hydrothermal vents, Princeton University Press, Princeton, NJ

van Nugteren P, Herman P, Moodley L, Middelburg J, Vos M, Heip C (2009) Spatial distribution of detrital resources determines the outcome of competition between bacteria and a facultative detritivorous worm. Limnol Oceanogr 54:1413-1419

Vetter EW, Dayton PK (1998) Macrofaunal communities within and adjacent to a detritus-rich submarine canyon system. Deep Sea Research Part II: Topical Studies in Oceanography 45:25-54

Vetter Y, Deming J, Jumars P, Krieger-Brockett B (1998) A predictive model of bacterial foraging by means of freely released extracellular enzymes. Microbial ecology 36:75-92

Vinogradov M, Tseitlin V (1983) Deep-sea pelagic domain (aspects of bioenergetics). In: Rowe GT (ed) Deep-sea biology. Wily-Interscience, New York, p 123-165

Wade TL, Soliman Y, Sweet ST, Wolff GA, Presley BJ (2008) Trace elements and polycyclic aromatic hydrocarbons (PAHs) concentrations in deep Gulf of Mexico

sediments. Deep Sea Research Part II: Topical Studies in Oceanography 55:2585-2593

Wei C-L, Rowe G, Hubbard G, Scheltema A, Wilson G, Petrescu I, Foster J, Wicksten M, Chen M, Davenport R, Soliman Y, Wang Y (2010a) Bathymetric zonation of deep-sea macrofauna in relation to export of surface phytoplankton production. Marine Ecology Progress Series 399:1-14

Wei C-L, Rowe GT (2009) Faunal zonation of large epibenthic invertebrates off North Carolina revisited. Deep Sea Research Part II: Topical Studies in Oceanography 56:1830-1833

Wei C-L, Rowe GT, Briones EE, Nunnally C, Soliman4 Y (In preparation) Standing stocks and body size of deep-sea macrofauna: A baseline prior to the 2010 BP oil spill in the northern Gulf of Mexico.

Wei C-L, Rowe GT, Escobar-Briones E, Boetius A, Soltwedel T, Caley MJ, Soliman Y, Huettmann F, Qu F, Yu Z, Pitcher CR, Haedrich RL, Wicksten MK, Rex MA, Baguley JG, Sharma J, Danovaro R, MacDonald IR, Nunnally CC, Deming JW, Montagna P, Lévesque M, Weslawski JM, Wlodarska-Kowalczuk M, Ingole BS, Bett BJ, Billett DSM, Yool A, Bluhm BA, Iken K, Narayanaswamy BE (2010b) Global patterns and predictions of seafloor biomass using Random Forests. PLoS One 5:e15323

Westberry T, Behrenfeld M, Siegel D, Boss E (2008) Carbon-based primary productivity modeling with vertically resolved photoacclimation. Global Biogeochemical Cycles 22:GB2024

Whittaker RH (1960) Vegetation of the Siskiyou Mountains, Oregon and California. Ecological Monographs 30:279-338

Whittaker RH (1972) Evolution and measurement of species diversity. Taxon 21:213-251

Wicksten MK, Packard JM (2005) A qualitative zoogeographic analysis of decapod crustaceans of the continental slopes and abyssal plain of the Gulf of Mexico. Deep Sea Research Part I: Oceanographic Research Papers 52:1745-1765

Williams RG, Follows MJ (2003) Physical transport of nutrients and the maintenance of biological production. In: Fasham M (ed) Ocean biogeochemistry: The role of the ocean carbon cycle in global change. Springer, p 19-51

Wilson GDF (2008) Local and regional species diversity of benthic Isopoda (Crustacea) in the deep Gulf of Mexico. Deep Sea Research Part II: Topical Studies in Oceanography 55:2634-2649

Wiseman WJ, Sturges W (1999) Physical oceanography of the Gulf of Mexico: Processes that regulate its biology. In: Kumpf H, Steidinger K, Sherman K (eds) The Gulf of Mexico large marine ecosystem: Assessment, sustainability and management. Blackwell Science, Malden, MA, p 77-92

Witte U, Wenzhofer F, Sommer S, Boetius A, Heinz P, Aberle N, Sand M, Cremer A, Abraham WR, Jorgensen BB, Pfannkuche O (2003) In situ experimental evidence of the fate of a phytodetritus pulse at the abyssal sea floor. Nature 424:763-766

Xu P, Jelinek F (2004) Random forests in language modeling Proceedings of EMNLP 2004. Association for Computational Linguistics, Barcelona, Spain, p 325-332

Yool A, Shepherd JG, Bryden HL, Oschlies A (2009) Low efficiency of nutrient translocation for enhancing oceanic uptake of carbon dioxide. Journal of Geophysical Research 114:C08009

Young CM (2003) Reproduction, development and life-history traits. In: Tyler PA (ed) Ecosystems of the deep oceans. Elsevier, Amsterdam, p 381-426

Zar J (1984) Biostatistical analysis. Prentice Hall, New Jersey

Zardus JD (2002) Protobranch bivalves. In: Advances in marine biology, Vol 42. Academic Press, p 1-65

APPENDIX A

SUPPORTING FIGURES FOR CHAPTER II

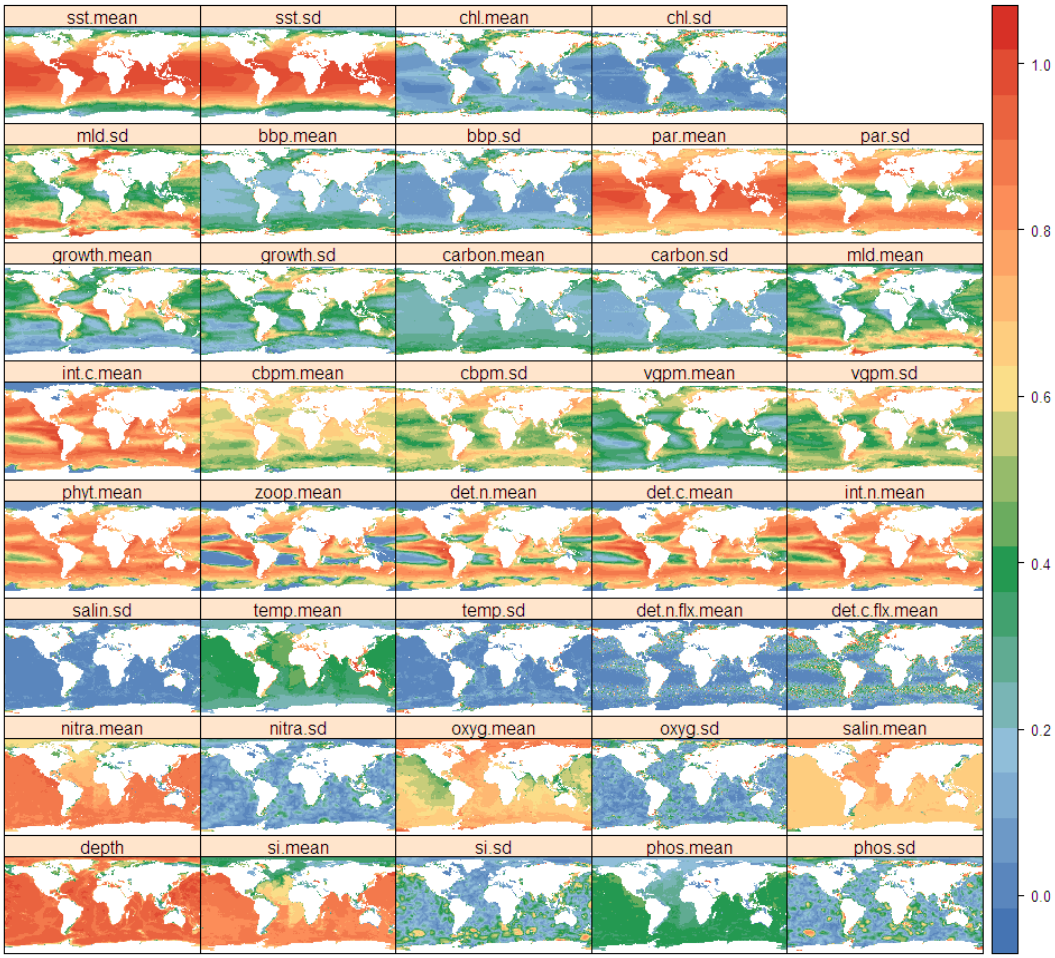

Fig. S1. Environmental predictors for Random Forest models. Data were logarithm transformed (base 10) and scaled to between 0 (minimum value) and 1 (maximum value). Detail description of the variable is given in Table 2.1. Abbreviations: mean = decadal or annual mean; sd = decadal or seasonal standard deviation.

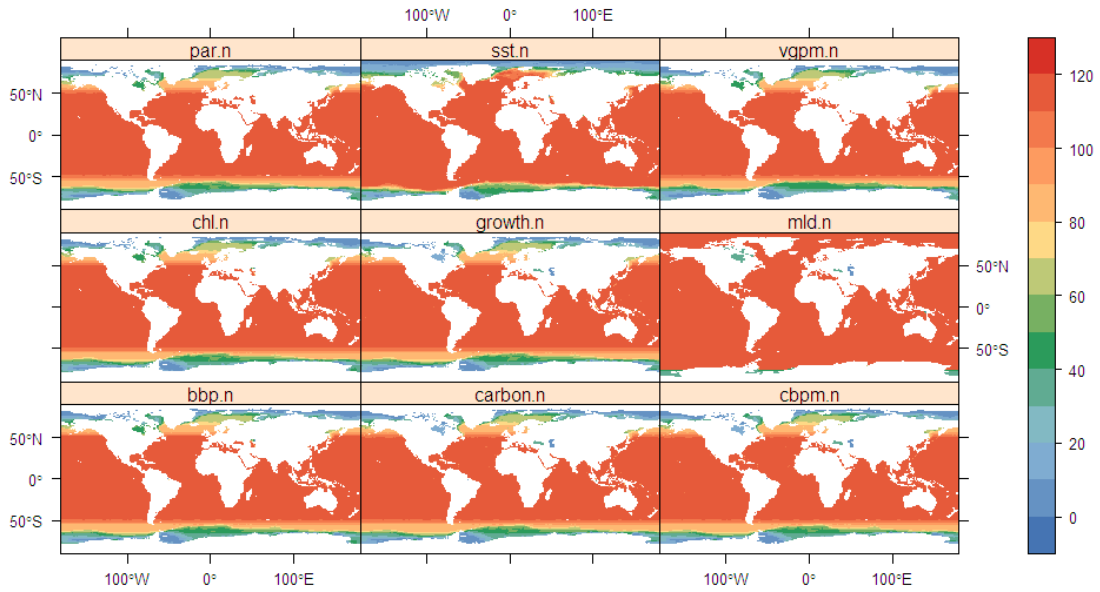

Fig. S2. Temporal coverage of primary productivity predictors between years of 1998 and 2007. Color ramp shows the sample size from 0 to 120 months of measurements. Detail description of the variable is given in Table 2.1. Abbreviations: n = sample size.

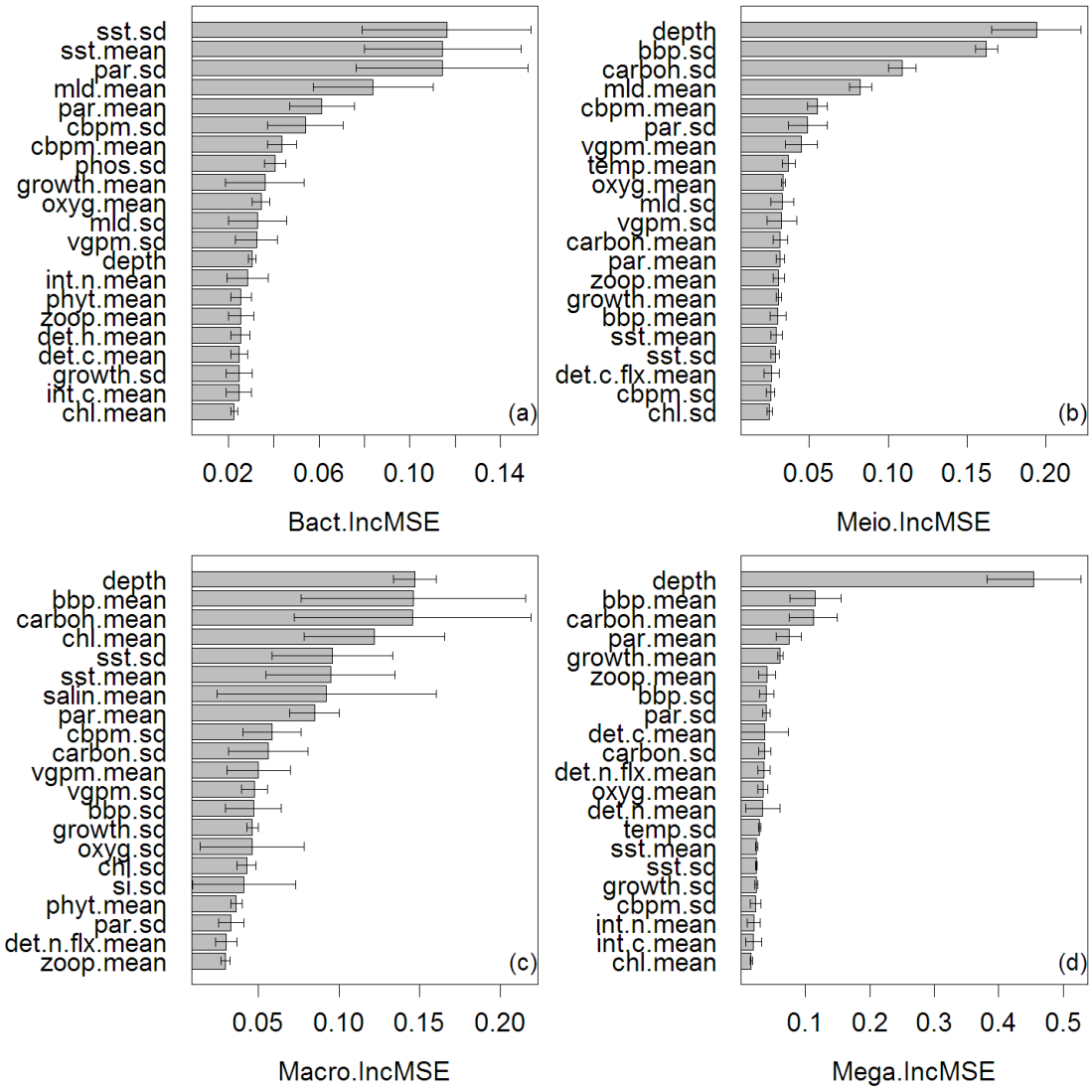

Fig. S3. Mean predictor Importance for biomass of (a) bacteria, (b) meiofauna, (c) macrofauna, and (d) megafauna. The mean ± S.D. (error bar) were calculated from 4 RF simulations. The top 20 most important variables are shown in descending order. Increase of mean square error (IncMSE) indicates the contribution to RF prediction accuracy for that variable. Detail description of the variable is given in Table 2.1. Abbreviations: mean = decadal or annual mean; sd = decadal or seasonal standard deviation.

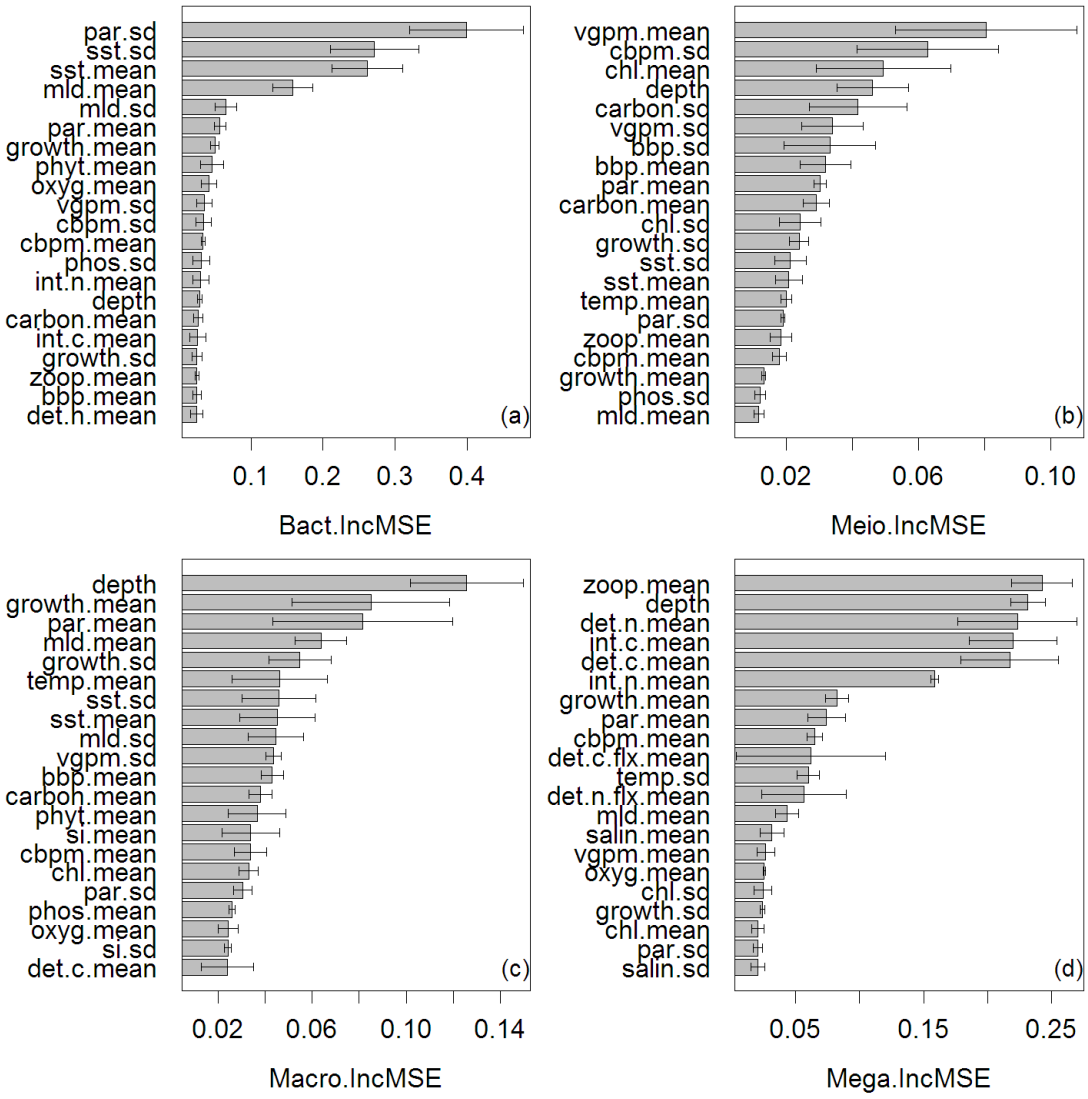

Fig. S4. Mean predictor Importance for abundance of (a) bacteria, (b) meiofauna, (c) macrofauna, and (d) megafauna. The mean ± S.D. (error bar) were calculated from 4 RF simulations. The top 20 most important variables are shown in descending order. Increase of mean square error (IncMSE) indicates the contribution to RF prediction accuracy for that variable. Detail description of the variable is given in Table 1. Abbreviations: mean = decadal or annual mean; sd = decadal or seasonal standard deviation.

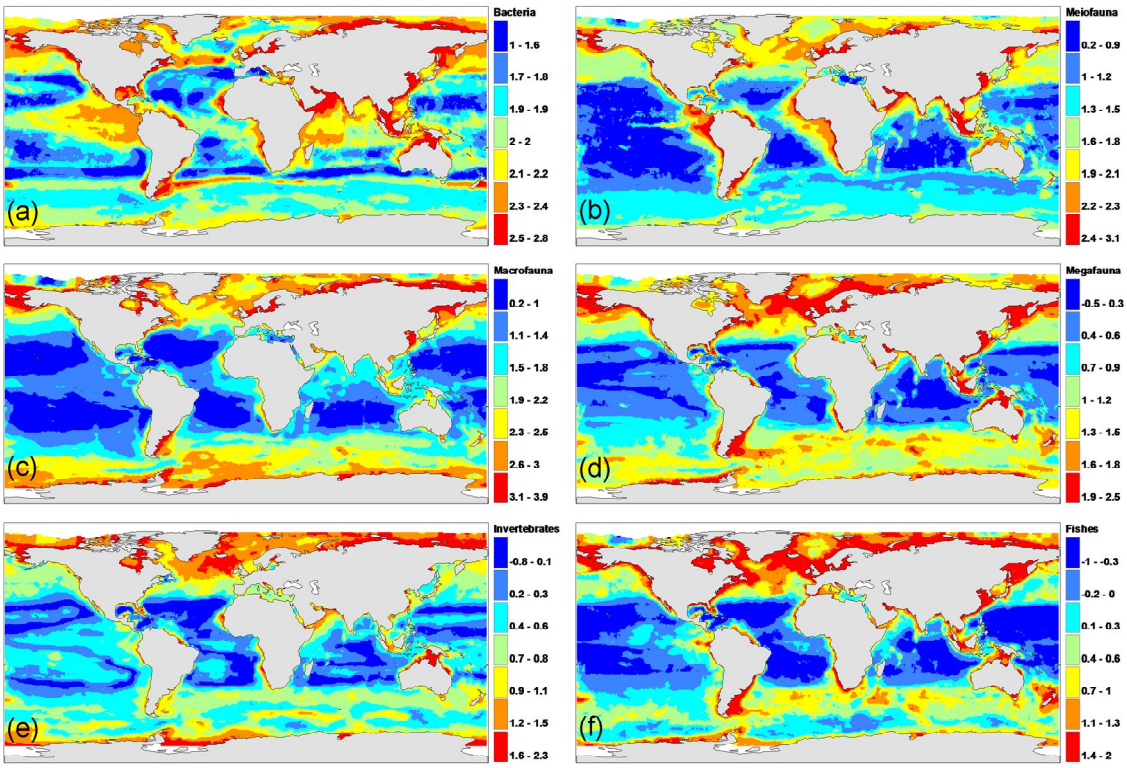

Fig. S5. Distribution of mean biomass predictions for (a) bacteria, (b) meiofauna, (c) macrofauna, (d) megafauna, (e) invertebrates, and (f) fishes. The mean biomass was computed from 4 RF simulations. Predictions were smoothed by Inverse Distance Weighting interpolation to 0.1 degree resolution and displayed in logarithm scale (base of 10).

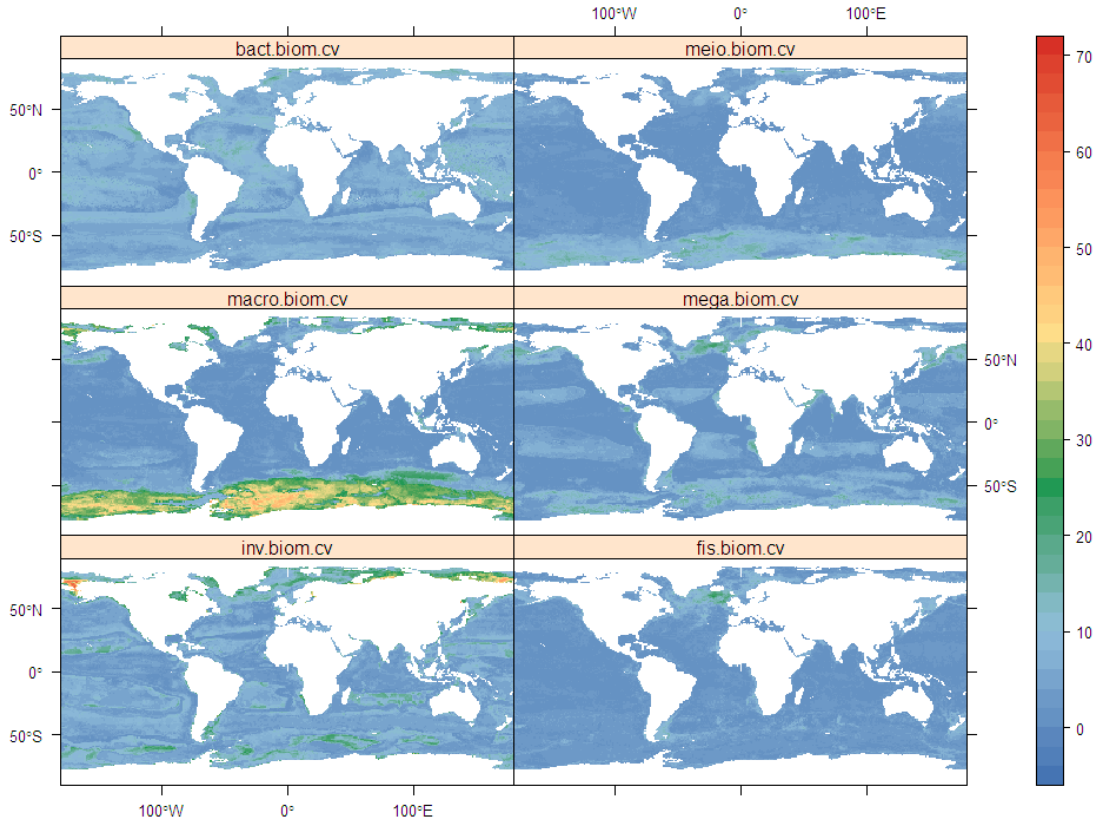

Fig. S6. Coefficient of variation (C.V.) for mean biomass predictions of each size class. The C.V. was computed as S.D. /mean * 100% from 4 RF simulations. The abbreviations are: bact = bacteria, meio = meiofauna, macro = macrofauna, mega = megafauna, inv = invertebrates, fis = fishes.

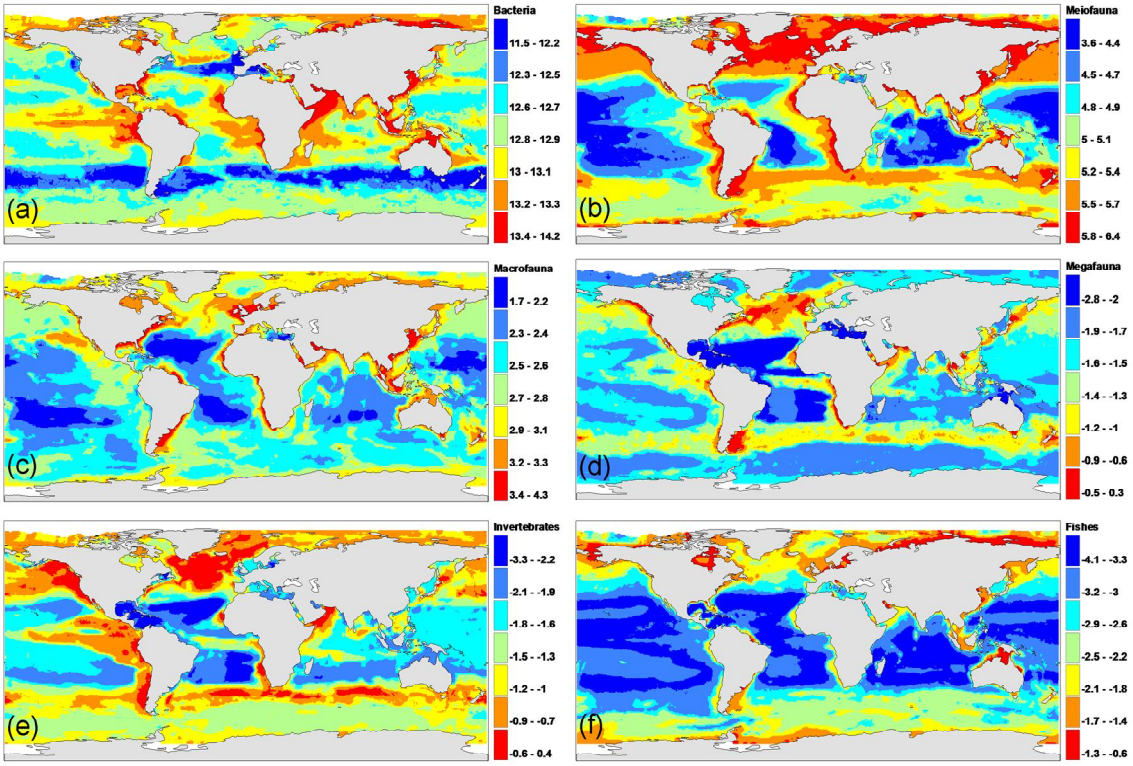

Fig. S7. Distribution of mean abundance predictions for (a) bacteria, (b) meiofauna, (c) macrofauna, (d) megafauna, (e) invertebrates, and (f) fishes. The mean abundance was computed from 4 RF simulations. Predictions were smoothed by Inverse Distance Weighting interpolation to 0.1 degree resolution and displayed in logarithm scale (base of 10).

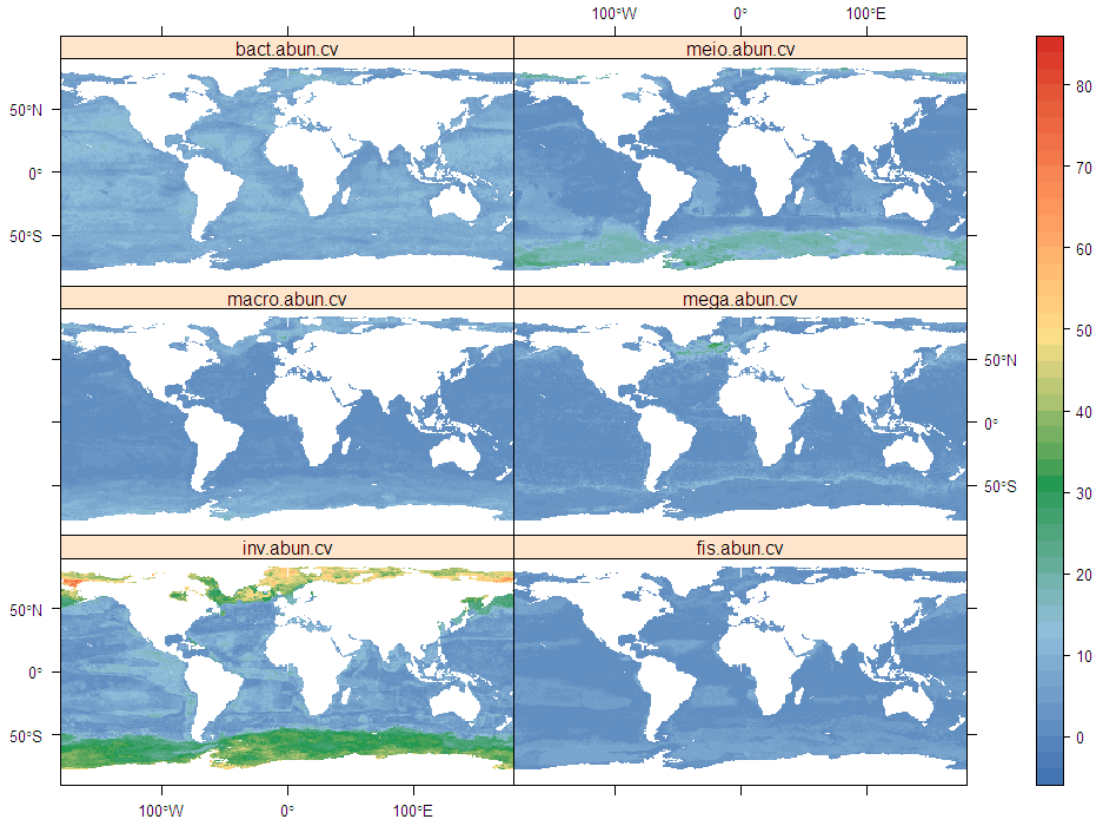

Fig. S8. Coefficient of variation (C.V.) for mean abundance predictions of each size class. The C.V. was computed as S.D. /mean * 100% from 4 RF simulations. The abbreviations are: bact = bacteria, meio = meiofauna, macro = macrofauna, mega = megafauna, inv = invertebrates, fis = fishes.

APPENDIX B

SUPPORTING REFERENCES FOR CHAPTER II

Table S1. The complete list of references for the "CoML Fresh Biomass Database".

Size Class	Dataset	Ocean/Sea	References
Bacteria	Biomass	Arabian Sea	[1]
		Arctic Ocean	[2-6]
		Atlantic Ocean	[7-14]
		Black Sea	[3]
		Caribbean Sea	[15]
		Gulf of Mexico	[16]
		Mediterranean	[3, 17, 18]
		Pacific Ocean	[3, 19]
	Abundance	Arabian Sea	[1]
		Arctic Ocean	[2-6, 20, 21]
		Atlantic Ocean	[3, 7, 8, 10, 12, 13, 22, 23]
		Black Sea	[3]
		Caribbean Sea	[15]
		Gulf of Mexico	[16, 24]
		Mediterranean	[3, 17, 25]
		Pacific Ocean	[3, 7, 26]
Meiofauna	Biomass	Arctic Ocean	[27]
		Atlantic Ocean	[7, 10, 11, 13, 28-43]
		Caribbean Sea	[13, 15, 44]
		Gulf of Mexico	[45-48]
		Indian Ocean	[49, 50]
		Mediterranean Sea	[18, 28, 51, 52]
		Pacific Ocean	[36, 53-59]
		Southern Ocean	[14, 29, 36, 60]

Table S1. Continued.

Size Class	Dataset	Ocean/Sea	References
Meiofauna	Abundance	Arctic Ocean	[20, 21, 27, 34, 61]
		Atlantic Ocean	[7, 10, 13, 14, 27, 28, 30-33, 35-43, 61-71]
		Caribbean Sea	[13, 15, 44]
		Gulf of Mexico	[45-48]
		Indian Ocean	[49, 50, 61, 72-75]
		Mediterranean Sea	[18, 28, 51, 52, 61, 76-80]
		Pacific Ocean	[26, 36, 53-59, 81-84]
		Red Sea	[85]
		Southern Ocean	[14, 29, 36, 60, 86]
Macrofauna	Biomass	Arctic Ocean	[20, 87-94]
		Atlantic Ocean	[7, 11, 30, 31, 37-39, 95-111]
		Baltic Sea	[112]
		Bohai/East China Sea	[113, 114]
		Caribbean Sea	[15, 115]
		Gulf of Mexico	[47, 48, 116-118]
		Indian Ocean	[49, 119-121]
		Pacific Ocean	[19, 58, 59, 84, 92-94, 122-130]
		Southern Ocean	[131-133]
	Abundance	Arctic Ocean	[20, 87-94]
		Atlantic Ocean	[7, 23, 30, 31, 37-39, 64, 70, 95-111, 134-144]
		Baltic Sea	[112]
		Bohai/East China Sea	[113, 114]
		Caribbean Sea	[15, 115]
		Gulf of Mexico	[48, 107, 116-118]
		Indian Ocean	[49, 119-121]
		Mediterranean Sea	[25, 145-147]
		Pacific Ocean	[26, 59, 84, 92-94, 122-127, 129, 148-151]
		Southern Ocean	[132, 133]

Table S1. Continued.

Size Class	Dataset	Ocean/Sea	References
Megafauna	Biomass	Atlantic Ocean	[32, 39, 152-154]
		Caribbean Sea	[15]
		Gulf of Mexico	[47, 117]
		Mediterranean	[155, 156]
		Pacific Ocean	[156, 157]
	Abundance	Atlantic Ocean	[32, 38, 39, 152-154, 158-160]
		Caribbean Sea	[15]
		Gulf of Mexico	[47, 117]
		Mediterranean	[155, 156, 161]
		Pacific Ocean	[26, 162, 163]
Invertebrates	Biomass	Arctic Ocean	[164]
		Atlantic Ocean	[31, 39, 152-154, 165-168]
		Gulf of Mexico	[47, 117]
		Mediterranean	[155, 156]
		Pacific Ocean	[157, 163]
	Abundance	Arctic Ocean	[164]
		Atlantic Ocean	[39, 152-154, 158, 159, 165-171]
		Gulf of Mexico	[47, 117]
		Mediterranean	[155, 156]
		Pacific Ocean	[162, 163, 172]
Fishes	Biomass	Atlantic Ocean	[39, 152-154]
		Gulf of Mexico	[47, 117]
		Mediterranean	[155, 156]
		Pacific Ocean	[157, 163]
	Abundance	Atlantic Ocean	[39, 152-154, 158, 159]
		Gulf of Mexico	[47, 117]
		Mediterranean	[155, 156]
		Pacific Ocean	[162, 163, 173]

Table S1. Continued.

Size Class	Dataset	Ocean/Sea	References
Nematodes	Biomass & Abundance	Atlantic Ocean	[32, 69, 174-177]
		Gulf of Mexico	[45, 47]
		Indian Ocean	[174]
		Mediterranean	[174, 178, 179]
Pelagic Decapods	Biomass & Abundance	Mid-Atlantic Ridge	[180]

1. Boetius A, Ferdelman T, Lochte K (2000) Bacterial activity in sediments of the deep Arabian Sea in relation to vertical flux. Deep Sea Research Part II: Topical Studies in Oceanography 47: 2835-2875.

2. Soltwedel T (2006). Atlantic Data Base for Exchange Processes at the Deep Sea Floor (ADEPD).

3. Danovaro R, Dell'Anno A, Corinaldesi C, Magagnini M, Noble R, et al. (2008) Major viral impact on the functioning of benthic deep-sea ecosystems. Nature 454: 1084-1087.

4. Kröncke I, Tan T, Stein R (1994) High benthic bacteria standing stock in deep Arctic basins. Polar Biology 14: 423-428.

5. Grahl C (1996) Mikrobielle Aktivität und Biomasse in den Sedimenten der Laptevsee (Arktis) [Diploma Thesis]: Universität Oldenburg.

6. Lochte K, Soltwedel T (1999) Atlantic Data Base for Exchange Processes at the Deep Sea Floor (ADEPD).

7. Aller JY, Aller RC, Green MA (2002) Benthic faunal assemblages and carbon supply along the continental shelf/shelf break-slope off Cape Hatteras, North Carolina. Deep Sea Research Part II: Topical Studies in Oceanography 49: 4599-4625.

8. Boetius A (2006). Atlantic Data Base for Exchange Processes at the Deep Sea Floor (ADEPD).

9. Deming J, Yager P (1992) Natural bacterial assemblages in deep-sea sediments: towards a global view. In: Rowe GT, Pariente V, editors. Deep-sea food chains and the global carbon cycle. Dordrecht, The Netherlands: Kluwer. pp. 11-27.

10. Relexans JC, Deming J, Dinet A, Gaillard JF, Sibuet M (1996) Sedimentary organic matter and micro-meiobenthos with relation to trophic conditions in the tropical northeast Atlantic. Deep Sea Research Part I: Oceanographic Research Papers 43: 1343-1368.

11. Rowe GT, Boland GS, Escobar Briones EG, Cruz-Kaegi ME, Newton A, et al. (1997) Sediment community biomass and respiration in the Northeast water polynya, Greenland: a numerical simulation of benthic lander and spade core data. Journal of Marine Systems 10: 497-515.

12. Soltwedel T, Vopel K (2001) Bacterial abundance and biomass in response to organism-generated habitat heterogeneity in deep-sea sediments. Marine Ecology Progress Series 219: 291-298.

13. Tietjen JH, Deming JW, Rowe GT, Macko S, Wilke RJ (1989) Meiobenthos of the hatteras abyssal plain and Puerto Rico trench: abundance, biomass and associations with bacteria and particulate fluxes. Deep Sea Research Part A Oceanographic Research Papers 36: 1567-1577.

14. Vanhove S, Wittoeck J, Desmet G, Van den Berghe B, Herman R, et al. (1995) Deep-sea meiofauna communities in Antarctica: structural analysis and relation with the environment. Marine Ecology Progress Series 127: 65-76.

15. Richardson MD, Young DK (1987) Abyssal benthos of the Venezuela Basin, Caribbean Sea: standing stock considerations. Deep Sea Research Part A Oceanographic Research Papers 34: 145-164.

16. Deming JW, Carpenter SD (2008) Factors influencing benthic bacterial abundance, biomass, and activity on the northern continental margin and deep basin of the Gulf of Mexico. Deep Sea Research Part II: Topical Studies in Oceanography 55: 2597-2606.

17. Boetius A, Scheibej S, Tselepides A, Thiel H (1996) Microbial biomass and activities in deep-sea sediments of the Eastern Mediterranean: trenches are benthic hotspots. Deep Sea Research Part I: Oceanographic Research Papers 43: 1439-1460.

18. Danovaro R, Croce ND, Eleftheriou A, Fabiano M, Papadopoulou N, et al. (1995) Meiofauna of the deep Eastern Mediterranean Sea: distribution and abundance in relation to bacterial biomass, organic matter composition and other environmental factors. Progress In Oceanography 36: 329-341.

19. Nodder SD, Pilditch CA, Probert PK, Hall JA (2003) Variability in benthic biomass and activity beneath the Subtropical Front, Chatham Rise, SW Pacific Ocean. Deep Sea Research Part I: Oceanographic Research Papers 50: 959-985.

20. Kröncke I, Vanreusel A, Vincx M, Wollenburg J, Mackensen A, et al. (2000) Different benthic size-compartments and their relationship to sediment chemistry in the deep Eurasian Arctic Ocean. Marine Ecology Progress Series 199: 31-41.

21. Soltwedel T (2000) Metazoan meiobenthos along continental margins: a review. Progress In Oceanography 46: 59-84.

22. Schaff TR, Levin LA (1994) Spatial heterogeneity of benthos associated with biogenic structures on the North Carolina continental slope. Deep Sea Research Part II: Topical Studies in Oceanography 41: 901-918.

23. Vanreusel A, Vincx M, Schram D, Gansbeke Dv (1995) On the Vertical Distribution of the Metazoan Meiofauna in Shelf Break and Upper Slope Habitats of the NE Atlantic. Internationale Revue der gesamten Hydrobiologie und Hydrographie 80: 313-326.

24. Yingst J, Rhoads D (1985) The structure of soft-bottom benthic communities in the vicinity of the Texas Flower Garden Banks, Gulf of Mexico. Estuarine, Coastal and Shelf Science 20: 569-592.

25. Duineveld GCA, Tselepides A, Witbaard R, Bak RPM, Berghuis EM, et al. (2000) Benthic-pelagic coupling in the oligotrophic Cretan Sea. Progress In Oceanography 46: 457-481.

26. Levin LA, Huggett CL, Wishner KF (1991) Control of deep-sea benthic community structure by oxygen and organic-matter gradients in the eastern Pacific Ocean. Journal of Marine Research 49: 763-800.

27. Pfannkuche O, Thiel H (1987) Meiobenthic stocks and benthic activity on the NE-Svalbard shelf and in the Nansen Basin. Polar Biology 7: 253-266.

28. Bianchelli S, Gambi C, Zeppilli D, Danovaro R (2010) Metazoan meiofauna in deep-sea canyons and adjacent open slopes: A large-scale comparison with focus on the rare taxa. Deep Sea Research Part I: Oceanographic Research Papers 57: 420-433.

29. Fabiano M, Danovaro R (1999) Meiofauna distribution and mesoscale variability in two sites of the Ross Sea (Antarctica) with contrasting food supply. Polar Biology 22: 115-123.

30. Flach E, Muthumbi A, Heip C (2002) Meiofauna and macrofauna community structure in relation to sediment composition at the Iberian margin compared to the Goban Spur (NE Atlantic). Progress In Oceanography 52: 433-457.

31. Galéron J, Sibuet M, Mahaut M-L, Dinet A (2000) Variation in structure and biomass of the benthic communities at three contrasting sites in the tropical Northeast Atlantic. Marine Ecology Progress Series 197: 121-137.

32. Heip CHR, Duineveld G, Flach E, Graf G, Helder W, et al. (2001) The role of the benthic biota in sedimentary metabolism and sediment-water exchange processes in the Goban Spur area (NE Atlantic). Deep Sea Research Part II: Topical Studies in Oceanography 48: 3223-3243.

33. Lambshead P, Elce B, Thistle D, Eckman J, Barnett P (1994) A comparison of the biodiversity of deep-sea marine nematodes from three stations in the Rockall Trough, Northeast Atlantic, and one station in the San Diego Trough, Northeast Pacific. Biodiversity Letters 2: 95-107.

34. Vanaverbeke J, Arbizu PM, Dahms HU, Schminke HK (1997) The metazoan meiobenthos along a depth gradient in the Arctic Laptev Sea with special attention to nematode communities. Polar Biology 18: 391-401.

35. Vanhove S, Vermeeren H, Vanreusel A (2004) Meiofauna towards the South Sandwich Trench (750-6300 m), focus on nematodes. Deep Sea Research Part II: Topical Studies in Oceanography 51: 1665-1687.

36. Danovaro R, Gambi C, Dell'Anno A, Corinaldesi C, Fraschetti S, et al. (2008) Exponential decline of deep-sea ecosystem functioning linked to benthic biodiversity loss. Current Biology 18: 1-8.

37. Pfannkuche O, Theeg R, Thiel H (1983) Benthos activity, abundance and biomass under an area of low upwelling off Morocco, Northwest Africa. Meteor Forschungsergebnisse, Reihe D Biologie 36: 85-96.

38. Sibuet M, Lambert CE, Chesselet R, Laubier L (1989) Density of the major size groups of benthic fauna and trophic input in deep basins of the Atlantic Ocean. Journal of Marine Research 47: 851-867.

39. Sibuet M, Monniot C, Desbruyères D, Dinet A, Khripounoff A, et al. (1984) Peuplements benthiques et caractéristiques trophiques du milieu dans la plaine abyssale de Demerara. Oceanologica Acta 7: 345-358.

40. Soltwedel T (1997) Meiobenthos distribution pattern in the tropical East Atlantic: indication for fractionated sedimentation of organic matter to the sea floor? Marine Biology 129: 747-756.

41. Vanreusel A, Vincx M, Gansbeke DV, Gijselinck. W (1992) Structural analysis of the meiobenthos communities of the shelf break area in 2 stations of the Gulf of Biscay (N.E. Atlantic). Belgian Journal of Zoology 122: 185-202.

42. Wigley RL, McIntyre AD (1964) Some quantitative comparisons of offshore meiobenthos and macrobenthos south of Martha's Vineyard. Limnology and Oceanography 9: 485-493.

43. Jensen P, Rumohr J, Graf G (1992) Sedimentological and biological differences across a deep-sea ridge exposed to advection and accumulation of fine-grained particles. Oceanologica Acta 15: 287-296.

44. Tietjen J (1984) Distribution and species diversity of deep-sea nematodes in the Venezuela Basin. Deep Sea Research Part A Oceanographic Research Papers 31: 119-132.

45. Baguley JG, Montagna PA, Hyde LJ, Rowe GT (2008) Metazoan meiofauna biomass, grazing, and weight-dependent respiration in the Northern Gulf of Mexico deep sea. Deep Sea Research Part II: Topical Studies in Oceanography 55: 2607-2616.

46. Escobar E, López M, Soto LA, Signoret M (1997) Density and biomass of the meiofauna of the upper continental slope in two regions of the gulf of mexico. Ciencias Marinas 23: 463-489.

47. Gallaway BJ (1988) Northern Gulf of Mexico continental slope study, final report: year 4. Volume II: Synthesis report. New Orleans, LA.: U.S. Department of the Interior, Minerals Management Service, Gulf of Mexico OCS Regional Office. 318 p.

48. Gettleson DA (1976) An ecological study of the benthic meiofauna and macroinfauna of a soft bottom area on the Texas outer continental shelf [Ph.D Thesis]. College Station: Texas A&M University.

49. Parulekar AH, Harkantra SN, Ansari ZA, Matondkar SGP (1982) Abyssal benthos of the central Indian Ocean. Deep Sea Research Part A Oceanographic Research Papers 29: 1531-1537.

50. Romano JC, Dinet A (1981) Re´lation entre l'abondance du me´iobenthos et la biomasse des se´dimento superficiels estime´e par la mesure des ade´nosines 5' phosphate (ATP, ADP, AMP). Ge´ochimie organique des se´diments marins profonds, ORGON IV, Golfe d' Aden, Mer d'Oman. Paris: CNRS. pp. 159–180.

51. Danovaro R, Marrale D, Dell'Anno A, Norberto Della C, Tselepides A, et al. (2000) Bacterial response to seasonal changes in labile organic matter composition on the continental shelf and bathyal sediments of the Cretan Sea. Progress In Oceanography 46: 345-366.

52. Gambi C, Danovaro R (2006) A multiple-scale analysis of metazoan meiofaunal distribution in the deep Mediterranean Sea. Deep Sea Research Part I: Oceanographic Research Papers 53: 1117-1134.

53. Brown C, Lambshead P, Smith C, Hawkins L, Farley R (2001) Phytodetritus and the abundance and biomass of abyssal nematodes in the central, equatorial Pacific. Deep Sea Research Part I: Oceanographic Research Papers 48: 555-565.

54. Danovaro R, Gambi C, Della Croce N (2002) Meiofauna hotspot in the Atacama Trench, eastern South Pacific Ocean. Deep Sea Research Part I: Oceanographic Research Papers 49: 843-857.

55. Grove SL, Probert PK, Berkenbusch K, Nodder SD (2006) Distribution of bathyal meiofauna in the region of the Subtropical Front, Chatham Rise, south-west Pacific. Journal of Experimental Marine Biology and Ecology 330: 342-355.

56. Renaud-Mornant J, Gourbault N (1990) Evaluation of abyssal meiobenthos in the eastern central Pacific (Clarion-Clipperton fracture zone). Progress In Oceanography 24: 317-329.

57. Shimanaga M, Nomaki H, Suetsugu K, Murayama M, Kitazato H (2007) Standing stock of deep-sea metazoan meiofauna in the Sulu Sea and adjacent areas. Deep Sea Research Part II: Topical Studies in Oceanography 54: 131-144.

58. Shirayama Y (1983) Size Structure of Deep-Sea Meio- and Macrobenthos in the Western Pacific. Internationale Revue der gesamten Hydrobiologie und Hydrographie 68: 799-810.

59. Snider LJ, Burnett BR, Hessler RR (1984) The composition and distribution of meiofauna and nanobiota in a central North Pacific deep-sea area. Deep Sea Research Part A Oceanographic Research Papers 31: 1225-1249.

60. Parulekar AH, Ansari ZA, Harkantra SN (1983) Benthic fauna of the Antarctic Ocean—quantitative aspects. New Delhi, India: Department of Ocean Development. 213-218 p.

61. Thiel H (1975) The size structure of the deep-sea benthos. Internationale Revue der gesamten Hydrobiologie und Hydrographie 60: 575-606.

62. Soltwedel T, Thiel H (1995) Biogenic sediment compounds in relation to marine meiofaunal abundances. Internationale Revue der gesamten Hydrobiologie und Hydrographie 80: 297-311.

63. Thiel H (1982.) Zoobenthos of the CINECA area and other upwelling regions. . Rapports et Procès-Verbaux des Réunions du Conseil International pour l'Exploration de la Mer 180: 323-334.

64. Thistle D, Yingst JY, Fauchald K (1985) A deep-sea benthic community exposed to strong near-bottom currents on the Scotian rise (Western Atlantic). Marine Geology 66: 91-112.

65. Tietjen JH (1971) Ecology and distribution of deep-sea meiobenthos off North Carolina. Deep Sea Research and Oceanographic Abstracts 18: 941-944, IN941-IN942, 945-957.

66. Pfannkuche O (1985) The deep-sea meiofauna of the Porcupine Seabight and abyssal plain (NE Atlantic): population structure, distribution, standing stocks. Oceanologica acta 8: 343-353.

67. Coull BC, Ellison RL, Fleeger JW, Higgins RP, Hope WD, et al. (1977) Quantitative estimates of the meiofauna from the deep sea off North Carolina, USA. Marine Biology 39: 233-240.

68. Dinet A (1973) Distribution quantitative du méiobenthos profond dans la région de la dorsale de Walvis (Sud-Ouest Africain). Marine Biology 20: 20-26.

69. Vanaverbeke J, Soetaert K, Heip C, Vanreusel A (1997) The metazoan meiobenthos along the continental slope of the Goban Spur (NE Atlantic). Journal of Sea Research 38: 93-107.

70. Galeron J, Sibuet M, Vanreusel A, Mackenzie K, Gooday A, et al. (2001) Temporal patterns among meiofauna and macrofauna taxa related to changes in sediment geochemistry at an abyssal NE Atlantic site. Progress In Oceanography 50: 303-324.

71. van der Loeff M, Lavaleye M (1986) Sediments, fauna and the dispersal of radionuclides at the NE Atlantic dumpsite for low-level radioactive waste. Report of the Dutch DORA program. Netherlands Institute for Sea Research. 134 p.

72. Ansari Z, Parulekar A, Jagtap T (1980) Distribution of sub-littoral meiobenthos off Goa coast, India. Hydrobiologia 74: 209-214.

73. Duineveld GCA, De Wilde PAWJ, Berghuis EM, Kok A, Tahey T, et al. (1997) Benthic respiration and standing stock on two contrasting continental margins in the western Indian Ocean: the Yemen-Somali upwelling region and the margin off Kenya. Deep Sea Research Part II: Topical Studies in Oceanography 44: 1293-1317.

74. Sommer S, Pfannkuche O (2000) Metazoan meiofauna of the deep Arabian Sea: standing stocks, size spectra and regional variability in relation to monsoon induced enhanced sedimentation regimes of particulate organic matter. Deep Sea Research Part II: Topical Studies in Oceanography 47: 2957-2977.

75. Thiel H (1966) Quantitative untersuchungen über die meiofauna des tiefseebodens. Veröffentlichungen des Instituts für Meeresforschung in Bremerhaven Supplement 2.

76. de Bovée F, Guidi LD, Soyer J (1990) Quantitative distribution of deep-sea meiobenthos in the northwestern Mediterranean (Gulf of Lions). Continental Shelf Research 10: 1123-1145.

77. Dinet A (1976) Études quantitatives du méiobenthos dans le sector nord de la Mer Égée. Acta Adriatica 18: 83-88.

78. Soetaert K, Heip C, Vincx M (1991) The Meiobenthos Along a Mediterranean Deep-Sea Transect off Calvi (Corsica) and in an Adjacent Canyon. Marine Ecology 12: 227-242.

79. Tahey TM, Duineveld GCA, Berghuis EM, Helder W (1994) Relation between sediment-water fluxes of oxygen and silicate and faunal abundance at continental shelf, slope and deep-water stations in the northwest Mediterranean. Marine Ecology Progress Series 104: 119-130.

80. Vivier MH (1978) Influence d'un déversement industriel profond sur la nématofauna (Canyon de Cassidaigne, Mediterranée). Tethys 8: 307-321.

81. Alongi DM, Pichon M (1988) Bathyal meiobenthos of the western Coral Sea: distribution and abundance in relation to microbial standing stocks and environmental factors. Deep Sea Research Part A Oceanographic Research Papers 35: 491-503.

82. Levin LA, Thomas CL (1989) The influence of hydrodynamic regime on infaunal assemblages inhabiting carbonate sediments on central Pacific seamounts. Deep Sea Research Part A Oceanographic Research Papers 36: 1897-1915.

83. Shirayama Y, Kojima S (1994) Abundance of deep-sea meiobenthos off Sanriku, Northeastern Japan. Journal of Oceanography 50: 109-117.

84. Alongi DM (1992) Bathymetric patterns of deep-sea benthic communities from bathyal to abyssal depths in the western South Pacific (Solomon and Coral Seas). Deep Sea Research Part A Oceanographic Research Papers 39: 549-565.

85. Thiel H (1979) First quantitative data on the deep Red Sea benthos. Marine Ecology Progress Series 1: 347-350.

86. Herman RL, Dahms HU (1992) Meiofauna communities along a depth transect off Halley Bay (Weddell Sea-Antarctica). Polar Biology 12: 313-320.

87. Clough L, Ambrose W (1997) Infaunal density, biomass and bioturbation in the sediments of the Arctic Ocean. Deep Sea Research Part II: Topical Studies in Oceanography 44: 1683-1704.

88. Kröncke I (1998) Macrofauna communities in the Amundsen Basin, at the Morris Jesup Rise and at the Yermak Plateau (Eurasian Arctic Ocean). Polar Biology 19: 383-392.

89. MacDonald IR, Bluhm BA, Iken K, Gagaev S, Strong S (2010) Benthic macrofauna and megafauna assemblages in the Arctic deep-sea Canada Basin. Deep Sea Research Part II: Topical Studies in Oceanography 57: 136-152.

90. Wlodarska-Kowalczuk M, Kendall MA, Marcin Weslawski J, Klages M, Soltwedel T (2004) Depth gradients of benthic standing stock and diversity on the continental margin at a high-latitude ice-free site (off Spitsbergen, 79°N). Deep Sea Research Part I: Oceanographic Research Papers 51: 1903-1914.

91. Wlodarska-Kowalczuk M, Pearson TH, Kendall MA (2005) Benthic response to chronic natural physical disturbance by glacial sedimentation in an Arctic fjord. Marine Ecology Progress Series 303: 31-41.

92. Dunton KH, Goodall JL, Schonberg SV, Grebmeier JM, Maidment DR (2005) Multi-decadal synthesis of benthic-pelagic coupling in the western arctic: Role of cross-shelf advective processes. Deep Sea Research Part II: Topical Studies in Oceanography 52: 3462-3477.

93. Grebmeier JM, Cooper LW, Feder HM, Sirenko BI (2006) Ecosystem dynamics of the Pacific-influenced Northern Bering and Chukchi Seas in the Amerasian Arctic. Progress In Oceanography 71: 331-361.

94. Oppel S, Huettmann F (2010) Using a Random Forest model and public data to predict the distribution of prey for marine wildlife management. In: Cushman SA, Huettmann F, editors. Spatial Complexity, Informatics, and Wildlife Conservation. pp. 151-163.

95. Flach E, Heip C (1996) Vertical distribution of macrozoobenthos within the sediment on the continental slope of the Goban Spur area (NE Atlantic). Marine Ecology Progress Series 141: 55-66.

96. Gage JD, Lamont PA, Kroeger K, Paterson GLJ, Gonzalez Vecino JL (2000) Patterns in deep-sea macrobenthos at the continental margin: standing crop, diversity and faunal change on the continental slope off Scotland. Hydrobiologia 440: 261-271.

97. Houston K, Haedrich R (1984) Abundance and biomass of macrobenthos in the vicinity of Carson Submarine Canyon, northwest Atlantic Ocean. Marine Biology 82: 301-305.

98. Khripounoff A, Desbruyeres D, Chardy P (1980) Les peuplements benthiques de la faille Vema: donnees quantitatives et bilan d'energie en milieu abyssal. Oceanologica Acta 3: 187–198.

99. Maciolek N, Grassle J, Hecker B, Boehm P, Brown B, et al. (1987) Study of biological processes on the US mid-Atlantic slope and rise. Final report. Washington, DC: US Department of the Interior, Mineral Management Service. pp. 310.

100. Narayanaswamy BE (2000) Macrobenthic ecology of the West Shetland Slope [Ph.D Thesis]: University of Southampton. 237 p.

101. Narayanaswamy BE, Bett BJ, Gage JD (2005) Ecology of bathyal polychaete fauna at an Arctic-Atlantic boundary (Faroe-Shetland Channel, North-east Atlantic). Marine Biology Research 1: 20-32.

102. Nichols J, Rowe G (1977) Infaunal macrobenthos off Cap Blanc, Spanish Sahara. Journal of Marine Research 35: 525–536.

103. Narayanaswamy BE, Bett BJ, Hughes DJ (2010) Deep-water macrofaunal diversity in the Faroe-Shetland region (NE Atlantic): a margin subject to an unusual thermal regime. Marine Ecology 31: 237-246.

104. Richardson M, Briggs K, Bowles F, Tietjen J (1995) A depauperate benthic assemblage from the nutrient-poor sediments of the Puerto Rico Trench. Deep Sea Research Part I: Oceanographic Research Papers 42: 351-364.

105. Rowe GT, Polloni PT, Haedrich RL (1975) Quantitative biological assessment of the benthic fauna in deep basins of the Gulf of Maine. Journal of Fisheries Research Board of Canada 32: 1805-1812.

106. Rowe GT, Polloni PT, Haedrich RL (1982) The deep-sea macrobenthos on the continental margin of the northwest Atlantic Ocean. Deep Sea Research Part A Oceanographic Research Papers 29: 257-278.

107. Rowe GT, Polloni PT, Horner SG (1974) Benthic biomass estimates from the northwestern atlantic ocean and the northern Gulf of Mexico. Deep Sea Research and Oceanographic Abstracts 21: 641-650.

108. Schaff T, Levin L, Blair N, DeMaster D, Pope R, et al. (1992) Spatial heterogeneity of benthos on the Carolina continental slope: large (100 km)-scale variation. Marine Ecology-Progress Series 88: 143-143.

109. Smith Jr. KL (1978) Benthic community respiration in the NW Atlantic Ocean: in situ measurements from 40 to 5200 m. Marine Biology 47: 337-347.

110. Romero-Wetzel M, Gerlach S (1991) Abundance, biomass, size-distribution and bioturbation potential of deep-sea macrozoobenthos on the Vøring Plateau (1200-1500 m, Norwegian Sea). Meeresforschung 33: 247-265.

111. Desrosiers G, Savenkoff C, Olivier M, Stora G, Juniper K, et al. (2000) Trophic structure of macrobenthos in the Gulf of St. Lawrence and on the Scotian Shelf. Deep Sea Research Part II: Topical Studies in Oceanography 47: 663-697.

112. Weslawski JM Data collected within the scope of Habitat Mapping project (http://www.pom-habitaty.eu/). Unpublished.

113. Han J, Zhang Z, Yu Z (2001) Study on the macrobenthic abundance and biomass in Bohai Sea. Journal of Ocean University of Qingdao 31: 889-869.

114. Rhoads DC, Boesch DF, Zhican T, Fengshan X, Liqiang H, et al. (1985) Macrobenthos and sedimentary facies on the Changjiang delta platform and adjacent continental shelf, East China Sea. Continental Shelf Research 4: 189-213.

115. Richardson M, Briggs K, Young D (1985) Effects of biological activity by abyssal benthic macroinvertebrates on a sedimentary structure in the Venezuela Basin. Marine Geology 68: 243-267.

116. Rowe GT, Menzel D (1971) Quantitative benthic samples from the deep Gulf of Mexico with some comments on the measurement of deep-sea biomass. Bulletin of Marine Science 21: 556-566.

117. Rowe GT, Wei C-L, Nunnally C, Haedrich R, Montagna P, et al. (2008) Comparative biomass structure and estimated carbon flow in food webs in the deep

Gulf of Mexico. Deep Sea Research Part II: Topical Studies in Oceanography 55: 2699-2711.

118. Wei C-L, Rowe GT, Briones EE, Nunnally C, Soliman Y (In Preparation) Standing stocks and body size of deep-sea macrofauna: A baseline prior 2010 BP oil spill in the northern Gulf of Mexico.

119. Ingole BS, Sautya S, Sivadas S, Singh R, Nanajkar M (2010) Macrofaunal community structure in the western Indian continental margin including the oxygen minimum zone. Marine Ecology 31: 148-166.

120. Levin L, Gage J, Martin C, Lamont P (2000) Macrobenthic community structure within and beneath the oxygen minimum zone, NW Arabian Sea. Deep Sea Research Part II: Topical Studies in Oceanography 47: 189-226.

121. Witte U (2000) Vertical distribution of metazoan macrofauna within the sediment at four sites with contrasting food supply in the deep Arabian Sea. Deep Sea Research Part II: Topical Studies in Oceanography 47: 2979-2997.

122. Carey Jr AG (1981) A comparison of benthic infaunal abundance on two abyssal plains in the northeast Pacific Ocean. Deep Sea Research Part A Oceanographic Research Papers 28: 467-479.

123. Carey Jr AG, Ruff R (1974) Ecological studies of the benthos in the western Beaufort Sea with special reference to bivalve molluscs. In: Dunbarnett MJ, editor. Polar Oceans. Calgary: Arctic Institute of North America. pp. 505-530.

124. Frankenberg D, Menzies RJ (1968) Some quantitative analyses of deep-sea benthos off Peru. Deep Sea Research and Oceanographic Abstracts 15: 623-626.

125. Griggs GB, Carey Jr AG, Kulm LD (1969) Deep-sea sedimentation and sediment-fauna interaction in Cascadia Channel and on Cascadia Abyssal Plain. Deep Sea Research and Oceanographic Abstracts 16: 157-166, IN153-IN156, 167-170.

126. Hecker B, Paul A (1974) Abyssal community structure of the benthic infauna of the eastern equatorial Pacific: DOMES sites A, B, and C. In: Bischoff JL, Piper DZ, editors. Marine geology and oceanography of the Pacific manganese nodule province. Palisades, New York: Plenum Press. pp. 287-308.

127. Palma M, Quiroga E, Gallardo VA, Arntz W, Gerdes D, et al. (2005) Macrobenthic animal assemblages of the continental margin off Chile (22° to 42°S). Journal of the Marine Biological Association of the UK 85: 233-245.

128. Smith Jr. KL (1987) Food energy supply and demand: A discrepancy between particulate organic carbon fluxand sediment community oxygen consumption in the deep ocean. Limnology and Oceanography 32: 201-220.

129. Smith Jr. KL, Baldwin RJ, Karl DM, Boetius A (2002) Benthic community responses to pulses in pelagic food supply: North Pacific Subtropical Gyre. Deep Sea Research Part I: Oceanographic Research Papers 49: 971-990.

130. Rowe GT (1971) Benthic biomass in the Pisco, Peru upwelling. Investigacion pesquera 35: 127-135.

131. Gerdes D, Klages M, Arntz WE, Herman RL, Galéron J, et al. (1992) Quantitative investigations on macrobenthos communities of the southeastern Weddell Sea shelf based on multibox corer samples. Polar Biology 12: 291-301.

132. Jażdżeski K, Jurasz W, Kittel W, Presler E, Presler P, et al. (1986) Abundance and biomass estimates of the benthic fauna in Admiralty Bay, King George Island, South Shetland Islands. Polar Biology 6: 5-16.

133. Sáiz-Salinas JI, Ramos A, García FJ, Troncoso JS, San Martin G, et al. (1997) Quantitative analysis of macrobenthic soft-bottom assemblages in South Shetland waters (Antarctica). Polar Biology 17: 393-400.

134. Blake J, Frederick Grassle J (1994) Benthic community structure on the US South Atlantic slope off the Carolinas: Spatial heterogeneity in a current-dominated system. Deep Sea Research Part II: Topical Studies in Oceanography 41: 835-874.

135. Blake J, Hilbig B (1994) Dense infaunal assemblages on the continental slope off Cape Hatteras, North Carolina. Deep Sea Research Part II: Topical Studies in Oceanography 41: 875-899.

136. Cosson N, Sibuet M, Galeron J (1997) Community structure and spatial heterogeneity of the deep-sea macrofauna at three contrasting stations in the tropical northeast Atlantic. Deep Sea Research Part I: Oceanographic Research Papers 44: 247-269.

137. Desbruyeres D, Bervas J, Khripounoff A (1980) Un cas de colonisation rapide d'un sediment profond. Oceanologica Acta 3: 285-291.

138. Gage J (1977) Structure of the abyssal macrobenthic community in the Rockall Trough. European Symposium on Marine Biology 11: 247-260.

139. Gage J (1979) Macrobenthic community structure in the Rockall Trough. Ambio Special Report: 43-46.

140. Grassle J, Morse-Porteous L (1987) Macrofaunal colonization of disturbed deep-sea environments and the structure of deep-sea benthic communities. Deep Sea Research Part A Oceanographic Research Papers 34: 1911-1915.

141. Grassle JF (1977) Slow recolonisation of deep-sea sediment. Nature 265: 618-619.

142. Laubier L, Sibuet M (1979) Ecology of the benthic communities of the deep North East Atlantic. Ambio Special Report: 37-42.

143. Sanders H (1969) Benthic marine diversity and the stability-time hypothesis. Brookhaven Symposia in Biology 22: 71-81.

144. Sanders HL, Hessler RR, Hampson GR (1965) An introduction to the study of deep-sea benthic faunal assemblages along the Gay Head-Bermuda transect. Deep Sea Research and Oceanographic Abstracts 12: 845-848.

145. Kröncke I, Türkay M, Fiege D (2003) Macrofauna communities in the eastern Mediterranean deep sea. Marine Ecology 24: 193-216.

146. Tselepides A, Eleftheriou A (1992) South Aegean (Eastern Mediterranean) continental slope benthos: macroinfaunal-environmental relationships. In: G. T. Rowe aVP, editor. Deep-sea food chains and the global carbon cycle. Dordrecht, The Netherlands: Kluwer. pp. 139-156.

147. Tselepides A, Papadopoulou K, Podaras D, Plaiti W, Koutsoubas D (2000) Macrobenthic community structure over the continental margin of Crete (South Aegean Sea, NE Mediterranean). Progress In Oceanography 46: 401-428.

148. Hessler RR, Jumars PA (1974) Abyssal community analysis from replicate box cores in the central North Pacific. Deep Sea Research and Oceanographic Abstracts 21: 185-209.

149. Hyland J, Baptiste E, Campbell J, Kennedy J, Kropp R, et al. (1991) Macroinfaunal communities of the Santa Maria Basin on the California outer continental shelf and slope. Marine Ecology Progress Series 78: 147-161.

150. Jumars P, Hessler R (1976) Hadal community structure: implications from the Aleutian Trench. Journal of Marine Research 34: 547-560.

151. Levin L, Thomas C (1989) The influence of hydrodynamic regime on infaunal assemblages inhabiting carbonate sediments on central Pacific seamounts. Deep Sea Research Part A Oceanographic Research Papers 36: 1897-1915.

152. Christiansen B, Thiel. H (1992) Deep-sea epibenthic megafauna of the Northeast Atlantic: Abundance and biomass at three mid-oceanic locations estimated from photographic transects. In: Rowe GT, Pariente V, editors. Deep-sea food chains and the global carbon cycle. Dordrecht, The Netherlands: Kluwer. pp. 125-138.

153. Haedrich RL, Rowe GT, Polloni PT (1980) The megabenthic fauna in the deep sea south of New England, USA. Marine Biology 57: 165-179.

154. Kröncke I, Türkay M (2003) Structural and functional aspects of the benthic communities in the deep Angola Basin. Marine Ecology Progress Series 260: 43-53.

155. Ramirez-Llodra E, Company JB, Sardà F, Rotllant G (2010) Megabenthic diversity patterns and community structure of the Blanes submarine canyon and adjacent

slope in the Northwestern Mediterranean: a human overprint? Marine Ecology 31: 167-182.

156. Sardà F, Cartes JE, Company JB (1994) Spatio-temporal variations in megabenthos abundance in three different habitats of the Catalan deep-sea (Western Mediterranean). Marine Biology 120: 211-219.

157. Pitcher C, Doherty P, Arnold P, Hooper J, Gribble N, et al. (2007) Seabed biodiversity on the continental shelf of the Great Barrier Reef world heritage area. AIMS/CSIRO/QM/QDPI CRC Reef Research Task Final Report. 320 p.

158. Bett BJ, Rice AL, Thurston MH (1995) A quantitative photographic survey of "spoke-burrow" type Lebensspuren on the Cape Verde Abyssal Plain. Internationale Revue der gesamten Hydrobiologie und Hydrographie 80: 153-170.

159. Grassle JF, Sanders HL, Hessler RR, Rowe GT, McLellan T (1975) Pattern and zonation: a study of the bathyal megafauna using the research submersible Alvin. Deep Sea Research and Oceanographic Abstracts 22: 457-462.

160. Hecker B (1990) Variation in megafaunal assemblages on the continental margin south of New England. Deep Sea Research Part A Oceanographic Research Papers 37: 37-57.

161. Kallianiotis A, Sophronidis K, Vidoris P, Tselepides A (2000) Demersal fish and megafaunal assemblages on the Cretan continental shelf and slope (NE Mediterranean): seasonal variation in species density, biomass and diversity. Progress In Oceanography 46: 429-455.

162. Kaufmann RS, Wakefield WW, Genin A (1989) Distribution of epibenthic megafauna and lebensspuren on two central North Pacific seamounts. Deep Sea Research Part A Oceanographic Research Papers 36: 1863-1896.

163. Ohta S (1983) Photographic census of large-sized benthic organisms in the bathyal zone of Suruga Bay, central Japan. Bulletin of the Ocean Research Institute, University of Tokyo 15: 1-244.

164. Bluhm BA, Iken K, Mincks Hardy S, Sirenko BI, Holladay BA (2009) Community structure of epibenthic megafauna in the Chukchi Sea. Aquatic Biology 7: 269-293.

165. Jackson P, Thurston M, Rice A (1991) Station data for the IOS Benthic Biological Survey of the Porcupine Seabight region (NE Atlantic) 1977-89. Institute of Oceanographic Sciences Deacon Laboratory. 88 p.

166. Lampitt RS, Billett DSM, Rice AL (1986) Biomass of the invertebrate megabenthos from 500 to 4100 m in the northeast Atlantic Ocean. Marine Biology 93: 69-81.

167. Lévesque M, Archambault P, Archambault D, Brêthes J-C, Vaz. S (2008) Epibenthic macrofauna community structure of the Gulf of St. Lawrence in relation to environmental factors and commercial fish assemblages : multivariate and geostatistic approaches. ICES Annual Science Conference CM 2008/L: 08.

168. Thurston MH, Rice AL, Bett BJ (1998) Latitudinal variation in invertebrate megafaunal abundance and biomass in the North Atlantic Ocean Abyss. Deep Sea Research Part II: Topical Studies in Oceanography 45: 203-224.

169. Dahl E, Laubier L, Sibuet M, Strömberg J-O (1976) Some quantitative results on benthic communities of the deep Norwegian Sea. Astarte 9: 61-79.

170. Rowe GT, Menzies RJ (1969) Zonation of large benthic invertebrates in the deep-sea off the Carolinas. Deep Sea Research and Oceanographic Abstracts 16: 531-532.

171. Wei C-L, Rowe GT (2009) Faunal zonation of large epibenthic invertebrates off North Carolina revisited. Deep Sea Research Part II: Topical Studies in Oceanography 56: 1830-1833.

172. Lauerman LML, Kaufmann RS, Smith KL (1996) Distribution and abundance of epibenthic megafauna at a long time-series station in the abyssal northeast Pacific. Deep Sea Research Part I: Oceanographic Research Papers 43: 1075-1103.

173. Sweatman HPA, Cheal AJ, Coleman GJ, Emslie MJ, Johns K, et al. (2008) Long-term monitoring of the Great Barrier Reef, Status Report. 8. Australian Institute of Marine Science. 369 p.

174. Soetaert K, Muthumbi A, Heip C (2002) Size and shape of ocean margin nematodes: morphological diversity and depth-related patterns. Marine Ecology Progress Series 242: 179-193.

175. Vanaverbeke J, Soetaert K, Vincx M (2004) Changes in morphometric characteristics of nematode communities during a spring phytoplankton bloom deposition. Marine Ecology Progress Series 273: 139-146.

176. Vanaverbeke J, Steyaert M, Soetaert K, Rousseau V, Van Gansbeke D, et al. (2004) Changes in structural and functional diversity of nematode communities during a spring phytoplankton bloom in the southern North Sea. Journal of Sea Research 52: 281-292.

177. Vanaverbeke J, Steyaert M, Vanreusel A, Vincx M (2003) Nematode biomass spectra as descriptors of functional changes due to human and natural impact. Marine Ecology Progress Series 249: 157-170.

178. Lampadariou N, Hatziyanni E, Tselepides A (2005) Meiofaunal community structure in Thermaikos Gulf: Response to intense trawling pressure. Continental Shelf Research 25: 2554-2569.

179. Lampadariou N, Tselepides A (2006) Spatial variability of meiofaunal communities at areas of contrasting depth and productivity in the Aegean Sea (NE Mediterranean). Progress In Oceanography 69: 19-36.

180. Wenneck T, Falkenhaug T, Bergstad O (2008) Strategies, methods, and technologies adopted on the RVGO Sars MAR-ECO expedition to the Mid-Atlantic Ridge in 2004. Deep-sea research Part 2 Topical studies in oceanography 55: 6-28.

APPENDIX C

SUPPORTING TABLES FOR CHAPTER III

Table S1. Locations of boxcorer sampling during DGoMB study.

Station	Latitude	Longitude	Depth	Date
RW1	27.4998	-96.0018	213	5/23/2000
RW2	27.2058	-95.7468	950	5/22/2000
RW3	27.0052	-95.4981	1329	5/22/2000
RW4	26.7502	-95.2484	1574	5/21/2000
RW5	26.5027	-95.0006	1620	5/21/2000
RW6	25.9992	-94.4945	3008	5/18/2000
W1	27.5779	-93.5500	405	5/13/2000
W2	27.4133	-93.3394	625	5/14/2000
W3	27.1734	-93.3224	863	5/14/2000
W4	26.7306	-93.3200	1452	5/15/2000
W5	26.2698	-93.3574	2753	5/16/2000
W6	25.9956	-93.3121	3146	5/17/2000
WC5	27.7795	-91.7645	345	5/4/2000
WC12	27.3225	-91.5530	1166	5/5/2000
B1	27.2024	-91.4042	2255	5/6/2000
B2	26.5511	-92.2197	2629	5/12/2000
B3	26.1649	-91.7343	2618	5/10/2000
NB2	27.1346	-91.9996	1530	5/7/2000
NB3	26.5547	-91.8233	1875	5/8/2000
NB4	26.2501	-92.3935	2042	5/11/2000
NB5	26.2500	-91.2112	2063	5/9/2000
C1	28.0597	-90.2493	336	5/30/2000
C7	27.7314	-89.9806	1069	5/30/2000 6/16/2001
C4	27.4551	-89.7732	1463	5/31/2000
C14	26.9315	-89.5699	2487	6/1/2000
C12	26.3781	-89.2408	2921	6/2/2000

Table S1. Continued.

Station	Latitude	Longitude	Depth	Date
MT1	28.5433	-89.8269	479	6/17/2000 6/2/2001 8/13/2002
MT2	28.4501	-89.6721	678	6/17/2000
MT3	28.2211	-89.5012	985	6/16/2000 6/4/2001
MT4	27.8289	-89.1661	1401	6/15/2000
MT5	27.3325	-88.6630	2275	6/3/2000
MT6	26.9971	-88.0035	2712	6/4/2000 6/13/2001
S35	29.3336	-87.0502	663	6/11/2000
S36	28.9164	-87.6691	1843	6/12/2000 6/10/2001 8/12/2002
S37	28.5550	-87.7633	2384	6/13/2000
S38	28.2771	-87.3314	2633	6/14/2000
S44	28.7503	-85.7484	213	6/11/2000
S43	28.5023	-86.0791	361	6/10/2000
S42	28.2528	-86.4216	770	6/9/2000 6/7/2001
S40	27.8382	-86.7515	2954	6/7/2000
S41	27.9954	-86.5740	2985	6/8/2000 6/8/2001
S39	27.4906	-86.9994	3001	6/6/2000
S5	25.4901	-88.2632	3314	6/13/2002
S4	24.2489	-85.4817	3409	6/10/2002
S1	25.0034	-92.0016	3526	6/3/2002
S3	24.7556	-90.7552	3675	8/6/2002
S2	23.5006	-92.0031	3732	6/6/2002
BH	27.7987	-91.4696	542	6/18/2001
HiPro	28.5521	-88.5733	1572	6/5/2001
GKF	26.9255	-90.2214	2465	6/15/2001
AC1	26.3903	-94.5598	2479	5/19/2000

Table S2. Average macrofaunal size for each taxon during DGoMB sampling. W = average size (mg individual-1). WC = average size (mg C individual^{-1}). CF = Conversion factor from preserved wet weight to organic carbon weight based on Rowe (1983). Average CF (3.28E-02) from all taxa was used when empirical measurements are not available in Rowe (1983). W = 0.126 (mean wet weight exlcuded Polychaete. Nemertini. Bivalve. & Ophiuroid) was used for the rest of the taxa that not measured.

TAXA	CF	W	WC
AMPHIPODA	4.50E-02	4.25E-01	1.91E-02
APLACOPHORA	5.70E-02	5.23E-02	2.98E-03
ASCIDIACEA	NA	8.59E-03	2.82E-04
BIVALVIA	3.40E-02	1.45E+00	4.93E-02
BRYOZOA	3.28E-01	1.63E-01	5.34E-03
CUMACEA	2.70E-02	3.56E-01	9.61E-03
GASTROPODA	3.40E-02	2.30E-02	7.83E-04
HARPACTICOIDA	NA	3.80E-03	1.25E-04
HOLOTHUROIDEA	1.90E-02	4.94E-01	9.39E-03
ISOPODA	NA	2.62E-02	8.59E-04
NEMATODA	3.20E-02	4.34E-03	1.39E-04
NEMERTINI	NA	1.22E+00	4.01E-02
OPHIUROIDEA	3.16E-02	2.32E+00	7.33E-02
OSTRACODA	NA	2.90E-01	9.52E-03
POLYCHAETA	5.10E-02	1.21E+00	6.18E-02
PORIFERA	8.00E-03	1.95E-03	1.56E-05
SCAPHOPODA	4.00E-02	2.51E-02	1.01E-03
SCYPHOZOA	NA	4.60E-02	1.51E-03
SIPUNCULIDA	5.20E-02	1.92E-02	1.00E-03
TANAIDACEA	2.90E-02	7.06E-02	2.05E-03

Table S3. Macrofaunal standing stocks and average size for NGoMCS sampling. n = number of sample. D = density (individual m^{-2}). B = preserved wet weight. (mg m^{-2}). BC = organic carbon weight. (mg C m^{-2}).

Station	Latitude	Longitude	Depth	n	D	s.d.	B	s.d.	BC	s.d.
C1	28.0596	-90.2543	351	17	3071	1311.2	1990.5	849.70	87.3	34.53
C11	27.2486	-89.6916	2101	6	1947	1279.4	588.6	326.86	23.6	13.39
C12	26.3850	-89.2360	2951	5	1082	1059.6	555.8	551.17	22.6	22.52
C2	27.9082	-90.0993	615	18	4139	2182.2	2194.6	1211.19	97.3	52.41
C3	27.8206	-90.1189	857	18	3443	1519.6	1898.4	779.65	81.8	36.43
C4	27.4735	-89.7800	1412	18	4580	1577.9	2230.0	778.53	96.2	35.56
C5	26.9618	-89.5605	2461	18	2653	1253.7	1077.8	570.88	44.2	23.23
C6	28.0297	-90.0994	492	6	2281	1668.2	1606.0	1141.23	76.6	55.15
C7	27.7416	-89.9850	1021	6	6839	3129.5	3447.2	1377.42	152.1	66.11
C8	27.5085	-89.8210	1192	6	4081	1618.0	2023.0	590.80	88.5	26.07
C9	27.4920	-89.7941	1430	6	6505	4245.6	2431.0	508.77	107.7	20.98
E1	28.4590	-86.0253	353	9	6012	792.5	2945.0	403.33	130.2	17.50
E1A	28.8898	-86.3923	352	6	4442	1059.4	2209.5	522.16	96.3	21.00
E1B	28.3338	-86.7786	346	6	5744	1784.6	2882.7	929.03	128.7	41.72
E1C	28.2022	-85.5251	352	6	6004	1197.1	3350.5	533.53	144.9	24.00
E2	28.2793	-86.2480	623	9	6290	1394.6	2814.8	647.85	126.2	28.21
E2A	28.5894	-86.7737	624	6	5596	1073.3	2519.2	348.74	109.0	14.52
E2B	28.3093	-86.3038	627	6	7849	1589.6	3135.2	876.17	134.3	40.81
E2C	28.2468	-86.1604	619	6	6730	1596.7	2941.0	516.88	130.2	21.70
E2D	28.1256	-85.8741	630	6	6544	1387.0	2702.0	498.99	119.5	23.92
E2E	28.0434	-85.6725	622	6	8365	1517.2	3727.3	463.95	163.4	18.24
E3	28.1572	-86.4179	828	9	4938	1375.8	2200.0	588.36	95.2	25.61
E3A	28.4807	-87.0004	856	6	5723	1154.6	2660.8	638.20	112.9	28.14
E3B	28.1184	-86.3219	860	6	5411	1080.8	2360.1	346.76	99.7	14.92
E3C	28.2621	-86.6151	849	6	6958	884.8	3076.5	454.54	129.0	20.34
E3D	28.3649	-86.7998	849	6	5358	1917.6	2830.5	924.82	119.2	38.86
E4	28.0725	-86.5783	1354	4	4716	1396.9	2044.6	634.08	87.1	26.20
E5	28.0059	-86.6476	2872	10	2072	442.3	811.8	186.81	33.4	8.14

Table S3. Continued.

Station	Latitude	Longitude	Depth	n	D	s.d.	B	s.d.	BC	s.d.
W1	27.5844	-93.5517	359	3	4253	482.4	2632.6	552.12	123.0	24.07
W2	27.4150	-93.3411	604	3	4618	493.9	2288.4	45.38	102.3	3.52
W3	27.1750	-93.3228	854	3	4007	664.5	1862.9	243.16	77.9	11.00
W4	26.7372	-93.3183	1410	3	2063	158.9	1207.5	180.32	51.9	7.51
W5	26.2844	-93.3211	2506	3	2000	744.0	570.7	160.41	24.2	6.74
WC1	27.7217	-92.8897	339	6	3761	768.2	2120.7	280.17	94.7	12.09
WC10	27.7546	-90.7948	748	6	2681	530.7	1258.8	199.36	54.6	9.57
WC11	27.3930	-92.7394	1226	6	2947	1021.0	1322.3	438.18	53.4	19.23
WC12	27.3304	-91.5490	1236	6	2460	553.1	1250.3	198.34	48.7	7.33
WC2	27.7312	-92.5031	550	6	3877	1231.4	2082.2	424.59	88.9	19.31
WC3	27.5940	-92.3614	750	6	3379	661.6	1646.3	436.96	69.5	18.21
WC4	27.7251	-92.1335	547	6	4165	801.5	2195.7	371.95	96.6	15.10
WC5	27.7849	-91.7690	298	6	7032	1906.7	3495.3	596.56	155.2	25.43
WC6	27.7115	-91.5503	563	6	6888	1656.2	3078.7	764.74	134.6	35.86
WC7	27.7615	-91.2198	453	6	4221	2210.5	1954.0	863.80	89.7	38.83
WC8	27.8409	-90.7346	547	6	5151	1364.8	2792.1	752.29	121.3	33.00
WC9	27.6922	-91.2977	759	6	3951	863.2	1909.4	368.65	80.4	16.80

Table S4. Historical macrofaunal standing stock and the southern Gulf of Mexico sampling. n = number of sample. D = density (individual m-2). B = preserved wet weight. (mg/m2). BC = organic carbon weight. (mg C m-2).

Study	Year	Station	Latitude	Longitude	Depth	D	B	BC
Rowe et al 2003	1997	LD 97	25.2500	-93.4333	3650	808	NA	32.5
Gettleson 1976	1974	8	28.1617	-94.3017	56	760	2327.0	100.1
Gettleson 1976	1974	16	28.1617	-94.3017	54	1028	5444.0	234.1
Gettleson 1976	1974	1	28.4000	-93.9583	49	430	752.0	32.3
Gettleson 1976	1974	2	28.3767	-94.0250	50	340	1419.0	61.0
Gettleson 1976	1974	5	28.3250	-94.1500	50	1041	4048.0	174.1
Gettleson 1976	1974	7	28.2667	-94.1083	53	1720	3352.0	144.1
Gettleson 1976	1974	8	28.2550	-94.0500	58	753	4570.0	196.5
Gettleson 1976	1974	9	28.3517	-93.6717	58	791	2370.0	101.9
Gettleson 1976	1974	11	28.3700	-93.8250	55	765	4863.0	209.1
Gettleson 1976	1974	12	28.3917	-93.8883	52	761	3993.0	171.7
Rowe et al 1974	NA	1	28.8991	-94.6040	16	1373	737.0	31.7
Rowe et al 1974	NA	2	28.5694	-94.5888	30	14623	4089.0	175.8
Rowe et al 1974	NA	3	27.0243	-93.0457	90	880	983.0	42.3
Rowe et al 1974	NA	4	27.6157	-93.7483	600	502	578.0	24.9
Rowe et al 1974	NA	8	29.7248	-88.8119	12	2893	404.0	17.4
Rowe et al 1974	NA	9	29.4495	-88.0198	40	3090	1351.0	58.1
Rowe et al 1974	NA	10	29.2622	-88.2125	190	1547	1082.0	46.5
Rowe et al 1974	NA	11	28.0734	-89.8020	200	2430	428.0	18.4
Rowe et al 1974	NA	12	28.0734	-89.2079	500	776	145.0	6.2
Rowe et al 1974	NA	13	27.5229	-89.5050	775	668	206.0	8.9
Rowe et al 1974	NA	14	27.0642	-89.7030	1280	102	188.0	8.1
Rowe et al 1974	NA	15	27.8899	-87.8218	2035	993	61.0	2.6
Rowe & Menzel 1971	NA	1251	24.0000	-84.8000	3440	26	53.2	0.8
Rowe & Menzel 1971	NA	1252	24.5667	-86.5000	3375	13	8.8	0.4
Rowe & Menzel 1971	NA	1254	24.0000	-86.8000	1100	437	768.0	30.7
Rowe & Menzel 1971	NA	1258	23.8167	-89.1833	2150	313	722.2	32.8
Rowe & Menzel 1971	NA	1259	23.4833	-89.6833	510	417	2145.0	28.5
Rowe & Menzel 1971	NA	1260	22.9500	-90.6500	960	95	371.0	4.5
Rowe & Menzel 1971	NA	1261	22.7833	-92.1000	3730	62	98.5	6.3
Rowe & Menzel 1971	NA	1262	23.9333	-92.3500	3780	113	155.5	2.8

Table S4. Continued.

Study	Year	Station	Latitude	Longitude	Depth	D	B	BC
Rowe & Menzel 1971	NA	1263	22.7000	-93.2000	3715	161	82.5	2.2
Rowe & Menzel 1971	NA	1264	22.4000	-93.2000	255	1095	7320.0	312.0
Rowe & Menzel 1971	NA	1265	22.5833	-90.5667	200	265	6800.0	180.5
Rowe & Menzel 1971	NA	1266	22.7500	-91.0000	2600	59	25.8	0.8
OGMEX14	1996	1	19.1917	-92.9917	130	NA	NA	60.0
OGMEX14	1996	3	22.0000	-90.5000	38	NA	NA	60.0
OGMEX14	1996	4	22.5000	-88.5000	42	NA	NA	40.0
OGMEX14	1996	5	23.3806	-87.5000	92.5	NA	NA	30.0
OGMEX14	1996	10	23.8833	-88.5000	251	NA	NA	40.0
OGMEX14	1996	11	23.5333	-88.5000	90	NA	NA	30.0
OGMEX14	1996	12	22.7833	-89.5000	78	NA	NA	180.0
OGMEX14	1996	13	23.2500	-89.5000	201	NA	NA	20.0
OGMEX14	1996	17	22.5500	-90.5000	117	NA	NA	40.0
OGMEX14	1996	18	22.2500	-91.5667	97	NA	NA	20.0
PROMEBIOI	1999	51	19.3328	-92.3397	57	1018	NA	476.0
PROMEBIOI	1999	52	19.4978	-92.3425	100	579	NA	326.0
PROMEBIOI	1999	66	19.2611	-92.8611	190	567	NA	329.0
PROMEBIOI	1999	65	19.4297	-92.8650	454	296	NA	96.0
PROMEBIOI	1999	78	19.5897	-93.3444	654	231	NA	128.0
PROMEBIOI	1999	64	19.5783	-92.8386	659	277	NA	140.0
SIGSBEE2	1999	1	21.0100	-96.9900	76	6971	NA	41.3
SIGSBEE2	1999	3	20.5800	-96.4100	690	1312	NA	20.4
SIGSBEE2	1999	4	20.5900	-96.3100	1400	1360	NA	7.2
SIGSBEE2	1999	5	20.5900	-96.2200	1680	1664	NA	16.8
SIGSBEE2	1999	6	20.5900	-96.1100	1920	1408	NA	8.1
SIGSBEE2	1999	7	21.5900	-95.4500	2300	741	NA	4.9
SIGSBEE2	1999	8	21.5900	-95.3000	2730	1296	NA	7.7
SIGSBEE2	1999	9	21.0000	-95.1600	2900	566	NA	4.8
SIGSBEE2	1999	10	20.5900	-95.0100	3360	1669	NA	6.3
SIGSBEE2	1999	11	20.5900	-94.3100	3300	1200	NA	4.2
SIGSBEE2	1999	12	21.3100	-94.0100	3290	1237	NA	14.9
SIGSBEE2	1999	13	21.5900	-93.3600	3300	1152	NA	6.3
SIGSBEE2	1999	14	22.3200	-93.0900	3600	555	NA	3.3

Table S4. Continued.

Study	Year	Station	Latitude	Longitude	Depth	D	B	BC
SIGSBEE2	1999	15	23.0100	-92.4600	3780	710	NA	5.2
SIGSBEE2	1999	16	23.3200	-92.1700	3795	374	NA	3.9
SIGSBEE2	1999	17	23.0800	-93.2200	3730	384	NA	2.0
SIGSBEE2	1999	18	22.3000	-94.2200	3750	230	NA	2.3
SIGSBEE2	1999	19	22.0000	-95.1600	3200	619	NA	5.6
SIGSBEE2	1999	20	21.3200	-96.1600	1960	864	NA	9.7
SIGSBEE2	1999	21	21.2000	-96.3600	1400	752	NA	4.4
SIGSBEE2	1999	21	21.2100	-96.3800	1365	902	NA	6.4
SIGSBEE3	2000	NA	22.0000	-97.1500	520	NA	NA	15.6
SIGSBEE3	2000	NA	23.0200	-97.1600	840	NA	NA	20.4
SIGSBEE3	2000	NA	22.5900	-95.1600	3380	NA	NA	14.9
SIGSBEE3	2000	NA	22.5900	-95.0200	3630	NA	NA	8.1
SIGSBEE3	2000	NA	23.0000	-94.4500	3680	NA	NA	33.4
SIGSBEE3	2000	NA	23.0000	-94.3100	3720	NA	NA	9.5
SIGSBEE3	2000	NA	22.3400	-94.2000	3730	NA	NA	3.9
SIGSBEE3	2000	NA	23.0000	-93.3000	3740	NA	NA	6.3
SIGSBEE3	2000	NA	23.0000	-94.0000	3760	NA	NA	5.2
SIGSBEE3	2000	NA	23.0000	-94.1600	3765	NA	NA	2.3
SIGSBEE3	2000	NA	23.0200	-93.4600	3775	NA	NA	2.0
SIGSBEE3	2000	NA	23.0000	-96.1600	2440	NA	NA	7.7
SIGSBEE3	2000	NA	23.0000	-96.0100	2524	NA	NA	4.8
SIGSBEE3	2000	NA	23.0000	-95.4600	2750	NA	NA	6.4
SIGSBEE3	2000	NA	23.0000	-95.3100	3200	NA	NA	5.6
SIGSBEE3	2000	NA	23.0100	-97.1100	1157	NA	NA	16.8
SIGSBEE3	2000	NA	22.5900	-97.0100	1510	NA	NA	7.2
SIGSBEE3	2000	NA	22.5900	-96.4500	1779	NA	NA	4.4
SIGSBEE3	2000	NA	23.0000	-96.3100	2210	NA	NA	4.9

Table S5. Mean density (individual m-2) for major macrofaunal taxa during DGoMB sampling. NEM = Nematoda. POL = Polychaeta. AMP = Amphipoda. HAR = Harpacticoida. SCY = Scyphozoa. TAN = Tanaidacea. BIV = Bivalvia. OST = Ostracoda. ISO = Isopoda. APL = Aplacophora. OTH = other taxa combined.

Station	NEM	POL	AMP	HAR	SCY	TAN	BIV	OST	ISO	APL	OTH
RW1	2461	2679	89	358	2343	181	307	246	64	53	420
RW2	1386	1411	66	261	74	225	192	167	78	29	294
RW3	1197	1047	38	128	160	121	64	46	59	3	148
RW4	1311	608	24	234	112	220	123	64	85	14	213
RW5	1092	633	8	204	208	172	125	86	75	6	145
RW6	676	365	10	176	9	59	77	57	26	6	163
W1	1368	2133	46	154	2479	150	224	184	85	48	461
W2	2259	2133	120	583	162	522	206	225	151	57	312
W3	1397	841	74	255	89	248	99	155	211	17	304
W4	1258	882	23	424	121	211	131	74	82	14	157
W5	719	392	5	116	60	42	53	39	41	1	65
W6	631	386	15	225	6	65	101	23	39	8	183
WC5	1389	2282	61	337	1355	130	162	140	42	23	326
WC12	1527	934	39	357	72	276	129	173	102	16	218
B1	1811	786	16	327	58	206	118	97	99	6	157
B2	743	325	10	134	29	124	95	13	28	2	63
B3	707	286	22	259	36	106	150	48	64	2	148
NB2	1147	916	30	340	78	232	140	137	82	14	208
NB3	778	656	8	253	176	169	96	48	64	8	163
NB4	807	655	21	239	140	158	154	93	67	3	245
NB5	519	292	23	166	57	103	56	63	49	6	121
C1	1197	1816	106	326	2187	209	102	153	85	77	249
C7	2212	1730	314	530	138	468	184	237	162	28	268
C4	2778	1598	117	592	187	365	263	184	190	31	293
C14	3209	889	13	444	276	90	184	104	112	7	137
C12	1747	705	16	696	108	175	163	151	117	13	188

Table S5. Continued.

Station	NEM	POL	AMP	HAR	SCY	TAN	BIV	OST	ISO	APL	OTH
MT1	86	4598	16250	49	2	314	305	3	3	42	148
MT2	1709	2503	971	101	36	1332	435	212	41	539	316
MT3	2949	2254	312	956	166	661	326	390	191	632	380
MT4	2470	1957	122	454	266	296	139	131	205	74	203
MT5	733	838	20	196	118	139	100	167	34	9	506
MT6	686	320	10	139	15	77	63	22	21	1	131
S35	4517	2974	195	664	75	630	312	686	235	277	321
S36	5194	2817	77	696	204	385	375	488	241	49	332
S37	3079	1312	12	802	106	267	148	157	138	15	195
S38	2175	877	26	550	70	131	77	99	67	23	175
S44	1366	3268	78	95	1413	56	125	52	19	31	272
S43	2713	1244	26	284	1949	145	250	194	24	64	563
S42	1655	1503	79	341	184	345	192	211	71	51	285
S40	584	341	16	228	19	80	75	32	20	7	171
S41	673	453	18	195	25	81	61	48	32	6	153
S39	649	415	13	119	54	64	63	58	38	6	116
S5	4606	681	12	759	101	70	313	165	194	20	154
S4	464	149	12	46	13	22	55	20	13	3	28
S1	736	348	9	310	29	32	49	49	23	0	26
S3	626	168	6	209	23	35	35	41	41	0	41
S2	470	171	6	130	23	12	41	20	9	0	101
BH	343	1926	79	383	63	335	245	30	250	30	216
HiPro	1386	3387	67	274	158	496	537	90	53	46	332
GKF	693	247	2	96	216	34	110	95	16	9	103
AC1	850	350	10	123	12	93	52	29	32	2	85

Table S6. Mean organic carbon biomass (mg C m-2) for major macrofaunal taxa during DGoMB sampling. POL = Polychaeta. BIV = Bivalvia. AMP = Amphipoda. ISO = Isopoda. OST = Ostracoda. OPH = Ophiuroidea. NEM = Nemertini. TAN = Tanaidacea. CUM = Cumacea. SCY = Scyphozoa. OTH = other taxa combined.

Station	POL	BIV	AMP	ISO	OST	OPH	NEM	TAN	CUM	SCY	OTH
RW1	107.2	16.8	1.6	1.9	2.3	2.9	3.4	0.9	2.4	3.5	2.8
RW2	56.5	10.5	1.2	2.3	1.6	2.3	2.1	1.1	0.4	0.1	1.6
RW3	41.9	3.5	0.7	1.7	0.4	0.5	1.0	0.6	0.1	0.2	1.1
RW4	24.3	6.7	0.4	2.5	0.6	0.1	1.2	1.1	0.1	0.2	2.1
RW5	25.3	6.9	0.1	2.2	0.8	0.1	1.0	0.8	0.1	0.3	1.0
RW6	14.6	4.2	0.2	0.8	0.5	0.3	0.3	0.3	0.1	0.0	0.6
W1	85.4	12.2	0.8	2.5	1.8	0.9	1.2	0.7	0.5	3.7	3.2
W2	85.4	11.3	2.1	4.4	2.1	2.0	2.7	2.5	1.2	0.2	2.1
W3	33.6	5.4	1.3	6.2	1.5	3.5	1.3	1.2	0.5	0.1	1.7
W4	35.3	7.2	0.4	2.4	0.7	0.0	0.9	1.0	0.4	0.2	1.1
W5	15.7	2.9	0.1	1.2	0.4	0.3	0.7	0.2	0.0	0.1	0.2
W6	15.4	5.5	0.3	1.2	0.2	0.1	0.6	0.3	0.1	0.0	0.9
WC5	91.3	8.9	1.1	1.2	1.3	0.8	1.8	0.6	1.1	2.0	2.0
WC12	37.4	7.0	0.7	3.0	1.6	1.4	0.9	1.3	0.6	0.1	1.3
B1	31.5	6.5	0.3	2.9	0.9	0.5	0.7	1.0	0.1	0.1	0.9
B2	13.0	5.2	0.2	0.8	0.1	0.1	0.5	0.6	0.0	0.0	0.6
B3	11.5	8.2	0.4	1.9	0.5	0.0	0.6	0.5	0.1	0.1	0.5
NB2	36.7	7.7	0.5	2.4	1.3	0.3	1.0	1.1	0.3	0.1	1.4
NB3	26.3	5.3	0.1	1.9	0.5	0.1	0.9	0.8	0.2	0.3	0.8
NB4	26.2	8.4	0.4	2.0	0.9	0.3	0.4	0.8	0.1	0.2	1.5
NB5	11.7	3.0	0.4	1.4	0.6	0.0	0.3	0.5	0.1	0.1	0.5
C1	72.7	5.6	1.9	2.5	1.5	0.7	3.4	1.0	0.6	3.3	1.7
C7	69.2	10.1	5.5	4.8	2.3	0.8	2.0	2.2	0.8	0.2	1.7
C4	63.9	14.4	2.1	5.6	1.8	1.0	1.1	1.7	0.5	0.3	2.0
C14	35.6	10.1	0.2	3.3	1.0	2.0	0.2	0.4	0.1	0.4	1.4
C12	28.2	8.9	0.3	3.4	1.4	0.2	0.4	0.8	0.3	0.2	2.0

Table S6. Continued.

Station	POL	BIV	AMP	ISO	OST	OPH	NEM	TAN	CUM	SCY	OTH
MT1	184.0	16.7	285.6	0.1	0.0	0.2	2.5	1.5	0.5	0.0	1.0
MT2	100.2	23.8	17.1	1.2	2.0	1.2	3.4	6.4	1.9	0.1	3.3
MT3	90.2	17.9	5.5	5.6	3.7	1.7	4.2	3.2	3.4	0.3	3.9
MT4	78.3	7.6	2.1	6.0	1.2	0.5	1.6	1.4	0.6	0.4	1.9
MT5	33.5	5.5	0.3	1.0	1.6	0.1	0.5	0.7	0.2	0.2	2.7
MT6	12.8	3.5	0.2	0.6	0.2	0.0	0.1	0.4	0.0	0.0	1.0
S35	119.0	17.1	3.4	6.9	6.5	1.5	3.7	3.0	2.1	0.1	2.8
S36	112.7	20.5	1.4	7.1	4.6	0.7	2.0	1.8	1.4	0.3	2.7
S37	52.5	8.1	0.2	4.1	1.5	0.1	0.7	1.3	1.3	0.2	1.5
S38	35.1	4.2	0.4	2.0	0.9	0.4	0.3	0.6	0.4	0.1	1.3
S44	130.8	6.9	1.4	0.5	0.5	3.6	1.5	0.3	1.3	2.1	1.1
S43	49.8	13.7	0.4	0.7	1.8	21.9	1.0	0.7	0.9	2.9	2.7
S42	60.2	10.5	1.4	2.1	2.0	2.4	0.8	1.6	0.7	0.3	1.8
S40	13.6	4.1	0.3	0.6	0.3	0.5	0.3	0.4	0.4	0.0	0.8
S41	18.1	3.3	0.3	0.9	0.5	0.0	0.1	0.4	0.2	0.0	1.0
S39	16.6	3.4	0.2	1.1	0.6	0.4	0.0	0.3	0.0	0.1	0.7
S5	27.3	17.1	0.2	5.7	1.6	0.6	0.1	0.3	0.2	0.2	2.4
S4	6.0	3.0	0.2	0.4	0.2	0.0	0.1	0.1	0.0	0.0	0.4
S1	13.9	2.7	0.2	0.7	0.5	0.0	0.1	0.2	0.1	0.0	0.4
S3	6.7	1.9	0.1	1.2	0.4	0.0	0.0	0.2	0.1	0.0	0.3
S2	6.8	2.2	0.1	0.3	0.2	0.0	0.0	0.1	0.0	0.0	0.3
BH	77.1	13.4	1.4	7.4	0.3	1.1	1.5	1.6	0.1	0.1	1.4
HiPro	135.5	29.4	1.2	1.6	0.9	1.4	4.0	2.4	0.5	0.2	1.9
GKF	9.9	6.0	0.0	0.5	0.9	0.3	0.0	0.2	0.1	0.3	1.2
AC1	14.0	2.9	0.2	1.0	0.3	0.2	0.2	0.4	0.0	0.0	0.5

APPENDIX D

SUPPORTING TABLES FOR CHAPTER V

Table S1. Coordinates and depth (m) of the box core locations.

Station	Latitude	Longitude	Depth
RW1	27.4998	-96.0018	213
RW2	27.2058	-95.7468	950
RW3	27.0052	-95.4981	1329
RW4	26.7502	-95.2484	1574
RW5	26.5027	-95.0006	1620
RW6	25.9992	-94.4945	3008
W1	27.5779	-93.5500	405
W2	27.4133	-93.3394	625
W3	27.1734	-93.3224	863
W4	26.7306	-93.3200	1452
W5	26.2698	-93.3574	2753
W6	25.9956	-93.3121	3146
WC5	27.7795	-91.7645	345
WC12	27.3225	-91.5530	1166
B1	27.2024	-91.4042	2255
B2	26.5511	-92.2197	2629
B3	26.1649	-91.7343	2618
NB2	27.1346	-91.9996	1530
NB3	26.5547	-91.8233	1875
NB4	26.2501	-92.3935	2042
NB5	26.2500	-91.2112	2063
C1	28.0597	-90.2493	336
C7	27.7314	-89.9806	1069
C4	27.4551	-89.7732	1463
C14	26.9315	-89.5699	2487
C12	26.3781	-89.2408	2921

Table S1. Continued.

Station	Latitude	Longitude	Depth
MT1	28.5433	-89.8269	479
MT2	28.4501	-89.6721	678
MT3	28.2211	-89.5012	985
MT4	27.8289	-89.1661	1401
MT5	27.3325	-88.6630	2275
MT6	26.9971	-88.0035	2712
S35	29.3336	-87.0502	663
S36	28.9164	-87.6691	1843
S37	28.5550	-87.7633	2384
S38	28.2771	-87.3314	2633
S44	28.7503	-85.7484	213
S43	28.5023	-86.0791	361
S42	28.2528	-86.4216	770
S40	27.8382	-86.7515	2954
S41	27.9954	-86.5740	2985
S39	27.4906	-86.9994	3001
S5	25.4901	-88.2632	3314
S4	24.2489	-85.4817	3409
S1	25.0034	-92.0016	3526
S3	24.7556	-90.7552	3675
S2	23.5006	-92.0031	3732
BH	27.7987	-91.4696	542
HiPro	28.5521	-88.5733	1572
GKF	26.9255	-90.2214	2465
AC1	26.3903	-94.5598	2479

Table S2. Breakdown of average Bray-Curtis similarity (SIMPER) within zones. Five species with the most similarity-percent contribution are listed for each faunal zone. POL: polychaetes, BIV: bivalves, ISO: isopods, Abund: average species abundance (inds. core^{-1}) in each zone, Contrib%: percent contribution of species to the average Bray-Curtis similarity within the zone, Cum%: cumulative species contribution.

Zone	Taxon	Species	Occurrence	Abund	Contrib%	Cum%
1	POL	*Tharyx marioni*	1,2W,2E,3W,3E,4	75	4.1	4.1
	POL	*Aricidea simplex*	1,2W,2E,3W,3E	78	3.7	7.8
	POL	*Levinsenia gracilis*	1,2W,2E,3E	38	3.3	11.1
	POL	*Levinsenia uncinata*	1,2W,2E,3W,3E,4	27	3.3	14.4
	POL	*Aricidea suecica*	1,2W,2E,3W,3E	88	2.8	17.2
2E	POL	*Aricidea suecica*	1,2W,2E,3W,3E	54	2.2	2.2
	POL	*Exogone sp. A*	1,2W,2E,3W,3E	30	1.9	4.1
	POL	*Levinsenia uncinata*	1,2W,2E,3W,3E,4	31	1.8	5.9
	POL	*Paralacydonia paradoxa*	1,2W,2E,3W,3E	44	1.6	9.1
	POL	*Tharyx annulosus*	1,2W,2E,3W,3E,4	45	1.5	10.6
2W	POL	*Paraonella monilaris*	1,2W,2E,3W,3E,4	50	4.1	4.1
	POL	*Levinsenia uncinata*	1,2W,2E,3W,3E,4	35	4	8.1
	POL	*Tharyx marioni*	1,2W,2E,3W,3E,4	59	3.6	11.7
	POL	*Aricidea suecica*	1,2W,2E,3W,3E	27	3.6	15.2
	POL	*Tachytrypane sp. A*	1,2W,2E,3W,3E,4	20	3.3	18.5

Table S2. Continued.

Zone	Taxon	Species	Occurrence	Abund	Contrib%	Cum%
3E	POL	*Paraonella monilaris*	1,2W,2E,3W,3E,4	96	6.7	6.7
	POL	*Tharyx marioni*	1,2W,2E,3W,3E,4	36	5.2	11.9
	BIV	Heterodonta sp. *B*	1,2W,2E,3W,3E,4	32	5.2	17.1
	BIV	Heterodonta sp. *C*	1,2W,2E,3W,3E,4	49	4.3	21.4
	POL	*Tachytrypane sp. A*	1,2W,2E,3W,3E,4	15	4.2	25.6
3W	BIV	Heterodonta sp. *C*	1,2W,2E,3W,3E,4	17	6.2	6.2
	BIV	Heterodonta sp. *B*	1,2W,2E,3W,3E,4	27	6.2	12.4
	POL	*Tachytrypane sp. A*	1,2W,2E,3W,3E,4	19	5.9	18.3
	POL	*Levinsenia uncinata*	1,2W,2E,3W,3E,4	30	4.8	23.1
	POL	*Paraonella monilaris*	1,2W,2E,3W,3E,4	26	4.1	27.2
4	BIV	*Dacrydium vitreum*	1,3W,3E,4	9	11.6	11.6
	BIV	Heterodonta sp. *B*	1,2W,2E,3W,3E,4	7	11.3	22.9
	BIV	*Vesicomya vesica*	1,2W,2E,3W,3E,4	5	8.1	40.6
	POL	*Paraonella monilaris*	1,2W,2E,3W,3E,4	13	7.7	48.2
	ISO	*Macrostylis 519*	2W,3W,3E,4	6	7.4	55.6

Table S3. Five most abundant species in each faunal zone. AMP: amphipods, POL: polychaetes, BIV: bivalves, ISO: isopods, Abund: average species abundance (inds. core^{-1}) in each zone, Contrib%: percent contribution of species to the total abundance within the zone, Cum%: cumulative species contribution.

Zone	Taxon	Species	Occurrence	Abund	Contrib%	Cum%
1	AMP	*Ampelisca mississippiana*	1,2W,2E,3W	2744	44.9	44.9
	POL	*Litocorsa antennata*	1,2E,3E	232	3.8	48.7
	BIV	Heterodonta sp. *A*	1,2W,2E,3W,3E,4	139	2.3	50.9
	POL	*Prionospio cirrifera*	1,2E,3E	92	1.5	52.4
	POL	*Aricidea suecica*	1,2W,2E,3W,3E	88	1.4	53.9
2E	POL	*Litocorsa antennata*	1,2E,3E	85	3.5	3.5
	POL	*Aricidea suecica*	1,2W,2E,3W,3E	54	2.2	5.8
	BIV	Heterodonta sp. *D*	1,2W,2E,3W,3E	46	1.9	7.7
	POL	*Tharyx marioni*	1,2W,2E,3W,3E,4	45	1.9	9.5
	POL	*Paralacydonia paradoxa*	1,2W,2E,3W,3E	44	1.8	11.3
2W	POL	*Tharyx marioni*	1,2W,2E,3W,3E,4	59	5.7	5.7
	POL	*Paraonella monilaris*	1,2W,2E,3W,3E,4	50	4.8	10.5
	POL	*Levinsenia uncinata*	1,2W,2E,3W,3E,4	35	3.4	13.9
	POL	*Macrochaeta clavicornis*	1,2W,2E,3W,3E,4	27	2.6	16.5
	POL	*Aricidea suecica*	1,2W,2E,3W,3E	27	2.6	19.2

Table S3. Continued

Zone	Taxon	Species	Occurrence	Abund	Contrib%	Cum%
3E	POL	*Paraonella monilaris*	1,2W,2E,3W,3E,4	96	10.2	10.2
	BIV	Heterodonta sp. *C*	1,2W,2E,3W,3E,4	49	5.2	15.4
	POL	*Tharyx marioni*	1,2W,2E,3W,3E,4	36	3.8	19.2
	BIV	Heterodonta sp. *B*	1,2W,2E,3W,3E,4	32	3.4	22.6
	ISO	*Macrostylis 519*	2W,3W,3E,4	26	2.8	25.4
3W	POL	*Levinsenia uncinata*	1,2W,2E,3W,3E,4	30	5.5	5.5
	BIV	Heterodonta sp. *B*	1,2W,2E,3W,3E,4	27	4.9	10.4
	POL	*Paraonella monilaris*	1,2W,2E,3W,3E,4	26	4.8	15.2
	POL	*Tachytrypane* sp. *A*	1,2W,2E,3W,3E,4	19	3.5	18.6
	ISO	*Macrostylis 256*	1,2W,2E,3W,3E	18	3.3	21.9
4	POL	*Paraonella monilaris*	1,2W,2E,3W,3E,4	13	6.7	6.7
	POL	*Sigambra tentaculata*	1,2W,2E,3E,4	11	5.7	12.4
	BIV	*Dacrydium vitreum*	1,3W,3E,4	9	4.5	16.9
	POL	*Tharyx marioni*	1,2W,2E,3W,3E,4	7	3.6	20.5
	BIV	Heterodonta sp. *B*	1,2W,2E,3W,3E,4	7	3.6	24.1

Table S4. Breakdown of average Bray-Curtis dissimilarity (SIMPER) between zone 3W and GKF, 3E and GKF, and Zone 1 and WC5. The 5 species that contribute the most to discriminating distinct sites from the adjacent zones are listed. POL: polychaetes, CUM: cumaceans, ISO: isopods, AMP: amphipods, Abund: average species abundance (inds. core^{-1}) in each zone, Contrib%: percent contribution of species to the average Bray-Curtis dissimilarity within the zone, Cum%: cumulative species contribution.

Taxon	Species	Range	Abund	Abund	Contrib%	Cum%
			Zone 3W	GKF		
POL	*Fauveliopsis* sp. *A*	1,2W,2E,3E,4	0	3	2.1	2.1
POL	*Leitoscoloplos* sp.	1,2W,2E	0	2	1.9	3.9
POL	*Sthenelais* sp. *A*	1,2W,2E,3E	0	2	1.9	5.8
CUM	*Leucon n.* sp. *5*	2E,3E	0	2	1.9	7.7
ISO	*Prochelator 290*	1,2E,3E	1	2	1.8	9.5
			Zone 3E	GKF		
AMP	Lysianassidae undet.	1,2W,2E,3W,4	0	2	1.5	1.5
POL	*Leitoscoloplos* sp.	1,2W,2E	0	2	1.5	3.0
POL	*Exogone longicirrus*	1,2W,2E,3W,3E	22	4	1.5	4.5
POL	*Cossura delta*	1,2E,3W,3E	1	3	1.34	5.81
ISO	*Prochelator 290*	1,2E,3E	0	2	1.31	7.12
			Zone 1	WC5		
POL	*Prionospio cristata*	1,2E,3W	10	302	1.9	1.9
POL	*Prionospio heterobranchia*	1,2W,2E	17	24	1.0	2.9
POL	*Gymnonereis* sp.	1,2W,2E,3E	1	13	0.9	3.7
POL	*Aricidea simplex*	1,2W,2E,3W,3E	78	0	0.8	4.5
POL	*Paleanotus* sp. *A*	WC5	0	5	0.8	5.3

Table S5. Global list of macrofaunal species in the Deep Gulf of Mexico Benthos (DGoMB) project. AMP: amphipods, APL: aplacophorans, BIV: bivalves, CUM: cumaceans, ISO: isopods, POL: polychaetes.

Taxon	Species	Occurrence
ALP	*Falcidens* sp. *I*	2W , 3E
	Falcidens sp. *J*	2E , 3E
	Falcidens sp. *K*	2W , 3W
	Psilodens sp. *A*	1 , 2E
	Scutopus sp. *A*	1 , 2E
	Neomeniomorpha sp. *A*	2E
	Neomeniomorpha sp. *B*	2E , 2W
	Neomeniomorpha sp. *C*	2E
	Neomeniomorpha sp. *D*	1 , 2E
	Neomeniomorpha sp. *E*	1 , 2E , 3E
	Neomeniomorpha sp. *F*	1 , 2E
	Neomeniomorpha sp. *G*	1
	Neomeniomorpha sp. *H*	2E , 3E
	Neomeniomorpha sp. *I*	2E
	Neomeniomorpha sp. *J*	3E , 3W
	Neomeniomorpha sp. *K*	1 , 2E , 2W
	Neomeniomorpha sp. *L*	2E
	Neomeniomorpha sp. *M*	2E
	Neomeniomorpha sp. *N*	2E
	Neomeniomorpha sp. *O*	2E
	Neomeniomorpha sp. *P*	1 , 2E , 2W , 3E , WC5
	Neomeniomorpha sp. *Q*	1 , 2E
	Neomeniomorpha sp. *R*	2E
	Neomeniomorpha sp. *S*	3E

Table S5. Continued.

Taxon	Species	Occurrence
AMP	*Ampelisca mississippiana*	1 , 2E , 2W , 3W
	Ampelisca sp. *72*	2E
	Byblis sp. *44*	1 , 2E , 3E , WC5
	Byblis cf giamardi sp. *84*	1
	Byblis brachycephala	3W
	Haploops sp. *14*	1 , 2E , 2W , 3E , WC5
	Haploops sp. *63*	2W , 3E , 4
	Ampeliscidae undet.	1 , 2E , 3E , 3W
	Byblis undet.	1
	Aoridae sp. *16*	1 , 2E , 2W , 3W
	Aoridae sp. *99*	2W
	Aoridae sp. *102*	WC5
	Aoridae sp. *110*	1
	Unciola sp. *52*	2W
	Aoridae undet.	1 , 2E
	Undet. sp. 22	2E
	Ericthonius cf rubicornis sp.*57*	1 , 2E
	Corophium sp. *13*	1
	Corophiidae undet.	1 , 2E , 2W
	Corophium sp. *100*	2W
	Lepechinella sp. *24*	2E
	Eusirius sp. *95*	1
	Rachytrophis sp. *37*	1
	Rachytrophis sp. *93*	1
	(Haustoroidea) sp. *36*	2E
	Haustoriidae sp. *23*	2E
	Lysianassidae sp. *45*	1
	Lysianassidae sp. *34*	2E
	Hippomedon sp. *28*	2E
	Lysianassidae sp. *61*	2E
	Lysianassidae sp. *74*	2W
	Schisturella cf robusta sp. *49*	2W
	Orchomella sp. *59*	2E , 2W
	Orchomella cf thomasi sp. *101*	WC5
	Icnopus sp. *67*	2E , 3E
	Lysianassidae undet.	1 , 2E , 2W , 3W , 4 ,
	Concarnes cf. concavus	2E

Table S5. Continued.

Taxon	Species	Occurrence
AMP	*Eriopisa cf elongata* sp.*1*	1 , 2E , 4
	Maera sp. *43*	WC5
	Cheirocratus cf. 105	1
	Melita sp. *5*	2E , 2W , WC5
	Melitidae sp. *31*	2E
	Melitidae sp. *39*	2E , WC5
	Elasmopus sp. *78*	2E
	Melitidae undet.	1 , 2E , 2W
	Bathymedon sp. *96*	1
	Perioculodes cf longimanus sp. *58*	2E
	Undet. genus 11 undet.	2E
	Undet. genus 6 undet.	1 , 2E
	Undet. genus 18 undet.	1
	Monoculodes sp. *40*	1 , 2E
	Oedicerotidae undet.	1 , 2E , 2W , 3W , WC5
	Monoculodes sp. *80*	1
	Westwoodilla sp. *107*	1
	Halicoides sp. *38*	1 , 2W , 4
	Rhynohalicella cf. halona sp. *48*	2E , 3W
	Pardalisca sp. *55*	2W , 3E
	Undet. genus 8 undet.	2E , 2W , 3E , 3W
	Parpano cf. cebeus sp. *68*	3E
	Halice sp. *9*	2E , 3W
	Pardalicella sp. *73*	2E , 2W
	Pardaliscidae undet.	1 , 2E , 2W , 3E , 3W , 4
	Nicippe sp. *83*	2E , 3W
	Nicippe sp. *111*	3E
	Pardaliscidae sp. *103*	2W
	Pardaliscidae sp. *104*	4
	Pardaliscidae sp. *106*	3W
	Leptophoxus cf falcatus	1 , 2E , 2W
	Proharpinia cf. antipoda sp. *25*	1 , 2E
	Phoxocephalidae *cf Joubinella* sp. *7*	1 , 2E , 2W , 4
	Phoxocephalidae sp. *10*	2E
	Harpinia cf propinqua sp. *33*	1 , 2E , 2W
	Pseudharpinia sp. *54*	1
	Harpiniopsis cf emeryi sp. *32*	1 , 2E , 2W , 3W

Table S5. Continued.

Taxon	Species	Occurrence
AMP	*Harpiniopsis cf profundis* sp. *109*	2W
	Harpinia sp. *64*	2E , 3E , 3W , 4
	Proharpinia sp. *56*	2E , 4
	Heterophoxus sp. *70*	1 , 2E , 3W
	Phoxocephalidae undet.	1 , 2E , 2W , 3E , 3W , 4 , WC5
	Paraphoxus undet.	3E
	Harpinia undet.	1 , 2W , 3E , WC5
	Paraphoxus sp. *87*	1 , 2E
	Phoxocephalidae sp. *66*	2E , 3E , 3W , 4
	Skaptopus cf brychis	2E
	Platyschnopidae undet.	2E
	Podoceridae sp. *21*	1 , 2E
	Andaniopsis sp. *108*	1
	Parametopella sp. *46*	1 , WC5
	Syrrhoe sp. *26*	1 , 2E , 2W , 3W
	Synopidae sp. *62*	2E
	Syrrhoe sp. *71*	2W
	Syrrhoe sp. *85*	2W
	Syrrhoe cf longifrons	1
	Syrrhoites sp. *75*	2E
	Synopidae sp. *60*	2E
	Synopidae sp. *107*	2E , 2W
	Pseudotiron sp. *42*	3E
	Pseudotiron sp. *76*	2E
	Pseudotiron sp. *76*	3W
	Synopidae undet.	1 , 2E , 2W , 3E
	Syrrhoe undet.	1 , 2E
	Syrrhoe sp. *97*	3E
	Carangolia cf puliciformis sp. *35*	1 , 2E , 2W , 3E
	Undet. sp.*19*	1
	Undet. sp. *20*	1
	Undet. sp. *22*	2E
	Undet. sp. *29*	2E
	Undet. sp. *65*	3E
	Undet. sp. *77*	2E
	Undet. sp. *79*	1
	Undet. sp. *88*	1

Table S5. Continued.

Taxon	Species	Occurrence
AMP	Undet. sp. *91*	2E
	Undet. sp. *98*	2W
	Undet. sp. *99*	2W
	Phtisica marina	1
	Paracaprella cf pusilla sp. *50*	2W , 3E
	Proaeginina cf norvegica	2W
	Undet. sp. *53*	2W
	Caprellidea undet.	2E , 2W , 3W
	Undet. sp. *69*	2E , 3E , 3W
BIV	Heterodonta sp. *A*	1 , 2E , 2W , 3E , 3W , 4
	Heterodonta sp. *B*	1 , 2E , 2W , 3E , 3W , 4 , WC5
	Heterodonta sp. *C*	1 , 2E , 2W , 3E , 3W , 4
	Heterodonta sp. *D*	1 , 2E , 2W , 3E , 3W
	Nucula sp. *A*	1 , 2E , 2W , 3E , 3W , 4
	Vesicomya vesica	1 , 2E , 2W , 3E , 3W , 4 , WC5
	Bathyarca sp. *A*	1 , 2E , 2W , 3E , 3W , 4 , WC5
	Tindariopsis aeolata	2E , 2W , 3E , 3W , 4
	Palaeotaxodonta sp. *A*	1 , 2E , 2W , 3E , 3W , 4
	Tindariopsis sp. *A*	2E , 3E , 3W , WC5
	Nuculana sp. *A*	1 , 2E , 2W , 3E , 3W , 4 , WC5
	Heterodonta sp. *E*	1 , 2E , 2W , 3E , 3W , 4
	Tellina sp.	2E , 2W , WC5
	Limopsis sp. *A*	1 , 2E , 2W , 3E , 3W , 4
	Heterodonta sp. *F*	2E , 2W
	Limopsis sp. *B*	1 , 2E , 2W , 3W
	Dacrydium vitreum	1 , 3E , 3W , 4 , WC5
	Heterodonta sp. *G*	1 , 2E , 2W , 3E , 3W
	Pristigloma nitens	1 , 2E , 2W , 3E , 3W , 4
	Heterodonta sp. *H*	2E , 3E , 4
	Bivalve sp. *A*	1 , 2E , 2W , 3E , 3W , WC5
	Malletiidae sp. *A*	2E , 3E , 3W , 4
	Tindariopsis agathida	1 , 2E , 2W , 3E , 3W
	Heterodonta sp. *I*	1 , 2E , 2W
	Limopsis sp. *C*	1 , 2E , 2W , 4
	Modiolinae sp. *A*	2E , 2W , 3E , 3W
	Palaeotaxodonta sp. *B*	2E , 3E , 3W , 4

Table S5. Continued.

Taxon	Species	Occurrence
BIV	Bivalve sp. *B*	2E , 2W , 3E , 3W , 4
	Tindariopsis sp. *B*	2E , 2W , 3E , 3W , 4 , WC5
	Bivalve sp. *C*	1 , 2E , 2W , 3E , WC5
	Nucula sp. *B*	1 , 2E , 2W , 3E , 4
	Nucula sp. *C*	1 , 2E , 2W , 3W , WC5
	Bathyarca sp. *B*	1 , 2E , 2W , 3E , 3W
	Lucina sp. *A*	1 , 2E , 2W , 3E
	Limea sp.	1 , 2E
	Bivalve sp. *D*	1 , 2E , 3E
	Nucula sp.	1 , WC5
	Bivalve sp. *E*	1 , 4
	Heterodonta sp. *J*	2E , 2W , 3E , 3W
	Bivalve sp. *F*	1 , 2E , 2W
	Lucina sp. *B*	1 , 2E , 2W , 3E , 3W
	Palaeotaxodonta sp. *C*	1 , 2E , 2W , 3E , 3W , 4 , WC5
	Pectinidae sp.	1 , 2E
	Bathyarca sp. *C*	2E , 2W , 3E , 3W
	Nuculanidae sp.	1 , WC5
	Malletiidae sp. *B*	1 , 2E , 2W , 3W
	Nucula sp. *D*	2E , 2W
	Neilonella sp.	1 , 2E , 2W
	Bivalve sp. *G*	2E , 2W , WC5
	Heterodonta sp. *K*	1
	Nuculana sp. *B*	1 , 2E , 2W , 3E , 3W , WC5
	Heterodonta sp. *L*	3E
	Neilo sp.	1 , 2E , 3W
	Heterodonta sp. *M*	1
	Bivalve sp. *H*	2E , 2W , 3W
	Limopsis sp. *D*	1 , 2W , 3E , 3W
	Bivalve sp. *I*	2E , 2W
	Limopsacea sp.	2E , 2W , 3E , 3W
	Bivalve sp. *J*	1 , 2E
	Nuculana sp. *C*	1 , 2E
	Limopsis sp. *E*	1 , 2E , 2W
	Anodontia sp.	1 , 2E
	Palaeotaxodonta sp. *D*	2E , 3E
	Bivalve sp. *K*	1 , 2E , 2W

Table S5. Continued.

Taxon	Species	Occurrence
BIV	Bivalve sp. *L*	2W , 3W , WC5
	Bivalve sp. *M*	2W , 3E , WC5
	Verticordia sp.	2E , 2W , WC5
	Cyrtodaria sp.	1 , 2E , 3E , 3W
	Palaeotaxodonta sp. *E*	1 , 3E , WC5
	Limopsis sp. *F*	2E , 2W
	Tindaria sp. *A.*	2E , 2W
	Tindaria sp. *B*	1 , 2E
	Palaeotaxodonta sp. *F*	1 , 2W
	Bivalve sp. *N*	1 , 2E , 2W
	Malletia sp.	1 , 2W , 3E , 3W
	Neilonella sp.	3E
	Bivalve sp. *O*	2E , 2W
	Cuspidaria sp.	2W , 3E , 3W
	Limea sp.	1
	Verticordia sp.	2E , 2W
	Malletiidae sp. *C*	1 , 2E , 2W , WC5
	Tindaria sp. *C*	1 , WC5
	Bivalve sp. *P*	1 , 2E
	Modiolinae sp. *B*	2E , 3W
	Bivalve sp. *Q*	2E
	Palaeotaxodonta sp. *G*	1 , 2W , 3E
	Palaeotaxodonta sp. *H*	2W
	Heterodonta sp. *N*	1 , 2E , WC5
	Palaeotaxodonta sp. *I*	1 , WC5
	Astarte sp.	1 , 2E
	Nuculana platessa	1
	Periploma sp.	2E , 3W
	Nuculana solidula	3W
	Bivalve sp. *R*	3W
CUM	*Ekleptostylis n.* sp. *1*	1
	Eudorella sp.	1
	Leucon tener	3E
	Leucon tenuirostris	2E
	New genus n. sp. *3*	2E
	Styloptocuma concinna	2E

Table S5. Continued.

Taxon	Species	Occurrence
CUM	*Bathylamprops motasi*	1
	Bathylamprops n. sp.	2E
	Campylaspis bicarinata	1 , 2E
	Campylaspis mansa	1 , 3W
	Campylaspis n. sp. *1*	2E , 2W
	Campylaspis n. sp. *2*	1 , 2E
	Campylaspis n. sp. *3*	3E
	Campylaspis n. sp. *6*	2W
	Campylaspis n. sp. *7*	2E , WC5
	Campylaspis pilosa	2W
	Campylaspis sp.	2E , 4
	Campylaspis sp. *B*	2E
	Campylaspis valida	1
	Cumacea sp.	1 , 2E , 2W , 3E , 3W
	Cumela garrityi	1 , 2E
	Cumella ocellata	1
	Cumella polita	1
	Cumella somersi	1
	Cumellopsis bicostata	1 , 2E , 2W , 3E
	Cumellopsis helgae	2E
	Cumellopsis puritani	1 , 2E
	Cyclaspis longicaudata	1 , 2E , 3E , WC5
	Cyclaspoides n. sp.	2W
	Cyclaspoides n. sp. *1*	2E
	Diastylid sp.	2E
	Diastylis n. sp.	1 , 2E
	Diastylis n. sp. *4*	2E
	Diastylis sp.	1 , 2E
	Eudorella hispida	1 , 2E , 3E , 3W
	Eudorella n. sp.	1
	Eudorellopsis n. sp. *1*	1
	Gaussicuma n. sp. *1*	2E , 2W
	Leptostylis ampullacea	1 , 2E , 2W , 3E , 3W
	Leptostylis crassicauda	2E
	Leptostylis n. sp.	3E
	Leptostylis n. sp. *2*	2E , 2W
	Leptostylis n. sp. *3*	2E

Table S5. Continued.

Taxon	Species	Occurrence
CUM	*Leptostylis* n. sp. *4*	1 , 2E
	Leptostylis n. sp. *5*	2E
	Leptostylis n. sp. *6*	2E
	Leptostylis n. sp. *7*	1
	Leptostylis n. sp. *8*	2E
	Leptostylis sp.	2E , 2W , 3E , 3W
	Leptostylis sp. *A*	2E , 2W
	Leptostylis villosa	2E
	Leucon americanus	2E
	Leucon ensis	1 , 2E
	Leucon homorhynchus	1 , 2E , 2W , 3E , 3W , 4
	Leucon longirostris	1 , 2E , 3E
	Leucon n. sp. *1*	1 , 3E
	Leucon n. sp. *2*	1
	Leucon n. sp. *3*	1
	Leucon n. sp. *5*	2E , 3E , GKF
	Leucon n. sp. *6*	2E
	Leucon n. sp. *7*	3E
	Leucon siphonatus	1 , 2E , 3E , 4
	Leucon sp.	2E , 3E
	Leucon spiniventris	1 , 2E , 2W , 3E
	Leucon turgidulus	1 , 2E , 2W , 3E , 3W , WC5
	Makrokylindrus n. sp.	1
	Makrokylindrus n. sp. *1*	1 , 2E
	Makrokylindrus n. sp. *2*	2E
	Makrokylindrus n. sp. *3*	2E
	Makrokylindrus sp.	2E
	Makrokylindrus tubulicauda	2E , 3W
	New genus n. sp. *1*	1 , 2E , 3E
	New genus n. sp. *2*	1
	New genus n. sp. *3*	1
	New genus n. sp. *4*	1
	Oxyurostylis n. sp. *1*	2E
	Paralamprops n. sp. *1*	1 , 2E , 2W , 4
	Paralamprops n. sp. *2*	2E
	Paralamprops n. sp. *3*	2W
	Paralamprops n. sp. *4*	2E

Table S5. Continued.

Taxon	Species	Occurrence
CUM	*Paralamprops* n. sp. *5*	2E , 4
	Petalosarsia longirostris	1 , 2E
	Platycuma marginale	2E
	Procampylaspis acanthomma	1 , 2E , 3E
	Procampylaspis armata	1 , 2E , 2W , 3E , 4
	Procampylaspis bonnieri	1 , 2W
	Procampylaspis n. sp. *1*	1 , 2E , 2W
	Procampylaspis n. sp. *2*	1 , 2E , 2W , 3E , 3W , 4
	Procampylaspis n. sp. *3*	1
	Procampylaspis n. sp. *4*	2W
	Procampylaspis ommidion	2E , 2W
	Procampylaspis sp. *A*	3W
	Schizocuma n. sp.	1
	Schizotrema n. sp. *1*	1 , 3E
	Styloptocuma aculeatum	2E
	Styloptocuma acuminatum	1 , 2E , 3E
	Styloptocuma antipai	2E , 2W , 3W
	Styloptocuma bacescui	2E
	Styloptocuma bishopi	1 , 2E
	Styloptocuma cf gracillimum	3W
	Styloptocuma echinatum	2W
	Styloptocuma erectum	2E
	Styloptocuma gracillimum	1 , 2E , 2W , 3E , 3W
	Styloptocuma n. sp.	2E
	Styloptocuma n. sp. *1*	2E , 3E
	Styloptocuma n. sp. *2*	2E
	Styloptocuma n. sp. *3*	2E
	Styloptocuma sp.	2W
	Styloptocuma sp. *A*	1 , 3E , 3W
	Styloptocuma sp. *B*	1
	Sympodomma n. sp.	1
	Sympodomma n. sp. *1*	1
	Vemacumella n. sp. *1*	1 , 2E , WC5
	Vemacumella n. sp. *5*	2E
	Vemacumella n. sp. *6*	2W
	Vemacumella n. sp. *7*	1
	Vemakylindrus n. sp.	2E

Table S5. Continued.

Taxon	Species	Occurrence
CUM	*Vemakylindrus* n. sp. *1*	1 , 2E
	Vemakylindrus sp.	2E
	Vemakylindrus sp. *A*	2E
ISO	*Gnathia 201*	1 , 2E , 2W
	Prochelator 202	1 , WC5
	Torwolia 203	1 , 2E , 2W , 3E , 3W , 4 , WC5
	Lipomera (Tetracope) 204	1 , WC5
	Leptanthura 205	2E , 2W
	Notoxenoides 206	1 , 2E , 2W , 3W , 4
	Haplomesus 207	2E
	Ischnomesus 208	1 , 2E , 2W
	Prochelator 209	1 , 2E , 2W , 3E , 3W , 4
	Gnathia 210	1
	Gnathia 211	1
	Chelator 212	2E , 3E , 3W
	Conilera 214	1
	Eugerda 215	2E , 2W , 3E , 3W
	Whoia 216	2E , 2W , 3E , 3W
	Ilyarachna 218	1 , 2E , 2W
	Leptanthura 219	2E , 2W , 3W
	Belonectes 220	2E
	Regabellator 221	2E
	Ischnomesus 222	2E , 3W
	Macrostylis 223	2E , 2W
	Panetela 224	2E , 2W , 3E , 3W , 4
	Whoia 225	1 , 2E , 2W , 3E , 3W
	Gnathia 226	2E , 2W
	Prochelator 228	1 , 2E , 2W , WC5
	Eugerdella 229	1 , 2E
	New genus *G 230*	2E
	Acanthocope 231	2E
	Exiliniscus 232	1 , 2E , 2W , 3E , 3W
	Nannoniscus 233	1 , 2E , 3E
	Haploniscus 234	2E , 2W , 3W , 4
	Prochelator 235	1 , 2E , 2W , 3E , 3W , WC5
	Eugerda 236	1 , 2E

Table S5. Continued.

Taxon	Species	Occurrence
ISO	*Chelator 237*	1 , 2E , 3E
	Prochelator 238	1 , 2E , WC5
	Haplomesus 239	1 , 2E , 2W , 3E , 3W
	Nannonisconus 240	1 , 2E , 2W , 3E , 3W , 4
	Eugerdella 241	2E , 2W , 3E , 3W
	Nannoniscus 242	1 , 2E , 2W , 3E , 3W
	Thambema 243	2E , 2W , 3W
	Katianira 244	2E , 3W
	Hapsidohedra 245	1 , 2E , 2W
	Dendrotion 246	2E , 2W , 4
	Ischnomesus 247	2E , 2W , 3E
	Desmosoma 248	1
	Dendromunna 249	2W
	Nannoniscoides 250	2E , 2W
	Chelator 251	2E , 2W , 3W
	Mirabilicoxa 254	2E , 2W
	Exiliniscus 255	2E , 2W , 3E , 3W , GKF
	Macrostylis 256	1 , 2E , 2W , 3E , 3W , GKF
	Cryptoniscid undet. *257*	1 , 2E , 2W , 3E , 4
	New genus *X2 258*	1 , 2W
	Desmosoma 260	1 , 2E , 2W
	Mirabilicoxa 261	1 , 2E , 2W
	Disconectes 262	1 , 2E , 2W
	Malacanthura 263	2E
	Whoia 264	1
	Rapaniscus 265	1 , 2E , 2W , 3E , 3W , 4
	Hyssura 266	WC5
	Mirabilicoxa 269	1 , 2E , 2W , 3E , 3W
	Whoia (cf) 270	2E , 2W
	New genus *B 271*	1 , 2E , 2W
	Haploniscus 273	2W , 3E , 4
	Ischnomesus 275	2E , 2W , 3E , 3W , 4
	Ischnomesus 276	2E
	Eurycope 277	2E , 2W , 3E , 3W
	Ischnomesus 278	2E , 3E , 4
	Thaumastasoma 279	2W , 3E , 3W , GKF
	Lipomera (Paralipomera) 280	2E , 2W

Table S5. Continued.

Taxon	Species	Occurrence
ISO	*Pseudarachna 281*	1 , 2E , 2W
	Chelator 284	1 , 2E , 2W , 3E , 3W , WC5
	Heteromesus 288	2E , 2W
	Eugerda 289	2E , 3W
	Prochelator 290	1 , 2E , 3E , GKF
	Echinopleura 291	2E , 2W
	Pseudomesus 293	2W , 3E , 3W , 4
	Acanthocope 295	2E
	Eurycope 401	2E
	Disconectes 402	1
	Eurycope 403	2E , 3W
	Munnopsurus 405	2E
	Ischnomesus 406	2E
	Prochelator 408	1 , 2E , WC5
	Chelator 409	1 , 2E , 2W , 3E
	Ischnomesus 410	2E
	Haplomesus 412	2E
	Aspidoniscus 413	2W
	Eugerda 414	2E , 2W , 3E , 3W , GKF
	Chelator 418	2W , 3E , 3W
	Cryodesma 419	2E , 2W , 3W
	Haplomesus 420	2E
	Austroniscus 421	2E
	Katianira (Abyssijaera) 422	2E , 3W
	Eugerda 423	2E , 4
	Thambema 424	2E , 2W , 3E , 3W , 4
	Gnathia 425	2W
	Gnathia 427	2E
	Gnathia 500	2E
	Genus undet. *501*	2E , 2W
	Disconectes 502	2E
	New genus *d 503*	2E
	Momedossa (?) *504*	2E
	Mirabilicoxa 505	1
	Prochelator 506	1 , 3E , 3W
	Torwolia-like new genus *507*	2E , 3E

Table S5. Continued.

Taxon	Species	Occurrence
ISO	*Rapaniscus 508*	3E , 4
	Heteromesus 509	3E
	Hebefustis 510	2E , 3E
	Sugoniscus 511	3W
	Syneurycope 512	2W
	Katianira 513	2W
	Haploniscus 514	2W
	Politolana 515	1
	Eugerdella 516	2E
	Chelator-like new genus *517*	2E
	Mirabilicoxa 518	1 , 2E , 3E
	Macrostylis 519	2W , 3E , 3W , 4
	Mesosignum 520	3E , 4
	Thaumastosoma 521	3W , 4
	Undet. *522*	4
	Undet. *523*	4
	Paramunna-like *524*	1
	Bathybadistes 525	2E
	Pleurogonium 526	2E
	Hydroniscus 527	2E
	Ilyarachna 528	2E
	Chauliodoniscus 529	3E
	Pilosanthura 530	1
	Hyssura 531	2W , 3W
	Exiliniscus 532	3E , 3W , 4
	Munella 533	4
	Syneurycope 534	3E
	Exiliniscus 535	3E , 4
	Panetela 536	3E
	Chelator 999	1 , 2E , 2W , 3E , 3W , 4 , GKF , WC5
POL	*Aberranta* sp.	2E , 3E
	Acrocirrus frontifilis	2E , 3E , 3W
	Macrochaeta clavicornis	1 , 2E , 2W , 3E , 3W , 4
	Macrochaeta sp.	2W , 3E , 3W
	Macrochaeta sp. *A*	2E

Table S5. Continued.

Taxon	Species	Occurrence
POL	*Ampharete* sp. *A*	1 , 2E , 2W , 3E
	Amphicteis gunneri	1 , 2E
	Amphicteis scaphobranchiata	1
	Amphicteis sp.	1
	Genus A *(Ampharetidae)* sp.	2E
	Genus A *(Ampharetidae)* sp.	2E
	Hobsonia sp.	1
	Isolda pulchella	1 , 2E
	Melinna cristata	1
	Melinna maculata	1
	Chloeia viridis	1 , 2E
	Eurythoe sp. *A*	1 , 2E
	Eurythoe sp. *B*	2E , 3E
	Paramphinome jeffreysii	1 , 2E , 2W , 3E , 3W , GKF
	Paramphinome sp.	1 , 2E , 4
	Paramphinome sp. *A*	2E , 2W , 3E , 3W
	Paramphinome sp. *B*	2E
	Barantolla sp. *A*	1 , 2E
	Capitella capitata	2E , WC5
	Decamastus gracilis	1 , 2E
	Decamastus sp. *A*	1 , 2E
	Genus A (Capitellidae) sp.	1 , 2E , WC5
	Genus C (Capitellidae) sp.	1 , 2E
	Genus D (Capitellidae) sp.	1
	Genus E (Capitellidae) sp.	4
	Genus G (Capitellidae) sp.	1 , 2E , WC5
	Genus H (Capitellidae) sp.	1
	Genus K (Capitellidae) sp.	2E
	Genus L (Capitellidae) sp.	1
	Genus O (Capitellidae) sp.	1 , 2E , 2W , 3E
	Genus P (Capitellidae) sp.	1 , 3E
	Genus Q (Capitellidae) sp.	1 , 2E
	Genus R (Capitellidae) sp.	1 , 2E
	Genus S (Capitellidae) sp.	2E , 2W
	Genus T (Capitellidae) sp.	2E
	Genus X (Capitellidae) sp.	1
	Genus Y (Capitellidae) sp.	1 , 2E , 3E

Table S5. Continued.

Taxon	Species	Occurrence
POL	Genus Z (Capitellidae) sp.	1 , 3W
	Genus AA (Capitellidae) sp.	1 , 2E , 2W , 3E
	Genus AC (Capitellidae) sp.	2E
	Genus AE (Capitellidae) sp.	2E
	Genus AF (Capitellidae) sp.	1 , 2E
	Genus AG (Capitellidae) sp.	1
	Genus AK(Capitellidae) sp.	2E , 2W , 3E
	Genus AL (Capitellidae) sp.	WC5
	Genus AM (Capitellidae) sp.	1
	Genus AN (Capitellidae) sp.	2E
	Genus AQ (Capitellidae) sp.	1 , WC5
	Genus AR (Capitellidae) sp.	1
	Genus AS (Capitellidae) sp.	1
	Heteromastus sp. *A*	2E
	Mediomastus californiensis	1 , 2E , 2W , WC5
	Neoheteromastus sp. *B*	1 , 2E , 2W , WC5
	Neomediomastus sp. *A*	1 , 2E , WC5
	Notomastus americanus	1 , 2E
	Notomastus hemipodus	1 , 2E
	Notomastus latericeus	1 , 2E , 3E , WC5
	Paraleiocapitella sp.	2E , GKF
	Chaetopterus sp.	2W
	Spiochaetopterus costarum	1 , 2E , 3W
	Dysponetus sp. *A*	1 , 2E , 3W , WC5
	Dysponetus sp. *B*	1 , 2E , 2W , 3E , 3W , 4
	Paleanotus sp. *A*	WC5
	Caulleriella sp. *A*	2E
	Chaetozone sp.	1 , 2E , 3E , 3W , 4
	Chaetozone sp. *A*	1 , 2E , 2W
	Chaetozone sp. *C*	4
	Cirriformia sp.	1
	Cirriformia sp. *A*	2E , 3E
	Cirriformia sp. *B*	2E
	Cirriformia sp. *C*	2E
	Tharyx annulosus	1 , 2E , 2W , 3E , 3W , 4 , WC5
	Tharyx marioni	1 , 2E , 2W , 3E , 3W , 4 , GKF , WC5
	Tharyx sp.	1 , 3E , 3W , WC5

Table S5. Continued.

Taxon	Species	Occurrence
POL	*Cossura alba*	1
	Cossura delta	1 , 2E , 3E , 3W , GKF , WC5
	Cossura heterochaeta	2E
	Cossura laeviseta	1
	Cossura rostrata	1
	Cossura soyeri	1 , 2E , WC5
	Cossura sp. *A*	1 , 2E , 3E
	Dorvillea sp. *A*	1
	Dorvillea sp. *C*	1
	Genus (Dorvilleidae) A	1 , 2E , 4
	Genus (Dorvilleidae) C	2E
	Meiodorvillea sp.	1
	Meiodorvillea sp. *A*	1 , 2E , 2W , 3E , 3W
	Meiodorvillea sp. *B*	1 , 2E , 3W , WC5
	Meiodorvillea sp. *C*	1
	Ophryotrocha sp. *A*	2E
	Pettiboneia sp.	1 , 2E
	Pettiboneia sp. *A*	1
	Pettiboneia sp. *B*	1
	Protodorvillea kefersteini	2E , 2W
	Schistomeringos pectinata	3E
	Schistomeringos rudolphi	1 , 2E
	Schistomeringos sp.	1 , 2E
	Schistomeringos sp. *B*	1 , 2E
	Eunice filamentosa	2E
	Eunice tenuis	1 , 2W
	Eunice vittata	1
	Euniphysa aculeata	1
	Lysidice ninetta	1
	Marphysa belli	1
	Marphysa conferta	2E
	Marphysa sp. *A*	1
	Nematonereis hebes	3E
	Palola siciliensis	2E
	Paramarphysa longula	2E
	Euphrosine armadilloides	2E
	Euphrosine sp. *A*	1

Table S5. Continued.

Taxon	Species	Occurrence
POL	*Euphrosine triloba*	2W
	Fauveliopsis sp.	2E
	Fauveliopsis sp. *A*	1 , 2E , 2W , 3E , 4 , GKF
	Fauveliopsis sp. *B*	1 , 2E , 2W , 3E , 3W , 4 , WC5
	Fauveliopsis sp. *C*	2E
	Brada sp.	2E
	Brada villosa	2E , 3W
	Diplocirrus capensis	1 , 2E , 2W , 3E , 3W , WC5
	Diplocirrus sp.	2E
	Diplocirrus sp. *A*	1 , 2E , 2W , WC5
	Diplocirrus sp. *B*	2E
	Flabelliderma sp.	2W
	Flabelligera sp.	1
	Pherusa inflata	1
	Pherusa sp.	2E , 2W , 3E , 3W , GKF
	Therochaeta sp. *A*	2E , 3E
	Glycera sp.	1 , 2E , 2W , 3E , 3W , 4 , WC5
	Hemipodus sp.	1 , 2E , 2W , 3E
	Bathyglycinde sp. *A*	3E , WC5
	Bathyglycinde sp. *B*	2E , 3E
	Glycinde nordmanni	3W
	Glycinde sp.	3W
	Goniada maculata	1 , 3E
	Goniada teres	3W
	Goniadella sp.	3W
	Goniadella sp. *A*	2E , 2W , 3E , 3W , 4
	Ophioglycera sp.	3E
	Ophioglycera sp. *A*	2W , 3E
	Progoniada regularis	1 , WC5
	Genus A (Hesionidae) sp.	1 , 2E
	Gyptis brevipalpa	1 , WC5
	Gyptis sp.	1
	Gyptis vittata	1 , 2E
	Hesiospina sp. *A*	2E
	Nereimyra sp.	1
	Podarke agilis	WC5
	Phalacrophorus pictus	3E

Table S5. Continued.

Taxon	Species	Occurrence
POL	*Heterospio longissima*	1 , 2E , 2W , 3E , 4
	Augeneria bidens	1 , 2E , 2W , 3E , 3W , WC5
	Lumbrinerides acuta	1 , 2E , 3E , GKF
	Lumbrinerides dayi	1 , 2E , 2W , 3E , 3W , 4 , GKF
	Lumbrinerides sp.	1 , 3E
	Lumbrinerides sp. *A*	2E , 3E
	Lumbrineriopsis paradoxa	1 , 2E , 2W , 3E
	Lumbrineriopsis sp.	2E
	Lumbrineris brevipes	1 , 2E
	Lumbrineris candida	1 , 2E , 2W
	Lumbrineris coccinea	2E
	Lumbrineris ernesti	1
	Lumbrineris latrielli	1 , 4
	Lumbrineris sp.	2E
	Lumbrineris sp. *A*	2E
	Lumbrineris sp. *B*	1 , 2E
	Lumbrineris sp. *C*	1 , 2E
	Lumbrineris sp. *D*	3E
	Lumbrineris sp. *E*	1
	Lumbrineris verrilli	1 , 2E , 2W , WC5
	Ninoe sp. *A*	1 , 2E , 2W , 3E , 3W , GKF , WC5
	Ninoe sp. *C*	1
	Magelona pettiboneae	2W
	Magelona riojai	3E
	Magelona sp.	1 , 2W , 3E , 3W , WC5
	Magelona sp. *A*	2W
	Magelona sp. *B*	1
	Magelona sp. *C*	1
	Magelona sp. *D*	1
	Magelona sp. *F*	1 , 2E
	Magelona sp. *G*	1
	Asychis atlanticus	2E
	Axiothella sp. *A*	3E
	Clymenella torquata	2E
	Euclymene sp. *A*	2E
	Maldane glebifex	2E

Table S5. Continued.

Taxon	Species	Occurrence
POL	*Maldane* sp.	2E
	Maldane sp. *A*	1 , 2E , 2W
	Micromaldane sp.	1 , 2E , 2W , 3E , WC5
	Petaloproctus sp.	3E
	Aglaophamus circinata	2E , 2W , 3E , GKF
	Aglaophamus verrilli	1 , 2E , WC5
	Micronephthys minuta	1 , 2E , 2W , 3E , 3W , WC5
	Nephtys incisa	2W , 3W , WC5
	Nephtys picta	1 , 2E , 2W , 3W
	Nephtys sp.	1
	Nephtys squamosa	1 , 2E
	Ceratocephale loveni	1 , 2E , 2W , 3E
	Ceratocephale oculata	1 , 2E , 2W , 3E , 3W , 4
	Ceratocephale websteri	2E
	Ceratonereis sp.	3E
	Gymnonereis sp.	1 , 2E , 2W , 3E , WC5
	Hyalinoecia sp.	1 , WC5
	Kinbergonuphis proalopus	1
	Kinbergonuphis sp.	1 , 2W
	Kinbergonuphis sp. *A*	1
	Nothria sp.	1
	Nothria textor	2E
	Onuphis geophiliformis	2W
	Onuphis sp.	2E
	Paradiopatra abranchiata	2E
	Paradiopatra abyssia	1
	Sarsonuphis fragosa	2E , 2W
	Sarsonuphis hartmanae	1 , 2E , 2W , 3E , 3W , 4
	Armandia agilis	1 , 2E , 2W , WC5
	Armandia maculata	1 , 2E , 2W , 3E , WC5
	Armandia sp.	1 , GKF
	Kesun sp. *A*	1 , 2E , 2W , 3E , 3W
	Ophelia denticulata	2E
	Ophelina cylindricaudata	1 , 2E , 2W , 3E , WC5
	Ophelina sp. *A*	1 , 2E , 3E , 3W
	Ophelina sp. *B*	2E
	Ophelina sp. *C*	1 , 2E , 3E

Table S5. Continued.

Taxon	Species	Occurrence
POL	*Ophelina* sp. *D*	1 , 2W
	Ophelina sp. *E*	2E
	Ophelina sp. *F*	2E , GKF
	Polyophthalmus sp. *A*	2E
	Polyophthalmus sp. *B*	1 , 2E
	Tachytrypane jeffreysii	1 , 2E , 2W , 3W
	Tachytrypane sp. *A*	1 , 2E , 2W , 3E , 3W , 4 , GKF , WC5
	Tachytrypane sp. *C*	1 , 2E , 3E , 3W
	Califia calida	1 , 2E
	Leitoscoloplos fragilis	1 , 2E
	Leitoscoloplos robustus	1 , 2E , 3E
	Leitoscoloplos sp.	1 , 2E , 2W , GKF
	Leitoscoloplos sp. *A*	1 , 2E , 2W
	Naineris laevigata	2E
	Orbinia americana	2E , 2W
	Proscoloplos sp. *A*	2E
	Scoloplos rubra	2E
	Scoloplos sp.	2E
	Myriochele heeri	1 , 2E , 2W
	Myriochele oculata	1 , 2E
	Myriochele sp. *A*	1 , 2E , 2W , 3E , 3W , 4
	Myriowenia sp. *A*	1 , 2E , 2W , 3E
	Owenia sp. *A*	2E
	Paralacydonia paradoxa	1 , 2E , 2W , 3E , 3W
	Paralacydonia sp. *A*	2E
	Aedicira belgicae	1 , 2E , 2W , 3W
	Aedicira sp.	1 , 2E , 2W , 3E , 3W
	Aricidea abranchiata	2E
	Aricidea alisdairi	1
	Aricidea catherinae	1 , 2E , 2W , 3E
	Aricidea cerrutii	1 , 2E
	Aricidea fragilis	1 , 2E , 2W , 3E , 3W , 4 , WC5
	Aricidea lopezi	1 , 2E , 3E , 3W
	Aricidea minuta	1
	Aricidea mirifica	1 , 2E
	Aricidea quadrilobata	1

Table S5. Continued.

Taxon	Species	Occurrence
POL	*Aricidea simplex*	1 , 2E , 2W , 3E , 3W , GKF
	Aricidea sp.	1 , 2E , 2W , 3E , 3W
	Aricidea suecica	1 , 2E , 2W , 3E , 3W , GKF , WC5
	Aricidea trilobata	1 , 2E , 2W , 3W , WC5
	Aricidea wassi	1
	Cirrophorus abranchiatus	2E , 2W , 3E , 3W
	Cirrophorus americanus	1 , 2E
	Cirrophorus branchiatus	1 , 2E , 4
	Cirrophorus brevicirratus	1 , 2E
	Cirrophorus forticirratus	2E
	Cirrophorus lyra	1 , 2E , 2W , 3E , 3W , 4 , GKF
	Cirrophorus neapolitanus	2E
	Cirrophorus sp.	1 , 2E
	Levinsenia brevibranchiata	1 , 2E , 3E
	Levinsenia flava	1 , 2E
	Levinsenia gracilis	1 , 2E , 2W , 3E
	Levinsenia oculata	1 , 2W
	Levinsenia oligobranchiata	1 , 2E , 2W , 3E , WC5
	Levinsenia sp.	1 , 2E , 4
	Levinsenia uncinata	1 , 2E , 2W , 3E , 3W , 4 , GKF
	Paraonella monilaris	1 , 2E , 2W , 3E , 3W , 4 , GKF
	Paraonella nordica	2E
	Paraonella rubriceps	2E
	Paraonella sp.	2E , 2W , 3W , WC5
	Paraonella sp. *A*	1 , 2E , 2W , 3E , 3W
	Sabidius cornatus	1 , 2E , 2W , 3E , 3W , GKF
	Sabidius sp.	2E
	Sabidius sp. *A*	1 , 2E , 3E
	Anaitides groenlandica	1
	Anaitides mucosa	1 , 2E
	Anaitides sp.	1
	Eteone heteropoda	2E
	Eteone lactea	4
	Genetyllis castanea	2E
	Genus A (Phyllodocidae) sp.	2E
	Hesionura sp. *A*	2E

Table S5. Continued.

Taxon	Species	Occurrence
POL	*Mystides borealis*	1 , 2E , 3E
	Paranaitis polynoides	1
	Paranaitis speciosa	2E
	Protomystides bidentata	1 , 2E , 2W , 3E , 3W , 4
	Ancistrosyllis sp.	1 , 3E , 4 , GKF
	Ancistrosyllis sp. *A*	1 , 3E , 4
	Ancistrosyllis sp. *B*	2E
	Cabira incerta	2W
	Litocorsa antennata	1 , 2E , 3E
	Pilargis berkeleyae	1 , 2E
	Sigambra bassi	1 , 2E , 2W
	Sigambra sp.	3E
	Sigambra tentaculata	1 , 2E , 2W , 3E , 4 , WC5
	Sigambra wassi	1
	Synelmis albini	1
	Synelmis klatti	1 , 2E , 2W , 3E , 3W , WC5
	Synelmis sp.	2W
	Synelmis sp. *B*	1 , 2E
	Genus A (Poecilochaetidae) sp. (uncertain)	3E
	Poecilochaetus fulgoris	1 , 2E , 2W
	Poecilochaetus johnsoni	3E
	Poecilochaetus sp.	1 , 2E
	Poecilochaetus vitjazi	1
	Genus A (Polynoidae) sp.	1
	Phalacrostemma elegans	3E
	Phalacrostemma sp. *A*	2E , 2W
	Chone americana	1 , 2E
	Chone sp.	2E , 2W , 3E
	Chone sp. *A*	1 , 2E , 2W
	Chone sp. *B*	1
	Chone sp. *D*	2W
	Chone sp. *E*	1 , 2W
	Chone sp. *F*	1 , 2E
	Chone sp. *G*	1 , 2E
	Chone sp. *H*	1 , 3E
	Chone sp. *I*	2E , 2W
	Chone sp. *M*	WC5

Table S5. Continued.

Taxon	Species	Occurrence
POL	*Chone* sp. *N*	2E , 3W , WC5
	Euchone incolor	1 , 2E , 2W
	Euchone rosea	2W
	Euchone sp.	1 , 2E
	Euchone sp. *A*	2E
	Fabricia sp.	4
	Fabricia sp. *A*	1 , 2E , 3E
	Fabricia sp. *B*	2E , 2W
	Sabella sp.	2E
	Asclerocheilus beringianus	2E , 4
	Asclerocheilus sp.	2E
	Scalibregma inflatum	1 , 2E
	Sclerobregma sp.	1
	Sclerocheilus sp.	2E
	(Scalibregmatidae) sp. *1*	WC5
	(Scalibregmatidae) sp. *2*	WC5
	Ehlersileanira incisa	1 , 2E , 3E
	Genus A (Sigalionidae) sp.	1
	Pholoe minuta	2W
	Pholoe sp.	2E
	Pholoe sp. *A*	2E
	Pholoe sp. *B*	1 , 2E
	Pholoe sp. *C*	1 , 2E
	Sthenelais sp.	2W , 3E
	Sthenelais sp. *A*	1 , 2E , 2W , 3E , GKF
	Sthenolepis sp. *A*	2E , 2W , 3E , 3W
	Thalenessa sp. *A*	2E
	Thalenessa spinosa	2E , 2W
	Ephesiella sp. *A*	2E
	Sphaerodoridium sp. *A*	1
	Sphaerodoropsis sp. *A*	1 , 2E , 2W , 3E , 4
	Sphaerodoropsis sp. *A*	2E
	Apoprionospio pygmaea	1
	Aurospio dibranchiata	1 , 2W , 3E , 3W , WC5
	Dispio sp.	1
	Genus B (Spionidae) sp.	1 , 2E , 3E , 4
	Laonice cirrata	1 , 2E , 3E

Table S5. Continued.

Taxon	Species	Occurrence
POL	*Malacoceros* sp.	1 , 2E
	Microspio pigmentata	2E , 3E
	Prionospio (Minuspio) sp.	1 , 3E , 3W
	Prionospio (Minuspio) sp. *A*	1 , 2E , 3E
	Prionospio (Prionospio) sp.	2E
	Prionospio aluta (uncertain)	1
	Prionospio cirrifera	1 , 2E , 3E , WC5
	Prionospio cirrobranchiata	1 , 2E
	Prionospio cristata	1 , 2E , 3W , WC5
	Prionospio delta	1
	Prionospio ehlersi	1 , 2E , 2W , WC5
	Prionospio fauchaldi	1
	Prionospio heterobranchia	1 , 2E , 2W , WC5
	Prionospio laciniosa	1
	Prionospio multibranchiata	1
	Prionospio perkinsi	1
	Prionospio pygmaea	2E
	Prionospio sp.	1 , 2E , 2W , 3E , 3W , WC5
	Prionospio steenstrupi	1 , 2E
	Rhynchospio sp.	2E
	Rhynchospio sp. *A*	2W
	Scolelepis sp.	2W , 3E
	Spio pettiboneae	1 , 2E
	Spio sp.	2E
	Spiophanes berkeleyorum	1 , 2E , 2W , 3E
	Spiophanes bombyx	1 , 2E , 2W , 3E
	Spiophanes kroyeri	1 , 2E
	Spiophanes missionensis	2E , 3E
	Spiophanes sp.	1 , 2E , 3E
	Spiophanes sp. *A*	2E
	Spiophanes sp. *D*	1 , 2E , 3E , 4 , WC5
	Spiophanes wigleyi	1 , 3E , 3W
	Streblospio benedicti	WC5
	Streblospio sp.	2E
	Spirorbis (Janua) corrugatus	1
	Sternaspis scutata	1
	Brania sp.	2W

Table S5. Continued.

Taxon	Species	Occurrence
POL	*Brania swedmarki*	3E
	Eusyllis lamelligera	1 , 2E
	Exogone atlantica	1 , 2E , 3E
	Exogone dispar	1 , 2E , 3E , 3W
	Exogone longicirrus	1 , 2E , 2W , 3E , 3W , GKF , WC5
	Exogone lourei	3E
	Exogone sp.	1 , 2E , 2W , 3E , 3W
	Exogone sp. *A*	1 , 2E , 2W , 3E , 3W , WC5
	Exogone sp. *B*	1 , 2E , 2W , 3E , GKF
	Exogone sp. *C*	2E , 2W
	Exogone sp. *D*	1 , 2E , 2W , 3E , 3W , 4 , WC5
	Exogone sp. *E*	2E
	Exogone sp. *F*	1 , 2E , 3E
	Exogone sp. *G*	1 , 2E , 3W
	Exogone sp. *H*	2E
	Exogone sp. *I*	3E
	Exogone sp. *J*	1 , 2E , 2W , 3E , 3W
	Exogone sp. *K*	1 , 2E , 3E
	Odontosyllis sp.	2W
	Parapionosyllis sp.	1
	Parapionosyllis sp. *A*	1
	Parapionosyllis sp. *D*	1
	Pionosyllis sp. *A*	2E
	Pionosyllis sp. *B*	1 , 2E
	Pionosyllis sp. *C*	1
	Pionosyllis sp. *D*	2E
	Sphaerosyllis aciculata	2E
	Sphaerosyllis glandulata	2E
	Sphaerosyllis longicauda	1 , 2E
	Sphaerosyllis magnidentata	2E
	Sphaerosyllis piriferopsis	1 , 2E , 2W , WC5
	Sphaerosyllis renaudae	1 , 2E , 2W , 3E , WC5
	Sphaerosyllis sp.	1 , 2E , 3E
	Sphaerosyllis sp. *B*	2E
	Sphaerosyllis taylori	2E , 2W , 3E
	Syllides floridanus	2E

Table S5. Continued.

Taxon	Species	Occurrence
POL	*Syllis (Ehlersia) cornuta*	1 , 2E
	Syllis (Ehlersia) ferrugina	1 , 2E
	Syllis (Ehlersia) sp.	2E
	Syllis (Ehlersia) sp. *A*	1 , 2E , WC5
	Syllis (Typosyllis) alternata	2E
	Syllis (Typosyllis) sp.	1 , 2E
	Lanassa sp. *A*	2E
	Neoleprea sp. *A*	3E
	Terebellides atlantis	1 , 2E , 2W , 3W
	Terebellides distincta	1 , 2E , 2W , 3E , 3W , 4
	Terebellides sp.	1 , 3E
	Terebellides stroemi	1
	Trichobranchus glacialis	1 , 3E
	Trochochaeta sp.	2W , 3E
	Travisiopsis dubia	1 , 2E
	Travisiopsis lobifera	2E
	Travisiopsis sp. *A*	4

APPENDIX E

SUPPORTING TABLES FOR CHAPTER VI

Table S1. Average latitude, longitude, and depth of epibenthic fish sampling locations in the northern Gulf of Mexico. Data were compiled from Pequegnat (1983), Gallaway (1998), and Rowe & Kennicutt (2009). Unit: Depth (m), Area (hecta)

Project	Station	Trawl	Latitude	Longitude	Depth	Gear	Date	Area
Alaminos	67A5-2H	63	28.3833	-88.3681	1829	Skimmer	NA	NA
Alaminos	67A5-4G	64	28.3000	-87.3500	2651	Skimmer	NA	NA
Alaminos	67A5-SD	65	28.5333	-87.3833	1453.5	Skimmer	NA	NA
Alaminos	67A5-6B	66	28.8000	-87.0500	788	Skimmer	NA	NA
Alaminos	67A5-7C	68	29.1667	-87.1000	853	Skimmer	NA	NA
Alaminos	67A5-8B	70	28.9167	-87.4000	1494	Skimmer	NA	NA
Alaminos	67A5-9A	72	29.4500	-86.9500	752	Skimmer	NA	NA
Alaminos	67A5-13E	79	29.4858	-86.8853	379	Skimmer	NA	NA
Alaminos	67A5-14E	81	28.6847	-87.6189	2367	Skimmer	NA	NA
Alaminos	67A5-15F	82	27.6344	-86.6333	3092	Skimmer	NA	NA
Alaminos	67A5-16E	84	25.4008	-86.1000	3255	Skimmer	NA	NA
Alaminos	68A7-1A	94	28.8500	-88.7847	696	Skimmer	NA	NA
Alaminos	68A7-2C	97	28.8514	-88.6167	696	Skimmer	NA	NA
Alaminos	68A7-4A	99	25.3333	-86.1167	3237	Skimmer	NA	NA
Alaminos	68A7-4E	100	25.4022	-86.2681	3255	Skimmer	NA	NA
Alaminos	68A7-7B	102	28.0000	-86.1347	1097	Skimmer	NA	NA
Alaminos	68A7-8A	103	29.5186	-86.4850	190	Skimmer	NA	NA
Alaminos	68A7-8C	104	29.5500	-86.5514	199	Skimmer	NA	NA
Alaminos	68A7-9A	105	29.4517	-86.7514	384	Skimmer	NA	NA
Alaminos	68A7-10A	106	29.2514	-86.9167	566	Skimmer	NA	NA
Alaminos	68A7-11A	107	29.2333	-87.0000	788	Skimmer	NA	NA
Alaminos	68A7-12B	109	29.2333	-86.9853	900	Skimmer	NA	NA
Alaminos	68A7-13A	110	29.0500	-87.2500	1061	Skimmer	NA	NA
Alaminos	68A7-13B	111	28.9847	-87.3508	1399	Skimmer	NA	NA
Alaminos	68A7-13D	112	28.9833	-87.3842	1463	Skimmer	NA	NA
Alaminos	68A7-14B	113	28.9333	-87.5353	1829	Skimmer	NA	NA
Alaminos	68A7-14C	114	28.8500	-87.5181	2103	Skimmer	NA	NA
Alaminos	68A7-15D	115	29.1675	-87.5181	1097	Skimmer	NA	NA
Alaminos	68A7-15H	116	29.1681	-87.2667	914	Skimmer	NA	NA

Table S1. Continued.

Project	Station	Trawl	Latitude	Longitude	Depth	Gear	Date	Area
Alaminos	68A7-16C	117	28.7689	-87.6011	2140	Skimmer	NA	NA
Alaminos	68A7-17B	118	29.1514	-87.0333	900	Skimmer	NA	NA
Alaminos	68A13-1	119	25.6333	-96.1175	878	Skimmer	NA	NA
Alaminos	68A13-4	121	25.6344	-96.3008	512	Skimmer	NA	NA
Alaminos	68A13-5	122	26.2014	-96.3189	274	Skimmer	NA	NA
Alaminos	68A13-7	123	26.2833	-96.3000	274	Skimmer	NA	NA
Alaminos	68A13-8	124	26.3000	-96.1333	732	Skimmer	NA	NA
Alaminos	68A13-11	127	25.3833	-95.9500	1216.5	Skimmer	NA	NA
Alaminos	68A13-12A	128	25.5167	-95.8500	1189	Skimmer	NA	NA
Alaminos	68A13-15	130	27.5681	-95.1681	759	Skimmer	NA	NA
Alaminos	68A13-17	132	27.8333	-95.2014	183	Skimmer	NA	NA
Alaminos	68A13-19	134	27.7358	-95.3336	361	Skimmer	NA	NA
Alaminos	68A13-21	135	27.6333	-95.3514	576	Skimmer	NA	NA
Alaminos	68A13-23	137	27.5833	-95.3833	732	Skimmer	NA	NA
Alaminos	68A13-24	138	27.4847	-95.5167	878	Skimmer	NA	NA
Alaminos	68A13-26	139	27.0008	-95.1333	1403.5	Skimmer	NA	NA
Alaminos	68A13-27	140	27.2847	-95.1347	1133.5	Skimmer	NA	NA
Alaminos	69A11-4	142	27.4025	-94.7347	1006	Skimmer	NA	NA
Alaminos	69A11-7	143	27.0175	-94.7181	1399	Skimmer	NA	NA
Alaminos	69A11-13	145	27.0183	-94.7000	1463	Skimmer	NA	NA
Alaminos	69A13-28	179	25.4500	-86.0667	3239	Skimmer	NA	NA
Alaminos	69A13-40	184	29.1167	-88.3000	476	Skimmer	NA	NA
Alaminos	69A13-41	185	29.1847	-88.2017	311	Skimmer	NA	NA
Alaminos	69A13-42	186	29.2333	-88.2500	183	Otter Trawl	NA	NA
Alaminos	69A13-43	187	29.2181	-88.2681	210	Skimmer	NA	NA
Alaminos	69A13-44	188	28.9667	-88.4667	752	Otter Trawl	NA	NA
Alaminos	71A7-7	193	26.4353	-96.1000	873.5	Skimmer	NA	NA
Alaminos	71A7-9	194	26.5333	-96.1167	906	20m Trawl	NA	NA
Alaminos	71A7-10	195	26.5358	-96.1011	937	20m Trawl	NA	NA
Alaminos	71A7-11	196	26.5342	-96.2175	636	20m Trawl	NA	NA
Alaminos	71A7-18	199	26.7667	-96.4333	229	20m Trawl	NA	NA
Alaminos	71A7-34	204	27.8667	-92.9167	192	20m Trawl	NA	NA
Alaminos	71A7-38	206	27.5850	-92.9683	533.5	20m Trawl	NA	NA
Alaminos	71A7-42	209	27.5011	-92.8175	936	Skimmer	NA	NA
Alaminos	71A7-43	210	27.4522	-92.7667	992	20m Trawl	NA	NA
Alaminos	71A1-49	213	27.4333	-92.7000	937	20m Trawl	NA	NA
Alaminos	71A7-56	214	27.5856	-93.0167	538	20m Trawl	NA	NA
Alaminos	71A7-57	215	26.9189	-92.9525	1225	20m Trawl	NA	NA
Alaminos	71A7-62	217	27.0000	-93.0181	1198	Skimmer	NA	NA
Alaminos	71A7-65	218	27.9500	-92.7358	237	Skimmer	NA	NA

Table S1. Continued.

Project	Station	Trawl	Latitude	Longitude	Depth	Gear	Date	Area
Alaminos	71A8-3	219	27.0500	-93.3833	1196	Skimmer	NA	NA
Alaminos	71A8-8	222	26.1333	-92.7192	2057	20m Trawl	NA	NA
Alaminos	71A8-10	223	26.1500	-92.8008	2077	20m Trawl	NA	NA
Alaminos	71A8-11	224	25.8500	-93.0500	3287	20m Trawl	NA	NA
Alaminos	71A8-13	225	25.8667	-93.2522	3267	20m Trawl	NA	NA
Alaminos	72A13-32	257	26.4167	-94.7847	1774	20m Trawl	NA	NA
Alaminos	72A13-39	258	27.4344	-94.1183	1061	20m Trawl	NA	NA
Alaminos	72A13-45	259	27.7686	-94.7847	412	20m Trawl	NA	NA
Alaminos	72A13-49	260	27.6667	-94.8189	585	20m Trawl	NA	NA
Alaminos	72A13-51	261	26.9183	-95.1681	1376	20m Trawl	NA	NA
Alaminos	72A13-53	262	27.4011	-94.9347	1161	20m Trawl	NA	NA
Alaminos	73A10-20	264	27.2508	-93.6844	969.5	20m Trawl	NA	NA
NGoMCS	C1	1C1	28.0678	-90.2847	329	9m Otter Trawl	Nov-83	2.87
NGoMCS	C2	1C2	27.8842	-90.0842	786	9m Otter Trawl	Nov-83	3.08
NGoMCS	C3	1C3	27.8000	-90.0508	850	9m Otter Trawl	Nov-83	6.25
NGoMCS	C1	2C1	28.0508	-90.2500	338	9m Otter Trawl	Apr-84	2.71
NGoMCS	C2	2C2	27.9011	-90.1000	603	9m Otter Trawl	Apr-84	2.67
NGoMCS	C3	2C3	27.8186	-90.1019	805	9m Otter Trawl	Apr-84	5.79
NGoMCS	C4	2C4	27.4669	-89.7183	1438	9m Otter Trawl	Apr-84	5.00
NGoMCS	C5	2C5	27.0178	-89.5008	2401	9m Otter Trawl	Apr-84	5.66
NGoMCS	E1	2E 1	28.4347	-86.0503	366.5	9m Otter Trawl	Apr-84	3.21
NGoMCS	E2	2E 2	28.2850	-86.2356	621.5	9m Otter Trawl	Apr-84	NA
NGoMCS	E3	2E 3	28.1686	-86.4183	840	9m Otter Trawl	Apr-84	5.58
NGoMCS	E4	2E 4	28.1000	-86.5842	1170	9m Otter Trawl	Apr-84	5.29
NGoMCS	E5	2E 5	28.0192	-86.6669	2857.5	9m Otter Trawl	Apr-84	NA
NGoMCS	W1	2W1	27.6167	-93.5517	342	9m Otter Trawl	Apr-84	2.83
NGoMCS	W2	2W2	27.4014	-93.3025	654	9m Otter Trawl	Apr-84	2.58
NGoMCS	W3	2W3	27.1344	-93.3850	828	9m Otter Trawl	Apr-84	6.62
NGoMCS	W4	2W4	26.7344	-93.3017	1413	9m Otter Trawl	Apr-84	5.75
NGoMCS	C1	3C1	28.0342	-90.2564	346	9m Otter Trawl	Dec-84	2.62
NGoMCS	C2	3C2	27.9008	-90.0314	632	9m Otter Trawl	Dec-84	3.46
NGoMCS	C3	3C3	27.8269	-90.0403	802.5	9m Otter Trawl	Dec-84	2.87
NGoMCS	C4	3C4	27.3503	-89.7514	1510	9m Otter Trawl	Dec-84	NA
NGoMCS	C5	3C5	26.9353	-89.5017	2504.5	9m Otter Trawl	Dec-84	5.12
NGoMCS	C6	3C6	28.0167	-90.0836	474.5	9m Otter Trawl	Dec-84	2.50
NGoMCS	C7	3C7	27.7347	-90.0181	964.5	9m Otter Trawl	Dec-84	NA
NGoMCS	C8	3C8	27.5186	-89.8258	1064	9m Otter Trawl	Dec-84	3.91
NGoMCS	C10	3C10	27.4167	-89.7006	1735	9m Otter Trawl	Dec-84	NA
NGoMCS	C11	3C11	27.2186	-89.6022	2074	9m Otter Trawl	Dec-84	NA
NGoMCS	E1	4E1	28.4797	-86.0422	354	9m Otter Trawl	Jun-85	2.50

Table S1. Continued.

Project	Station	Trawl	Latitude	Longitude	Depth	Gear	Date	Area
NGoMCS	E2	4E2	28.2678	-86.2014	615.5	9m Otter Trawl	Jun-85	2.50
NGoMCS	E3	4E3	28.1597	-86.3989	871	9m Otter Trawl	Jun-85	2.50
NGoMCS	E1A	4ElA	28.9061	-86.4006	351	9m Otter Trawl	Jun-85	2.29
NGoMCS	E1B	4E1B	28.3111	-85.7389	345	9m Otter Trawl	Jun-85	2.42
NGoMCS	E1C	4E1C	28.2186	-85.5656	350	9m Otter Trawl	Jun-85	2.42
NGoMCS	E2A	4E2A	28.5836	-86.7622	625	9m Otter Trawl	Jun-85	3.96
NGoMCS	E2B	4E2B	28.3161	-86.3156	612.5	9m Otter Trawl	Jun-85	2.46
NGoMCS	E2C	4E2C	28.2258	-86.1108	618	9m Otter Trawl	Jun-85	2.46
NGoMCS	E2D	4E2D	28.1272	-85.8600	627.5	9m Otter Trawl	Jun-85	2.50
NGoMCS	E2E	4E2E	28.0178	-85.6606	629	9m Otter Trawl	Jun-85	2.50
NGoMCS	E3A	4E3A	28.4994	-86.9692	812	9m Otter Trawl	Jun-85	1.83
NGoMCS	E3B	4E3B	28.1189	-86.2861	834	9m Otter Trawl	Jun-85	2.50
NGoMCS	E3C	4E3C	28.2667	-86.6044	842.5	9m Otter Trawl	Jun-85	2.79
NGoMCS	E3D	4E3D	28.3731	-86.8081	850.5	9m Otter Trawl	Jun-85	2.54
NGoMCS	WC1	5WC1	27.7161	-92.8681	368.5	9m Otter Trawl	Jun-85	NA
NGoMCS	WC10	5WC10	27.7547	-90.8003	746.5	9m Otter Trawl	Jun-85	NA
NGoMCS	WC11	5WC11	27.4125	-92.6344	1135.5	9m Otter Trawl	Jun-85	2.50
NGoMCS	WC12	5WC12	27.3269	-91.5225	1203	9m Otter Trawl	Jun-85	2.50
NGoMCS	WC2	5WC2	27.7522	-92.4856	551.5	9m Otter Trawl	Jun-85	2.50
NGoMCS	WC3	5WC3	27.5869	-92.3778	774.5	9m Otter Trawl	Jun-85	NA
NGoMCS	WC4	5WC4	27.7194	-92.1539	521.5	9m Otter Trawl	Jun-85	2.42
NGoMCS	WC5	5WC5	27.7839	-91.7294	423	9m Otter Trawl	Jun-85	2.50
NGoMCS	WC6	5WC6	27.7122	-91.5486	663	9m Otter Trawl	Jun-85	2.75
NGoMCS	WC7	5WC7	27.7589	-91.2269	464.5	9m Otter Trawl	Jun-85	2.50
NGoMCS	WC8	5WC8	27.8619	-90.7636	479	9m Otter Trawl	Jun-85	2.67
NGoMCS	WC9	5WC9	27.7131	-91.2531	751	9m Otter Trawl	Jun-85	2.46
DGoMB	B1	1-B1-1	27.1907	-91.4097	2250	10m Otter Trawl	6-May-00	4.21
DGoMB	B2	1-B2-3	26.5495	-92.2106	2230	10m Otter Trawl	19-Jun-00	5.75
DGoMB	B3	1-B3-1	26.1381	-91.7453	2460	10m Otter Trawl	10-May-00	6.75
DGoMB	C1	1-C1-1	28.0738	-90.2514	325	10m Otter Trawl	30-May-00	2.15
DGoMB	C12	1-C12-1	26.3889	-89.2513	2915	10m Otter Trawl	3-Jun-00	5.01
DGoMB	C4	1-C4-1	27.4810	-89.7862	1358.5	10m Otter Trawl	31-May-00	2.95
DGoMB	C7	1-C7-1	27.7379	-89.9841	997.5	10m Otter Trawl	31-May-00	2.91
DGoMB	MT1	1-MT1-1	28.5506	-89.8392	460.5	10m Otter Trawl	17-Jun-00	1.62
DGoMB	MT1	2-MT1-1	28.5569	-89.8458	461	10m Otter Trawl	3-Jun-01	0.88
DGoMB	MT2	1-MT2-1	28.4422	-89.6628	686	10m Otter Trawl	17-Jun-00	2.04
DGoMB	MT3	1-MT3-1	28.2143	-89.4839	1002	10m Otter Trawl	16-Jun-00	1.68
DGoMB	MT4	1-MT4-1	27.8603	-89.2249	1368.5	10m Otter Trawl	18-Jun-00	2.38
DGoMB	MT5	1-MT5-1	27.3283	-88.6706	2242.5	10m Otter Trawl	4-Jun-00	4.12
DGoMB	MT6	1-MT6-1	26.9851	-88.0004	2735	10m Otter Trawl	5-Jun-00	5.68

Table S1. Continued.

Project	Station	Trawl	Latitude	Longitude	Depth	Gear	Date	Area
DGoMB	NB2	1-NB2-1	27.1336	-92.0009	1532.5	10m Otter Trawl	7-May-00	3.28
DGoMB	NB3	1-NB3-1	26.5027	-91.8062	1880	10m Otter Trawl	8-May-00	4.63
DGoMB	NB5	1-NB5-1	26.2503	-91.2214	2105	10m Otter Trawl	9-May-00	3.78
DGoMB	RW1	1-RW1-1	27.5140	-96.0206	187.5	10m Otter Trawl	23-May-00	2.92
DGoMB	S1	3-S1-1	24.9456	-91.6452	3590	10m Otter Trawl	3-Aug-02	2.86
DGoMB	S3	3-S3-1	24.8137	-90.5202	3655	10m Otter Trawl	7-Aug-02	7.49
DGoMB	S35	1-S35-1	29.3459	-87.0375	670	10m Otter Trawl	12-Jun-00	1.79
DGoMB	S36	1-S36-1	28.9332	-87.6450	1783.5	10m Otter Trawl	13-Jun-00	3.7
DGoMB	S37	1-S37-1	28.5875	-87.7479	2369	10m Otter Trawl	13-Jun-00	5.07
DGoMB	S38	1-S38-1	28.3201	-87.3489	2607.5	10m Otter Trawl	15-Jun-00	5.5
DGoMB	S4	3-S4-1	24.2553	-85.6850	3402.5	10m Otter Trawl	9-Aug-02	4.62
DGoMB	S40	1-S40-1	27.8564	-86.7482	3010	10m Otter Trawl	8-Jun-00	5.88
DGoMB	S41	1-S41-1	27.9881	-86.5561	2980	10m Otter Trawl	9-Jun-00	6.21
DGoMB	S42	1-S42-1	28.2489	-86.4109	785	10m Otter Trawl	10-Jun-00	2.17
DGoMB	S42	2-S42-1	28.2663	-86.4642	767	10m Otter Trawl	8-Jun-01	1.99
DGoMB	S43	1-S43-1	28.4990	-86.0782	359	10m Otter Trawl	10-Jun-00	2.03
DGoMB	S44	1-S44-1	28.7383	-85.7467	215.5	10m Otter Trawl	11-Jun-00	2.09
DGoMB	S5	3-S5-1	25.3916	-88.0253	3355	10m Otter Trawl	8-Aug-02	4.99
DGoMB	W1	1-W1-1	27.5695	-93.5407	400	10m Otter Trawl	14-May-00	2.1
DGoMB	W3	1-W3-1	27.1482	-93.3198	950	10m Otter Trawl	15-May-00	2.78
DGoMB	W6/RW6	1-W6-1	26.0014	-93.8477	3075	10m Otter Trawl	20-Jun-00	5.18
DGoMB	WC12	1-WC12-1	27.3240	-91.6025	1100	10m Otter Trawl	6-May-00	2.18
DGoMB	WC5	1-WC5-1	27.6905	-91.6514	757.5	10m Otter Trawl	5-May-00	2.11

Table S2. Species list of deep-sea epibenthic fishes during Alaminos, NGoMCS, and DGoMB surveys in the northern Gulf of Mexico. Data were compiled from Pequegnat (1983), Gallaway (1998), and Rowe & Kennicutt (2009). Only species with valid scientific names were listed.

Code	Species Name	Code	Species Name
SP001	*Acanthonus armatus*	SP138	*Anacanthobatis folirostris*
SP002	*Aldrovandia affinis*	SP139	*Apristurus laurussonii*
SP003	*Aldrovandia gracilis*	SP140	*Apristurus parvipinnis*
SP004	*Alepocephalus agassizii*	SP141	*Bathypterois bigelowi*
SP005	*Ancylopsetta dilecta*	SP142	*Bathypterois grallator*
SP006	*Apristurus profundorum*	SP143	*Bathypterois phenax*
SP007	*Argentina striata*	SP144	*Bathypterois viridensis*
SP008	*Barathronus bicolor*	SP145	*Borostomias antarcticus*
SP009	*Bassozetus normalis*	SP146	*Brosmiculus imberbis*
SP010	*Bathophilus pawneei*	SP147	*Coryphaenoides rudis*
SP011	*Bathygadus favosus*	SP148	*Cruriraja cadenati*
SP012	*Bathygadus macrops*	SP149	*Cruriraja rugosa*
SP013	*Bathygadus melanobranchus*	SP150	*Decapterus punctatus*
SP014	*Bathyonus pectoralis*	SP151	*Dysommina rugosa*
SP015	*Bathypterois longipes*	SP152	*Epigonus denticulatus*
SP016	*Bathypterois quadrifilis*	SP153	*Epigonus macrops*
SP017	*Bathytroctes macrolepis*	SP154	*Epigonus occidentalis*
SP018	*Bathyuroconger vicinus*	SP155	*Epigonus pandionis*
SP019	*Bellator militaris*	SP156	*Eptatretus minor*
SP020	*Bembrops anatirostris*	SP157	*Eptatretus springeri*
SP021	*Bembrops gobioides*	SP158	*Etmopterus gracilispinis*
SP022	*Bregmaceros atlanticus*	SP159	*Etmopterus virens*
SP023	*Cetonurus globiceps*	SP160	*Exechodontes daidaleus*
SP024	*Chauliodus sloani*	SP161	*Gadomus dispar*
SP025	*Chaunax pictus*	SP162	*Halosaurus ovenii*
SP026	*Chimaera monstrosa*	SP163	*Helicolenus dactylopterus*
SP027	*Chlorophthalmus agassizi*	SP164	*Heptranchias perlo*
SP028	*Chlorophthalmus chalybeius*	SP165	*Hoplostethus occidentalis*
SP029	*Citharichthys gymnorhinus*	SP166	*Kuronezumia bubonis*
SP030	*Coelorinchus caribbaeus*	SP167	*Lophiodes monodi*
SP031	*Coelorinchus caelorhincus*	SP168	*Lophius gastrophysus*

Table S2. Continued.

Code	Species Name	Code	Species Name
SP032	*Coelorinchus occa*	SP169	*Luciobrotula corethromycter*
SP033	*Conger oceanicus*	SP170	*Lycenchelys bullisi*
SP034	*Conocara macropterum*	SP171	*Manducus maderensis*
SP035	*Coryphaenoides carapinus*	SP172	*Melanonus zugmayeri*
SP036	*Coryphaenoides carminifer*	SP173	*Myxine glutinosa*
SP037	*Coryphaenoides mexicanus*	SP174	*Nezumia suilla*
SP038	*Coryphaenoides zaniophorus*	SP175	*Notacanthus chemnitzii*
SP039	*Decodon puellaris*	SP176	*Ophichthus cruentifer*
SP040	*Dibranchus atlanticus*	SP177	*Peristedion ecuadorense*
SP041	*Dicrolene introniger*	SP178	*Peristedion miniatum*
SP042	*Dicrolene kanazawai*	SP179	*Polyacanthonotus merretti*
SP043	*Diplacanthopoma brachysoma*	SP180	*Rajella purpuriventralis*
SP044	*Etmopterus pusillus*	SP181	*Rhynchoconger guppyi*
SP045	*Etmopterus schultzi*	SP182	*Rinoctes nasutus*
SP046	*Etmopterus spinax*	SP183	*Saccogaster staigeri*
SP047	*Fenestraja sinusmexicanus*	SP184	*Sciadonus galatheae*
SP048	*Foetorepus agassizii*	SP185	*Sciadonus pedicellaris*
SP049	*Gadella imberbis*	SP186	*Scyliorhinus retifer*
SP050	*Gadella maraldi*	SP187	*Stomias affinis*
SP051	*Gadomus arcuatus*	SP188	*Synagrops bellus*
SP052	*Gadomus longifilis*	SP189	*Synagrops spinosus*
SP053	*Gnathagnus egregius*	SP190	*Trachyscorpia cristulata*
SP054	*Halosaurus guentheri*	SP191	*Ventrifossa macropogon*
SP055	*Haptenchelys texis*	SP192	*Zenopsis conchifera*
SP056	*Hemanthias leptus*	SP193	*Alepocephalus productus*
SP057	*Hemanthias vivanus*	SP194	*Anoplogaster cornuta*
SP058	*Histiobranchus bathybius*	SP195	*Antigonia capros*
SP059	*Hollardia hollardi*	SP196	*Argentia striata*
SP060	*Hoplostethus mediterraneus*	SP197	*Argyropelecus aculeatus*
SP061	*Hoplunnis macrurus*	SP198	*Argyropelecus affinis*
SP062	*Hoplunnis schmidti*	SP199	*Argyropelecus gigas*
SP063	*Hoplunnis tenuis*	SP200	*Ariosoma balearicum*
SP064	*Hydrolagus alberti*	SP201	*Aristostomias xenostoma*
SP065	*Hydrolagus media*	SP202	*Barathrites iris*
SP066	*Hydrolagus mirabilis*	SP203	*Barathrodemus manatinus*
SP067	*Hymenocephalus italicus*	SP204	*Bassogigas gillii*
SP068	*Ilyophis brunneus*	SP205	*Bassozetus robustus*

Table S2. Continued.

Code	Species Name	Code	Species Name
SP069	*Ipnops murrayi*	SP206	*Bathylagus longirostris*
SP070	*Laemonema barbatulum*	SP207	*Bathysaurus mollis*
SP071	*Lepophidium brevibarbe*	SP208	*Bathytroctes microlepis*
SP072	*Leptoderma macrops*	SP209	*Bathytyphlops sewelli*
SP073	*Leucoraja garmani*	SP210	*Benthodesmus tenuis*
SP074	*Macroramphosus scolopax*	SP211	*Caelorinchus caelorhinchus*
SP075	*Malacocephalus occidentalis*	SP212	*Caelorinchus caribbaeus*
SP076	*Malacosteus niger*	SP213	*Caelorinchus occa*
SP077	*Melanostomias biseriatus*	SP214	*Caranx hippos*
SP078	*Merluccius albidus*	SP215	*Chauliodus danae*
SP079	*Merluccius bilinearis*	SP216	*Chaunax suttkusi*
SP080	*Monolene sessilicauda*	SP217	*Citharichthys cornutus*
SP081	*Monomitopus agassizii*	SP218	*Coloconger meadi*
SP082	*Myrophis punctatus*	SP219	*Coryphaenoides mediterraneus*
SP083	*Neobythites gilli*	SP220	*Coryphaenoides alateralis*
SP084	*Neobythites marginatus*	SP221	*Cyclothone alba*
SP085	*Neoscopelus macrolepidotus*	SP222	*Cyclothone pallida*
SP086	*Nettastoma melanurum*	SP223	*Cyttopsis roseus*
SP087	*Nettenchelys pygmaea*	SP224	*Diaphus lucidus*
SP088	*Nezumia aequalis*	SP225	*Gadomus longifilus*
SP089	*Nezumia atlantica*	SP226	*Gadomus macrops*
SP090	*Nezumia bairdii*	SP227	*Gibberichthys pumilus*
SP091	*Nezumia cyrano*	SP228	*Gigantura indica*
SP092	*Nezumia sclerorhynchus*	SP229	*Gonostoma atlanticum*
SP093	*Oneirodes eschrichtii*	SP230	*Gonostoma elongatum*
SP094	*Parahollardia lineata*	SP231	*Holtbyrnia innesi*
SP095	*Parasudis truculenta*	SP232	*Howella sherborni*
SP096	*Penopus microphthalmus*	SP233	*Hygophum taaningi*
SP097	*Peristedion greyae*	SP234	*Hymenocephalus billsam*
SP098	*Phycis chesteri*	SP235	*Kali indica*
SP099	*Physiculus fulvus*	SP236	*Laemonema goodebeanerum*
SP100	*Physiculus kaupi*	SP237	*Leucoraja lentiginosa*
SP101	*Poecilopsetta beanii*	SP238	*Malacocephalus laevis*
SP102	*Polyacanthonotus africanus*	SP239	*Merluccius albides*
SP103	*Polymetme corythaeola*	SP240	*Microstoma microstoma*
SP104	*Polymixia lowei*	SP241	*Monolene sessilcauda*
SP105	*Pontinus longispinis*	SP242	*Monomitopus magnus*

Table S2. Continued.

Code	Species Name	Code	Species Name
SP106	*Porogadus catena*	SP243	*Narcetes stomias*
SP107	*Prionotus beanii*	SP244	*Neoscopelus microchir*
SP108	*Prionotus rubio*	SP245	*Notoscopelus resplendens*
SP109	*Prionotus stearnsi*	SP246	*Paralichthys squamilentus*
SP110	*Pristipomoides aquilonaris*	SP247	*Penopus macdonaldi*
SP111	*Pseudophichthys splendens*	SP248	*Peristedion thompsoni*
SP112	*Rajella bigelowi*	SP249	*Photostomias guernei*
SP113	*Rajella fuliginea*	SP250	*Phrynichthys wedii*
SP114	*Rhynchoconger flavus*	SP251	*Platytroctes apus*
SP115	*Saccogaster maculata*	SP252	*Poecilopsetta beani*
SP116	*Scorpaena plumieri*	SP253	*Polyipnus claris*
SP117	*Setarches guentheri*	SP254	*Pontus longispinis*
SP118	*Sphagemacrurus grenadae*	SP255	*Porogadus miles*
SP119	*Squalogadus modificatus*	SP256	*Poromitra crassiceps*
SP120	*Squalus cubensis*	SP257	*Poromitra megalops*
SP121	*Steindachneria argentea*	SP258	*Pseudoscopelus sp.*
SP122	*Stephanoberyx monae*	SP259	*Rajella purpurventralis*
SP123	*Symphurus marginatus*	SP260	*Remora brachyptera*
SP124	*Symphurus piger*	SP261	*Rhinochimaera atlantica*
SP125	*Synaphobranchus oregoni*	SP262	*Rouleina maderensis*
SP126	*Trachonurus villosus*	SP263	*Saurida normani*
SP127	*Trichopsetta ventralis*	SP264	*Scombrolabrax heterolepis*
SP128	*Uroconger syringinus*	SP265	*Sternoptyx diaphana*
SP129	*Urophycis cirrata*	SP266	*Sternoptyx pseudobscura*
SP130	*Urophycis floridana*	SP267	*Synaphobranchus affinis*
SP131	*Urophycis regia*	SP268	*Talismania antillarum*
SP132	*Venefica procera*	SP269	*Thaumatichthys pagidostomus*
SP133	*Xenomystax atrarius*	SP270	*Trachonurus sulcatus*
SP134	*Xenomystax bidentatus*	SP271	*Trichiurus lepturus*
SP135	*Xyelacyba myersi*	SP272	*Urophycis cinata*
SP136	*Yarrella blackfordi*	SP273	*Ventrifossa macrogon*
SP137	*Acromycter perturbator*	SP274	*Zalieutes mcgintyi*

Table S3. Occurrence and abundance of deep-sea epibenthic fishes during the Alaminos, NGoMCS, and DGoMB surveys in the northern Gulf of Mexico. Data were compiled from Pequegnat (1983), Gallaway (1998), and Rowe & Kennicutt (2009). The table header follows Table S2. P denotes "species presence"

Trawl	Code	Count	Trawl	Code	Count	Trawl	Code	Count	Trawl	Code	Count
63	SP106	P	213	SP081	P	3C7	SP016	1	5WC5	SP138	1
63	SP132	P	213	SP090	P	3C7	SP037	3	5WC5	SP146	2
63	SP135	P	213	SP119	P	3C7	SP038	1	5WC5	SP155	27
64	SP014	P	213	SP122	P	3C7	SP040	3	5WC5	SP165	4
65	SP002	P	213	SP125	P	3C7	SP051	1	5WC5	SP168	1
66	SP002	P	213	SP136	P	3C7	SP052	8	5WC5	SP178	1
66	SP081	P	214	SP006	P	3C7	SP054	6	5WC6	SP012	3
66	SP125	P	214	SP013	P	3C7	SP068	5	5WC6	SP025	8
68	SP040	P	214	SP020	P	3C7	SP091	1	5WC6	SP031	2
68	SP045	P	214	SP021	P	3C7	SP125	11	5WC6	SP040	33
68	SP052	P	214	SP027	P	3C7	SP132	1	5WC6	SP045	9
68	SP066	P	214	SP031	P	3C7	SP137	1	5WC6	SP047	2
70	SP003	P	214	SP040	P	3C7	SP144	1	5WC6	SP070	6
70	SP037	P	214	SP045	P	3C7	SP180	1	5WC6	SP075	1
70	SP122	P	214	SP046	P	3C8	SP002	4	5WC6	SP078	5
72	SP012	P	214	SP053	P	3C8	SP003	1	5WC6	SP086	2
72	SP013	P	214	SP064	P	3C8	SP008	1	5WC6	SP088	11
72	SP025	P	214	SP067	P	3C8	SP011	2	5WC6	SP089	1
72	SP043	P	214	SP070	P	3C8	SP013	1	5WC6	SP097	2
72	SP045	P	214	SP075	P	3C8	SP016	5	5WC6	SP123	1
72	SP085	P	214	SP079	P	3C8	SP037	5	5WC6	SP125	3
72	SP088	P	214	SP084	P	3C8	SP052	8	5WC6	SP146	1
72	SP103	P	214	SP097	P	3C8	SP068	37	5WC6	SP154	4
72	SP111	P	214	SP100	P	3C8	SP091	6	5WC6	SP161	2
72	SP123	P	214	SP129	P	3C8	SP118	6	5WC6	SP169	1
79	SP021	P	214	SP131	P	3C8	SP122	3	5WC6	SP175	1
79	SP031	P	214	SP132	P	3C8	SP125	23	5WC6	SP188	1
79	SP040	P	214	SP136	P	3C8	SP132	1	5WC7	SP021	16
79	SP097	P	215	SP011	P	3C8	SP137	9	5WC7	SP025	2
79	SP116	P	215	SP016	P	3C8	SP147	1	5WC7	SP027	26
81	SP042	P	215	SP038	P	3C8	SP174	1	5WC7	SP031	9
81	SP069	P	215	SP040	P	3C8	SP179	2	5WC7	SP040	76
82	SP009	P	215	SP041	P	3C10	SP002	3	5WC7	SP045	2
82	SP014	P	215	SP051	P	3C10	SP003	1	5WC7	SP047	2

Table S3. Continued.

Trawl	Code	Count	Trawl	Code	Count	Trawl	Code	Count	Trawl	Code	Count
84	SP009	P	215	SP081	P	3C10	SP008	1	5WC7	SP060	1
94	SP040	P	215	SP088	P	3C10	SP016	1	5WC7	SP067	77
94	SP050	P	215	SP122	P	3C11	SP037	1	5WC7	SP070	21
94	SP054	P	215	SP125	P	3C11	SP142	2	5WC7	SP075	6
94	SP097	P	215	SP132	P	3C11	SP147	1	5WC7	SP078	4
94	SP125	P	215	SP136	P	4E1	SP007	2	5WC7	SP095	4
94	SP136	P	217	SP034	P	4E1	SP020	1	5WC7	SP097	5
97	SP040	P	218	SP071	P	4E1	SP021	40	5WC7	SP117	1
97	SP065	P	218	SP105	P	4E1	SP027	106	5WC7	SP123	2
99	SP001	P	218	SP127	P	4E1	SP031	24	5WC7	SP129	15
100	SP017	P	219	SP037	P	4E1	SP040	1	5WC7	SP146	4
102	SP040	P	222	SP016	P	4E1	SP047	1	5WC7	SP151	1
103	SP020	P	223	SP016	P	4E1	SP053	1	5WC7	SP152	1
104	SP071	P	223	SP132	P	4E1	SP057	3	5WC7	SP155	20
104	SP099	P	224	SP009	P	4E1	SP067	9	5WC7	SP156	3
104	SP101	P	224	SP015	P	4E1	SP075	4	5WC7	SP159	8
104	SP105	P	224	SP076	P	4E1	SP078	41	5WC7	SP165	1
105	SP021	P	225	SP008	P	4E1	SP095	12	5WC7	SP168	2
105	SP022	P	225	SP009	P	4E1	SP097	25	5WC7	SP188	1
105	SP027	P	225	SP055	P	4E1	SP101	33	5WC8	SP021	31
105	SP031	P	225	SP068	P	4E1	SP104	3	5WC8	SP025	6
105	SP040	P	257	SP002	P	4E1	SP117	2	5WC8	SP027	1
105	SP047	P	258	SP004	P	4E1	SP121	4	5WC8	SP031	39
105	SP075	P	258	SP006	P	4E1	SP129	16	5WC8	SP040	63
105	SP079	P	258	SP008	P	4E1	SP130	5	5WC8	SP045	15
105	SP097	P	258	SP013	P	4E1	SP155	30	5WC8	SP067	71
105	SP124	P	258	SP016	P	4E1	SP164	1	5WC8	SP070	26
106	SP010	P	258	SP017	P	4E1	SP168	1	5WC8	SP075	5
106	SP031	P	258	SP032	P	4E1	SP183	1	5WC8	SP078	3
106	SP047	P	258	SP037	P	4E1	SP186	2	5WC8	SP088	1
106	SP088	P	258	SP038	P	4E1	SP188	3	5WC8	SP095	2
106	SP098	P	258	SP040	P	4E1	SP189	9	5WC8	SP097	17
106	SP099	P	258	SP041	P	4E2	SP008	2	5WC8	SP123	1
106	SP123	P	258	SP052	P	4E2	SP012	1	5WC8	SP125	1
106	SP136	P	258	SP075	P	4E2	SP025	9	5WC8	SP129	52
107	SP013	P	258	SP081	P	4E2	SP040	26	5WC8	SP146	3
107	SP025	P	258	SP088	P	4E2	SP045	2	5WC8	SP151	2
107	SP037	P	258	SP113	P	4E2	SP070	4	5WC8	SP155	12
107	SP038	P	258	SP118	P	4E2	SP078	1	5WC8	SP157	2
107	SP040	P	258	SP122	P	4E2	SP088	7	5WC8	SP159	3

Table S3. Continued.

Trawl	Code	Count	Trawl	Code	Count	Trawl	Code	Count	Trawl	Code	Count
107	SP041	P	258	SP126	P	4E2	SP091	1	5WC8	SP160	2
109	SP013	P	258	SP132	P	4E2	SP125	3	5WC8	SP168	1
109	SP038	P	259	SP021	P	4E2	SP129	1	5WC9	SP008	2
109	SP041	P	259	SP027	P	4E2	SP146	1	5WC9	SP012	12
109	SP052	P	259	SP028	P	4E2	SP190	1	5WC9	SP013	13
109	SP054	P	259	SP030	P	4E3	SP013	2	5WC9	SP025	4
109	SP081	P	259	SP031	P	4E3	SP037	1	5WC9	SP032	2
109	SP088	P	259	SP050	P	4E3	SP040	4	5WC9	SP037	1
109	SP112	P	259	SP053	P	4E3	SP054	2	5WC9	SP038	3
109	SP125	P	259	SP057	P	4E3	SP068	1	5WC9	SP040	26
109	SP132	P	259	SP060	P	4E3	SP072	1	5WC9	SP045	1
110	SP003	P	259	SP067	P	4E3	SP088	10	5WC9	SP051	1
110	SP016	P	259	SP075	P	4E3	SP091	2	5WC9	SP052	1
110	SP034	P	259	SP079	P	4E3	SP111	2	5WC9	SP054	3
110	SP041	P	259	SP101	P	4E3	SP125	3	5WC9	SP088	6
110	SP052	P	259	SP117	P	4E3	SP146	1	5WC9	SP111	4
110	SP068	P	259	SP129	P	4E3	SP161	2	5WC9	SP112	1
110	SP081	P	260	SP010	P	4E1A	SP007	1	5WC9	SP125	39
110	SP088	P	260	SP012	P	4E1A	SP020	2	5WC9	SP140	1
110	SP119	P	260	SP025	P	4E1A	SP021	68	5WC9	SP146	1
110	SP122	P	260	SP031	P	4E1A	SP027	28	5WC9	SP170	1
110	SP125	P	260	SP033	P	4E1A	SP030	20	5WC9	SP175	1
111	SP002	P	260	SP038	P	4E1A	SP031	6	1-B1-1	SP042	1
111	SP003	P	260	SP040	P	4E1A	SP040	4	1-B1-1	SP106	1
111	SP016	P	260	SP043	P	4E1A	SP057	8	1-B1-1	SP193	1
111	SP034	P	260	SP046	P	4E1A	SP067	4	1-B1-1	SP230	1
111	SP041	P	260	SP047	P	4E1A	SP075	3	1-B1-1	SP249	1
112	SP037	P	260	SP052	P	4E1A	SP078	11	1-B2-3	SP004	1
112	SP041	P	260	SP054	P	4E1A	SP095	4	1-B2-3	SP069	3
112	SP052	P	260	SP079	P	4E1A	SP097	5	1-B2-3	SP224	1
112	SP118	P	260	SP088	P	4E1A	SP101	15	1-B2-3	SP260	1
112	SP122	P	260	SP089	P	4E1A	SP105	24	1-B2-3	SP265	1
112	SP125	P	260	SP101	P	4E1A	SP117	3	1-B3-1	SP042	1
113	SP003	P	260	SP129	P	4E1A	SP121	2	1-B3-1	SP219	1
113	SP034	P	260	SP136	P	4E1A	SP123	1	1-C1-1	SP021	3
113	SP041	P	261	SP002	P	4E1A	SP129	11	1-C1-1	SP095	1
113	SP106	P	261	SP003	P	4E1A	SP138	1	1-C1-1	SP104	2
114	SP003	P	261	SP015	P	4E1A	SP155	21	1-C1-1	SP121	29
114	SP009	P	261	SP023	P	4E1A	SP165	3	1-C1-1	SP165	1
114	SP106	P	261	SP037	P	4E1A	SP178	1	1-C1-1	SP178	1

Table S3. Continued.

Trawl	Code	Count	Trawl	Code	Count	Trawl	Code	Count	Trawl	Code	Count
115	SP003	P	261	SP040	P	4E1A	SP181	1	1-C1-1	SP188	3
115	SP035	P	261	SP041	P	4E1A	SP188	5	1-C1-1	SP192	2
115	SP038	P	261	SP122	P	4E1A	SP189	2	1-C1-1	SP196	1
115	SP041	P	261	SP125	P	4E1B	SP007	1	1-C1-1	SP210	1
115	SP052	P	261	SP132	P	4E1B	SP020	2	1-C1-1	SP212	30
115	SP068	P	262	SP002	P	4E1B	SP021	11	1-C1-1	SP214	3
115	SP081	P	262	SP016	P	4E1B	SP027	8	1-C1-1	SP223	3
115	SP088	P	262	SP037	P	4E1B	SP031	14	1-C1-1	SP252	2
115	SP119	P	262	SP041	P	4E1B	SP053	1	1-C1-1	SP254	18
115	SP122	P	262	SP052	P	4E1B	SP057	2	1-C1-1	SP272	1
115	SP125	P	262	SP081	P	4E1B	SP075	11	1-C12-1	SP001	1
116	SP013	P	262	SP088	P	4E1B	SP078	7	1-C12-1	SP142	1
116	SP038	P	262	SP090	P	4E1B	SP095	2	1-C12-1	SP203	1
116	SP041	P	262	SP118	P	4E1B	SP097	7	1-C12-1	SP207	4
116	SP052	P	262	SP122	P	4E1B	SP101	3	1-C4-1	SP024	2
116	SP054	P	262	SP132	P	4E1B	SP117	1	1-C4-1	SP034	2
116	SP068	P	264	SP012	P	4E1B	SP129	22	1-C4-1	SP037	4
116	SP081	P	264	SP016	P	4E1B	SP130	1	1-C4-1	SP041	4
116	SP088	P	264	SP018	P	4E1B	SP148	4	1-C4-1	SP081	6
116	SP125	P	264	SP032	P	4E1B	SP155	4	1-C4-1	SP091	7
117	SP106	P	264	SP038	P	4E1B	SP177	1	1-C4-1	SP119	1
118	SP013	P	264	SP040	P	4E1B	SP188	1	1-C4-1	SP125	5
118	SP037	P	264	SP051	P	4E1B	SP189	1	1-C4-1	SP174	4
118	SP041	P	264	SP085	P	4E1B	SP192	1	1-C4-1	SP208	1
118	SP076	P	264	SP088	P	4E1C	SP021	69	1-C4-1	SP225	7
118	SP088	P	264	SP125	P	4E1C	SP025	1	1-C4-1	SP247	2
118	SP125	P	264	SP136	P	4E1C	SP027	13	1-C4-1	SP259	1
119	SP013	P	1C1	SP007	4	4E1C	SP031	31	1-C4-1	SP265	3
119	SP037	P	1C1	SP027	5	4E1C	SP047	2	1-C7-1	SP010	1
119	SP054	P	1C1	SP030	77	4E1C	SP053	1	1-C7-1	SP024	2
119	SP081	P	1C1	SP031	3	4E1C	SP057	2	1-C7-1	SP076	1
119	SP088	P	1C1	SP053	1	4E1C	SP075	5	1-C7-1	SP222	2
119	SP125	P	1C1	SP057	4	4E1C	SP078	6	1-C7-1	SP229	1
119	SP126	P	1C1	SP071	1	4E1C	SP095	1	1-C7-1	SP230	2
121	SP040	P	1C1	SP073	1	4E1C	SP097	12	1-C7-1	SP240	1
121	SP075	P	1C1	SP074	1	4E1C	SP101	15	1-C7-1	SP249	1
121	SP078	P	1C1	SP075	5	4E1C	SP117	2	1-MT1-1	SP012	26
121	SP088	P	1C1	SP078	2	4E1C	SP121	1	1-MT1-1	SP021	6
121	SP125	P	1C1	SP095	16	4E1C	SP129	19	1-MT1-1	SP040	6
121	SP131	P	1C1	SP097	2	4E1C	SP130	4	1-MT1-1	SP045	3

Table S3. Continued.

Trawl	Code	Count	Trawl	Code	Count	Trawl	Code	Count	Trawl	Code	Count
122	SP020	P	1C1	SP101	31	4E1C	SP155	5	1-MT1-1	SP049	2
122	SP030	P	1C1	SP104	2	4E1C	SP165	1	1-MT1-1	SP075	1
122	SP040	P	1C1	SP105	4	4E1C	SP168	2	1-MT1-1	SP091	1
122	SP053	P	1C1	SP109	1	4E1C	SP188	6	1-MT1-1	SP117	4
122	SP075	P	1C1	SP117	1	4E1C	SP189	1	1-MT1-1	SP121	4
122	SP101	P	1C1	SP121	2	4E2A	SP008	4	1-MT1-1	SP136	10
122	SP121	P	1C1	SP129	26	4E2A	SP012	51	1-MT1-1	SP155	3
122	SP129	P	1C1	SP130	5	4E2A	SP025	40	1-MT1-1	SP165	1
123	SP020	P	1C1	SP155	3	4E2A	SP038	8	1-MT1-1	SP186	1
123	SP021	P	1C1	SP165	1	4E2A	SP040	59	1-MT1-1	SP211	33
123	SP030	P	1C1	SP178	3	4E2A	SP045	4	1-MT1-1	SP212	18
123	SP067	P	1C2	SP012	2	4E2A	SP047	2	1-MT1-1	SP236	33
123	SP075	P	1C2	SP025	3	4E2A	SP078	2	1-MT1-1	SP239	2
123	SP095	P	1C2	SP030	1	4E2A	SP088	82	1-MT1-1	SP272	21
123	SP101	P	1C2	SP038	1	4E2A	SP089	3	2-MT1-1	SP024	2
123	SP121	P	1C2	SP088	6	4E2A	SP111	4	2-MT1-1	SP053	1
124	SP013	P	1C2	SP111	4	4E2A	SP123	2	2-MT1-1	SP123	2
124	SP041	P	1C2	SP125	3	4E2A	SP125	4	2-MT1-1	SP248	1
124	SP072	P	1C2	SP149	2	4E2A	SP129	3	1-MT2-1	SP012	13
124	SP101	P	1C2	SP150	1	4E2A	SP141	3	1-MT2-1	SP038	19
124	SP111	P	1C3	SP018	1	4E2A	SP160	1	1-MT2-1	SP040	1
124	SP125	P	1C3	SP037	4	4E2A	SP169	2	1-MT2-1	SP041	3
124	SP126	P	1C3	SP052	6	4E2A	SP170	1	1-MT2-1	SP043	1
127	SP003	P	1C3	SP088	1	4E2B	SP008	7	1-MT2-1	SP051	1
127	SP016	P	1C3	SP125	6	4E2B	SP025	12	1-MT2-1	SP072	1
127	SP041	P	1C3	SP136	1	4E2B	SP040	38	1-MT2-1	SP088	49
127	SP052	P	1C3	SP140	1	4E2B	SP045	2	1-MT2-1	SP122	1
127	SP102	P	1C3	SP154	1	4E2B	SP047	1	1-MT2-1	SP210	1
127	SP126	P	2C1	SP007	1	4E2B	SP070	7	1-MT3-1	SP013	3
128	SP003	P	2C1	SP021	5	4E2B	SP075	2	1-MT3-1	SP037	6
128	SP023	P	2C1	SP027	1	4E2B	SP088	11	1-MT3-1	SP038	16
128	SP037	P	2C1	SP030	34	4E2B	SP089	1	1-MT3-1	SP041	10
128	SP041	P	2C1	SP031	7	4E2B	SP111	2	1-MT3-1	SP066	2
128	SP052	P	2C1	SP057	1	4E2B	SP123	1	1-MT3-1	SP081	3
128	SP076	P	2C1	SP075	13	4E2B	SP125	4	1-MT3-1	SP091	61
128	SP081	P	2C1	SP078	3	4E2B	SP190	2	1-MT3-1	SP119	14
128	SP101	P	2C1	SP095	2	4E2C	SP006	1	1-MT3-1	SP139	2
128	SP122	P	2C1	SP101	13	4E2C	SP012	3	1-MT3-1	SP162	1
128	SP125	P	2C1	SP103	1	4E2C	SP013	1	1-MT3-1	SP225	2
128	SP132	P	2C1	SP105	1	4E2C	SP025	11	1-MT3-1	SP230	1

Table S3. Continued.

Trawl	Code	Count	Trawl	Code	Count	Trawl	Code	Count	Trawl	Code	Count
130	SP125	P	2C1	SP129	10	4E2C	SP040	34	1-MT3-1	SP250	1
132	SP082	P	2C1	SP130	1	4E2C	SP047	1	1-MT3-1	SP257	1
132	SP105	P	2C1	SP155	5	4E2C	SP070	3	1-MT4-1	SP034	1
134	SP021	P	2C2	SP008	1	4E2C	SP086	1	1-MT4-1	SP037	3
134	SP030	P	2C2	SP012	2	4E2C	SP088	8	1-MT4-1	SP040	1
134	SP053	P	2C2	SP013	1	4E2C	SP089	2	1-MT4-1	SP041	9
134	SP101	P	2C2	SP025	3	4E2C	SP111	1	1-MT4-1	SP064	1
134	SP115	P	2C2	SP038	1	4E2C	SP125	9	1-MT4-1	SP122	4
135	SP008	P	2C2	SP040	1	4E2C	SP149	1	1-MT4-1	SP125	1
135	SP040	P	2C2	SP045	2	4E2D	SP008	3	1-MT4-1	SP197	1
135	SP043	P	2C2	SP088	5	4E2D	SP012	5	1-MT4-1	SP230	1
135	SP067	P	2C2	SP101	1	4E2D	SP025	18	1-MT4-1	SP264	1
135	SP075	P	2C2	SP111	1	4E2D	SP040	23	1-MT4-1	SP271	1
135	SP076	P	2C2	SP136	1	4E2D	SP044	1	1-MT5-1	SP194	1
135	SP089	P	2C2	SP162	1	4E2D	SP045	3	1-MT5-1	SP205	2
137	SP015	P	2C3	SP008	1	4E2D	SP047	1	1-MT5-1	SP209	1
137	SP088	P	2C3	SP012	1	4E2D	SP070	1	1-MT5-1	SP219	2
137	SP125	P	2C3	SP013	3	4E2D	SP078	2	1-MT5-1	SP230	3
137	SP136	P	2C3	SP038	1	4E2D	SP086	1	1-MT5-1	SP231	1
138	SP040	P	2C3	SP040	5	4E2D	SP088	12	1-MT5-1	SP255	2
138	SP041	P	2C3	SP088	2	4E2D	SP089	6	1-MT5-1	SP265	1
138	SP054	P	2C3	SP101	1	4E2D	SP111	10	1-MT5-1	SP267	1
139	SP009	P	2C3	SP125	4	4E2D	SP125	5	1-MT6-1	SP024	1
139	SP034	P	2C3	SP136	1	4E2D	SP144	1	1-MT6-1	SP147	1
139	SP041	P	2C4	SP088	1	4E2D	SP151	1	1-MT6-1	SP199	1
139	SP122	P	2C4	SP180	1	4E2D	SP162	1	1-MT6-1	SP221	2
139	SP125	P	2C5	SP132	1	4E2D	SP185	1	1-MT6-1	SP230	2
139	SP132	P	2E1	SP021	19	4E2D	SP188	1	1-MT6-1	SP266	1
140	SP052	P	2E1	SP027	10	4E2E	SP012	3	1-NB2-1	SP135	1
140	SP068	P	2E1	SP031	3	4E2E	SP025	12	1-NB3-1	SP042	2
140	SP132	P	2E1	SP067	27	4E2E	SP040	1	1-NB3-1	SP198	2
142	SP016	P	2E1	SP075	1	4E2E	SP078	1	1-NB3-1	SP205	1
142	SP017	P	2E1	SP078	2	4E2E	SP088	3	1-NB3-1	SP230	2
142	SP034	P	2E1	SP097	14	4E2E	SP089	1	1-NB3-1	SP243	1
142	SP038	P	2E1	SP117	5	4E2E	SP111	4	1-NB3-1	SP245	1
142	SP041	P	2E1	SP123	1	4E2E	SP125	1	1-NB3-1	SP265	2
142	SP088	P	2E1	SP129	13	4E2E	SP175	1	1-NB3-1	SP269	1
142	SP122	P	2E1	SP155	6	4E2E	SP184	1	1-NB5-1	SP003	1
142	SP125	P	2E1	SP163	1	4E3A	SP006	1	1-NB5-1	SP042	1
142	SP132	P	2E1	SP165	1	4E3A	SP013	36	1-NB5-1	SP069	1

Table S3. Continued.

Trawl	Code	Count	Trawl	Code	Count	Trawl	Code	Count	Trawl	Code	Count
143	SP002	P	2E1	SP167	4	4E3A	SP037	6	1-NB5-1	SP132	1
143	SP041	P	2E1	SP188	2	4E3A	SP038	2	1-NB5-1	SP205	1
143	SP118	P	2E2	SP008	1	4E3A	SP040	10	1-NB5-1	SP256	1
145	SP003	P	2E2	SP012	7	4E3A	SP051	2	1-NB5-1	SP262	1
145	SP037	P	2E2	SP025	7	4E3A	SP052	11	1-NB5-1	SP266	1
145	SP041	P	2E2	SP038	1	4E3A	SP054	5	1-RW1-1	SP005	1
179	SP017	P	2E2	SP040	13	4E3A	SP068	3	1-RW1-1	SP020	2
184	SP021	P	2E2	SP045	2	4E3A	SP078	1	1-RW1-1	SP071	3
184	SP031	P	2E2	SP070	3	4E3A	SP088	15	1-RW1-1	SP127	1
184	SP040	P	2E2	SP088	7	4E3A	SP089	1	1-RW1-1	SP189	1
184	SP048	P	2E2	SP097	1	4E3A	SP091	9	1-RW1-1	SP254	1
184	SP092	P	2E2	SP101	2	4E3A	SP125	23	1-RW1-1	SP272	1
184	SP098	P	2E2	SP111	2	4E3B	SP012	1	3-S1-1	SP001	2
184	SP123	P	2E2	SP167	1	4E3B	SP013	9	3-S1-1	SP069	1
184	SP124	P	2E3	SP013	4	4E3B	SP037	3	3-S1-1	SP208	2
185	SP021	P	2E3	SP025	1	4E3B	SP040	2	3-S1-1	SP251	1
185	SP028	P	2E3	SP037	2	4E3B	SP068	3	3-S3-1	SP182	1
185	SP101	P	2E3	SP040	9	4E3B	SP091	3	3-S3-1	SP200	2
185	SP129	P	2E3	SP051	1	4E3B	SP113	4	3-S3-1	SP202	1
186	SP020	P	2E3	SP068	2	4E3B	SP125	7	3-S3-1	SP232	1
186	SP105	P	2E3	SP072	1	4E3B	SP141	1	1-S35-1	SP012	39
186	SP108	P	2E3	SP088	2	4E3B	SP160	1	1-S35-1	SP024	1
186	SP109	P	2E3	SP091	1	4E3C	SP006	1	1-S35-1	SP038	26
186	SP114	P	2E3	SP125	24	4E3C	SP013	12	1-S35-1	SP040	2
186	SP121	P	2E3	SP174	1	4E3C	SP037	3	1-S35-1	SP045	13
186	SP131	P	2E4	SP002	4	4E3C	SP038	1	1-S35-1	SP047	7
187	SP082	P	2E4	SP003	1	4E3C	SP040	12	1-S35-1	SP051	1
187	SP087	P	2E4	SP011	10	4E3C	SP052	8	1-S35-1	SP054	1
188	SP013	P	2E4	SP012	2	4E3C	SP054	1	1-S35-1	SP064	4
188	SP038	P	2E4	SP016	9	4E3C	SP068	4	1-S35-1	SP088	25
188	SP040	P	2E4	SP020	1	4E3C	SP088	3	1-S35-1	SP136	8
188	SP041	P	2E4	SP037	1	4E3C	SP091	2	1-S35-1	SP210	1
188	SP052	P	2E4	SP051	1	4E3C	SP125	22	1-S35-1	SP216	9
188	SP054	P	2E4	SP052	31	4E3C	SP179	2	1-S35-1	SP218	1
188	SP081	P	2E4	SP054	1	4E3D	SP006	1	1-S35-1	SP230	2
188	SP086	P	2E4	SP068	11	4E3D	SP013	3	1-S35-1	SP239	10
188	SP088	P	2E4	SP091	10	4E3D	SP038	1	1-S35-1	SP244	2
188	SP125	P	2E4	SP095	4	4E3D	SP040	7	1-S36-1	SP002	3
193	SP091	P	2E4	SP097	1	4E3D	SP051	1	1-S36-1	SP003	1

Table S3. Continued.

Trawl	Code	Count	Trawl	Code	Count	Trawl	Code	Count	Trawl	Code	Count
194	SP026	P	2E4	SP122	33	4E3D	SP068	3	1-S36-1	SP034	1
194	SP037	P	2E4	SP125	18	4E3D	SP086	1	1-S36-1	SP040	2
194	SP040	P	2E4	SP126	1	4E3D	SP088	2	1-S36-1	SP041	4
194	SP041	P	2E4	SP132	6	4E3D	SP091	4	1-S36-1	SP042	4
194	SP052	P	2E4	SP135	2	4E3D	SP125	21	1-S36-1	SP047	1
194	SP054	P	2E4	SP137	1	4E3D	SP146	1	1-S36-1	SP135	1
194	SP068	P	2E4	SP139	1	4E3D	SP170	1	1-S36-1	SP169	2
194	SP081	P	2E4	SP143	4	4E3D	SP172	1	1-S36-1	SP193	1
194	SP088	P	2E4	SP144	1	4E3D	SP173	1	1-S36-1	SP205	1
194	SP125	P	2E4	SP174	4	5WC1	SP007	2	1-S36-1	SP206	1
195	SP012	P	2E4	SP182	1	5WC1	SP020	1	1-S36-1	SP219	2
195	SP013	P	2E5	SP132	1	5WC1	SP021	10	1-S36-1	SP230	1
195	SP024	P	2W1	SP021	45	5WC1	SP027	27	1-S36-1	SP243	1
195	SP038	P	2W1	SP027	35	5WC1	SP030	10	1-S36-1	SP266	1
195	SP040	P	2W1	SP030	3	5WC1	SP031	1	1-S37-1	SP003	2
195	SP041	P	2W1	SP031	4	5WC1	SP057	2	1-S37-1	SP042	3
195	SP054	P	2W1	SP047	3	5WC1	SP067	15	1-S37-1	SP106	2
195	SP058	P	2W1	SP053	3	5WC1	SP073	1	1-S37-1	SP147	1
195	SP077	P	2W1	SP057	2	5WC1	SP075	4	1-S37-1	SP193	1
195	SP081	P	2W1	SP067	3	5WC1	SP095	2	1-S37-1	SP230	1
195	SP088	P	2W1	SP075	4	5WC1	SP097	3	1-S37-1	SP243	1
195	SP093	P	2W1	SP078	3	5WC1	SP101	5	1-S38-1	SP001	2
195	SP096	P	2W1	SP095	1	5WC1	SP104	2	1-S38-1	SP142	1
195	SP113	P	2W1	SP097	2	5WC1	SP117	18	1-S38-1	SP205	2
195	SP118	P	2W1	SP101	24	5WC1	SP121	1	1-S38-1	SP219	3
195	SP125	P	2W1	SP103	2	5WC1	SP129	5	1-S38-1	SP228	1
195	SP136	P	2W1	SP105	1	5WC1	SP154	1	1-S38-1	SP243	2
196	SP012	P	2W1	SP117	59	5WC1	SP155	12	3-S4-1	SP207	1
196	SP013	P	2W1	SP129	8	5WC1	SP165	2	1-S40-1	SP143	1
196	SP025	P	2W1	SP146	5	5WC1	SP168	1	1-S40-1	SP201	1
196	SP026	P	2W1	SP155	15	5WC10	SP012	1	1-S40-1	SP204	1
196	SP036	P	2W1	SP165	1	5WC10	SP038	2	1-S40-1	SP205	2
196	SP038	P	2W1	SP178	1	5WC10	SP040	5	1-S40-1	SP230	1
196	SP040	P	2W1	SP189	1	5WC10	SP068	1	1-S41-1	SP001	3
196	SP043	P	2W2	SP012	3	5WC10	SP086	1	1-S41-1	SP014	4
196	SP044	P	2W2	SP021	1	5WC10	SP088	2	1-S41-1	SP024	1
196	SP049	P	2W2	SP025	2	5WC10	SP125	3	1-S41-1	SP219	1
196	SP050	P	2W2	SP038	1	5WC10	SP126	1	1-S41-1	SP230	1
196	SP054	P	2W2	SP040	15	5WC10	SP149	1	1-S41-1	SP233	1
196	SP079	P	2W2	SP070	2	5WC10	SP162	1	1-S41-1	SP255	1

Table S3. Continued.

Trawl	Code	Count	Trawl	Code	Count	Trawl	Code	Count	Trawl	Code	Count
196	SP082	P	2W2	SP078	1	5WC11	SP003	11	1-S42-1	SP012	3
196	SP089	P	2W2	SP086	1	5WC11	SP006	1	1-S42-1	SP038	1
196	SP104	P	2W2	SP088	5	5WC11	SP011	2	1-S42-1	SP040	5
196	SP125	P	2W2	SP136	1	5WC11	SP016	2	1-S42-1	SP041	7
196	SP129	P	2W2	SP176	1	5WC11	SP018	1	1-S42-1	SP081	3
196	SP136	P	2W3	SP013	2	5WC11	SP037	2	1-S42-1	SP085	3
199	SP005	P	2W3	SP037	5	5WC11	SP047	1	1-S42-1	SP088	8
199	SP007	P	2W3	SP040	2	5WC11	SP052	110	1-S42-1	SP125	1
199	SP019	P	2W3	SP054	7	5WC11	SP054	6	1-S42-1	SP136	41
199	SP020	P	2W3	SP091	2	5WC11	SP068	8	1-S42-1	SP162	1
199	SP031	P	2W3	SP125	27	5WC11	SP069	9	1-S42-1	SP218	1
199	SP040	P	2W3	SP144	1	5WC11	SP122	15	1-S42-1	SP219	3
199	SP063	P	2W3	SP153	2	5WC11	SP125	25	1-S42-1	SP226	2
199	SP078	P	2W3	SP155	3	5WC11	SP132	1	1-S42-1	SP230	6
199	SP080	P	2W3	SP174	2	5WC11	SP170	2	1-S42-1	SP239	1
199	SP101	P	2W4	SP002	2	5WC11	SP179	1	1-S42-1	SP270	1
199	SP104	P	2W4	SP069	1	5WC12	SP003	3	2-S42-1	SP024	2
199	SP105	P	2W4	SP122	1	5WC12	SP011	2	2-S42-1	SP197	1
199	SP110	P	2W4	SP125	1	5WC12	SP037	6	1-S43-1	SP021	8
199	SP111	P	3C1	SP021	4	5WC12	SP052	4	1-S43-1	SP097	6
199	SP120	P	3C1	SP027	5	5WC12	SP068	4	1-S43-1	SP121	5
199	SP121	P	3C1	SP030	20	5WC12	SP118	3	1-S43-1	SP168	1
199	SP129	P	3C1	SP047	1	5WC12	SP119	3	1-S43-1	SP188	1
199	SP134	P	3C1	SP053	1	5WC12	SP125	3	1-S43-1	SP212	5
204	SP005	P	3C1	SP057	1	5WC12	SP132	5	1-S43-1	SP239	1
204	SP020	P	3C1	SP073	1	5WC12	SP172	1	1-S43-1	SP252	1
204	SP029	P	3C1	SP075	5	5WC2	SP012	3	1-S43-1	SP272	1
204	SP039	P	3C1	SP078	2	5WC2	SP021	5	1-S43-1	SP273	3
204	SP040	P	3C1	SP095	2	5WC2	SP031	5	1-S44-1	SP005	1
204	SP048	P	3C1	SP101	4	5WC2	SP040	1	1-S44-1	SP020	1
204	SP053	P	3C1	SP104	3	5WC2	SP045	17	1-S44-1	SP110	1
204	SP056	P	3C1	SP121	27	5WC2	SP067	25	1-S44-1	SP178	10
204	SP059	P	3C1	SP129	20	5WC2	SP070	2	1-S44-1	SP195	34
204	SP061	P	3C1	SP146	10	5WC2	SP075	3	1-S44-1	SP217	1
204	SP062	P	3C1	SP155	2	5WC2	SP078	2	1-S44-1	SP237	4
204	SP063	P	3C1	SP165	1	5WC2	SP097	11	1-S44-1	SP241	2
204	SP071	P	3C1	SP171	3	5WC2	SP129	7	1-S44-1	SP246	1
204	SP073	P	3C1	SP188	5	5WC2	SP146	2	1-S44-1	SP263	2
204	SP074	P	3C2	SP012	6	5WC2	SP155	2	1-S44-1	SP274	2
204	SP079	P	3C2	SP013	3	5WC2	SP188	1	3-S5-1	SP069	1

Table S3. Continued.

Trawl	Code	Count	Trawl	Code	Count	Trawl	Code	Count	Trawl	Code	Count
204	SP083	P	3C2	SP025	1	5WC3	SP013	2	3-S5-1	SP207	2
204	SP094	P	3C2	SP031	7	5WC3	SP025	1	3-S5-1	SP242	1
204	SP101	P	3C2	SP038	3	5WC3	SP038	1	1-W1-1	SP021	15
204	SP105	P	3C2	SP040	18	5WC3	SP040	4	1-W1-1	SP024	1
204	SP107	P	3C2	SP047	2	5WC3	SP045	2	1-W1-1	SP027	27
204	SP108	P	3C2	SP070	6	5WC3	SP052	3	1-W1-1	SP040	16
204	SP110	P	3C2	SP075	2	5WC3	SP054	1	1-W1-1	SP045	4
204	SP127	P	3C2	SP086	2	5WC3	SP068	2	1-W1-1	SP047	2
204	SP128	P	3C2	SP088	19	5WC3	SP086	2	1-W1-1	SP095	9
204	SP129	P	3C2	SP125	1	5WC3	SP088	3	1-W1-1	SP103	1
204	SP130	P	3C2	SP129	7	5WC3	SP111	7	1-W1-1	SP104	1
204	SP131	P	3C2	SP136	1	5WC3	SP113	2	1-W1-1	SP155	5
204	SP133	P	3C2	SP145	1	5WC3	SP125	31	1-W1-1	SP165	3
206	SP012	P	3C2	SP157	1	5WC3	SP157	1	1-W1-1	SP210	2
206	SP031	P	3C2	SP158	1	5WC3	SP169	1	1-W1-1	SP211	1
206	SP040	P	3C2	SP166	1	5WC3	SP170	1	1-W1-1	SP223	1
206	SP050	P	3C2	SP187	1	5WC4	SP021	4	1-W1-1	SP234	15
206	SP067	P	3C3	SP013	4	5WC4	SP025	5	1-W1-1	SP238	2
206	SP075	P	3C3	SP037	6	5WC4	SP031	4	1-W1-1	SP239	3
206	SP088	P	3C3	SP038	2	5WC4	SP040	10	1-W1-1	SP252	1
206	SP097	P	3C3	SP040	15	5WC4	SP045	1	1-W1-1	SP253	8
206	SP131	P	3C3	SP054	2	5WC4	SP067	11	1-W1-1	SP272	2
209	SP091	P	3C3	SP088	7	5WC4	SP070	4	1-W3-1	SP051	1
210	SP002	P	3C3	SP125	19	5WC4	SP075	5	1-W3-1	SP091	1
210	SP003	P	3C3	SP136	5	5WC4	SP078	1	1-W3-1	SP197	1
210	SP011	P	3C3	SP140	1	5WC4	SP088	1	1-W3-1	SP220	1
210	SP013	P	3C3	SP146	1	5WC4	SP097	4	1-W6-1	SP001	3
210	SP037	P	3C3	SP180	2	5WC4	SP123	2	1-W6-1	SP017	1
210	SP038	P	3C4	SP037	1	5WC4	SP129	14	1-W6-1	SP024	1
210	SP040	P	3C4	SP122	1	5WC4	SP149	1	1-W6-1	SP142	1
210	SP041	P	3C4	SP125	2	5WC4	SP151	1	1-W6-1	SP203	1
210	SP051	P	3C5	SP001	2	5WC4	SP152	1	1-W6-1	SP205	1
210	SP052	P	3C5	SP142	3	5WC4	SP155	1	1-WC12-1	SP024	1
210	SP054	P	3C5	SP147	2	5WC4	SP157	1	1-WC12-1	SP258	1
210	SP081	P	3C6	SP021	12	5WC4	SP191	1	1-WC12-1	SP265	1
210	SP088	P	3C6	SP025	3	5WC5	SP021	16	1-WC5-1	SP024	1
210	SP090	P	3C6	SP031	46	5WC5	SP025	1	1-WC5-1	SP041	5
210	SP091	P	3C6	SP040	31	5WC5	SP027	39	1-WC5-1	SP091	1
210	SP122	P	3C6	SP070	16	5WC5	SP030	12	1-WC5-1	SP113	1
210	SP125	P	3C6	SP075	12	5WC5	SP040	16	1-WC5-1	SP136	1

Table S3. Continued.

Trawl	Code	Count	Trawl	Code	Count	Trawl	Code	Count	Trawl	Code	Count
210	SP136	P	3C6	SP078	1	5WC5	SP047	2	1-WC5-1	SP199	1
213	SP003	P	3C6	SP088	4	5WC5	SP053	5	1-WC5-1	SP213	1
213	SP011	P	3C6	SP097	13	5WC5	SP060	1	1-WC5-1	SP215	1
213	SP016	P	3C6	SP123	1	5WC5	SP067	10	1-WC5-1	SP225	5
213	SP037	P	3C6	SP129	100	5WC5	SP070	15	1-WC5-1	SP227	1
213	SP038	P	3C6	SP138	1	5WC5	SP075	20	1-WC5-1	SP230	2
213	SP040	P	3C6	SP146	1	5WC5	SP097	4	1-WC5-1	SP235	1
213	SP041	P	3C6	SP155	7	5WC5	SP101	8	1-WC5-1	SP261	1
213	SP051	P	3C6	SP157	1	5WC5	SP104	3	1-WC5-1	SP266	1
213	SP052	P	3C6	SP158	15	5WC5	SP117	2	1-WC5-1	SP268	2
213	SP054	P	3C6	SP159	1	5WC5	SP121	1			
213	SP068	P	3C6	SP165	2	5WC5	SP129	25			
213	SP076	P	3C7	SP013	1	5WC5	SP130	1			

Table S4. The characteristic epibenthic fish speices in the northern Gulf of Mexico. The top-10 species with the highest occurrence were listed for each faunal group based on the cluster analysis of pooled data (Fig. 6.5a). The depth ranges indicate depth distribution within the specific faunal group. The trophic level and economic value for each characteristic species were derived from the FishBase (Froese & Pauly 2000).

Group	Family	Species	Common Name	Depth	Occur	%Occur
Shelf Break	Percophidae	*Bembrops anatirostris*	Duckbill flathead	183-229	6	60
	Scorpaenidae	*Pontinus longispinis*	Longspine scorpionfish	183-237	6	60
	Paralichthyidae	*Ancylopsetta dilecta*	Three-eye flounder	188-229	4	40
	Ophidiidae	*Lepophidium brevibarbe*	Shortbeard cusk-eel	188-237	4	40
	Pleuronectidae	*Poecilopsetta beanii*	Deepwater dab	192-229	3	30
	Lutjanidae	*Pristipomoides aquilonaris*	Wenchman	192-229	3	30
	Bothidae	*Trichopsetta ventralis*	Sash flounder	188-237	3	30
	Ogcocephalidae	*Dibranchus atlanticus*	Atlantic batfish	192-229	2	20
	Nettastomatidae	*Hoplunnis tenuis*	Spotted pike-conger	192-229	2	20
	Ophichthidae	*Myrophis punctatus*	Speckled worm-eel	183-210	2	20
Upper Slope	Percophidae	*Bembrops gobioides*	Goby flathead	274-552	27	73
	Macrouridae	*Malacocephalus occidentalis*	Western softhead grenadier	274-576	25	68
	Ogcocephalidae	*Dibranchus atlanticus*	Atlantic batfish	274-1097	23	62
	Macrouridae	*Coelorinchus coelorhincus*	Hollowsnout grenadier	329-552	20	54
	Peristediidae	*Peristedion greyae*		329-696	20	54
	Phycidae	*Urophycis cirrata*	Gulf hake	274-552	20	54
	Epigonidae	*Epigonus pandionis*	Bigeye	329-552	18	49
	Chlorophthalmidae	*Chlorophthalmus agassizi*	Shortnose greeneye	329-538	17	46
	Merlucciidae	*Hymenocephalus italicus*	Glasshead grenadier	274-576	15	41
	Merlucciidae	*Merluccius albidus*	Offshore silver hake	329-552	15	41

Table S4. Continued.

Group	Family	Species	Common Name	Depth	Occur	%Occur
Upper to Mid Slope	Synaphobranchidae	*Synaphobranchus oregoni*		613-1510	52	76
	Macrouridae	*Nezumia aequalis*	Common Atlantic grenadier	566-1438	46	68
	Ogcocephalidae	*Dibranchus atlanticus*	Atlantic batfish	585-1376	40	59
	Macrouridae	*Coryphaenoides mexicanus*	Mexican grenadier	751-1510	32	47
	Macrouridae	*Coryphaenoides zaniophorus*	Thickbeard grenadier	585-1225	31	46
	Macrouridae	*Bathygadus melanobranchus*	Vaillant's grenadier	603-1064	30	44
	Ophidiidae	*Dicrolene introniger*	Digitate cusk eel	686-1463	26	38
	Macrouridae	*Bathygadus macrops*	Bullseye grenadier	585-1170	24	35
	Macrouridae	*Gadomus longifilis*	Treadfin grenadier	585-1463	24	35
	Halosauridae	*Halosaurus guentheri*		585-1170	21	31
Mid Slope	Halosauridae	*Aldrovandia affinis*	Gilbert's halosaurid fish	788-1774	7	64
	Halosauridae	*Aldrovandia gracilis*		1217-1829	4	36
	Ophidiidae	*Dicrolene introniger*	Digitate cusk eel	1217-1829	4	36
	Ipnopidae	*Bathypterois quadrifilis*		1217-1735	3	27
	Alepocephalidae	*Conocara macropterum*	Longfin smooth-head	1198-1829	3	27
	Synaphobranchidae	*Synaphobranchus oregoni*		759-1413	3	27
	Aphyonidae	*Barathronus bicolor*		1735-1735	1	9
	Macrouridae	*Gadomus longifilis*	Treadfin grenadier	1217-1217	1	9
	Ipnopidae	*Ipnops murrayi*		1413-1413	1	9
	Ophidiidae	*Monomitopus agassizii*		788-788	1	9
Mid to Lower Slope	Gonostomatidae	*Gonostoma elongatum*	Elongated bristlemouth fish	758-3010	10	67
	Ophidiidae	*Dicrolene kanazawai*		1784-2460	7	47
	Stomiidae	*Chauliodus sloani*	Sloane's viperfish	758-2980	6	40
	Ophidiidae	*Bassozetus robustus*	Robust assfish	1784-3010	5	33
	Macrouridae	*Coryphaenoides mediterraneus*	Mediterranean grenadier	1784-2980	4	27
	Sternoptychidae	*Sternoptyx diaphana*	Diaphanous hatchet fish	1100-2243	4	27
	Sternoptychidae	*Sternoptyx pseudobscura*	Highlight hatchetfish	758-2735	4	27
	Halosauridae	*Aldrovandia gracilis*		1784-2369	3	20
	Ipnopidae	*Ipnops murrayi*		2105-2367	3	20
	Alepocephalidae	*Alepocephalus productus*	Smalleye smooth-head	1784-2369	3	20

Table S4. Continued.

Group	Family	Species	Common Name	Depth	Occur	%Occur
Lower Slope to Abyssal Plain 1	Ophidiidae	*Bassozetus normalis*		2103-3287	5	36
	Nettastomatidae	*Venefica procera*		1134-2858	5	36
	Ophidiidae	*Porogadus catena*		1829-2140	3	21
	Ophidiidae	*Bathyonus pectoralis*		2651-3092	2	14
	Ipnopidae	*Bathypterois quadrifilis*		2057-2077	2	14
	Synaphobranchidae	*Ilyophis brunneus*	Muddy arrowtooth eel	1134-3267	2	14
	Ophidiidae	*Xyelacyba myersi*	Gargoyle cusk	1533-1829	2	14
	Halosauridae	*Aldrovandia gracilis*		2103-2103	1	7
	Aphyonidae	*Barathronus bicolor*		3267-3267	1	7
	Ipnopidae	*Bathypterois longipes*	Abyssal spiderfish	3287-3287	1	7
Lower Slope to Abyssal Plain 2	Ophidiidae	*Acanthonus armatus*	Bony-eared assfish	2505-3590	6	67
	Ipnopidae	*Bathypterois grallator*	Tripodfish	2074-3075	5	56
	Synodontidae	*Bathysaurus mollis*	Highfin lizardfish	2915-3403	3	33
	Ipnopidae	*Ipnops murrayi*		3355-3590	2	22
	Macrouridae	*Coryphaenoides rudis*	Rudis rattail	2074-2505	2	22
	Ophidiidae	*Barathrodemus manatinus*		2915-3075	2	22
	Ophidiidae	*Bassozetus robustus*	Robust assfish	2608-3075	2	22
	Alepocephalidae	*Bathytroctes macrolepis*	Koefoed's smooth-head	3075-3075	1	11
	Stomiidae	*Chauliodus sloani*	Sloane's viperfish	3075-3075	1	11
	Macrouridae	*Coryphaenoides mexicanus*	Mexican grenadier	2074-2074	1	11

APPENDIX F

ONLINE SUPPORTING FILES

A total of four online supporting files are available along with the electronic copy of this dissertation.

File S1. Google Earth file for the "CoML fresh biomass database".

File S2. Global seafloor biomass predictions. Predicted biomass (mg C m^{-2}) is in global 1 x 1 degree grids. Data fields include latitude, longitude, depth, and biomass of each size class. The biomass data are in logarithm scale (base 10).

File S3. Global seafloor abundance predictions. Predicted abundance (individual m^{-2}) is in global 1 x 1 degree grids. Data fields include latitude, longitude, depth, and abundance of each size class. The abundance data are in logarithm scale (base 10).

File S4. Gulf of Mexico macrofauna abundance and biomass predictions and the corresponding environmental data. Predicted abundance (individual m^{-2}) and biomass (mg C m-2) are in 5 x 5 arcminute grids. Data fields include latitude, longitude, abundance and biomass of benthic macrofauna, as well as the 19 environmental variables for Random Forest analyses (Table 3.1). The abundance data are in logarithm scale (base 10).

VITA

Chih-Lin Wei received his Bachelor of Science degree in zoology from National Chung-Hsing University in 1999 in Taiwan. He entered the Oceanography Department at Texas A&M University in September 2002 and received his Master of Science degree in December 2006 under the supervision of Dr. Gilbert T. Rowe. His research interests include ecology of deep-sea benthos. He plans to publish his dissertation on peer-review journals, focusing on his researches in the deep Gulf of Mexico.

Mr. Wei may be reached at Department of Marine Biology, Texas A&M University at Galveston, 1001 Texas Clipper Road, OCSB Bldg 3029 Room 240, Galveston, TX 77554. His email is weic@tamug.edu.

PUBLICATIONS:

Wei C-L, Rowe GT, Escobar-Briones E, et al. (2010) Global Patterns and Predictions of Seafloor Biomass Using Random Forests. PLoS One 5:e15323

Wei C-L, Rowe GT, Hubbard GF, et al. (2010) Feature Article: Bathymetric Zonation of Deep-Sea Macrofauna in Relation to Export Surface Phytoplankton Production. Marine Ecology Progress Series 399: 1-14

Wei C-L, Rowe GT (2009) Faunal zonation of large epibenthic invertebrates off North Carolina revisited. Deep Sea Research Part II: Topical Studies in Oceanography 56:1830-1833